

University of Alberta

Impact of Mountain Pine Beetle Attack on Water Balance of Lodgepole
Pine Forests in Alberta
by

Pablo César Piña Poujol

A thesis submitted to the Faculty of Graduate Studies and Research
in partial fulfillment of the requirements for the degree of

Doctor of Philosophy
in
Water and Land Resources

Department of Renewable Resources

©Pablo César Piña Poujol
Spring 2013
Edmonton, Alberta

Permission is hereby granted to the University of Alberta Libraries to reproduce single copies of this thesis and to lend or sell such copies for private, scholarly or scientific research purposes only. Where the thesis is converted to, or otherwise made available in digital form, the University of Alberta will advise potential users of the thesis of these terms.

The author reserves all other publication and other rights in association with the copyright in the thesis and, except as herein before provided, neither the thesis nor any substantial portion thereof may be printed or otherwise reproduced in any material form whatsoever without the author's prior written permission.

Dedication

To Anna, Maia and Tau
Capicúa, Gaia y Sol

Abstract

In recent decades mountain pine beetle (MPB) has become an important natural disturbance agent in western Canada, thus the impact of this disturbance will likely be an important component affecting water resources in this region.

Despite the widespread recognition of the potential changes, there has been limited research focused on how MPB affects key hydrological processes in lodgepole pine forests throughout west central Alberta.

To better understand how water inputs and outputs are modified at stand scales after the MPB attack I investigated: 1) the initial effects of simulated MPB on individual components of the stand water balance, including forest evapotranspiration (rainfall interception, transpiration and forest floor evaporation) and soil moisture as these components along with precipitation regulate water production from forested regions; and 2) the likely integrated effect of these components on the water balance of Alberta's lodgepole pine forests.

My research indicated that rainfall interception dominates the evaporative losses from mature lodgepole pine stands, and while the impact of MPB on water balance increases in proportion to the intensity of the attack, lower intensities of attack (affecting $<1/3$ of the stand) may not result in increased drainage or runoff because of increased water use by surviving trees. MPB impacts on forest water balance is likely greatest in the regions of Alberta where growing season precipitation is greatest. Thus, interactions among water balance components such as forest floor rainfall interception, and highly variable changes in transpiration can moderate the impacts of MPB on water balance across a

gradient of increasing intensity of MPB attack.

I also found that intensively MPB attacked forests can exhibit strong seasonal variations in drainage that parallels the distribution of summer rain. Thus, soil moisture during the growing season in attacked stands may not be as reliant on strong snowmelt recharge as in healthy forests.

These findings are novel because impacts of MPB attack on the components regulating stand water balance have not been previously documented. Thus the combined effect of MPB on the processes that govern water cycling in MPB affected pine forests have been speculative prior to this study.

Acknowledgements

I am most grateful to my academic advisors for their ongoing support. A deep appreciation to my supervisor, Uldis Silins; it has been a tremendous experience growing together, having you as mentor, to work in your lab and to know you as a person. Thank you for this shared adventure. Ellen MacDonald, I am particularly thankful for your bright comments and positive, constructive advice. By allowing me to take part in your lab meetings, I have gained an invaluable interaction with your students over the past years. To John Gamon, thank you for your thoughtful questions and insightful direction.

The university is a wonderful place to explore and exchange endless hours of insights. Thank you Mike Wagner, Anne McIntosh, Melissa Hairabedian, Chris Williams and Jocelyn Howery. Thank you Peter Presant for your tremendous help and friendship. Long hours of fieldwork were greatly complemented with topics of major thoughts and laughing. I would also like to thank all of the folks that helped me out in the field; after all, the basis of this dissertation refers directly to your hard work: Emily Turton, Sheelah Griffith, Samantha Karpyskin, Travis Cooper, Kim Stang and Halley Coxson. Thank you to the people in the forest hydrology lab and Silviculture research group, in particular to Eckhart Marenholtz and Devin Goodsman, for the logistical help.

My family. Anna, your support and joy through this journey leave me silent. From here I smile, to you. Maia, dear daughter... you have taught me great perspective starting with your birth, and I am delighted to share The Path with you. Tau, Sol... you were born and all of a sudden all happened, love. The family. Abue and Xitla, from within I thank you too.

This work was financially supported by a PhD scholarship from the Mexican National Council for Science and Technology (CONACYT, Doctoral scholarship #189271/230786) as well as by the Foothills Research Institute through the Forest Resource Improvement Association of Alberta.

Table of Contents

Chapter 1. INTRODUCTION.....	1
1.1. Ecohydrology, an overview	1
1.2. Lodgepole pine forests.....	2
1.2.1. Hydrology	2
1.2.2. Mountain Pine Beetle.....	3
1.2.3. Ecohydrology of MPB affected forests	4
1.3. Forest interception.....	4
1.4. Transpiration.....	5
1.5. Soil moisture	6
1.6. Overview of studies.....	6
1.6.1. Vertical water balance framework and structure of the dissertation ...	7
1.7. References.....	10
1.8. Figures	17
Chapter 2. VERTICAL ANALYSIS OF RAINFALL INTERCEPTION AND INITIAL EFFECTS OF MOUTAIN PINE BEETLE ATTACK ON INTERCEPTION IN A MATURE LODGEPOLE PINE FOREST	19
2.1. Introduction	19
2.2. Materials and methods	21
2.2.1. Study site description.....	21
2.2.2. Site description and experimental design	22
2.2.3. Micrometeorological measurements	22
2.2.4. Interception measurements	23
2.2.4.1. Throughfall	23
2.2.4.2. Stemflow	24
2.2.4.3. Recharge into the mineral soil	24
2.2.5. Calculation of canopy, forest floor, and total forest interception.....	25
2.2.6. Forest floor water content.....	25
2.2.7. Modeling rainfall interception	26
2.2.7.1. Canopy interception sub-model.....	26
2.2.7.2. Forest floor interception sub-model	28
2.2.7.3. Forest interception model	28
2.2.7.4. Model validation.....	29
2.2.8. Statistical analysis.....	29
2.3. Results.....	30
2.3.1. Rainfall interception dynamics.....	30
2.3.2. Early effect of MPB attack on rainfall interception.....	32
2.3.3. Modeled interception	33
2.4. Discussion	34
2.4.1. Canopy interception	34
2.4.2. Forest floor interception	35
2.4.3. Total forest interception	36
2.4.4. Early effect of MPB attack (red attack) on canopy interception.....	37
2.4.5. Modeled interception	37
2.5. Conclusions.....	38
2.6. References.....	39
2.7. Tables	45
2.8. Figures	52

Chapter 3. EARLY EFFECT OF VARIABLE INTENSITY MOUNTAIN PINE BEETLE ATTACK ON MICROCLIMATE AND TRANSPIRATION DYNAMICS OF LODGEPOLE PINE.....	60
3.1. Introduction	60
3.2. Materials and methods	62
3.2.1. Study site description	62
3.2.2. Experimental design	62
3.2.3. Effectiveness of treatments.....	63
3.2.4. Micrometeorological measurements	64
3.2.5. Transpiration measurements	65
3.2.6. Scaling transpiration to the treatment unit scale.....	67
3.2.7. Scenarios for stand transpiration.....	67
3.2.8. Data analysis.....	68
3.3. Results.....	69
3.3.1. Effectiveness of treatments.....	69
3.3.2. Micrometeorology.....	69
3.3.3. Transpiration	70
3.4. Discussion	72
3.4.1. Microclimate.....	73
3.4.2. Transpiration dynamics of individual trees.....	74
3.4.3. Transpiration response of lodgepole pine to variable intensity MPB attack.....	76
3.5. Conclusions.....	77
3.6. References.....	78
3.7. Tables	83
3.8. Figures	87
Chapter 4. EARLY EFFECTS OF FOREST HARVESTING AND VARIABLE INTENSITY MOUNTAIN PINE BEETLE ATTACK ON SOIL MOISTURE IN MATURE LODGEPOLE PINE FORESTS OF WESTERN ALBERTA.....	95
4.1. Introduction	95
4.2. Materials and Methods	97
4.2.1. Study site description	97
4.2.2. Site description and experimental design	97
4.2.3. Micrometeorological measurements	98
4.2.4. Soil moisture measurements.....	98
4.2.4.1. Continuous soil moisture series	98
4.2.4.2. Spatially distributed soil moisture	99
4.2.5. Data analysis.....	99
4.2.5.1. Soil moisture response by depth.....	100
4.2.5.2. Spatial patterns in surface soil moisture	100
4.3. Results.....	101
4.3.1. Soil moisture response.....	101
4.3.1.1. Seasonal patterns of soil moisture	101
4.3.1.2. Soil moisture response to canopy disturbance.....	102
4.3.2. Spatial patterns of soil moisture	103
4.4. Discussion	104
4.4.1. Soil moisture response to canopy disturbance	104
4.4.2. Spatial and temporal variability in soil moisture responses.....	105

4.5. Conclusion.....	107
4.6. References.....	108
4.7. Tables.....	112
4.8. Figures.....	118
Chapter 5. IMPACT OF VARIABLE INTENSITY MOUNTAIN PINE BEETLE ATTACK ON VERTICAL WATER BALANCE OF MATURE LODGEPOLE PINE FORESTS IN WESTERN ALBERTA.....	125
5.1. Introduction.....	125
5.2. Materials and methods.....	126
5.2.1. Interception.....	127
5.2.2. Transpiration.....	128
5.2.3. Evapotranspiration and Water balance.....	129
5.2.4. Statistical analysis.....	129
5.3. Results.....	130
5.3.1. Regional water balance.....	130
5.3.2. Effect of the MPB in the water balance.....	130
5.3.2.1. Rainfall interception and total evapotranspiration.....	130
5.3.2.2. Storage and drainage.....	132
5.4. Discussion.....	133
5.4.1. Effects of MPB on rainfall interception.....	133
5.4.2. Effects of MPB on water balance.....	134
5.5. Conclusions.....	136
5.6. References.....	137
5.8. Figures.....	145
Chapter 6. SYNTHESIS OF CONCLUSIONS.....	152
6.1. Research contributions.....	152
6.1.2. Effects of MPB on water balance of lodgepole pine forests in Alberta	154
6.2. Unanswered questions.....	156
6.3 Final statement.....	157
6.3. References.....	159
6.4. Figures.....	160

List of Tables

Table 2-1. Meteorological instrumentation used in this study. The quantity refers to the number of instruments deployed per treatment unit 45

Table 2-2. Total seasonal gross precipitation (P_G), throughfall (T_h), stemflow (S_F), canopy interception (I_c), forest floor interception (I_F), total forest interception (I_{tf}), and recharge into mineral soil (F). Values in brackets indicate percentage of gross precipitation 46

Table 2-3. Components of tree, forest floor and meteorological parameters. Parameters are: canopy cover fraction (c), mean rainfall and net precipitation rate (R, R_n), mean canopy per unit area and forest floor evaporation rate (E_c, E_F), canopy (with gaps) and forest floor storage capacity (S_c, S_{Fl}), trunk storage capacity (S_T), storage capacity of the stand and forest floor (C_{mc}, S_{Fl}), and drainage partitioning coefficient (pd) 47

Table 2-4. Seasonal total gross precipitation (P_G), throughfall (T_h), stemflow (S_F), and canopy interception (I_c) of control, 50-, and 100% mortality treatment units before (2008) and after (2010) treatment application. Values in brackets indicate percentage of gross precipitation 48

Table 2-5. Rainfall interception model performance: Root Mean Square Error ($RMSE$) and linear regression coefficients 49

Table 2-6. Differences (Δ) between measured and predicted (measured - predicted) throughfall (ΔT_h), stemflow (ΔS_F), canopy interception (ΔI_c), forest floor interception (ΔI_F), total forest interception (ΔI_{tf}), and recharge into mineral soil (ΔF). Negative and positive values denote over-, and underestimation compared to measured values, respectively. Values in brackets indicate percentage of gross precipitation ...50

Table 2-7. Total seasonal gross precipitation (P_G), and predicted (modeled) components of rainfall interception; throughfall (T_h), stemflow (S_F), canopy interception (I_c), forest floor interception (I_F), total forest interception (I_{tf}), and recharge into mineral soil (F). Values in brackets indicate percentage of gross precipitation51

Table 3-1. Median sap velocity (S_v), sap flow (S_f), transpiration per unit leaf area (T_l), transpiration per unit ground area (T_g), and canopy conductance (g_c) before and after treatment application of live, live within dead (50% mortality unit), and fading trees (100% mortality unit). Live 1, 2 and 3 correspond to transpiration measured in the control, 50% and 100% mortality sites prior to treatment application, respectively83

Table 3-2. Relative change in median sap velocity (S_v), sap flow (S_f), transpiration per unit leaf area (T_l), transpiration per unit ground area (T_g), and canopy conductance (g_c) after application of treatments for live, live within dead, and fading trees adjusted relative to live trees in the control. Relative change for each variable after treatment was calculated as $1 + [((\text{post-treatment treated unit})/(\text{post-treatment live1 unit})) - ((\text{pre-treatment treated unit})/(\text{pre-treatment Live1 unit}))]$ where 1 indicates no relative adjusted change after treatment .	84
Table 3-3. Median T_{st} (mm d^{-1}) before and after treatment application in the control, 50% and 100% mortality (mort.) sites	85
Table 3-4. Percentage of trees in three categories used in scenarios and corresponding total seasonal (May-Sept, 2010) stand-scale transpiration (T_{st}) for each of four scenarios of partial MPB attack. The reference T_{st} (control conditions) was 77 mm	86
Table 4-1. Tests for coincidental regressions ($P > F $) among regression relationships between mean daily soil moisture in treated units and the control unit by depth before and after treatment application. Relationships are based on mean daily VWC for the continuously measured dataset and on mean of weekly measurements for three increasingly deep soil profiles in the manually sampled dataset. R^2 indicates goodness of fit of the linear regressions before and after treatments and * indicates $P < 0.05$	112
Table 4-2. Mean manually measured (TDR dataset) and modeled (GAMM) VWC for three increasingly deep soil profiles before (Bfr) and after (Aft) treatment application. BACI columns refer to the scaled relative (adjusted) treatment effect relative to control conditions where 1 indicates no relative adjusted change after treatment. The Error column indicates the difference between measured and modeled BACI	113
Table 4-3. Mean monthly soil moisture storage (mm) for each experimental unit at 5 cm depth. Confidence intervals (95%) shown in brackets	114
Table 4-4. Coefficients for exponential models fit to soil moisture storage (mm) at 5 cm depth	115
Table 4-5. Summary of the 1000 Monte Carlo simulations of soil moisture storage (mm) drawn from the probability density functions for soil moisture storage at 5 cm depth	116
Table 4-6. Mean percentage of samples ($n = 1000$) from Monte Carlo simulations exceeding the mean soil moisture storage of the reference site (control). Values shown in brackets indicate the mean % difference between treatments and the control site	117
Table 5-1. Climate stations in the study region with 32 years of continuous records (May-September) of daily rainfall and air temperature. Station locations (easting and northing) are UTM coordinates for zone 11 using ellipsoid GRS80 and datum NAD83. Elevation units are in meters	140

Table 5-2. Long-term mean (32 years) growing season rainfall (P_G), canopy interception (I_c), throughfall (T_h), forest floor interception (I_F), total forest interception (I_{tf}), recharge into the mineral soil (F), transpiration (T), evapotranspiration (E_t), and drainage and storage (Q) from 48 climate stations across the study region. Summaries below stations refer to mean, standard deviation (Std) and coefficient of variation (CV) across stations. The CV of Q was adjusted to account for the presence of negative numbers	142
Table 5-3. Mean growing season canopy interception (I_c), forest floor interception (I_F), total forest interception (I_{tf}), recharge into the mineral soil (F), evapotranspiration (E_t), and drainage and storage (Q) across the 48 climate stations. Mean growing season rainfall (P_G) was 272 mm. Values in brackets indicate the percentage of P_G	144

List of Figures

Figure 1-1. Vertical water balance of a mature stand with a well-developed forest floor layer	17
Figure 1-2. Vertical water balance components following a gradient of intensity of mountain pine beetle attack. The size of the rectangles correspond to the amount of water on each water balance component relative to the size of the “Rainfall” rectangle	18
Figure 2-1. Location of the 2.2 ha research sites and general layout of measurements (approximate locations). Asterisks refer to measurements that were rotated every year	52
Figure 2-2. Frequencies of rain events recorded during the study period (2008-2010) with their respective relative contribution to total rain in cumulative terms	53
Figure 2-3. Funnelling ratios related to tree size and rain depth. A) Scatter plot of funnelling ratio as a function of P_G events for each DBH (cm) class. B) Boxplots with notches of funnelling ratio as a function of DBH class, whiskers indicate extremes (1.5 X interquartile range), and circles indicate outliers. The y-axis is in logarithmic scale. The widths of the notches are proportional to the square root of the samples sizes	54
Figure 2-4. Measured interception as a function of the range of P_G events along with the fit of the model. The panels A) and B) illustrate the boxplots of canopy and forest floor interception respectively. The width of the boxplots is proportional to the square root of the samples sizes, whiskers indicate extremes (1.5 X interquartile range), and circles indicate outliers. Panel C illustrates the scatter plot of total forest interception	55
Figure 2-5. Series of forest floor water content and gross precipitation in 2009 and 2010. The dashed line represents a smoothed spline over the forest floor water content. The dashed vertical line indicated the forest floor’s maximum water holding capacity	56
Figure 2-6. Relationships between control and treated sites for canopy interception I_c (mm) before (hollow symbols) and after (filled symbols) the treatment application. Dashed lines represent linear regressions before treatment for 50%- ($y = 0.91x + 0.01$) and 100% mortality units ($y = 0.93 + 0.03$), and after treatment for 50%- ($y = 1.02x - 0.01$) and 100% mortality units ($y = 0.96x + 0.00$). Variables were log transformed. The continuous line represents the 1:1 relationship	57
Figure 2-7. Modeled interception as a function of field measurements. Both variables were log transformed. The continuous line represents the fit of the linear regression between modeled and measured. The dashed line is the 1:1 relationship. Panel A) illustrates canopy interception, and B) forest floor interception	58

Figure 2-8. Gross precipitation and recharge (F) into the mineral soil (left axis), along with cumulative trend of canopy (I_c), forest (I_F), and total forest interception (I_{TF}) respectively for the 2010 season (right axis). Vertical lines indicate rainfall-recharge events (positive = rainfall, negative = recharge). Horizontal dashed line indicates total season gross rainfall (at end of season). A) indicates measured interception components, B) indicates measured P_G and modeled interception components ..	59
Figure 3-1. Study location and layout of treatment units (2.2 ha. each), climate stations, sapflow measurements. Dotted pattern indicates presence of dead trees (red foliage) from supervised classification of a color orthophoto taken in 2010. Asterisks indicate the approximate location of sapflow measurements (re-located within units every year)	87
Figure 3-2. Relationship of mean daily air temperature (T °C), relative humidity (RH), wind speed ($m\ s^{-1}$), and net radiation ($W\ m^{-2}$) in the 50% (left) and 100% (right) mortality units with that of the control unit before (filled symbols) and after (hollow symbols) treatment application	88
Figure 3-3. Mean air temperature (T °C), relative humidity (RH), wind speed ($m\ s^{-1}$), and net radiation ($W\ m^{-2}$) of control, 50% and 100% mortality units before and after treatment application. Error bars indicate 95% confidence intervals	89
Figure 3-4. Distribution of transpiration (T_t , $m^3\ m^2\ day^{-1}$) of live, live within dead, and fading trees before and after treatment application. Dark horizontal lines on boxplots indicate median, boxes indicate inter-quartile range (IQR), whiskers (extremes) indicate extreme range ($1.5 \times IQR$), box widths are proportional to square root (n), and notches indicate approximate 95% confidence intervals [$\pm 1.58 IQR/\text{square root } (n)$]	90
Figure 3-5. Typical diurnal patterns of median hourly transpiration (T_g , $mm\ d^{-1}$, unit ground area basis) of live, live within dead, and fading trees in the control, 50%, and 100% mortality sites, respectively, during sunny, clear-sky conditions (Julian days 133-135, 2011)	91
Figure 3-6. Median daily transpiration per unit ground area (T_g , mm) of live, live within dead and fading trees in 2010. Symbols indicate daily medians ($n=7$) embedded in shaded bands/edge lines representing the upper and lower inter-quartile range of each tree category	92

Figure 3-7. Relationships between median daily transpiration per unit ground area (T_g , mm) of live within dead (50 % mortality unit), and fading trees (100% mortality unit) trees with live trees (control unit) before (filled symbols) and after (hollow symbols) treatment application. Short-dashed lines indicate linear regressions before treatment for 50% ($y = 0.85x + 0.13$, $R^2 = 0.63$) and 100% mortality ($y = 0.99 + 0.20$, $R^2 = 0.57$) units, whereas long-dashed lines indicate relationships after treatment for 50% ($y = 1.29x + 0.01$, $R^2 = 0.84$), and 100% mortality ($y = 0.70x + 0.00$, $R^2 = 0.75$) units	93
Figure 3-8. Relationship between mean daily estimated stand scale transpiration (T_{st} , mm day ⁻¹) for four scenarios of partial MPB attack comprised of 75- (A), 50- (B), and 25% (C), and (D) 5% live trees (surrounded by fading and dead trees) and control (E - 100% live trees) with that of control conditions. Grey bands indicate 95% confidence intervals	94
Figure 4-1. Layout of the four treatment units (2.2 ha size with 20 m treated inner-buffers). Filled circles indicate the sampling locations for the manual TDR measurements of 3 increasingly deep soil layers (2008-2010), and hollow circles denote the sampling grid for the surface (5 cm depth) soil measurements (2010 only)	118
Figure 4-2. Scaled relative soil moisture storage (mm) in the top 60cm of the soil profile during the frost-free period from Sept. 2008 to Dec. 2010. Relative soil moisture storage represents the actual storage minus the minimum value of storage recorded in the series for each site. The blank frames represent the periods of frozen soil. Vertical bars indicate daily gross precipitation (mm)	119
Figure 4-3. Relationship between mean weekly manually sampled VWC (n=8) in the control and treated units before and after treatment application for three increasingly deep soil profile depths. Lines indicate linear regressions before (long-dashed) and after (short-dashed) treatment application for 50%, 100% and clearcut units	120
Figure 4-4. Relationship between mean modeled VWC (n=8) in the control and treated units before and after treatment application for three increasingly deep soil profile depths. GAM modeled VWC reflects variation in moisture content due to only the fixed effects of treatment, the three profile depths, and time	121
Figure 4-5. Precipitation (mm) and median (n=81) soil VWC at 5 cm depth in 2010. Arrows indicate the four dates used for the spatial analysis	122
Figure 4-6. Probability Density Functions (PDF) of the simulations (n=1000) of moisture storage at 5 cm depth for four treatment units. The panels represent the four dates used in the spatial analysis	123

Figure 4-7. Proportion of area in each treated unit exceeding the mean soil moisture storage (mm) at 5 cm depth of the control unit (indicated in titles for each date) for four dates during 2010. Vertical lines indicate the mean proportion of area for each site	124
Figure 5-1. Distribution of lodgepole pine in Alberta and location of climate stations used in this study	145
Figure 5-2. Linear relationships between mean daily tree transpiration (T_g) in 2010 for three categories of trees after MPB attack and potential evapotranspiration. Live trees ($y = 0.14 \times ET_0 - 0.10$, $R^2 = 0.76$); live within dead trees ($y = 0.14 \times ET_0 - 0.09$, $R^2 = 0.59$); and dying (fading) trees ($y = 0.08 \times ET_0 - 0.02$, $R^2 = 0.71$)	146
Figure 5-3. Boxplots of total growing season rainfall across 54 climate stations in the study region (1979-2010). The boxplots width is proportional to sample size (i.e., number of stations with data available for the respective year). Horizontal dashed lines indicate median (273 mm) and both upper (342 mm) and lower (202 mm) interquartile range (IQR), whiskers indicate extremes (1.5 x IQR), and circles indicate outliers	147
Figure 5-4. Mean daily (A, mm and %) and annual (B, mm/yr) rainfall interception I_{rf} across the 48 climate stations for control, MPB1, MPB2 and MPB3 scenarios. Vertical lines in panel A represent the range of daily rainfall where the maximum percentage difference between the control and the MPB scenarios was evident. Lines shown in panel B indicate the linear fit, upper and lower 95% confidence intervals	148
Figure 5-5. Relationships between daily recharge into the mineral soil F , and total rainfall interception I_{rf} , as a function of daily rainfall. Exponential trends in both panels represent F . Quasi-asymptotic trends represent I_{rf} . Vertical and horizontal lines denote the points where I_{rf} is equal to F in the control and three mountain pine beetle attack scenarios	149
Figure 5-6. Mean daily storage and drainage (Q) across the 48 climate stations for control, MPB1, MPB2 and MPB3 scenarios	150
Figure 5-7. The relationship between mean annual storage and drainage (Q) and mean growing season precipitation across the 48 climate stations for control, MPB1, MPB2 and MPB3 scenarios (panel A) and mean annual Q across 32 years for these scenarios. The dashed lines in panel A indicate the linear relationship, upper and lower 95% confidence intervals for each scenario. The solid lines refer to the range of value in rain where Q equalled zero in the control and MPB1 scenario. The horizontal dashed line in panel B indicates the long-term mean Q for control conditions across all years, and the solid line indicates zero Q	151

Figure 6-1. A hypothesis tree of potential effects of MPB on key water budget components in a mature lodgepole pine forest after Adams et al. (2011). Possible effects include increases and decreases in total forest interception (I_{tf}), soil moisture, stand transpiration (T_{st}), evapotranspiration (E_t) and soil moisture storage or drainage. Important factors for determining these outcomes include the total amount of annual rainfall during the growing season, the dominance of snowmelt on water flows, percent tree cover lost from mortality, the degree of development of forest floor and rainfall interception response, and the effect of tree mortality and the compensatory response in stand transpiration. These hypotheses represent an assessments of the empirical analysis conducted in Chapters 2 to 5	160
Figure 6-2. Changes in components of forest water balance with increasing intensity of MPB attack. Components include total forest interception I_{tf} , stand transpiration T_{st} , and water balance (storage and/or drainage) Q as a percentage of annual rainfall in healthy forests and MPB scenarios reflecting a gradient of intensity from MPB1-MPB3 (after Chapter 5). Scenarios were defined by decreasing both canopy cover and overstory transpiration	161
Figure 6-3. Components of water balance in healthy forests and MPB scenarios reflecting a gradient of intensity in MPB attack from MPB1- MPB3 (after Chapter 5). Scenarios were defined by decreasing both values of canopy cover and of overstory transpiration. The width of the each box corresponds to the percentage of rainfall during the growing season	162

Chapter 1. INTRODUCTION

1.1. Ecohydrology, an overview

Ecohydrology is a comparatively new scientific discipline that focuses on the interaction of global water cycles with biota (D'Odorico et al., 2010). The name has been associated with integrated studies of ecological and hydrological processes in wetlands (Ingram 1987, Zalewski 1997) and terrestrial ecosystems (Vertessy et al. 1996, Baird and Wilby 1999, Rodríguez-Iturbe 2000), and relationships between freshwater river flows and ecosystem services (Gordon and Folke 2000). The emphasis on bridging scientific understanding between water cycles and ecosystem dynamics is attracting the attention of an increasingly broad segment of the science community and even triggering the development of new academic programs (D'Odorico et al., 2010). From a theoretical perspective, ecohydrology offers rich opportunities for development of unifying concepts and new theories to help understand complex patterns and processes in ecosystems (D'Odorico et al., 2010). From a practice perspective, the discipline faces a pressing global challenge because of the highly diverse dimensions of uncertainty in predicting ecosystems trajectories associated with disturbance and human activities. In the case of terrestrial ecohydrology, the emerging picture of global changes to ecology suggests the potential of large-scale changes in vegetation (Jackson et al., 2009; Wilcox 2010) has the potential to produce rapid and abrupt changes in water resources (Allen and Breshears, 1998; Overpeck and Cole, 2006; Backlund *et al.*, 2008).

Vegetation dynamics, unlike other physical attributes in the landscape occur within relatively short time frames, reflecting seasonality, developmental changes, and disturbance conditions. Vegetation dynamics can occur on temporal scales similar to changing patterns of human water demand and land use management (Brooks and Vivoni, 2008). Evaluating future water availability is currently challenged by important hydrological changes to water budgets (Troch *et al.*, 2009) that parallel the current trends in both climate and vegetation shifts in much of the world (Jackson *et al.*, 2009; Wilcox 2010). Of particular concern is increasing drought and warmer temperatures, which combined with human-influences on landscapes have had triggered a widespread infestation by pathogen and/or pests in vegetation (Allen *et al.*, 2010). As a result, forest decline over the past 30 years on all six continents supporting forests suggests that climate-driven forest die-off may be emerging as a global phenomenon of considerable importance (Allen et al., 2010). Adams et al. (2011) compiled several recently documented die-off events affecting large areas including 130 000 km² of pine (*Pinus* spp.) forests in western Canada by the end of 2006, loss of 55 000 km² of Australian eucalypts (*Eucalyptus* spp.) by the late 1990s, and over 600 000 km² of non-contiguous coniferous forests in western North America in the last decade (Fensham and Holman, 1999; Kurz et al., 2008; Bentz et al., 2009; Fensham et al., 2009; Allen et al., 2010). In the particular case of lodgepole pine forests (*Pinus contorta* Dougl. ex Loud.) in western North America, a combination of warm winter temperatures and an abundance of mature stands have created optimal conditions for the

development of an unprecedented outbreak of mountain pine beetle (MPB; *Dendroctonus ponderosae* Hopkins) (Taylor et al., 2006; Robertson et al., 2007).

1.2. Lodgepole pine forests

The lodgepole pine has been a component of the coniferous forest of western North America for millions of years. Its widespread distribution ranges from 31° N in Baja California to about 64° N in the Yukon Territory. Lodgepole pine forests occupy 22% of forested land in western Canada; 15% in the US portion of the Rocky Mountains and 4% in the coastal states (Despain, 2001). Lodgepole pine forests dominate much of the mountainous environment located from Colorado to northern Alberta, and often forms monospecific stands. Lodgepole pine is relatively shade-intolerant species and has adapted to grow on sites that are marginal for other tree species. Disturbance is another relevant factor that helps lodgepole pine compete with other species by providing seedbeds enabling germination and establishment. Natural disturbances associated with lodgepole pine forests include fire, insect outbreaks, mistletoe infestations, and windstorms. While bark beetle epidemics or windstorms may create the openings necessary for lodgepole pine regeneration, severe stand-replacing wildfires have been the primary disturbances occurring at 100- to 400-year intervals throughout much of the home range of lodgepole pine (Arno, 1980; Romme et al., 1986). After a fire, biomass re-accumulates following a predictable pattern of accretion of the major forest components (live plant, forest floor, and dead wood biomasses). The maximum rate of biomass accretion occurs in the fourth or fifth decade of forest development. In the period between fires, annual net primary productivity continually exceeds annual respiration by heterotrophic organisms (Yavitt & Fahey, 1986). This situation differs from other forests where equilibrium in total biomass at maturity is hypothesized (Bormann & Likens, 1979; Fahey & Knight, 1986).

1.2.1. Hydrology

The annual hydrological pattern in the Canadian Rocky Mountains can be divided into three primary phases: 1) an extended period of snow accumulation with little movement of water in the liquid state, usually from October until April; 2) shorter phase in May and June during which the accumulated snow melts and saturates the soil, contributing to groundwater and streamflow; and 3) a relatively dry summer period between July and September during which evapotranspiration reduces soil water content, often leading to tree water stress. Most summer rains do not significantly contribute to soil moisture beyond the rooting zone (Reynolds & Knight, 1973). During this phase, much more water can move via transpiration than from direct soil evaporation (Fahey & Knight, 1986).

Understanding the hydrophysiology of lodgepole pine is required to predict water fluxes throughout the year, and how variation in biotic, climatic, and soil conditions affects these fluxes. For example, tree density and composition influence the water yield; water outflow beyond the rooting zone in the spring

would be much greater in a stand dominated by deciduous aspen (*Populus tremuloides* Michx.) than a lodgepole pine because essentially no vernal transpiration occurs when the trees are leafless (Fahey & Knight, 1986). One primary effect of timber harvest, fire, or insect epidemics is lowering tree density and canopy leaf area index (LAI), which can lead to an earlier and shorter snowmelt period and higher streamflow. This effect is magnified with the possibility of snow redistribution by wind from the forest into small openings (Troendle, 1983; Wittwer et al., 1975). Reducing LAI by 45% in a girdled lodgepole pine stand and by 99% in a clearcut stand (from 9.1 to 5.2 and 0.1) led to an estimated increase of annual water outflow of 92% and 277% (from 13 cm to 25 and 49 cm) respectively (Knight et al., 1991).

1.2.2. Mountain Pine Beetle

While fire is the dominant natural disturbance affecting lodgepole pine forests in western Canada, MPB has been expanding to become a serious disturbance agent (Nealis and Peter 2008). Furthermore, MPB distribution is not considered to be constrained by the availability of suitable host tree species (Carroll et al. 2006) but by climate, and more specifically by low winter temperatures (Safranyik 1978, Carroll et al. 2004). In the last decade, favorable climate (mild winters) has promoted significant expansion of MPB (Logan and Powell 2001; Carroll et al. 2004). In Alberta, MPB has expanded its range in pine forests (Safranyik et al. 2010). Although the future course of the attack of MPB in Alberta is not yet known, MPB is likely to remain in Alberta (Schneider et al. 2010) due to both climate and vegetation shifts (Mbogga et al., 2009; Gray and Hammann, 2011). As a result, MPB will likely modify the historic disturbance regimes for Alberta's pine forests.

Tree mortality in MPB affected stands can range widely along environmental gradients (elevation, climate, topography); overstory tree mortality in MPB affected stands in British Columbia typically ranges between 25% and 50% (Shore et al. 2006). MPB is a unique disturbance agent. Compared to other disturbance agents such as fire and wind, MPB has no direct impacts on the understory or soil (Burton, 2008). Three stages of effects on foliage are recognized in trees successfully attacked by MPB. First, a green attack stage occurs during host colonization and early establishment by the beetle population. At this stage, there are no apparent visual symptoms detectable at the canopy level. Initially during this phase, attacked trees are still physiologically alive and although often stressed beyond recovery they do not usually die in this phase (Chojnacky et al., 2000; Neiman and Vistintini, 2004). Inside the host tree, MPB resides in the cambial zone and inoculates fungi that occlude the ray cells and vertical tracheids thereby reducing sapwood hydraulic conductance and water supply to the crown (Ballard et al., 1982, 1984). The red attack and gray attack stages usually develop within one and three years, respectively, from the time of the initial mass attack (Chojnacky et al., 2000; Neiman and Vistintini, 2004). During these stages, the tree canopy first gradually turns red-brown (hence the name red attack) followed by progressive defoliation in the gray attack phase, though some overlap is usually observed

between the development of red attack and the onset of gray attack phases.

1.2.3. Ecohydrology of MPB affected forests

In the early MPB attack phase (i.e., green towards red attack) a major abiotic change occurs in stand-level hydrology. In particular, death of the forest canopy results in increased water availability (Knight et al. 1991, Schnorbus 2011). Pine mortality from MPB primarily affects tree transpiration, and thus, modifies the link between soil and atmospheric evaporative demand. Because MPB also changes the structure of the canopy in latter phase (via loss of foliage and chlorosis), other changes occur in the canopy including changing radiation dynamics, wind penetration, and a range of other microclimatic conditions (Boon 2009, 2012; Winkler et al., 2010). Changes in microclimate also drive further changes in evaporative processes, which result in more water available for streamflow (Redding et al., 2008). These ecohydrological effect at the stand scale aggregate to manifest changes at the scale of regional surface and groundwater resources (Brooks and Vivoni, 2008). Therefore, increases in soil moisture can produce increases in groundwater recharge and runoff generation in MPB affected landscapes.

The potential impacts of MPB on the hydrology of pine forest has prompted a wide range of research focusing on evaluating changes in water yield, peak flows and low flows, channel changes associated with increased runoff, as well as impacts on aquatic habitat and drinking water (Uunila et al., 2006; Redding et al., 2008; Schnorbus, 2011). However, much of this research has largely been limited to potential influences of MPB on landscape or watershed scale hydrology. Catchment-scale water balance studies across a broad range of forest biomes have provided fundamental information regarding the effects of forest development and land-use on water yield (Bosch & Hewlett, 1982). However, because water yield reflects the integrated effects of precipitation interception, transpiration, and soil evaporation, the processes driving changes in water yield are not easily separated. To understand the factors that govern forest water use it is essential to examine the responses to variable external environmental factors such as water supply for tree water use, precipitation, soil moisture, and evaporative demand (Phillips & Oren, 2001). Thus, the prediction of how MPB affects the forest, climate and soil requires also a clear understanding of the factors that govern the water balance in forests at the stand scale (Phillips & Oren, 2001; Simonin et al., 2007, Adams et al., 2011). In particular, the literature suggests the need of research that includes short- to long-term stand-level field studies (Hélie et al., 2005) within a before, after, control, impact (BACI) framework (Uunila et al., 2006). Key research priorities include forest interception, transpiration, and soil moisture dynamics (Hélie et al., 2005; Adams, 2011).

1.3. Forest interception

Interception is the fraction of precipitation that is intercepted by the earth's surface and subsequently evaporated back to the atmosphere. Research typically

focuses on interception dynamics of the different forms of precipitation including rain, snow, or fog and relationships with characteristics of the intercepting surfaces such as vegetation canopies, ground layers, or man-made structures. Rainfall interception in particular, is one of the most conspicuous ecohydrological processes in forests. Potentially only a fraction of the rainfall reaches the forest floor and infiltrates into the soil under some conditions. Interception of precipitation may indirectly affect the functioning of forest ecosystems (Helvey & Patric, 1965; Reynolds & Knight, 1973; Forgeard *et al.*, 1980; Pitman, 1989; Johnson, 1990; Navar & Bryan, 1990; Klaassen *et al.*, 1998; Zeng *et al.*, 2000; McJannet *et al.*, 2007). However, interception processes are not as extensively represented in the research literature compared to other pathways of evaporative water loss in forests. Furthermore, literature on rainfall related studies mainly emphasizes aboveground (canopy) water losses whereas relatively little attention has focused on the role of rainfall interception in regulating the recharge of soil moisture in forests (Guevara-Escobar *et al.*, 2007; Shachnovich *et al.*, 2008; Gerrits *et al.*, 2010). With the exception of one recent study (Guerrits *et al.* 2010) very little interception research has attempted to integrate the combined effect of canopy and forest floor layers.

1.4. Transpiration

Water loss from the forest canopy is another important component of stand water balance (Whitehead and Jarvis, 1981; Whitehead and Kelliher, 1991). However, very little research has contrasted transpiration with other pathways of evaporative water losses from forests (Kaufmann, 1985; Simonin, 2007). Transpiration is influenced by factors such as climate, forest age, species, structure, and soil-moisture conditions (Roberts, 1983). Transpiration also affects various ecosystem characteristics such as cooling of soil, air, and plant tissues when incoming energy is dissipated as latent heat of vaporization (Simonin *et al.*, 2007), increases the depth to which soil water contributes to forest floor evaporation (Dawson, 1996), and alters soil surface energy budgets and thus the overall rates of soil evaporation (Breshears *et al.*, 1998). The effects of transpiration can even extend to biogeochemistry; if a large portion of incoming precipitation is lost to transpiration, transpiration can reduce nutrient leaching from deep percolation (Simonin *et al.*, 2007).

Research has provided much insight into differential transpiration and stomatal controls among a broad range of tree species (e.g., Oren *et al.*, 1999; Phillips and Oren, 2001; Bladon, *et al.*, 2006; Ford *et al.*, 2007; McDowel *et al.*, 2008). Yet, there is very little understanding of how disturbance affects transpiration and how transpiration modifies the hydrological cycle by extrapolating detailed fine-scale measurements from the tree- or leaf-level to the stand-level (Gebre *et al.*, 1998; Ewers *et al.*, 2002; Kostner *et al.*, 2002; Adams, 2011). It is clear however, that changes in vegetation cover influence the relative contributions of plant transpiration to total ecosystem evapotranspiration.

1.5. Soil moisture

Soil water content affects vegetation and at the same time is affected by vegetation. This close coupling between soil water and vegetation is and an important determinant of many ecological processes (Rutter, 1966; Tanner, 1968; Rodríguez-Iturbe et al., 1999; Porporato et al., 2004; Guswa, 2005). Soil moisture is the fundamental state variable in hydrological studies of the land surface (Rodríguez-Iturbe, 2000, 2003; Rodríguez-Iturbe et al., 1999) and most hydrological models are centered on soil moisture accounting (e.g. Chen and Dudhia, 2001; Feddes et al., 2001; Guswa et al., 2002; Simunek et al., 1998). However, complexity arises since the driving elements of soil and vegetation dynamics are heavily dependent on the space and time scales at which systems are observed (Rodríguez-Iturbe et al., 1999).

Soil moisture reflects the difference between precipitation inputs and outputs in the form of evapotranspiration, runoff and drainage. During the spring period, the capacity of the soil to store melting snow water depends directly on the soil pore space emptied of water by evapotranspiration during the previous summer and fall. The primary variable affecting the amount of available pore spaces is the total leaf area from which transpiration occurs (Fahey and Knight, 1986). For mature, closed-canopy stands in dry environments, the amount of LAI varies in response to the degree of water stress developed during the growing season (Grier & Running, 1977; Knight et al., 1981). In lodgepole pine forests, LAI is closely related to the soil storage capacity, as most of the water available to the trees each year is that retained in the soil during the snowmelt period (Fahey & Knight, 1986). Research relating soil moisture to ecological processes typically stresses the need to consider the role of regional seasonality (Rodríguez-Iturbe et al., 2001; Rodríguez-Iturbe, 2003; Verstraeten et al., 2005; Christiansen et al., 2006; Small and McConnell, 2008); however the role of stand development including disturbance regime is an important modifying component. As a forest canopy alters both, the distribution of precipitation as well as water extraction from the soil, it can be postulated that both changes produced by stand development (and seasonality) and disturbance alter the connection between climate, soil and vegetation in forests.

1.6. Overview of studies

widespread latitudinal extent makes lodgepole pine forest a key component in the study of terrestrial ecosystems in North America (Koch, 1996). The MPB is the most serious insect pest of lodgepole pine in the mountain regions of western Canada and the United States (Taylor, 2006). This dissertation is focused on providing critical information on how hydrological processes in the lodgepole pine forests in Alberta's Upper Foothills are likely to respond to the MPB attack. The results will help inform forest management planning for this region by providing key insights needed to forecast MPB effects on the hydrology of MPB affected landscapes. The information available in the literature on lodgepole pine water fluxes is mostly related to short-term periods (1 or 2 years) and usually accounts only for one of the components of the water cycle. However, water yield from forested landscapes is determined by complex

interactions among various components of regulating the water cycle. Current approaches using information and models developed on harvested sites (e.g., Spittlehouse, 2007; Dubé and Rex, 2008; Schnorbus, 2011) cannot accomplish these goals, because key eco-hydrological processes in MPB affected forests likely differ from those of harvested forests but have not been researched. A more complete understanding of this disturbance is critical for scientists and resource managers to plan for potential hydrological changes produced by MPB in forested landscapes. Thus, research is needed to document the explicit linkages between precipitation, forest interception, transpiration, soil recharge, and recharge of water tables in MPB affected forests (Hélie et al., 2005; Uulina, 2006; Adams, 2011). This dissertation focuses on developing the quantitative, process focused understanding of how water inputs and outputs are modified at stand scales after the MPB attack that can be directly applied to lodgepole pine forests in west central Canada. This research had two main objectives: 1) to describe the initial effects of MPB on individual components of the stand water balance, including forest evapotranspiration (i.e., rainfall interception, transpiration and forest floor evaporation) and soil moisture as these components (along with precipitation) regulate water production from forested regions; and 2) to model the integrated effect of these water balance components following the lodgepole pine distribution in Alberta.

1.6.1. Vertical water balance framework and structure of the dissertation

This dissertation was divided in four chapters based on a vertical water balance framework (Figure 1-1). The water balance of a conifer stand consists of a tree canopy and a well-developed forest floor as follows:

$$Q = P_G - (I_{tf} + T_{st}) \quad (1)$$

where Q is the net amount of water added to storage and/or drainage in the soil and P_G , I_{tf} and T_{st} are average rainfall, total forest interception, and stand overstory transpiration, respectively (Figure 1-1). The individual responses of water balance components to precipitation was analyzed for healthy forest conditions along with two levels of intensity MPB attack (Figure 1-2). Evapotranspiration was assumed to be the dominant component on the water balance, represented here as the sum of I_{tf} and T_{st} . It is expected that an immediate change in stand conditions after a MPB attack result in an increase in tree mortality, which should be manifested as crown reddening and needle cast and an overall decrease in canopy cover. These immediate changes in early MPB attacked stands could result in significant decreases in evapotranspiration and a subsequent increases in Q . As a first general hypothesis, a change in the response on forest rainfall interception would be primarily driven by a reduction in canopy cover. A reduction in the canopy cover represents a direct reduction in the canopy interception capacity, which in turn results in an increase in net precipitation. The increase in net precipitation has the potential to increase both the amount of rainfall intercepted by the forest floor and the amount of water recharging the mineral soil (Figure 1-2). Thus, a significant reduction in canopy interception could produce a significant increase in forest floor interception,

where the role of the forest floor in the total forest interception could become critical in the forest evaporative loss. As a second general hypothesis, the response in transpiration could be driven by changes in two conditions: microclimate and soil water availability. A reduction in the canopy cover could increase light and wind penetration within the stand. Furthermore, a reduction in the amount of evaporative loss in the canopy by reducing both canopy interception and overstory transpiration could result in a reduction of latent heat fluxes, which could produce an increase of sensible heat fluxes resulting in increased air temperature. The overall changes in microclimate could resemble thinning harvesting practices, where the stands experience a general increase in evaporative demand. Also, the increase in tree mortality results in a decrease in transpiration and thus, a decrease in soil moisture water extraction. This increase in soil moisture water extraction could result in significant increases in soil water availability. These changes in environmental conditions could increase individual tree transpiration in healthy un-attacked trees. Microclimate could increase evaporative demand and soil conditions might favour the overall tree water uptake, resulting in a significant increase in individual tree transpiration rates. As a result of individual tree transpiration response in early MPB attacked stands, changes in transpiration at the stand level could be buffered, reflecting the integrated stand-scale effect of the differential transpiration responses of remaining strata in the stands represented by healthy un-attacked trees and dying trees (Figure 1-2). These hypothetical responses were evaluated based as follows:

Chapter 2 focuses on the total forest interception component of the water balance in Equation 1 (see Figure 1-1). The goal of the research described in Chapter 2 was to analyze and characterize the total forest rainfall interception in a lodgepole pine stand in western Alberta. Main objectives were: 1) to characterize the major components of canopy interception and forest floor interception in mature lodgepole pine stands at risk from MPB attack; 2) to explore the early impact of MPB attack on these processes, and 3) to develop and test a revised rainfall interception model incorporating both canopy and forest floor interception to represent the entire vertical profile of regulating interception dynamics.

Chapter 3 focuses on the transpiration component of the water balance in Equation 1 (see Figure 1-1). The goal of the research described in this Chapter was to analyze the initial transpiration response of a mature lodgepole pine forest to the early green-red attack phase of MPB attack by integrating the differential whole-tree water use responses of live, dying, and dead individuals in the stand. Specific research objectives included evaluating the effect of variable intensity MPB attack on: 1) changes in the canopy micrometeorology; 2) transpiration response of individual trees including surviving live, fading, and dying trees; 3) integrated these differential responses to estimate changes in total stand-scale transpiration; and lastly, 4) to model the effects on stand scale transpiration of a wider range of MPB disturbance scenarios in mature lodgepole pine forests.

Chapter 4 focuses on the overall soil moisture component of the water balance in Equation 1 (part of storage and/or drainage in the soil, see Figure 1-1). The purpose of Chapter 4 was to analyze the soil moisture response after a variable intensity MPB red attack and salvage logging in a mature lodgepole pine stand. The objectives of this study were to determine the impact of variable intensity MPB green and red attack along with and salvage logging on 1) differential soil moisture response in both shallow and increasingly depth soil profile layers and 2) to explore the variation in soil moisture responses throughout the growing season, and 3) explore how these are associated with spatial variation in soil moisture response to MPB attack.

Chapter 5 represents an integration of the relationships developed in the vertical water balance components of Chapters 2 (I_{ef}) and 3 (T_{st}) to provide insights into the likely stand or forest scale impacts of MPB attack in Alberta. The primary objectives of this study were: 1) to examine rainfall interception, transpiration, and drainage dynamics across a range of MPB attack intensities using historical precipitation regimes characteristic of the region supporting lodgepole pine forests in Alberta; and 2) to examine the interaction these components in regulating overall vertical water balance.

Chapter 6 represents a synthesis of results from these studies (i.e., Chapters 2 to 5) to highlight contributions of this work to the literature, discuss broader inferences than can be drawn from the work, and comment on directions for future work.

1.7. References

- Adams, H. D., C. H. Luce, et al. (2011). "Ecohydrological consequences of drought- and infestation- triggered tree die-off: insights and hypothesis." Ecohydrology **5**(2): 145-159.
- Allen, C. D. and D. D. Breshears (1998). "Drought-induced shift of a forest- woodland ecotone: Rapid landscape response to climate variation." Proceedings of the National Academy of Sciences of the United States of America **95**(25): 14839-14842.
- Allen, C. D., A. K. Macalady, et al. (2010). "A global overview of drought and heat- induced tree mortality reveals emerging climate change risks for forests." Forest Ecology and Management **259**(4): 660-684.
- Arno, S. F. (1980). "Forest fire history in the northern rockies." Journal Of Forestry **78**(8): 460-465.
- Backlund, P., D. Schimel, et al. (2008). The effects of climate change on agriculture, land resources, water resources, and biodiversity in the United States. U.S. Climate Change Science Program and the Subcommittee on Global Change Research. Washington, DC, U.S. Department of Agriculture: 362.
- Baird, A. J. and R. L. Wilby, Eds. (1999). Eco-hydrology: plants and water in terrestrial and aquatic environments. London, Routledge.
- Ballard, R. G., M. A. Walsh, et al. (1982). "Blue-stain fungi in xylem of lodgepole pine - a light-microscope study on extent of hyphal distribution." Canadian Journal of Botany-Revue Canadienne De Botanique **60**(11): 2334-2341.
- Ballard, R. G., M. A. Walsh, et al. (1984). "The penetration and growth of blue- stain fungi in the sapwood of lodgepole pine attacked by mountain pine- beetle." Canadian Journal of Botany-Revue Canadienne De Botanique **62**(8): 1724-1729.
- Bentz, B. J., J. A. Logan, et al. (2009). Bark Beetle Outbreaks in Western North America: Causes and Consequences. Salt Lake City, University of Utah Press.
- Bladon, K. D., U. Silins, et al. (2006). "Differential transpiration by three boreal tree species in response to increased evaporative demand after variable retention harvesting." Agricultural And Forest Meteorology **138**(1-4): 104-119.
- Boon, S. (2009). "Snow ablation energy balance in a dead forest stand." Hydrological Processes **23**(18): 2600-2610.
- Boon, S. (2012). "Snow accumulation following forest disturbance." Ecohydrology **5**(3): 279-285.
- Bormann, F. H. and G. Likens (1979). Pattern and process in a forested ecosystem. New York, USA, Springer-Verlag.
- Bosch, J. M. and J. D. Hewlett (1982). "A review of catchment experiments to determine the effect of vegetation changes on water yield and evapo- transpiration." Journal of Hydrology **55**(1-4): 3-23.
- Breshears, D. D., J. W. Nyhan, et al. (1998). "Effects of woody plants on microclimate in a semiarid woodland: Soil temperature and evaporation in canopy and intercanopy patches." International Journal of Plant

- Sciences **159**(6): 1010-1017.
- Brooks, K. N., P. F. Ffolliott, et al. (2003). Hydrology and the management of watersheds. USA, Iowa State Press.
- Brooks, P. D. and E. R. Vivoni (2008). "Mountain ecohydrology: quantifying the role of vegetation in the water balance of montane catchments." Ecohydrology **1**(3): 187-192.
- Burton, P. J. (2008). "The mountain pine beetle as an agent of forest disturbance: From Lessons Learned to Community-based Solutions Conference Proceedings." BC Journal of Ecosystems and Management **9**(3): 9-13.
- Carroll, A. L., J. Régnière, et al. (2006). Impacts of climate change on range expansion by the mountain pine beetle. Victoria, Natural Resources Canada, Canadian Forest Service, Pacific Forestry Centre: 20.
- Carroll, A. L., S. W. Taylor, et al. (2004). Effects of climate change on range expansion by the mountain pine beetle in British Columbia. Mountain Pine Beetle Symposium: challenges and solutions, Kelowna, B.C., Natural Resources Canada, Canadian Forest Service, Pacific Forestry Centre.
- Chen, F. and J. Dudhia (2001). "Coupling an advanced land surface-hydrology model with the Penn State-NCAR MM5 modeling system. Part I: Model implementation and sensitivity." Monthly Weather Review **129**(4): 569-585.
- Chojnacky, D. C., B. J. Bentz, et al. (2000). Mountain pine beetle attack in ponderosa pine: Comparing methods for rating susceptibility Research Paper. Fort Collins, U.S. Department of Agriculture, Forest Service, Rocky Mountain Research Station: 10 p.
- Christiansen, J. R., B. Elberling, et al. (2006). "Modelling water balance and nitrate leaching in temperate Norway spruce and beech forests located on the same soil type with the CoupModel." Forest Ecology and Management **237**(1-3): 545-556.
- D'Odorico, P., F. Laio, et al. (2010). "Ecohydrology of terrestrial ecosystems." Bioscience **60**(11): 898-907.
- Dawson, T. E. (1996). "Determining water use by trees and forests from isotopic, energy balance and transpiration analyses: The roles of tree size and hydraulic lift." Tree Physiology **16**(1-2): 263-272.
- Despain, D. G. (2001). "Dispersal ecology of lodgepole pine (*Pinus contorta* Dougl.) in its native environment as related to Swedish forestry." Forest Ecology and Management **141**: 59-68.
- Dubé, S. and J. Rex (2008). "Hydrologic effects of mountain pine beetle infestation and salvage-harvesting operations." B.C. Journal of Ecosystem Management **9**(3): 134.
- Ewers, B. E., D. S. Mackay, et al. (2002). "Tree species effects on stand transpiration in northern Wisconsin." Water Resources Research **38**(7).
- Fahey, T. and D. H. Knight (1986). "Lodgepole pine ecosystems." BioScience **36**(9): 610-617.
- Feddes, R. A., H. Hoff, et al. (2001). "Modeling root water uptake in hydrological and climate models." Bulletin of The American Meteorological Society **82**(12): 2797-2809.
- Fensham, R. J., R. J. Fairfax, et al. (2009). "Drought-induced tree death in savanna." Global Change Biology **15**(2): 380-387.

- Fensham, R. J. and J. E. Holman (1999). "Temporal and spatial patterns in drought-related tree dieback in Australian savanna." Journal of Applied Ecology **36**(6): 1035-1050.
- Ford, C. R., R. M. Hubbard, et al. (2007). "A comparison of sap flux-based evapotranspiration estimates with catchment-scale water balance." Agricultural and Forest Meteorology **145**(3-4): 176-185.
- Forgeard, F., J. C. Gloaguen, et al. (1980). "Interception of precipitations and mineral supply to the soil by rainfall and leaching in an Atlantic beech forest and in some coniferous stands in Brittany." Annales des Sciences Forestieres **37**(1): 53-71.
- Gebre, G. M., T. J. Tschaplinski, et al. (1998). "Water relations of several hardwood species in response to throughfall manipulation in an upland oak forest during a wet year." Tree Physiology **18**(5): 299-305.
- Gerrits, A. M. J., L. Pfister, et al. (2010). "Spatial and temporal variability of canopy and forest floor interception in a beech forest." Hydrological Processes **24**(21): 3011-3025.
- Gordon, L. and C. Folke (2000). "Ecohydrological landscape management for human well-being." Water International **25**(2): 178-184.
- Gray, L. K. and A. Hamann (2011). "Strategies for reforestation under uncertain future climates: guidelines for Alberta, Canada." PLoS ONE **6**(8): e22977.
- Grier, C. C. and S. W. Running (1977). "Leaf area of mature northwestern coniferous forests - relation to site water-balance." Ecology **58**(4): 893-899.
- Guevara-Escobar, A., E. Gonzalez-Sosa, et al. (2007). "Experimental analysis of drainage and water storage of litter layers." Hydrology and Earth System Sciences **11**(5): 1703-1716.
- Guswa, A. J. (2005). "Soil-moisture limits on plant uptake: an upscaled relationship for water-limited ecosystems " Advances in Water Resources(28): 543-552.
- Guswa, A. J., M. A. Celia, et al. (2002). "Models of soil moisture dynamics in ecohydrology: A comparative study." Water Resources Research **38**(9).
- Hélie, J. F., D. L. Peters, et al. (2005). Review and synthesis of potential hydrologic impacts of mountain pine beetle and related harvesting activities in British Columbia. Mountain Pine Beetle Initiative Working Paper. Victoria, Natural Resources Canada, Canadian Forest Service, Pacific Forestry Centre. **2005-23**: 34.
- Helvey, J. D. and J. H. Patric (1965). "Canopy and litter interception of rainfall by hardwoods of eastern United States." Water Resources Research **1**(2): 193-206.
- Ingram, H. A. P. (1987). "Ecohydrology of Scottish peatlands." Earth and Environmental Science Transactions of the Royal Society of Edinburgh **78**(04): 287-296.
- Jackson, S. T., J. L. Betancourt, et al. (2009). "Ecology and the ratchet of events: Climate variability, niche dimensions, and species distributions." Proceedings of the National Academy of Sciences of the United States of America **106**: 19685-19692.
- Johnson, R. C. (1990). "The interception, throughfall and stemflow in a forest in highland scotland and the comparison with other upland forests in the

- UK." Journal of Hydrology **118**(1-4): 281-287.
- Kaufmann, M. R. (1985). "Annual transpiration in subalpine forests: large differences among four tree species." Forest Ecology and Management **13**: 235-246.
- Klaassen, W., F. Bosveld, et al. (1998). "Water storage and evaporation as constituents of rainfall interception." Journal of Hydrology **213**(1-4): 36-50.
- Knight, D. H., T. Fahey, et al. (1981). "Transpiration from 100-yr-old Lodge Pole pine forests estimated with whole-tree potometers." Ecology **62**(3): 717-726.
- Knight, D. H., J. B. Yavitt, et al. (1991). "Water and nitrogen outflow from lodgepole pine forest after 2 levels of tree mortality." Forest Ecology and Management **46**(3-4): 215-225.
- Koch, P. (1996). Lodgepole Pine in North America. Madison, Forest Products Society.
- Kostner, B., E. Falge, et al. (2002). "Age-related effects on leaf area/sapwood area relationships, canopy transpiration and carbon gain of Norway spruce stands (*Picea abies*) in the Fichtelgebirge, Germany." Tree Physiology **22**(8): 567-574.
- Kurz, W. A., C. C. Dymond, et al. (2008). "Mountain pine beetle and forest carbon feedback to climate change." Nature **452**(7190): 987-990.
- Logan, J. A. and J. A. Powel (2001). "Ghost forests, global warming , and the mountain pine beetle (Coleoptera: Scolytidae)." American Entomologist **47**(3): 160-172.
- Mbogga, M. S., A. Hamann, et al. (2009). "Historical and projected climate data for natural resource management in western Canada." Agricultural and Forest Meteorology **149**(5): 881-890.
- McDowell, N. G., S. White, et al. (2008). "Transpiration and stomatal conductance across a steep climate gradient in the southern Rocky Mountains." Ecohydrology **1**: 193-204.
- McJannet, D., J. Wallace, et al. (2007). "Precipitation interception in Australian tropical rainforests: I. Measurement of stemflow, throughfall and cloud interception." Hydrological Processes **21**: 1692-1702.
- Navar, J. and R. Bryan (1990). "Interception loss and rainfall redistribution by 3 semiarid growing shrubs in northeastern Mexico." Journal of Hydrology **115**(1-4): 51-63.
- Nealis, V. G. and B. Peter (2008). Risk assessment of the threat of mountain pine beetle to Canada's boreal and eastern pine forests. Information Report Victoria, Natural Resources Canada, Canadian Forest Service, Pacific Forestry Centre. **BC-X-417**: 38.
- Neimann, K. O. and F. Visintini (2004). Assessment of potential for remote sensing detection of bark beetle-infested areas during a green attack: a literature review. Mountain Pine Beetle Initiative. Victoria, Natural Resources Canada, Canadian Forest Service.
- Oren, R., N. Phillips, et al. (1999). "Sap-flux-scaled transpiration responses to light, vapour pressure deficit, and leaf area reduction in a flooded *Taxodium distichum* forest." Tree Physiology **19**: 337-347.
- Overpeck, J. T. and J. E. Cole (2006). Abrupt change in Earth's climate system.

- Annual Review of Environment and Resources. **31**: 1-31.
- Phillips, N. and R. Oren (2001). "Intra- and inter-annual variation in transpiration of a pine forest." Ecological Applications **11**(2): 385-396.
- Pitman, J. I. (1989). "Rainfall interception by bracken in open habitats - relations between leaf-area, canopy storage and drainage rate." Journal of Hydrology **105**(3-4): 317-334.
- Porporato, A., E. Daly, et al. (2004). "Soil water balance and ecosystem response to climate change." The American Naturalist **164**(5).
- Redding, T. E., R. D. Winkler, et al. (2008). Mountain pine beetle and watershed hydrology: A synthesis focused on the Okanagan. One Watershed – One Water, Kelowna, BC, Canadian Water Resources Association.
- Reynolds, J. F. and D. H. Knight (1973). "The magnitude of snowmelt and rainfall interception by litter in lodgepole pine and spruce-fir forests in Wyoming." Northwest Science **47**(1): 50-60.
- Roberts, J. (1983). "Forest transpiration - a conservative hydrological process." Journal Of Hydrology **66**(1-4): 133-141.
- Robertson, C., T. A. Nelson, et al. (2007). "Mountain pine beetle dispersal: the spatial-temporal interaction of infestations." Forest Science **53**(3): 395-404.
- Rodríguez-Iturbe, I. (2000). "Ecohydrology: A hydrologic perspective of climate-soil-vegetation dynamics." Water Resources Reseach **36**(1): 3-9.
- Rodríguez-Iturbe, I. (2003). "Hydrologic dynamics and ecosystem structure." Water Science & Technology **47**(6): 17-24.
- Rodríguez-Iturbe, I., A. Porporato, et al. (2001). "Plants in water-controlled ecosystems: active role in hydrologic processes and response to water stress - I. Scope and general outline." Advances in Water Resources **24**(7): 695-705.
- Rodríguez-Iturbe, I., A. Porporato, et al. (1999). "Probabilistic modelling of water balance at a point: the role of climate, soil and vegetation." Proceedings of the Royal Society of London. Series A **455**: 3789-3805.
- Romme, W. H., D. H. Knight, et al. (1986). "Mountain pine beetle outbreaks in the Rocky Mountains: regulatory of primary productivity?" The American Naturalist **127**(4): 484-494.
- Rutter, A. J. (1966). "Studies on water relations of *Pinus sylvestris* in plantation conditions. 4. direct observations on rates of transpiration evaporation of intercepted water and evaporation from soil surface." Journal of Applied Ecology **3**(2): 393-&.
- Safranyik, L. (1978). Effects of climate and weather on mountain pine beetle populations. Symposium on theory and practice of mountain pine beetle management in lodgepole pine forests, University of Idaho, Moscow, Idaho, Washington State University, Pullman, Washington.
- Safranyik, L., A. L. Carroll, et al. (2010). "Potential for range expansion of mountain pine beetle into the boreal forest of North America." Canadian Entomologist **142**(5): 415-442.
- Schneider, R. R., M. C. Latham, et al. (2010). "Effects of a severe mountain pine beetle epidemic in western Alberta, Canada under two forest management scenarios." International Journal of Forestry Research(417595): 7.

- Schnorbus, M. (2011). A synthesis of the hydrological consequences of large-scale mountain pine beetle disturbance. Mountain Pine Beetle Working Paper 2010-01. Victoria, Natural Resources Canada, Canadian Forest Service, Pacific Forestry Centre: 30.
- Shachnovich, Y., P. R. Berliner, et al. (2008). "Rainfall interception and spatial distribution of throughfall in a pine forest planted in an arid zone." Journal of Hydrology **349**: 168-177.
- Shore, T. L., L. Safranyik, et al. (2006). Effects of the mountain pine beetle on lodgepole pine stand structure and dynamics. The mountain pine beetle: a synthesis of biology, management, and impacts on lodgepole pine. L. Safranyik and W. R. Wilson. Victoria, B.C., Natural Resources Canada, Canadian Forest Service, Pacific Forestry Centre: 95-114.
- Simonin, K., T. E. Kolb, et al. (2007). "The influence of thinning on components of stand water balance in a ponderosa pine forest stand during and after extreme drought " Agricultural and Forest Meteorology **143**: 266-276.
- Simunek, J., M. Sejna, et al. (1998). The Hydrus-ID software package for simulating the one-dimensional movement of water, heat, and multiple solutes in variably saturated media. I. G. W. M. Centre. Golden, CO. **Version 2.0, IGWMC-TPS-70**.
- Small, E. E. and J. R. McConnell (2008). "Comparison of soil moisture and meteorological controls on pine and spruce transpiration." Ecohydrology **1**: 205-214.
- Spittlehouse, D. L. (2007). Influence of the mountain pine beetle on the site water balance. Mountain Pine Beetle and Watershed Hydrology Workshop: Preliminary results of research from BC, Alberta, and Colorado, Kelowna, BC, FORREX, BC Ministry of Environment, Forest Service BC, Canadian Water Resources Association.
- Tanner, C. B. (1968). Evaporation of water from plants and soil. Water deficits and plant growth. T. Kozlowski. New York, Academic Press. **I**: 73-106.
- Taylor, S. W., A. L. Carrol, et al. (2006). Forest, climate and mountain pine beetle dynamics. The mountain pine beetle: A synthesis of its biology, management and impacts on lodgepole pine. L. Safranyik and W. B., Natural Resources Canada, Canadian Forest: 67-94.
- Troch, P. A., G. F. Martinez, et al. (2009). "Climate and vegetation water use efficiency at catchment scales." Hydrological Processes **23**(16): 2409-2414.
- Troendle, C. A. (1983). "The potential for water yield augmentation from forest management in the rocky-mountain region." Water Resources Bulletin **19**(3): 359-373.
- Uunila, L., B. Guy, et al. (2006). "Hydrologic effects of mountain pine beetle in the interior pine forests of British Columbia: key questions and current knowledge." Streamline **9**(2): 1-6.
- Verstraeten, W. W., B. Muys, et al. (2005). "Comparative analysis of the actual evapotranspiration of Flemish forest and cropland, using the soil water balance model WAVE." Hydrology and Earth System Sciences **9**: 225-241.
- Vertessy, R. A., T. J. Hatton, et al. (1996). "Long-term growth and water balance predictions for a mountain ash (*Eucalyptus regnans*) forest catchment subject to clear-felling and regeneration." Tree Physiology **16**(1-2): 221-

232.

- Whitehead, D. and P. G. Jarvis (1981). Coniferous forests and plantations. Water deficits and plant growth. T. Kozlowski. New York, USA: 49-152.
- Whitehead, D. and F. M. Kelliher (1991). "A canopy water-balance model for a pinus-radiata stand before and after thinning." Agricultural And Forest Meteorology **55**(1-2): 109-126.
- Wilcox, B. P. (2010). "Transformative ecosystem change and ecohydrology: ushering in a new era for watershed management." Ecohydrology **3**(1): 126-130.
- Winkler, R., S. Boon, et al. (2010). "Assessing the effects of post-pine beetle forest litter on snow albedo." Hydrological Processes **24**(6): 803-812.
- Wittwer, R. F., A. L. Leaf, et al. (1975). "Biomass and chemical composition of fertilized and-or irrigated *Pinus resinosa* ait plantations." Plant and Soil **42**(3): 629-651.
- Yavitt, J. B. and T. J. Fahey (1986). "Litter decay and leaching from the forest floor in *Pinus-contorta* (lodgepole pine) ecosystems." Journal of Ecology **74**(2): 525-545.
- Zalewski, M., G. A. Janauer, et al. (1997). Ecohydrology: a new paradigm for sustainable management of aquatic resources. UNESCO International Hydrological Programme. U. I. T. D. i. H. N. 7. Paris, UNESCO.
- Zeng, N., J. W. Shuttleworth, et al. (2000). "Influence of temporal variability of rainfall on interception loss. Part I. Point analysis." Journal of Hydrology **228**(3-4): 228-241.

1.8. Figures

Figure 1-1. Vertical water balance of a mature stand with a well-developed forest floor layer.

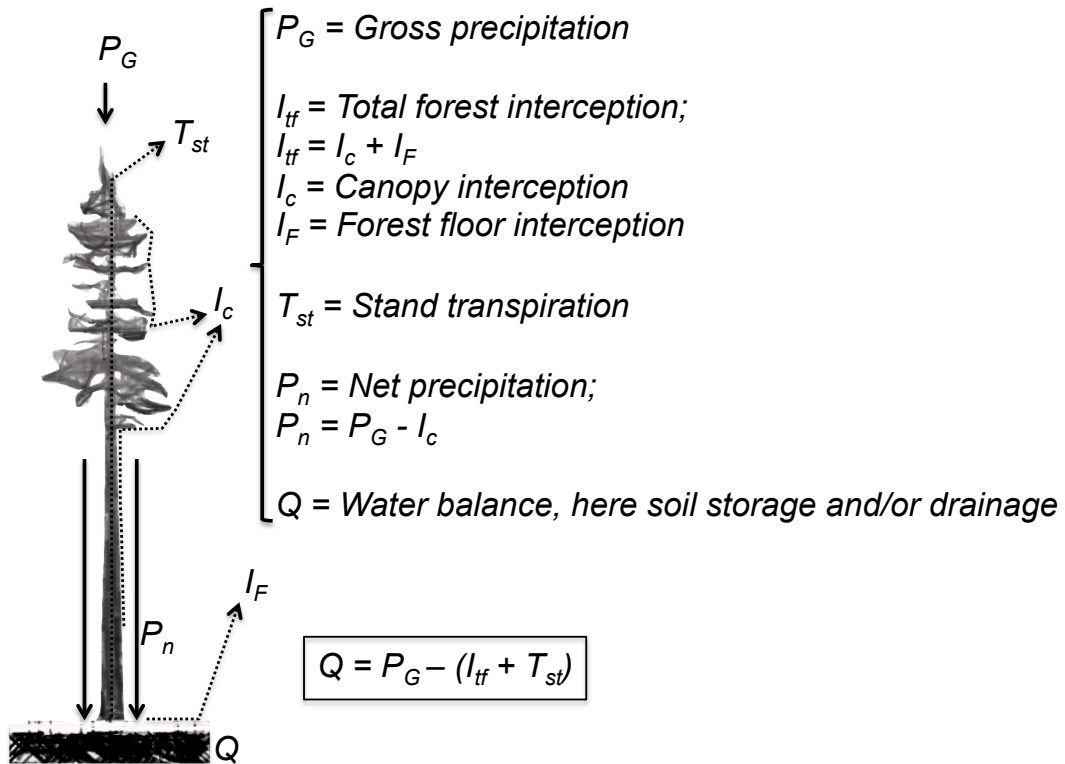
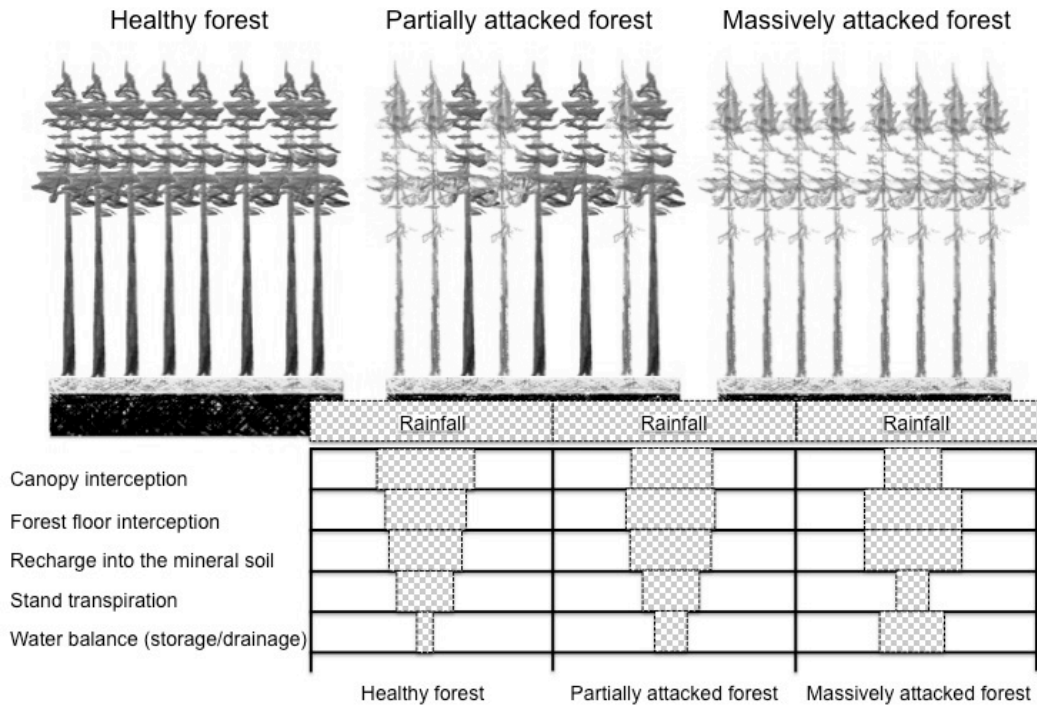


Figure 1-2. Vertical water balance components following a gradient of intensity of mountain pine beetle attack. The size of the rectangles correspond to the amount of water on each water balance component relative to the size of the “Rainfall” rectangle.



Chapter 2. VERTICAL ANALYSIS OF RAINFALL INTERCEPTION AND INITIAL EFFECTS OF MOUNTAIN PINE BEETLE ATTACK ON INTERCEPTION IN A MATURE LODGEPOLE PINE FOREST

2.1. Introduction

Lodgepole pine forests are an important component of western North American forests and play a key role regulating a range of ecological goods and services including water resources. However, despite previous research, the role of lodgepole pine as a key regulator of water balance in regions dominated by this type of forest is not yet available. A better understanding of hydro-ecological processes such as rain/snow interception, transpiration, and water storage dynamics is needed to enable a predicting how different types of forest disturbances are likely to affect water cycling in these forests across regions (Hélie et al., 2005; Uunila et al., 2006; Adams, 2011).

Interception of precipitation by forest vegetation and its subsequent evaporation back to the atmosphere, is one of the most conspicuous hydro-ecological processes in forests. However, research on interception is limited when compared to research on other components of evaporative loss in forests. Recent studies suggest that interception may represent a critical component regulating water cycling in many forests by potentially limiting recharge of soil moisture to only a fraction of total gross precipitation (Guevara-Escobar et al., 2007; Shachnovich et al., 2008; Gerrits et al., 2010). In addition, interception may also indirectly affect the functioning of forest ecosystems as a key regulator for soil moisture recharge into the mineral soil (Helvey and Patric, 1965; Reynolds and Knight, 1973; Forgeard et al., 1980; Pitman, 1989; Johnson, 1990; Navar and Bryan, 1990; Klaassen et al., 1998; Zeng et al., 2000; McJannet et al., 2007).

While both rain and snow interception are important components of total interception losses in northern temperate regions such as Alberta, rainfall interception is particularly essential to water cycling in Alberta's forests because 60-70% of total annual precipitation typically occurs as rain (Longley, 1972; Nkemdirim and Weber, 1976). Rainfall interception processes are governed by both aboveground and ground level components of forest structure. In conifer forests, rainfall intercepted by tree crowns, branches, and boles (canopy interception) can vary between 14% to 60%, depending upon the characteristics of the rainfall (i.e., number of rain events, distribution of storm sizes, and intensity), as well as the structure and composition of the forest (Dunne and Leopold, 1978; Forgeard et al., 1980; Anderson and Pyatt, 1986; Spittlehouse, 1998; Huber and Iroume, 2001; Samba et al., 2001; Holko et al., 2009; Gerrits et al., 2010). Previous research suggests strong similarity of rainfall interception losses in lodgepole pine across differing climatic regions. Wilm and Niederhof (1941) studied mature lodgepole pine stands in Colorado and found canopy rainfall interception losses of 31% of total annual rainfall. Similarly, Anderson and Pyatt (1986) reported an interception of 30% for young lodgepole pine stands in the U.K., while Brabender (2005) reported canopy interception losses of 27.4% in 30-year-old stands and 37% in 115-year-old stands in west-central Alberta. Moore et al. (2008) indicated that 30-40% of growing season rainfall

was lost as interception loss in a mature stand in the Canadian West Coast. While this previous research establishes rainfall interception as an important component of evaporative losses that regulate water balance in these forests, most of this research does not directly enable predicting changes in interception after disturbance. For example, most of these earlier works did not document stemflow, throughfall, or interception using some features of the stands that allow an adequate extrapolation to other regions (e.g., interception as a function of canopy or stand attributes).

An additional fraction of rainfall that penetrates through the canopy can also be intercepted by the ground level components of the forest, including ground vegetation and soil litter/duff. Forest floor interception is governed by the amount of material on the forest floor capable of intercepting and temporarily storing rainfall before it percolates into the mineral soil below the forest floor. Hence, the forest floor interception capacity is a function of the mass of litter on the ground and its drying rate (Putuhena and Cordery, 1996; Sato et al., 2004; Guevara-Escobar et al., 2007; Gerrits et al., 2010). Forest floor interception is not typically explored in forest rainfall interception studies (Schaap et al., 1997; Gerrits et al., 2007; Guevara-Escobar et al., 2007), yet, many authors argue that both forest floor and canopy interception should be considered equally important in overall forest evaporative losses (Mader and Lull, 1968; Walsh and Voight, 1977; Putuhena and Cordery, 1996; Schaap et al., 1997; DeLuca et al., 2002; O'Connell et al., 2003; Bond-Lamberty et al., 2011). Estimates of forest floor interception reported in the few studies on forest floor interception vary considerably among studies, making it difficult to generalize this process between broadleaved and coniferous litter types. For example, Kelliher et al. (1992) reported forest floor interception storage capacity for *Pinus radiata* slash of 0.7 mm, while Putuhena and Cordery (1996) reported 0.96 and 1.12 mm for coniferous and eucalyptus litter types. Sato et al. (2004) reported 0.27 to 3.05 mm for a range of coniferous and broadleaved litter types. However, no previous studies (to my knowledge) have reported on forest floor interception in lodgepole pine. Thus, presently there is very limited understanding of this critical element regulating rainfall interception dynamics. Consequently, there is limited understanding of overall interception processes in lodgepole pine forests.

Mountain pine beetle (MPB), *Dendroctonus ponderosae* Hopkins, is the most serious insect pest of pine in the mountain regions of western Canada and the United States. British Columbia and Alberta have recently experienced the worst outbreak of MPB ever reported (Robertson et al., 2007). The combination of warm winter temperatures and abundance of mature lodgepole pine stands has created optimal conditions for the development of outbreak MPB populations (Taylor et al., 2006). External (foliar) symptoms of trees attacked by MPB include crown foliar chlorosis (green attack) followed by death and retention of dead needles in the crown (red attack) for a period of 1-3 years (Chojnacky et al., 2000; Neiman and Vistintini, 2004). These dead needles are eventually shed during the final phase of the attack (grey attack). Because of the critical role of the forest canopy in regulating water cycling in pine forests, a growing body of

research has explored (mainly by modelling) the potential impact of MPB attack in western North American forests (e.g., Adams et al., 2011; Schnorbus, 2011). However, despite the particularly key ecohydrological role of rainfall interception, no studies (to my knowledge) have documented the impact of MPB on rainfall interception.

An additional area of interception research has focused on developing empirical and process-based models that help predict canopy-rainfall relations. Process-based models include numerical models such as the Rutter model (Rutter et al., 1971; 1975), and analytical approaches such as the Gash (1979) and Liu (1997) models. These models represent the major physical processes that govern rainfall interception dynamics, and conceptually enable prediction of rainfall interception across varied ecosystems (e.g., differing forest vegetation types and precipitation regimes). However, no studies (to my knowledge) have reported on either the parameters needed to apply these models, nor explored the suitability of various models in representing rainfall interception dynamics in lodgepole pine. Furthermore, only one study (to my knowledge) has explored the impact of measuring and subsequently modeling the combined effect of canopy and forest floor interception on total forest interception in a European hardwood forest (Gerrits et al., 2010). Model parameterization of rainfall interception may assist in estimating regional forest-atmosphere water balances (Valente et al., 1997; Liu, 2001) and in better-forecasting scenarios of climate change and its impact on forest water balance components such as forest rainfall interception and soil water availability (Wallace et al., 2006; Scott et al., 2005; Zimmermann et al., 2006).

The objectives of the present study were: 1) to characterize the major components of canopy interception and forest floor interception in mature lodgepole pine stands at risk from MPB attack; 2) to explore the early impact of MPB attack on these processes, and 3) to develop and test a revised rainfall interception model incorporating both canopy and forest floor interception to represent the entire vertical profile of regulating interception dynamics.

2.2. Materials and methods

2.2.1. Study site description

The present research was conducted in the upper montane forested region of west-central Alberta, Canada. The region is characterized by pure lodgepole pine (*Pinus contorta* Dougl.), along with mixed conifer stands that include white spruce (*Picea glauca* (Moench) Voss), balsam fir (*Abies balsamea* (L.) Mill.) and subalpine fir (*Abies lasiocarpa* (Hook.) Nutt. (Beckingham et al., 1996). The area experiences a temperate continental climate where mean daily maximum air temperatures during the growing season range from 16.2 °C in May to 20.6 °C in August. The precipitation in the area is usually controlled by cyclonic activity (Nkemdirim and Weber, 1976), although localized convective storms are also frequent from late May to July (Longley, 1972). Mean monthly precipitation from May to August ranges from 57.9 mm to 82.2 mm, and the mean annual

precipitation is 562.4 mm.

2.2.2. Site description and experimental design

This research was part of a larger study focused on examining changes in the forest water balance in response to a potential MPB attack in the foothills region of west-central Alberta, Canada. Study sites were part of a healthy, homogeneous lodgepole pine stand of old age classes (> 100 yrs. old). Tree height ranged from 20.2 to 23.5 m, basal area ranged from 32.8 to 54.9 m² ha⁻¹, and stem density ranged from 1044 to 1343 trees ha⁻¹. The understory was dominated by three dominant bryophyte species (*Pleurozium schreberi* (Brid.) Mitt., *Polytrichum commune* Hedw., and *Ptilium crista-castrensis* (Hedw.) De Not.). Mean depth of these mosses at the base of the trees was 16.8 cm (ranging from 16.3 cm to 17.6 cm) that decreased to 10.8 cm at a distance of 50 cm from the tree trunks. The forest floor layer consisted of 19% living vascular and non-vascular plant forms, 25% coarse material (e.g., needles, sticks, twigs, pine cones), and 56% fine material (i.e., fragmented material and humus).

The experimental design for this larger study employed a “before/after; control/impact” approach (BACI; Green, 1979; Stewart-Oaten et al., 1986, 1992). Three treatments were applied to four experimental units: control (untreated), two levels of simulated MPB attack (50% and 100% mortality), and a fourth experimental unit that was harvested to represent a salvage logged management treatment comparison. Individual tree application of glyphosate was used (“EZ-Ject” lance system, Herbicide System corp., MA, USA) to kill individual lodgepole pine trees as this type of treatment closely approximates the external morphological symptoms of post-MPB green-, red-, and grey-attack phases (i.e., foliar chlorosis followed by reddening of crowns and eventual needle cast as trees die). The experimental units were 2.2 ha in size and contained internal research plots surrounded by a 20 m treated buffer to minimize edge effects within interior portions of the experimental units where measurements were conducted. The pre-treatment period ran from May 2008 to mid-June 2009. At the completion of the pre-treatment measurement period, treatments were applied to all three experimental units in the last two weeks of June 2009.

Rainfall interception measurements took place in all four experimental units during three rainfall seasons from May through September during 2008-2010, except for the harvested unit in which measurements were discontinued once harvest operations began in July 2009 (Figure 2-1). Measurements and instrumentation deployment aimed to maximize capturing the range of variation (including a treatment response) of each variable, where the number of units employed to characterize each variable was mainly determined by the budget available to conduct the research.

2.2.3. Micrometeorological measurements

Climate stations were established approximately in the center of each of the four experimental units. Each station enabled measurements of air temperature,

relative humidity, and wind speed at two heights; mid-canopy (21 m) and above the understory (3 m, Table 2-1). Net radiation was measured near the top of the canopy (top of each climate station, Table 2-1). Radiation reaching the forest floor was estimated using four quantum sensors at 1 m height (Table 2-1). Net radiation was estimated from photo flux density using the relationship between net radiation in the control experimental unit and photon flux density in the nearby harvested site after harvesting in 2009 (linear regression, $R^2 = 0.86$). Air temperature/relative humidity (RH) and wind speed/direction were measured using electronic hydrometers and wind sensors at both heights at each climate station (Table 2-1). All variables were sampled every five seconds and averaged after 10 minutes using a datalogger (CR1000 system, Campbell Scientific, Inc., Utah, USA).

Gross precipitation P_G (mm) was measured in a nearby clear-cut 300-600 m from the study sites. Two types of precipitation gauges were used in a cluster to measure both total annual and summer storm rainfall precipitation (Table 2-1). A universal precipitation gauge was used to measure precipitation throughout the year, and three adjacent tipping bucket rain gauges were used to provide higher resolution for estimates of mean total precipitation for the rainfall events occurring each summer. Precipitation from each gauge was recorded using dataloggers (Hobo Event loggers and U12-008, Onset Computer Corporation) MA, USA).

2.2.4. Interception measurements

Canopy rainfall interception I_c (mm) was measured indirectly as the difference between P_G and the sum of rain falling to the ground without being intercepted by the canopy T_h (throughfall, mm) and rain reaching the ground via the trunks of the trees S_F (stemflow, mm) for each discrete rainfall event during the three study seasons. Similarly, forest floor interception I_F (mm) was estimated indirectly from net precipitation reaching the forest floor P_n (effectively used here as T_h) and recharge into the mineral soil F (mm) below the forest floor.

2.2.4.1. Throughfall

Throughfall was measured in each experimental unit using four trough gauges (Table 2-1), which were randomly re-located each summer. Each gauge consisted of two troughs (3 m long, 11.5 cm wide) both of which drained into a central plastic reservoir (16 L capacity). The reservoir regulated water flow through a tipping bucket rain gauge with data loggers (Hobo Event loggers, Onset Computer Corporation) to record the total water volume collected by both troughs during precipitation events. Plastic reservoirs were used to collect, slowly release, and accurately measure large volumes of water during high intensity events. This was necessary because high rainfall volumes produced by high intensity storms could not be reliably measured using the trough gauge – rain gauge system employed in this study.

2.2.4.2. Stemflow

Stemflow was measured using stemflow gauges installed on three randomly located trees within each of the four sites (Table 2-1). These trees were selected across a range of diameter at breast height (DBH) classes representative of canopy trees (dominant and co-dominant) in the four study units. The same trees were used each year to capture seasonal variation of stemflow across tree size classes. Stemflow gauges consisted of a spiral collar constructed from split vinyl tubing (15 mm diameter) of sufficient length to wrap around the circumference of each tree a minimum of 2 to 3 times. The spiral collars were sealed against the bark with silicone adhesive, and drained into a covered tipping bucket rain gauge / data logger unit (as above) to measure total stemflow volume during each precipitation event. Stemflow depth (mm) was calculated from stemflow volume after Price and Carlyle-Moses (2003) as:

$$S_F = S_F(L) * S_D \quad (1)$$

where S_F is stemflow on a unit-area basis (mm), $S_F(L)$ is the mean measured stemflow volume (L) from instrumented trees, and S_D is the stem density (# of trees m^{-2}). Mean stem density was measured from four fixed 8 m radius plots (one per site) that provided tree height, crown height, DBH and sapwood area (based on translucence of 2 perpendicular increment cores per tree) on a per ground area basis. Additionally, funnelling ratio F_r (dimensionless) for stemflow was calculated as in Herwitz (1986):

$$F_r = \frac{S_F(L)}{B * P_G} \quad (2)$$

where B is the trunk basal area (m^2). The funnelling ratio is the ratio of the precipitation delivered to the base of the tree to the rainfall that would have reached the ground in the absence of the tree. This ratio describes the efficiency of rainfall capture and funnelling to the ground; a funnelling ratio > 1 indicates more efficient water delivery to the ground than would be evident in the absence of the tree.

2.2.4.3. Recharge into the mineral soil

The recharge into the mineral soil below the forest floor was measured directly during the 2010 growing season in four 0.5 x 0.5 m forest-floor quadrats in the control unit only (Table 2-1, Figure 2-1). Each quadrat was lined with polyethylene plastic, which collected and routed water through a tipping bucket rain gauge installed into a soil pit excavated into the center of the quadrat to enable direct measurement of precipitation draining from the forest floor. A screened, sand filled funnel buried flush with the mineral soil surface was used to direct water through the tipping bucket rain gauge installed in the pit below. Drainage volume measured with the tipping bucket gauge was converted into depth (mm) based on the quadrat area (0.25 m^2). The forest floor interception quadrats were randomly located to capture a range of forest floor moss thicknesses (6 to 15 cm) characteristic of the stand.

2.2.5. Calculation of canopy, forest floor, and total forest interception

Canopy interception I_c , was estimated from gross precipitation P_G , throughfall T_h , and stemflow S_F , for each rainfall event as:

$$I_c = P_G - (T_h + S_F) \quad (3)$$

Similarly, interception by the forest floor I_F , was estimated from throughfall T_h , and recharge into the mineral soil F , for each rainfall event as:

$$I_F = T_h - F \quad (4)$$

Total forest interception I_{tf} (mm) was calculated using two approaches: firstly as the sum of estimated canopy and forest floor interception:

$$I_{tf} = I_c + I_F \quad (5)$$

and secondly, from gross precipitation P_G , and recharge into the mineral soil F , as:

$$I_{tf} = P_G - F \quad (6)$$

Total forest interception was calculated only for the 2010 season when data from both forest floor and canopy layers were available.

2.2.6. Forest floor water content

Seasonal forest floor water content F_d (mm) was measured to explore variation in moisture storage dynamics of the forest floor moss/duff. Forest floor water content was measured by removing and replacing intact 0.5 x 0.5 m areas of forest floor moss/duff layers over 0.5 x 0.5 m wire mesh quadrats framed by PVC pipe. Four quadrats were established in each site and weighed on a weekly basis during the summers of 2009 and 2010. All quadrats were destructively sampled at the end of each growing season to measure the dry mass that was needed to calculate the seasonal variation of forest floor water content for each quadrat. Water content (mm) was calculated by dividing the volumetric water content by the quadrat area (0.25 m²).

In a separate experiment, the maximum water holding capacity F_{max} (mm) of the forest floor moss/duff layer was determined in the summer of 2009 in four quadrats in the control unit that were shielded from the rain (covered with a 1 m² tarp) to produce a standardized condition of moisture status governed only by drainage and evaporative processes. These four quadrats were saturated with a watering can until no subsequent change in weight was observed, and then allowed to drain freely until a stable weight was again recorded (F_{max}). The moisture content was then determined one week later to establish a standardized moisture content $F_{d std}$, that reflected only local evaporative

conditions over one week, and the water retention characteristics of the forest floor at each quadrat. This experiment was repeated seven times during the 2009 season. The mean forest floor storage capacity S_{Fl} (mm) was then determined as the mean difference between F_{max} and $F_{d\ std}$ for all four quadrats over the seven repeated watering experiments. As with F_d , all quadrats were destructively sampled at the end of each growing season to measure the dry mass that was needed to calculate the water content in mm, by dividing the volumetric water content (excluding the dry mass) by the quadrat area. Additionally, a forest floor storage opportunity F_{op} (mm) was calculated by subtracting the F_d values (unshielded plots) from the F_{max} .

2.2.7. Modeling rainfall interception

Rainfall interception measurements along with the tree, stand, and forest floor descriptors were used to develop and evaluate an analytical model for the canopy and forest floor layers. This involved parameterizing and combining the canopy interception model by Carlyle-Moses and Price (2007) modified from Liu (1997) with a similar formulation adapted and parameterized herein to model forest floor interception. The dual layer analytical model developed or adapted here consisted of canopy and forest floor interception sub-models implemented in series to model total forest interception dynamics.

2.2.7.1. Canopy interception sub-model

Liu (1997) developed an analytical model for canopy rainfall interception I_c , for single-storms, where the canopy was assumed to be completely dry before each rain event:

$$I_c = C_m \left[1 - \exp \left(- \frac{(1-p)}{C_m} P_G \right) \right] \left[1 - \frac{E_c}{(1-p)R} \right] + \frac{E_c}{R} P_G \quad (7)$$

where C_m is the stand storage capacity (mm), which conceptually includes both canopy S , and trunk S_T , storage capacities. However, no techniques for parameterization of this term were developed (Liu 1997). Carlyle-Moses and Price (2007) modified this model by explicitly re-defining C_m as an explicit stand storage capacity term C_{mc} , for a canopy with gaps S_c , and trunks S_T , where $C_{mc} = S_c + S_T$ and $S_c = S/c$. The threshold event size of 4 mm over no longer than 24 hr identified by Valente et al. (1997) was used to parameterise S . S was calculated as the absolute value of the negative intercept of the forced envelope line between P_G and T_h divided by $1-pd$; where the coefficient pd (dimensionless) represented the drainage partitioning coefficient after Valente et al. (1997). S was then scaled by cover fraction (c or $1-p$) as $S_c = S/c$. p is the free throughfall coefficient or canopy openness, which represents the proportion of throughfall that reaches the forest floor by passing directly through the canopy. p is often estimated as $p = 1 - c$ (Valente et al., 1997). The factor p was determined by averaging twelve hemispherical photographs taken across three sites (excluding a harvested experimental unit) at a height of 60 cm above ground. Photographs were taken with a Nikon Coolpix 4500 equipped with a Nikon Fisheye Converter

FC-E8 0.21x converter and analyzed using the software Gap Light Analyzer (GLA) (Frazer et al., 1999), with an azimuth of 36 and 20 zenith regions after Park and Cameron (2008). p was calculated as the percentage of the total open sky pixels to total pixels within the zenith regions between 0° -directly overhead- to 45° (11 regions in total).

Trunk storage S_T , was estimated after Carlyle-Moses et al., (2010), by solving the volumetric canopy water balance for the a rainfall event representing the maximum funnelling ratio for the stand:

$$S_T = P_{gFc} - T_{hd} - S_c - EL_c - SF_c \quad (8)$$

where P_{gFc} is the rainfall depth that corresponds to the maximum funnelling ratio derived for the stand or tree of interest, T_{hd} represents the amount of T_h that drains from the canopy ($T_{hd} = T_h \times c$), EL_c is the evaporative loss [$(E/R) \times P_{gFc}$], and SF_c represents the stemflow. All of these individual tree parameters were expressed in units of volume and then converted to an equivalent depth (mm) based on the area of the tree crowns after Carlyle-Moses et al., (2010). A one-sided projected leaf area (A_L m²) was used as a proxy for crown area. Crown leaf area was determined by destructive sampling of the crowns of eight trees collected from an adjacent plot off-site to avoid destructive sampling within the research area. The eight sampled trees crowns were divided into top, middle, and bottom sections, and collected along with sub-sample of 150 needles for each section. Samples and sub-samples were dried (70 °C until weight stabilized) and weighed. Projected leaf area of sub-samples was measured using image analysis software (WinFolia, Regent Instruments Inc.) to calculate specific leaf area (S_{LA} , m² g⁻¹). A_L was calculated as the product of S_{LA} and total leaf dry weight (g) for each tree. The sapwood area at breast height was measured on the same eight trees by cutting a small section of the stem (cookie). Samples were dried (54 °C for three days), sanded and dyed using bromocresol green stain at 0.0413% (Kutscha and Irving, 1962). Sapwood area was quantified with the Sigma Scan software (Aspire Software International Com.). The leaf area of these eight trees was used to develop a linear relationship (linear regression, $R^2 = 0.76$) between sapwood area at breast height and crown leaf area that was then used to estimate A_L of trees within the study sites. The sapwood area of trees in the experimental units was estimated from the length of sapwood determined visually by distinguishing the natural changes in wood color (Simonin et al., 2007) and assuming a circular bole cross-section.

E_c (i.e., E^*c) and R represent the mean evaporative and rainfall rate respectively. Mean rainfall intensity R (mm) was estimated as the average intensity of rainfall events larger than 4 mm (events potentially able to saturate the canopy) and with a duration less than 24 hr. Micrometeorological data were used to calculate evaporation rate for both canopy and understory layers based on the Penman-Monteith equation (Monteith, 1964) for rainfall conditions with canopy resistance set to zero, and following the momentum method for estimation of aerodynamic resistance as in Whitehead and Kelliher (1991):

$$E = \frac{\Delta R_n + \rho c_p D g_a}{\lambda(\Delta + \gamma)} \quad (9)$$

where Δ is the slope of saturated vapour pressure as a function of temperature ($\text{KPa } ^\circ\text{C}^{-1}$), R_n the net radiation (W m^{-2}), ρ the density of dry air (Kg m^{-3}), c_p the specific heat of air ($\text{J g}^{-1} \text{K}^{-1}$), D the vapour pressure deficit (Kpa), g_a the aerodynamic conductance as conductance for momentum transfer between a height z and a reference plane (m S^{-1}), λ the latent heat of vaporization of water (Mj Kg^{-1}), and γ the psychrometric constant ($\text{Kpa } ^\circ\text{C}^{-1}$). g_a was calculated as in Jones (1992) for canopy boundary layer conductance for momentum:

$$g_a = \frac{k^2 u_z}{\{\ln[(z-d)/z_0]\}^2} \quad (10)$$

where k is the von Karman's constant (dimensionless), u_z the wind speed (m s^{-1}), z (m) the height of the sensor, d the zero plane displacement (m), and z_0 the roughness length for momentum (m).

2.2.7.2. Forest floor interception sub-model

The model used in canopy interception was modified to predict forest floor interception I_F . Modification included replacement of C_{mc} with forest floor storage capacity S_{Fl} (mm) and the representation of the forest floor as a continuous layer analogous to full canopy cover fraction and zero canopy openness ($c=1, p=0$):

$$I_F = S_{Fl} \left[1 - \exp\left(-\frac{1}{S_{Fl}} P_n\right) \right] \left[1 - \frac{E_F}{R_{net}} \right] + \frac{E_F}{R_{net}} P_n \quad (11)$$

where E_F is the evaporative demand in the forest floor, P_n represents net precipitation ($P_n = T_h$), and R_{net} is the mean rate of net precipitation. Net precipitation was calculated from the same subset of P_G events used to calculate R . Stemflow was excluded from P_n and R_{net} calculations because: a) funnelling ratios in the stand were consistently less than 1; and, b) the quadrats that measured recharge into the mineral soil did not contain trees contributing to the stemflow. S_{Fl} was determined from the forest floor watering experiment conducted in 2009 as the mean difference between $F_{d\text{std}}$ before and after each watering test (see section 2.2.6.).

2.2.7.3. Forest interception model

The canopy and forest floor interception sub-models were linked in series to model total forest interception I_{tf} , in four sequential steps: 1) gross precipitation triggered canopy interception I_c ; 2) canopy interception triggered net precipitation to the forest floor; 3) net precipitation triggered forest floor interception I_F ; and, 4) forest floor interception triggered recharge into the mineral soil below the forest floor. The combined output of both canopy and forest floor layer interception sub-models represented the estimate for modeled

total forest interception I_{tf} . Because stemflow was not included in the forest floor sub-model, S_F was calculated as the residual of $P_G - (I_{tf} + F)$.

2.2.7.4. Model validation

Model parameters were verified against values found in the literature for forest under similar conditions. It was assumed that the model validation through RMSE, sensitivity and regression analysis encompassed a sufficient degree of independence. While the process of validation involved model parameters (e.g., rainfall rate and canopy storage capacity) that were derived from the measurements of interception, the vast majority of the model structure was derived from independent datasets.

Performance analysis of the analytical model, as a means of model validation, was done using the Root Mean Square Error (*RMSE*) (Mayer and Butler, 1993):

$$RMSE = \sqrt{\frac{\sum_{i=1}^n (I_i - I_{p,i})^2}{n}} \quad (12)$$

where I_i and $I_{p,i}$ are the measured and predicted interception of the i_{th} rain event in a dataset, and n is the number of pairs in that data set. Linear regressions between modeled and observed values were also used to assess the model variables with log transformed values in order to meet the assumption of normality in the residuals.

The sensitivity of the model to errors in parameters c , C_{mc} , E and R was assessed using the following sensitivity index (Liu, 2001):

$$Sensitivity = \frac{\frac{(I_c - I_b)}{I_b}}{\frac{(par_c - par_b)}{par_b}} * 100 \quad (13)$$

where I_b is the predicted interception using the base value (par_b) of a specific parameter, and I_c is the predicted interception based on a different value of the same parameter (par_c , change in c magnitude). The sensitivity analysis was done for both the canopy and forest floor interception, and the change in magnitude c of the parameters was increased by 30% (i.e., $par_c = 1.3 par_b$) as in Liu (2001).

2.2.8. Statistical analysis

Two approaches were used for analysis of results. Because the early effect of MPB attack simulated using herbicide produced no detectable influence on rainfall interception processes in either the 50% or 100% MPB treatments (section 2.3.2) rainfall interception measurements from all four treatment units (with the exception of the harvested treatment after harvesting) were used to examine precipitation-interception dynamics characteristic of mature lodgepole pine. Because of the widely spaced distribution of individual throughfall troughs, stemflow gauges, forest floor moisture measurement plots, and soil moisture

recharge gauges (Figure 2-1), spatial variation in canopy condition and actual precipitation across these measurement locations was assumed to be sufficient to permit treating these measurement plots as replicates or independent observations of the interception dynamics (interaction among precipitation and canopy controls over these processes) for each discrete rainfall event.

Throughfall measured for each rainfall event was averaged for all 16 trough gauges (4 treatment units x 4 gauges) in 2008 and 2009 (up to the beginning of the harvest), while 12 gauges were used for the latter half of 2009 and 2010 (measurements discontinued in the harvested treatment). Similarly, mean stemflow for each discrete rainfall event was averaged across the 12 gauges prior to the harvest in 2009 and 9 gauges after the harvest. Forest floor moisture plots were averaged for each measurement period using 16 and 12 plots, before and after harvesting. Relationships between precipitation and funnelling ratios were tested using linear regression and Kruskal-Wallis rank sum tests ($\alpha = 0.05$), while differences in funnelling ratios between DBH classes were tested using 95% confidence intervals from box plots. Where shown, box plot widths are proportional to the square root of the number of observations in groups, and notches extend to ± 1.58 interquartile/square root (n), which indicates 95% confidence interval for the difference in two medians.

The effect of MPB treatments on canopy interception were tested using a BACI approach to compare linear regressions between interception in the control unit with the 50% and 100% treatment units before and after application of the treatments. Because treatments were applied mid-summer in 2009, the effect of the treatments was evaluated using interception measurements in 2010 (full post-treatment season) compared to observations in 2008 (full pre-treatment season). Student's t test of equality of two population regression coefficients (Zar, 1999) was used to test differences in slopes and intercepts among regressions. All numerical analysis were performed using R version 2.15.1 (R Core Team, 2012).

2.3. Results

2.3.1. Rainfall interception dynamics

Mean gross precipitation P_G (mm) from May to August was 353 mm and was generally similar across the three years of the study (318-397 mm, Table 2-2). Growing season P_G in the area generally comprised approximately 65% of total annual precipitation. Over the 3 seasons, 149 individual P_G events were observed ranging from 0.016-70 mm per event. While the vast majority of the individual P_G events (93%) were less than 12 mm (Figure 2-2), the less frequent storms (greater than 12 mm) accounted for half (48, 53, and 52% for 2008, 2009, and 2010 respectively) of the total growing season P_G (Figure 2-2).

The relative proportion of all interception components (throughfall, stemflow, both canopy and forest floor interception, and recharge into the mineral soil) as a fraction of precipitation was strongly related to the magnitude of individual

rainfall events. For smaller rain events ($< 3\text{ mm}$) T_h represented a smaller fraction (34%) of P_G while a larger fraction ($> 56\%$) of P_G was observed as T_h for larger rainfall events $> 12\text{ mm}$. Mean growing season T_h for the three years of the study was 188 mm ranging from 169-221 mm which represented 51- 56% of the P_G across the three seasons (Table 2-2)

Stemflow accounted for a very small portion of P_G , and despite some variation in P_G , mean annual S_F was only 2mm each of the three seasons (0.5-0.6% of seasonal P_G , Table 2-2). This represented a mean S_F volume of approximately 18 L/tree per season. Mean trunk storage capacity of trees instrumented with stemflow gauges was 5.22 mm (Table 2-3). This corresponded to the strong variability in stemflow across rainfall event sizes, where generally no measureable S_F was observed for rainfall events $< 5\text{ mm}$, whereas stemflow increases proportionally with rainfall for events $> 5\text{ mm}$. This was consistent with the observation that funnelling ratios were generally very low (below 0.1) for rainfall events $< 6\text{-}8\text{ mm}$ in magnitude. However, while highly variable among individual trees, funnelling ratio increased substantially for larger event sizes ($> 10\text{ mm}$, Figure 2-3 A). Funnelling ratios did not exceed 0.75 even for some of the larger rainfall events (25mm, Figure 2-3 A). Funnelling ratios were also strongly variable among tree size classes. The increase in funnelling ratio with storm magnitude was greatest in the smallest DBH classes ($p < 0.05$), and this pattern of greater funnelling ratio in smaller trees (15-19 cm DBH) was also strongly evident in variation in median funnelling ratio across the full range of rainfall event magnitudes observed during 2008-2010 (Figure 2-3 B).

Mean canopy interception I_c , across three years was 162 mm (146-173 mm), representing a mean interception loss of 46% (44-48%) of P_G (Table 2-2). During the 2010 season when both canopy and forest floor interception components were measured, I_F accounted for 74 mm, which represented an additional interception loss of 22% of P_G (Table 2-2). Both I_c and I_F were strongly related to the magnitude of individual rainfall events. A weakly non-linear relationship between I_c and precipitation, and a non-linear (quasi-asymptotic) relationship between I_F and P_n were evident (Figures 2-4 A and B). Canopy interception storage capacity was 10.6 mm (Table 2-3, see 2.2.7.1). I_c as a fraction of P_G was very high (close to 90%) for small rainfall events ($< 3\text{ mm}$) and decreased strongly as event size increased to $< 25\%$ for larger rainfall events ($> 25\text{ mm}$). A similar pattern was evident for I_F as a fraction of P_n , however, this fraction showed a strong decline but for smaller P_G events (18 mm) than evident for I_c . In 2010, total seasonal rainfall interception was 240 mm, which represented 70% of P_G (Table 2-2). I_{tf} obtained with Equation 6 was 66% of P_G , indicating a difference of 4% between estimates for I_{tf} using Equation 5. As with I_c and I_F , total forest interception was strongly related (non-linearly) to the magnitude of P_G events (Figure 2-4 C), where total forest interception as a fraction of P_G decreased from 90% of small rainfall events to approximately 35% of large events.

In 2010 when all of these vertical interception components were measured, the fraction of precipitation that represented net recharge into the mineral soil (i.e.,

not lost through interception) was 118 mm (34% of total P_G ; Table 2-2). As with I_c , I_f , and I_{tf} , the proportion of P_G observed as F was also strongly related to the magnitude of rainfall events (data not shown). For rain events smaller than 5 mm, F represented less than 10% of P_G (less than 60% of net precipitation); whereas for events larger than 10 mm, > 50% of P_G (80% of net precipitation) was observed as F .

The water content of the forest floor F_d , was highly variable within each season (2009-2010) but mean F_d was only marginally greater during the somewhat wetter 2010 season (11.5 and 12.8 mm in 2009 and 2010, respectively; Figure 2-5). Mean F_d over these two seasons was 11.8 mm, with a maximum and minimum of 17.8 and 6.3 mm respectively. In contrast, the mean maximum forest floor water holding capacity F_{max} , determined from the watering experiment was 18.7 mm (16.3-24 mm). This corresponded with a mean storage capacity for the forest floor S_{Fl} , of 5.6 mm (Table 2-3). While variation in F_d was positively associated with the timing and magnitude of precipitation events over the two seasons, F_d did not reach F_{max} at any time during 2009-2010 (Figure 2-5). The storage opportunity of the forest floor was inversely associated with variation in F_d for 2009 and 2010, when forest floor storage opportunities were 7.24 mm and 6.57 mm, respectively.

The total combined forest rainfall interception storage capacity of both C_{mc} (15.8 mm) and S_{Fl} (5.6 mm) was 21.4 mm for this lodgepole pine stand (Table 2-3).

2.3.2. Early effect of MPB attack on rainfall interception

Herbicide treatments to simulate the effects of MPB attack (hereafter referred to 50% and 100 % mortality treatments) were successful in producing signs of foliar chlorosis consistent with the green and early red attack phases of MPB attack. Herbicide treated trees in the 50% and 100% mortality units showed no initial signs of foliar chlorosis from date of application through to the late fall of 2009. Some initial foliar chlorosis became apparent on a fraction of herbicide treated trees by the spring of 2010. Many of these trees were beginning to develop signs of transition from chlorotic to reddening crowns consistent with the transition from green attack to red attack by late fall of 2010. However, the crowns of many treated trees also remained green through the 2010 growing season. No indication of needle cast was observed on any of the trees showing reddening by late fall of 2010. Thus, by the end of the 2010 growing season, the treatments produced canopy conditions approximating the red attack.

Throughfall, stemflow, and canopy interception were all marginally greater in each of the control, 50% and 100 % mortality units in 2008 (prior to the application of the herbicide treatments) than was observed during the full post-treatment season in 2010 (Table 2-4). However, 2008 received 397 mm of rainfall while only 344 mm (87%) was observed in 2010. Comparison of pre- and post-treatment regressions between I_c in the control unit and 50% MPB treatment across a range of precipitation event sizes indicated no difference in either slopes ($p=0.21$) or intercepts ($p=0.56$) of these relationships were

evident (Figure 2-5). Similarly, no difference in the slopes ($p=0.71$) or intercepts ($p=0.50$) of pre- versus post-treatment relationships for I_c were evident for the 100% MPB treatment. Thus there was no detectable effect of red attack conditions on any of the components that govern canopy interception in either of the two MPB treatments.

2.3.3. Modeled interception

The revised dual-layer interception model predicted the non-linear relationships of I_c and I_F that very closely paralleled field observations for these components in 2008-2010 (I_c) and 2010 (I_F) (Figures 2-4 A and B). Model performance was assessed by comparing predicted I_c and I_F to field measured values for these components (linear regression) across a range of event sizes (Figure 2-7). Canopy interception was predicted with both high accuracy (close to a 1:1 relationships for predicted versus observed; Figure 2-7 A) and precision ($R^2=0.92$ and $RMSE=0.73$; Table 2-5); whereas both the accuracy (Figure 2-7 B) and precision of modeled I_F were weaker ($R^2=0.67$, $RMSE=0.131$, Table 2-5). While the model over-estimated I_F for a fraction of the larger rainfall event sizes, this over-estimation for larger rainfall events was not consistent across rainfall events; the majority of the predicted values closely approximated observed I_F (i.e., close to a 1:1 relationship). Despite some moderate differences in accuracy and precision of modeled I_c and I_F , the modeled estimates for I_{tf} properly represented the measured relationship between I_{tf} and P_G events (Figure 2-4 C) showing the same non-linear relationship between these variables. Variation in predicted I_{tf} as a fraction of P_G indicated that the relationship became asymptotic at $P_G \approx 35\%$, suggesting no further change in I_{tf} for P_G events larger than 40 mm.

All model parameters were sensitive to variation in magnitude of P_G events. A 30% increase in c , C_{mc} and E increased I_c , whereas R decreased I_c . The sensitivity in all parameters increased as magnitude of P_G increased, with the exception of c . The canopy interception sub-model (I_c) was most sensitive to variation in c , and less sensitive to variation in C_{mc} and R , suggesting that I_c in the model is most influenced by changes in canopy structure (particularly for small rain events). A 30% increase in parameter values for the forest floor layer submodel (I_F) showed no clear response in terms of interception relationships with P_G , except for the forest floor storage capacity. As with the canopy sub-model, sensitivity in all parameters governing P_G and I_F relationships increased as P_G size increased, except for S_{Fl} which produced an initial increase in I_F followed by a slight decrease for $P_G > 25$ mm. The submodel for I_F was most sensitive to variation in S_{Fl} .

The complete series of all interception components measured in 2010 enabled examining the correspondence of cumulative interception components for both measured and modeled interception (Figure 2-8 A and B). The precipitation period governed by rain began in mid-May (Julian day 133) and spanned approximately 103 days. A very similar temporal pattern in cumulative interception or recharge response to P_G events was evident between measured and modeled interception. While I_{tf} and F were most similar between measured

and modeled interception, the model underestimated I_c and overestimated I_F (which in turn led to an underestimation of F). The additive effect of these errors was most clearly evident in accumulated interception or recharge at the end of the season. The modeling of individual responses to rain events was mainly affected by large rain events. However, the cumulative response of the model adequately summarized the measured series of rainfall interception (Figure 2-8, Table 2-6).

Despite these smaller individual errors, the dual layer model permitted the prediction all the interception components (including those that were not measured in the field) over the three seasons of the study (Table 2-7). Variation in total seasonal predicted T_h , S_F , and I_c was very similar to the measured seasonal interception components (Table 2-2). Furthermore, the model enabled the exploration of annual variation in predicted forest floor interception I_F , total forest interception I_{tf} , and recharge into mineral soil F , for the three seasons. Consistent with annual variation in other measured interception components, modeled I_{tf} and F were positively associated with variation in P_G across these seasons (Table 2-7).

While minor deviation of predicted from observed interception components for individual events was evident, the total seasonal interception components as a fraction of P_G were all less than 10% (Table 2-6). Over the three seasons, mean T_h and S_F were overestimated by 6.2 and 0.3% respectively, while I_c was underestimated by 6.5%. These general patterns were consistent over the three years of the study. In 2010, under-estimation of I_c (and subsequent over-estimation 6.1%) of I_F produced balancing errors that resulted in a very minor over-estimation of total forest interception of 3 mm (0.9%; Table 2-7).

2.4. Discussion

2.4.1. Canopy interception

Canopy interception was the dominant component of rainfall interception (Table 2-2) with annual variability in I_c as a fraction of P_G ranging from 44 to 48% through the three seasons of the study. Canopy interception observed in this study was generally higher than what other researchers have reported for lodgepole pine across a broad range of stand conditions. Both Wilm and Niederhof (1941) and Anderson and Pyatt (1986) found I_c to be 30-31% of P_G in both mature lodgepole pine stands in Colorado, and young lodgepole pines stands in the U.K. (respectively), while Moore et al. (2008) observed 30-40% canopy rainfall interception in a mature stand in the Canadian West Coast. Brabender (2005) reported I_c was sensitive to variation in age and stand structure in west central Alberta where I_c varied from 27.4% in 30 year old stands to 37% for 115 year old stands. The greater fractional I_c observed in this study compared to that reported elsewhere might be associated with the fact that the period of years when the study was conducted was relatively dry, as the long-term records for the area indicate (mean annual total rainfall of 420.4 mm, 1971-2000; Environment Canada, 2011). However, while these previous studies

show general similarity, I_c as a fraction of P_G variation in rainfall interception is ultimately driven by the distribution of rain events in relation to canopy storage capacity within years. Thus, while drier seasons generally exhibit greater I_c as a fraction of total seasonal rainfall than wetter seasons, a consistent fraction of rainfall interception losses among seasons or regions cannot be expected. Nonetheless, the range of I_c as a fraction of P_G in the area could be as wide as 35-44%, based on a simulation done by applying the model developed for I_c over historical records in the area on a Julian day basis (data not shown).

Unfortunately, while many of these studies in lodgepole pine interception report on measured I_c , only Brabender (2005) reported canopy storage capacities that would support broad generalizations about interception processes in lodgepole pine forests. Furthermore, relatively few previous studies have reported all of the components of canopy rainfall interception such as throughfall and stemflow which makes comparisons with previous research difficult. In the present study both canopy and trunk storage capacities, as integrated aboveground components of I_c (i.e., branches, needles and trunks), were the main sources of interception loss in the forest canopy (Tables 2-2 and 2-3). Furthermore, the effects of canopy storage seem to extend beyond the reported estimates of their respective storage capacities. For example, while mean trunk interception storage capacity was 5.2 mm (Table 2-3), however the generally low funnelling ratios observed in this study (which did not approach 0.75 even for rainfall events larger than 25 mm) suggest that trunk storage likely has a meaningful effect on canopy interception even for very large events (> 25 mm Figure 2-3). Moreover, the low range of values for funnelling ratios (Figure 2-3) and the tendency of these ratios to rise with an increase in P_G (Figure 2-3 A) support Carlyle-Moses' and Prices' (2006) suggestion of analysing the trunks' storage capacity by using Herwitzs' (1986) funnelling ratio concept. Because funnelling ratio describes the efficiency of rainfall capture and funnelling to the ground by the trees, the concept helps to clarify the link between evaporative losses from trunks and moisture recharge into the mineral soil via preferential flow *versus* simply that of net precipitation and trunk storage capacity. This supports viewing stemflow as a point-scale water flux (e.g., Crabtree and Trudgill, 1985; Taniguchi et al., 1996) without having to scale stemflow into a depth (mm) in order to relate it to P_G or T_h . Carlyle-Moses and Price (2006) demonstrated that typical methods employed to analyze stemflow (e.g., Valente et al., 1997) tend to greatly underestimate the values of rain required to satisfy the storage capacity of trunks and canopy.

2.4.2. Forest floor interception

The forest floor interception is only rarely explored as a component in forest rainfall interception research (Schaap et al., 1997; Gerrits et al., 2007; Guevara-Escobar, et al., 2007). Moreover, no previous studies have documented forest floor interception in lodgepole pine forests (to my knowledge). Nevertheless, the variation in forest floor water content along with a high maximum forest floor water holding capacity and forest floor storage opportunity (Figure 2-5) indicates that forest floor interception and the subsequent evaporative loss

represent approximately 1/3 of the total forest interception loss. Additionally, the variation in forest floor water and high forest floor storage opportunity suggest that forest floor interception should be considered a highly significant component in total forest evaporative loss, also as indicated in other studies conducted in different forest environments (Mader and Lull, 1968; Walsh and Voight, 1977; Putuhena and Cordery, 1996; Schaap et al., 1997; DeLuca et al., 2002; O'Connell et al., 2003; Bond-Lamberty et al., 2011). While forest floor storage capacity observed in this study was similar to that reported by Guevara-Escobar et al. (2007) for poplar leaves and fresh grass (0.4 to 0.7 mm), and *Pinus radiata* slash (0.7 mm, Kelliher et al. 1992), these are generally lower than those reported for most forest floor litter types. For example, Putuhena and Cordery (1996) observed 0.96 and 1.12 mm for coniferous and eucalyptus litter types, while Marin et al. (2000) reported 1.5 mm storage after drainage for Amazonian rainforest litter, Sato et al. (2004) found S_{Fl} in the range of 0.27-3.05 mm for coniferous and broadleaved litter types, and 1.63 mm was reported by Pitman (1989) for bracken litter. The discrepancies likely reflect variation in forest floor litter depth, litter type, and different methodological approaches to simulate rainfall (Guevara-Escobar et al., 2007).

The seasonal monitoring of F_d in this study showed that only infrequent rain events (extremely intense or very long) might potentially saturate the forest floor layer (F_{max}) and overwhelm forest floor storage (Figure 2-5). Mean F_d was ~ 12.1 mm, which corresponds to a mean seasonal storage opportunity of 6.6 mm. The slight discrepancy between F_{op} and S_{Fl} (1 mm difference), along with the fact that F_{max} was never observed during two seasons of forest floor water content monitoring, suggests that the water status in the forest floor has a clear potential to exceed its mean seasonal conditions. Mean seasonal water conditions in the forest floor are strongly dependant on the characteristics of net precipitation, which is primarily conditioned by the canopy and trunk rainfall storage capacities. The later suggest that the canopy layer exerts a strong control over the forest floor's water status, idea also supported by the notion that the water input-outputs in bryophytes (the dominant plants in the forest floor) are controlled by canopy structural properties (Proctor, 1980; Zotz et al., 2000; Rice and Schneider, 2004) as opposed to vascular plants that have leaf stomata regulating water fluxes.

2.4.3. Total forest interception

The relative contribution of total seasonal interception to P_G was strongly regulated by the distribution rain event magnitudes. Sites characterized by a cyclonic storm regime tend to have frequent small rain events, which in turn increases the seasonal contribution of interception loss. In this study, more than half of the rain reaching the forest was lost as I_{tf} (Figure 2-8, Table 2-2). These high values for I_{tf} indicate that rainfall interception not only plays a critical role in evaporative loss, but also in controlling the soil moisture recharge in lodgepole pine forests. Given the very high I_{tf} observed in this study, characterizing rainfall interception dynamics is critical for both understanding the water cycle and the potential impact of a broad range of forest disturbances

that affect hydrology of lodgepole pine forests.

2.4.4. Early effect of MPB attack (red attack) on canopy interception

While the effects of MPB on water cycling and hydrology in lodgepole pine forests are driven by tree mortality since it regulates evaporative losses (interception and transpiration), very few studies have explored these effects. Boon (2009, 2011) and Winkler et al. (2010) described the effects of MPB on snow interception and ablation losses; however no studies (to my knowledge) have documented impacts of MPB on rainfall interception processes.

Along the gradient of impacts on pine canopies from MPB attack, needles are typically retained during the green- and red-attack phases then are shed during the latter grey attack phase. However, because no previous studies have documented any of these changes on rainfall interception, changes to rainfall interception dynamics along this gradient have been uncertain. No detectable effect of green- or red-attack on canopy interception or any of the components regulating interception dynamics were observed in this study. While this is likely consistent with expectations based on needle retention during this phase, subtle changes in needle morphology could have influenced water storage in tree crowns after rainfall events.

2.4.5. Modeled interception

Model estimates of interception on an annual basis indicated minor discrepancies with the measurements (Table 2-6). The main discrepancy in modeled interception was in the forest floor component, with an estimated I_F ~14% more than what was measured. The performance analysis indicated that the canopy layer was the best represented of the two sub-models (Table 2-6, Figures 2-4 A and 2-7 A) and the combination of the two model layers as I_{tf} adequately predicted the field measured rainfall interception (Figures 2-4 C and 2-8). Discrepancies between simulated and observed season-long or annual interception are likely a consequence of the approach used to estimate E , since several studies have shown that E estimated from relationships of P_G with P_n is usually higher than E derived using the Penman-Montieth equation (Carlyle-Moses and Gash, 2011). Advection originating from within the forest and especially from a relatively warm-dry immediate landscape characterized by a large proportion of clearcuts might be the source of energy responsible for potential enhancement of E (Carlyle-Moses and Gash, 2011).

No previous studies (to my knowledge) have parameterized or modeled rainfall interception processes in lodgepole pine forests. Moreover, results of this study clearly illustrate the importance of including forest floor interception in efforts to model forest rainfall interception. The vast majority of rainfall interception modeling studies across a wide range of forest environments characterize overall forest interception losses using only the canopy interception component (e.g., Carlyle-Moses et al., 2010; Carlyle-Moses and Price, 2007; Gash, 1979; Gash et al., 1995; Hall, 2003; Herbst et al., 2006; Liu, 1997; Rutter et al., 1971; Rutter

et al., 1972; Valente et al., 1997; Wallace and McJannet, 2006). However, the dual-layer (canopy and forest floor) forest interception model developed herein represents a meaningful advance in modeling forest interception losses. If total rainfall interception in this study had been approximated using only I_c as has typically been done by others, mean seasonal interception over the three years of study would have been underestimated by 109 mm / yr (44%).

2.5. Conclusions

Given both the broad importance of lodgepole pine and the impacts of MPB attack affecting these forests in western North America, information on rainfall interception dynamics is a key component of understanding water balance and hydrology of these western forests. As no previous studies have documented all of the components regulating rainfall interception losses in lodgepole pine, the results of this study constitute an important contribution to understanding the vertical dynamics of rainfall interception processes in lodgepole pine.

Previous research on rainfall interception dynamics in other forest types has usually neglected the role of the forest floor layer and focused primarily on the canopy layer. The present research highlights the importance of analyzing the process of rainfall interception as a dual layer. In the aboveground components regulating rainfall interception processes, the analysis of stemflow/funnelling ratios permitted to: 1) highlight trunk storage capacity as an important element in the interception loss; and, 2) assess the magnitude of funnelling ratios as a function of P_G in order to properly link rainfall interception with moisture recharge into the mineral soil. These relationships, in turn, allowed the identification of the particular importance of the forest floor layer to the regulation of net precipitation and forest recharge.

Assessing the impact of MPB on interception and evaporative processes has been described as one of the key information gaps in understanding the impact of the current western North American MPB epidemic on hydrology of lodgepole pine forests (Hélie et al., 2005). The present study represents the first work (to my knowledge) that examines the impacts of MPB on rainfall interception. It showed that during the green and initial red phases of MPB attack, there was no evident change in canopy rainfall interception, though much larger effects on interception during the latter grey attack phase would be expected.

The dual-layer analytical interception model developed in this study effectively predicted values of interception components that are comparable with their values measured in the field. Hence, the model and parameters used represent an accurate baseline to encourage further analysis of rainfall interception in lodgepole pine forests. Unlike most hydrological models, process-based modeling for interception is transferrable among forest types and other vegetation cover. Specifically, the present research may enable better forecasts of the impact of climate change and other types of forest disturbances (e.g., wildfire, MPB, harvesting, etc.) on water cycling and hydrology of lodgepole pine forests.

2.6. References

- Adams, H. D., C. H. Luce, et al. (2011). "Ecohydrological consequences of drought- and infestation- triggered tree die-off: insights and hypothesis." Ecohydrology **5**(2): 145-159.
- Anderson, A. R. and D. G. Pyatt (1986). "Interception of precipitation by pole-stage sitka spruce and lodgepole pine and mature sitka spruce at kielder forest, Northumberland." Forestry **59**(1): 29-38.
- Beckingham, J. D., J. H. Archibald, et al. (1996). Field guide to ecosites of west-central Alberta. Edmonton, Northern Forestry Centre.
- Bond-Lamberty, B., S. T. Gower, et al. (2011). "Measurement and modelling of bryophyte evaporation in a boreal forest chronosequence." Ecohydrology **4**(1): 26-35.
- Boon, S. (2009). "Snow ablation energy balance in a dead forest stand." Hydrological Processes **23**(18): 2600-2610.
- Brabender, B. (2005). Scaling Leaf Area Index and rainfall interception in lodgepole pine. Renewable Resources. Edmonton, University of Alberta. **Master of Science: 91**.
- Burles, K. and S. Boon (2011). "Snowmelt energy balance in a burned forest plot, Crowsnest Pass, Alberta, Canada." Hydrological Processes **25**(19): 3012-3029.
- Carlyle-Moses, D. E. (2007). Measurement and modelling of mountain pine beetle impacts on annual forest water balance. Final Report, Ministry of Forests and Range: 26.
- Carlyle-Moses, D. E. and J. H. C. Gash (2011). Rainfall interception loss by forest canopies. Forest hydrology and biogeochemistry: Synthesis of past research and future directions. D. F. Levia, D. CarlyleMoses and T. Tanaka. New York, Springer. **216**: 407-423.
- Carlyle-Moses, D. E., A. D. Park, et al. (2010). "Modelling rainfall interception loss in forest restoration trials in Panama." Ecohydrology **3**(3): 272-283.
- Carlyle-Moses, D. E. and A. G. Price (2006). "Growing-season stemflow production within a deciduous forest of southern Ontario." Hydrological Processes **20**(17): 3651-3663.
- Chojnacky, D. C., B. J. Bentz, et al. (2000). Mountain pine beetle attack in ponderosa pine: Comparing methods for rating susceptibility Research Paper. Fort Collins, U.S. Department of Agriculture, Forest Service, Rocky Mountain Research Station: 10 p.
- Crabtree, R. W. and S. T. Trudgill (1985). "Hillslope hydrochemistry and stream response on a wooded, permeable bedrock - the role of stemflow." Journal Of Hydrology **80**(1-2): 161-178.
- DeLuca, T. H., O. Zackrisson, et al. (2002). "Quantifying nitrogen-fixation in feather moss carpets of boreal forests." Nature **419**(6910): 917-920.
- Dunne, T. and L. B. Leopold (1978). Water in environmental planning. San Francisco, W.H. Freeman.
- Forgeard, F., J. C. Gloaguen, et al. (1980). "Interception of precipitations and mineral supply to the soil by rainfall and leaching in an Atlantic beech forest and in some coniferous stands in Brittany." Annales des Sciences Forestieres **37**(1): 53-71.

- Frazer, G. W., C. D. Canham, et al. (1999). GAP light analyzer (GLA). Burnaby, Simon Fraser University. The Institute of Ecosystem Studies.
- Gash, J. H. C. (1979). "Analytical model of rainfall interception by forests." Quarterly Journal Of The Royal Meteorological Society **105**(443): 43-55.
- Gash, J. H. C., C. R. Lloyd, et al. (1995). "Estimating sparse forest rainfall interception with an analytical model." Journal of Hydrology **170**(1-4): 79-86.
- Gerrits, A. M. J., L. Pfister, et al. (2010). "Spatial and temporal variability of canopy and forest floor interception in a beech forest." Hydrological Processes **24**(21): 3011-3025.
- Gerrits, A. M. J., H. H. G. Savenije, et al. (2007). "New technique to measure forest floor interception - an application in a beech forest in Luxembourg." Hydrology And Earth System Sciences **11**(2): 695-701.
- Green, R. H. (1979). Sampling design and statistical methods for environmental biologists. New York, Wiley.
- Guevara-Escobar, A., E. Gonzalez-Sosa, et al. (2007). "Experimental analysis of drainage and water storage of litter layers." Hydrology and Earth System Sciences **11**(5): 1703-1716.
- Hall, R. L. (2003). "Interception loss as a function of rainfall and forest types: stochastic modelling for tropical canopies revisited." Journal Of Hydrology **280**(1-4): 1-12.
- Hélie, J. F., D. L. Peters, et al. (2005). Review and synthesis of potential hydrologic impacts of mountain pine beetle and related harvesting activities in British Columbia. Mountain Pine Beetle Initiative Working Paper. Victoria, Natural Resources Canada, Canadian Forest Service, Pacific Forestry Centre. **2005-23**: 34.
- Helvey, J. D. and J. H. Patric (1965). "Canopy and litter interception of rainfall by hardwoods of eastern United States." Water Resources Research **1**(2): 193-206.
- Herbst, M., J. M. Roberts, et al. (2006). "Measuring and modelling the rainfall interception loss by hedgerows in southern England." Agricultural and forest meteorology **141**: 244-256.
- Herwitz, S. R. (1986). "Infiltration-Excess Caused By Stemflow In A Cyclone-Prone Tropical Rain-Forest." Earth Surface Processes and Landforms **11**(4): 401-412.
- Holko, L., J. Skvarenina, et al. (2009). "Impact of spruce forest on rainfall interception and seasonal snow cover evolution in the Western Tatra Mountains, Slovakia." Biologia **64**(3): 594-599.
- Huber, A. and A. Iroume (2001). "Variability of annual rainfall partitioning for different sites and forest covers in Chile." Journal Of Hydrology **248**(1-4): 78-92.
- Johnson, R. C. (1990). "The interception, throughfall and stemflow in a forest in highland scotland and the comparison with other upland forests in the UK." Journal of Hydrology **118**(1-4): 281-287.
- Jones, H. G. (1992). Plants and microclimate: a quantitative approach to environmental plant physiology. UK, Cambridge University Press.

- Kelliher, F. M., D. Whitehead, et al. (1992). "Rainfall Interception By Trees And Slash In A Young Pinus-Radiata D Don Stand." Journal of Hydrology **131**(1-4): 187-204.
- Klaassen, W., F. Bosveld, et al. (1998). "Water storage and evaporation as constituents of rainfall interception." Journal of Hydrology **213**(1-4): 36-50.
- Liu, S. G. (1997). "A new model for the prediction of rainfall interception in forest canopies." Ecological Modelling **99**(2-3): 151-159.
- Liu, S. G. (2001). "Evaluation of the Liu model for predicting rainfall interception in forests world-wide." Hydrological Processes **15**(12): 2341-2360.
- Longley, L. W. (1972). Precipitation in the canadian praires. Atmospheric Environment Service. Toronto, Canadian Department of the Environment.
- Mader, H. W. and H. W. Lull (1968). Depth, weight, and water storage of the forest floor in white pine stands in Massachusetts. Research Paper. Upper Darby, US Department of Agriculture.
- Marin, C. T., I. W. Bouten, et al. (2000). "Forest floor water dynamics and root water uptake in four forest ecosystems in northwest Amazonia." Journal of Hydrology **237**(3-4): 169-183.
- Mayer, D. G. and D. G. Butler (1993). "Statistical validation." Ecological Modelling **68**(1-2): 21-32.
- McJannet, D., J. Wallace, et al. (2007). "Precipitation interception in Australian tropical rainforests: I. Measurement of stemflow, throughfall and cloud interception." Hydrological Processes **21**: 1692-1702.
- Monteith, J. L. (1964). Evaporation and environment The state and movement of water in living organisms, Swansea, Symposia of the Society for Experimental Biology.
- Moore, R. D., R. D. Winkler, et al. (2008). "Watershed response to the mclure forest fire: Presentation summaries from the fishtrap creek workshop, March 2008." Streamline **12**(1).
- Navar, J. and R. Bryan (1990). "Interception loss and rainfall redistribution by 3 semiarid growing shrubs in northeastern Mexico." Journal of Hydrology **115**(1-4): 51-63.
- Neimann, K. O. and F. Visintini (2004). Assessment of potential for remote sensing detection of bark beetle-infested areas during a green attack: a literature review. Mountain Pine Beetle Initiative. Victoria, Natural Resources Canada, Canadian Forest Service.
- Nkemdirim, L. C. and L. Weber (1976). "Wet and dry sequences in precipitation regimes." Geografiska Annaler Series a-Physical Geography **58**(4): 303-315.
- O'Connell, K. E. B., S. T. Gower, et al. (2003). "Comparison of net primary production and light-use dynamics of two boreal black spruce forest communities." Ecosystems **6**(3): 236-247.
- Park, A. and J. L. Cameron (2008). "The influence of canopy traits on throughfall and stemflow in five tropical trees growing in a Panamanian plantation." Forest Ecology and Management **255**(5-6): 1915-1925.

- Pitman, J. I. (1989). "Rainfall interception by bracken in open habitats - relations between leaf-area, canopy storage and drainage rate." Journal of Hydrology **105**(3-4): 317-334.
- Price, A. G. and D. E. Carlyle-Moses (2003). "Measurement and modelling of growing-season canopy water fluxes in a mature mixed deciduous forest stand, southern Ontario, Canada." Agricultural and Forest Meteorology **119**(1-2): 69-85.
- Proctor, M. C. F. (1980). Diffusion resistance in bryophytes. Plants and their atmospheric environment. J. Grace, E. D. Ford and P. G. Jarvis. Oxford, Blackwell Scientific: 219-229.
- Putuhen, W. M. and I. Cordery (1996). "Estimation of interception capacity of the forest floor." Journal of Hydrology **180**: 283-299.
- R Core Team (2012). R: A language and environment for statistical computing. Vienna, R Foundation for Statistical Computing.
- Reynolds, J. F. and D. H. Knight (1973). "The magnitude of snowmelt and rainfall interception by litter in lodgepole pine and spruce-fir forests in Wyoming." Northwest Science **47**(1): 50-60.
- Rice, S. K. and N. Schneider (2004). "Cushion size, surface roughness and the control of water balance and carbon flux in the cushion moss *Leucobryum glaucum* (Leucobryaceae)." American Journal of Botany **91**(8): 1164-1172.
- Robertson, C., T. A. Nelson, et al. (2007). "Mountain pine beetle dispersal: the spatial-temporal interaction of infestations." Forest Science **53**(3): 395-404.
- Rutter, A. J., K. A. Kershaw, et al. (1971). "A predictive model of rainfall interception on forests. I. Derivation of the model from observations in a plantation of Corsican pine." Agricultural Meteorology **9**: 367-384.
- Rutter, A. J., A. J. Morton, et al. (1975). "A predictive model of rainfall interception in forests. II. Generalization of the model and comparison with observations in some coniferous and hardwood stands." Journal of Applied Ecology **12**: 367-386.
- Rutter, A. J., P. C. Robins, et al. (1972). "Predictive model of rainfall interception in forests, .1. derivation of model from observations in a plantation of corsican pine." Agricultural Meteorology **9**(5-6): 367-384.
- Samba, S. A. N., C. Camire, et al. (2001). "Allometry and rainfall interception of *Cordyla pinnata* in a semi-arid agroforestry parkland, Senegal." Forest Ecology And Management **154**(1-2): 277-288.
- Sato, Y., T. Kumagai, et al. (2004). "Experimental analysis of moisture dynamics of litter layers - the effects of rainfall conditions and leaf shapes." Hydrological Processes **18**(16): 3007-3018.
- Schaap, M. G., W. Bouten, et al. (1997). "Forest floor water content dynamics in a Douglas fir stand." Journal of Hydrology **201**(1-4): 367-383.
- Schnorbus, M. (2011). A synthesis of the hydrological consequences of large-scale mountain pine beetle disturbance. Mountain Pine Beetle Working Paper 2010-01. Victoria, Natural Resources Canada, Canadian Forest Service, Pacific Forestry Centre: 30.

- Scott, D. F., L. A. Bruijnzeel, et al. (2005). The hydrological and soil impact of forestation in the tropics. Forests, water and People in the humid tropics: past, present and future hydrological research for integrated land and water management. M. Bonnell and L. A. Bruijnzeel. Cambridge, UK, Cambridge University Press, UNESCO: 622-651.
- Shachnovich, Y., P. R. Berliner, et al. (2008). "Rainfall interception and spatial distribution of throughfall in a pine forest planted in an arid zone." Journal of Hydrology **349**: 168-177.
- Simonin, K., T. E. Kolb, et al. (2007). "The influence of thinning on components of stand water balance in a ponderosa pine forest stand during and after extreme drought " Agricultural and Forest Meteorology **143**: 266-276.
- Spittlehouse, D. L. (1998). Rainfall interception in young and mature conifer forest in British Columbia. Conference on Agricultural and Forest Meteorology, Albuquerque, N.M., USA, American Meteorological Society.
- Stewart-Oaten, A., J. R. Bence, et al. (1992). "Assessing effects of unreplicated perturbations: no simple solutions." Ecology **73**(4): 1396-1404.
- Stewart-Oaten, A., W. W. Murdoch, et al. (1986). "Environmental-impact assessment - pseudoreplication in time." Ecology **67**(4): 929-940.
- Taniguchi, M., M. Tsujimura, et al. (1996). "Significance of stemflow in groundwater recharge .1. Evaluation of the stemflow contribution to recharge using a mass balance approach." Hydrological Processes **10**(1): 71-80.
- Taylor, S. W., A. L. Carrol, et al. (2006). Forest, climate and mountain pine beetle dynamics. The mountain pine beetle: A synthesis of its biology, management and impacts on lodgepole pine. L. Safranyik and W. B., Natural Resources Canada, Canadian Forest: 67-94.
- Uunila, L., B. Guy, et al. (2006). "Hydrologic effects of mountain pine beetle in the interior pine forests of British Columbia: key questions and current knowledge." Streamline **9**(2): 1-6.
- Valente, F., J. S. David, et al. (1997). "Modelling interception loss for two sparse eucalypt and pine forests in central Portugal using reformulated Rutter and Gash analytical models." Journal of Hydrology **190**(1-2): 141-162.
- Wallace, J. and D. McJannet (2006). "On interception modelling of a lowland coastal rainforest in northern Queensland, Australia." Journal of Hydrology **329**(3-4): 477-488.
- Walsh, R. P. D. and P. J. Voight (1977). "Vegetation litter: an underestimated variable in hydrology and geomorphology." Journal of Biogeography **4**: 253-274.
- Whitehead, D. and F. M. Kelliher (1991). "A canopy water-balance model for a pinus-radiata stand before and after thinning." Agricultural And Forest Meteorology **55**(1-2): 109-126.
- Wilm, H. G. and C. H. Niederhof (1941). "Interception of rainfall by mature lodgepole pine." Transactions-American Geophysical Union **22**: 660-665.
- Winkler, R., S. Boon, et al. (2010). "Assessing the effects of post-pine beetle forest litter on snow albedo." Hydrological Processes **24**(6): 803-812.
- Zar, J. (1999). Biostatistical analysis. Upper Saddle River, Prentice Hall.

- Zeng, N., J. W. Shuttleworth, et al. (2000). "Influence of temporal variability of rainfall on interception loss. Part I. Point analysis." Journal of Hydrology **228**(3-4): 228-241.
- Zimmermann, B., H. Elsenbeer, et al. (2006). "The influence of land-use changes on soil hydraulic properties: Implications for runoff generation." Forest Ecology and Management **222**(1-3): 29-38.
- Zotz, G., A. Schweikert, et al. (2000). "Water relations and carbon gain are closely related to cushion size in the moss *Grimmia pulvinata*." New Phytologist **148**(1): 59-67.

2.7. Tables

Table 2-1. Meteorological instrumentation used in this study. The quantity refers to the number of instruments deployed per treatment unit.

Variable	Instrument	Quantity	Height (m)	Location
Air temperature and relative humidity	HMP50 hygrometer (Campbell Scientific, Utah, USA)	1	21 & 3	Climate station / each treatment unit
Net radiation	NR-LITE net radiometer (Kipp & Zonen, Netherlands)	1	21	Climate station / each treatment unit
	GaAsP quantum sensor (Pontaller, 1990)	4	1	Climate station / each treatment unit
Precipitation	Alter shielded universal precipitation gauge (Belfort Instruments Company, MD, USA)	1	1.5	Nearby clearcut
	Tipping bucket rain gauges (Davis Instruments Corporation, CA, USA)	3	1	Nearby clearcut
Stemflow	Spiral collar with tipping bucket rain gauge	3	1.5	Each treatment unit
Throughfall	Trough gauges draining through reservoir and tipping bucket rain gauge	4	1	Each treatment unit
Recharge into the mineral soil	Lined forest floor quadrat draining through buried tipping bucket rain gauge	4	0.60 below ground	Control treatment unit only

Table 2-2. Total seasonal gross precipitation (P_G), throughfall (T_h), stemflow (S_F), canopy interception (I_c), forest floor interception (I_F), total forest interception (I_{tf}), and recharge into mineral soil (F). Values in brackets indicate percentage of gross precipitation.

Year	P_G	T_h	S_F	I_c	I_F	I_{tf}	F	# rain events
2008	397	221 (56%)	2 (0.5%)	173 (44%)	-	-	-	40
2009	318	170 (53%)	2 (0.6%)	146 (46%)	-	-	-	58
2010	344	175 (51%)	2 (0.6%)	166 (48%)	74 (22%)	240 (70%)	118 (34%)	51
Mean	352	188	2	161				52

Note that the sum of $I_{tf} + F$ does not equal P_G in 2010 as these components were measured independently.

Table 2-3. Components of tree, forest floor and meteorological parameters. Parameters are: canopy cover fraction (c), mean rainfall and net precipitation rate (R, R_n), mean canopy per unit area and forest floor evaporation rate (E_c, E_F), canopy (with gaps) and forest floor storage capacity (S_c, S_{Fl}), trunk storage capacity (S_T), storage capacity of the stand and forest floor (C_{mc}, S_{Fl}), and drainage partitioning coefficient (pd).

Parameter	Canopy	Forest floor
c	0.48	NA
R, R_n (mm hr-1)	1.06	0.53
E_c, E_F (mm hr-1)	0.08	0.0086
S_c, S_{Fl} (mm)	10.60	5.6
S_T (mm)	5.22	NA
C_{mc}, S_{Fl} (mm)	15.83	5.6
pd	0.03	NA

Table 2-4. Seasonal total gross precipitation (P_G), throughfall (T_h), stemflow (S_F), and canopy interception (I_c) of control, 50-, and 100% mortality treatment units before (2008) and after (2010) treatment application. Values in brackets indicate percentage of gross precipitation.

Year	P_G	Treatment	T_h	S_F	I_c
2008	397	Control	223 (56%)	1.3 (0.3%)	172 (43%)
		50% MPB	217 (55%)	1.4 (0.3%)	178 (45%)
		100% MPB	213 (54%)	1.1 (0.2%)	183 (46%)
2010	344	Control	182 (53%)	1.09 (0.3%)	160 (47%)
		50% MPB	170(49%)	3.3 (0.9%)	170 (49%)
		100% MPB	171 (50%)	8.3 (2.4%)	165 (48%)

Table 2-5. Rainfall interception model performance: Root Mean Square Error (*RMSE*) and linear regression coefficients.

Statistic	Canopy	Forest floor
<i>RMSE</i>	0.73	1.31
R ²	0.92	0.67

Table 2-6. Differences (Δ) between measured and predicted (measured - predicted) throughfall (ΔT_h), stemflow (ΔS_F), canopy interception (ΔI_c), forest floor interception (ΔI_F), total forest interception (ΔI_{tf}), and recharge into mineral soil (ΔF). Negative and positive values denote over-, and underestimation compared to measured values, respectively. Values in brackets indicate percentage of gross precipitation.

Year	ΔT_h	ΔS_F	ΔI_c	ΔI_F	ΔI_{tf}	ΔF
	-16	-1	17			
2008	(4.0 %)	(0.3 %)	(4.3 %)			
	-20	-1	21			
2009	(6.3 %)	(0.3 %)	(6.6 %)			
	-29	-1	29	-33	-3	21
2010	(8.4 %)	(0.3 %)	(8.4 %)	(9.6 %)	(0.9 %)	(6.1 %)
	-22	-1	22			
Mean	(6.2 %)	(0.3 %)	(6.5 %)			

Table 2-7. Total seasonal gross precipitation (P_G), and predicted (modeled) components of rainfall interception; throughfall (T_h), stemflow (S_F), canopy interception (I_c), forest floor interception (I_F), total forest interception (I_{tf}), and recharge into mineral soil (F). Values in brackets indicate percentage of gross precipitation.

Year	P_G	T_h	S_F	I_c	I_F	I_{tf}	F
2008	397	237 (60%)	3 (0.8%)	156 (39%)	122 (31%)	279 (70%)	115 (29%)
2009	318	190 (60%)	3 (0.9%)	125 (40%)	97 (30%)	222 (70%)	93 (29%)
2010	344	204 (59%)	2 (0.6%)	137 (40%)	107 (31%)	244 (71%)	97 (28%)
Mean	352	210	3	139	109	248	102

2.8. Figures

Figure 2-1. Location of the 2.2 ha research sites and general layout of measurements (approximate locations). Asterisks refer to measurements that were rotated every year.

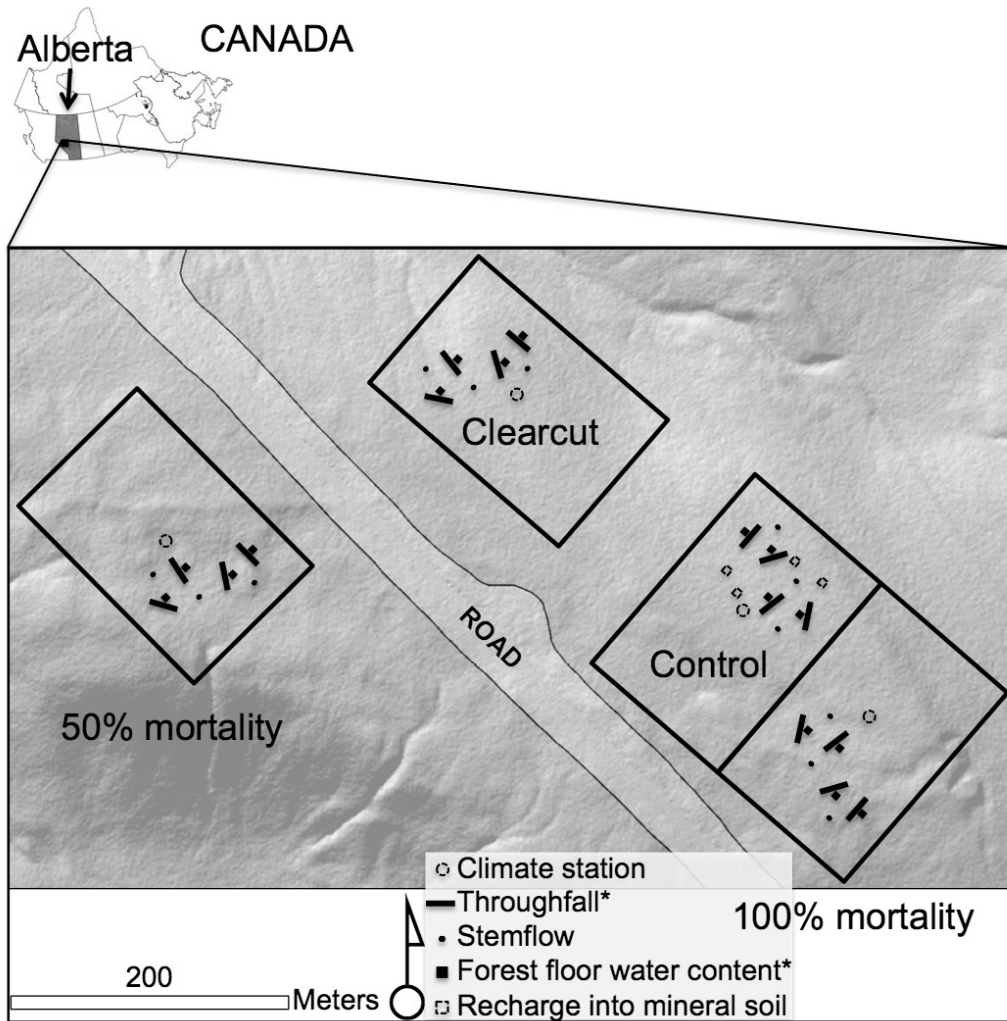


Figure 2-2. Frequencies of rain events recorded during the study period (2008-2010) with their respective relative contribution to total rain in cumulative terms.

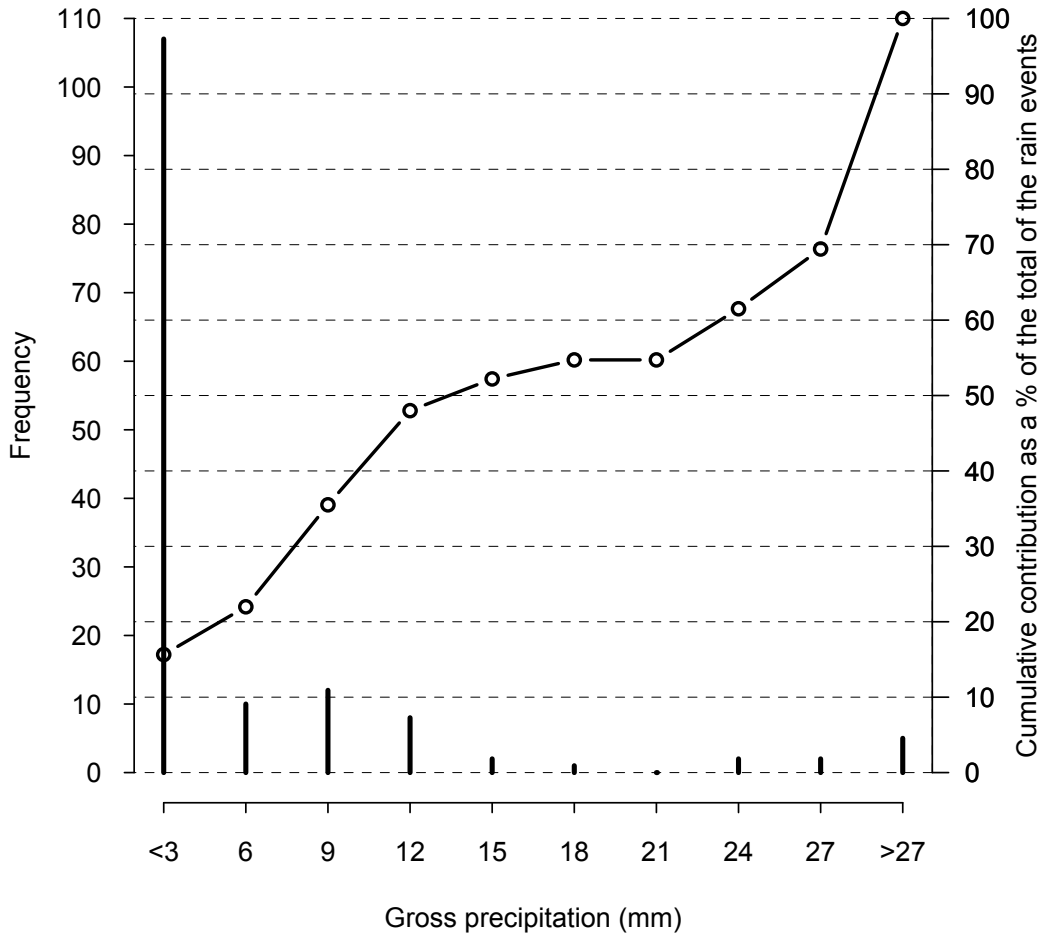


Figure 2-3. Funnelling ratios related to tree size and rain depth. A) Scatter plot of funnelling ratio as a function of P_G events for each DBH (cm) class. B) Boxplots with notches of funnelling ratio as a function of DBH class, whiskers indicate extremes (1.5 X interquartile range), and circles indicate outliers. The y-axis is in logarithmic scale. The widths of the notches are proportional to the square root of the samples sizes.

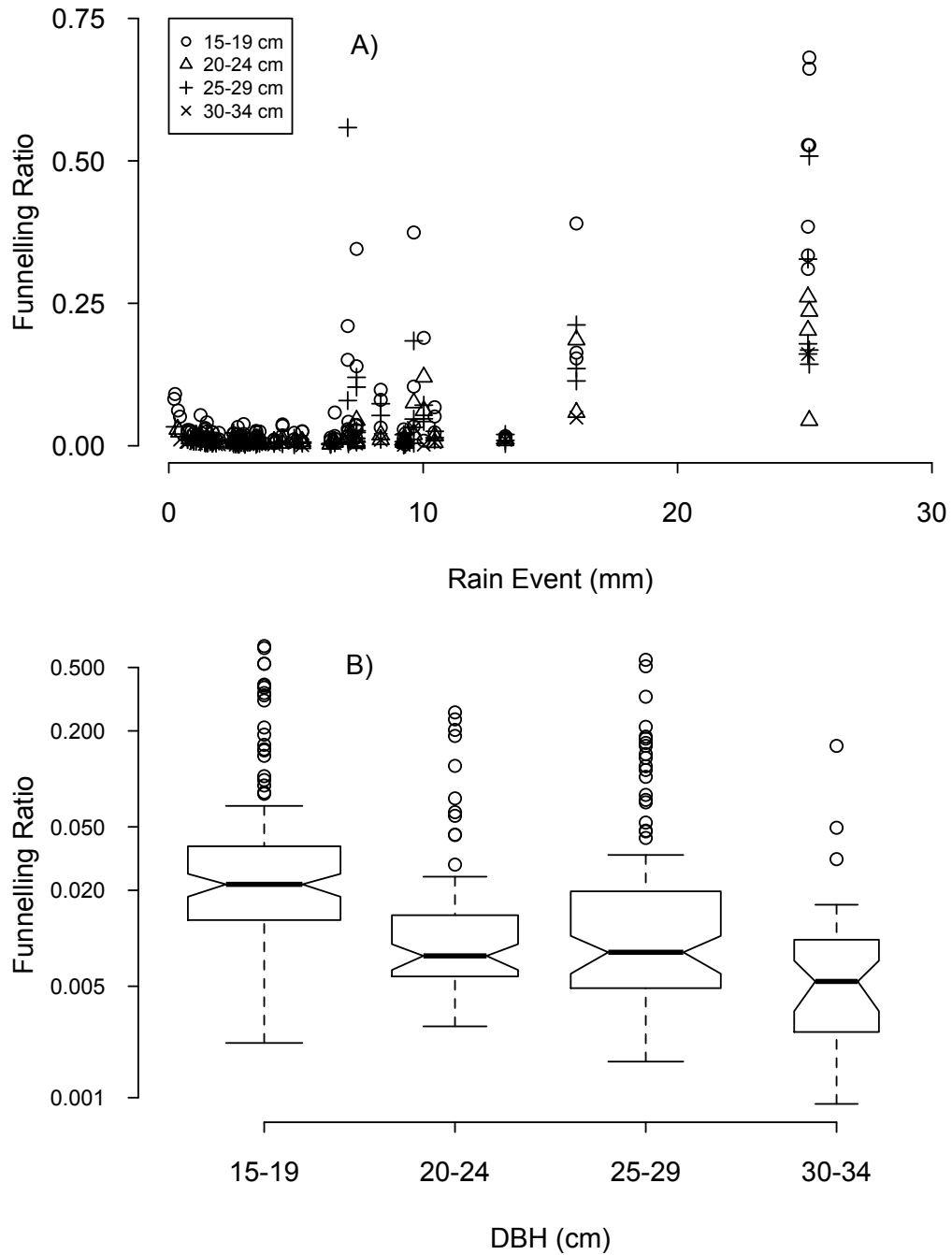


Figure 2-4. Measured interception as a function of the range of P_G events along with the fit of the model. The panels A) and B) illustrate the boxplots of canopy and forest floor interception respectively. The width of the boxplots is proportional to the square root of the samples sizes, whiskers indicate extremes (1.5 X interquartile range), and circles indicate outliers. Panel C illustrates the scatter plot of total forest interception.

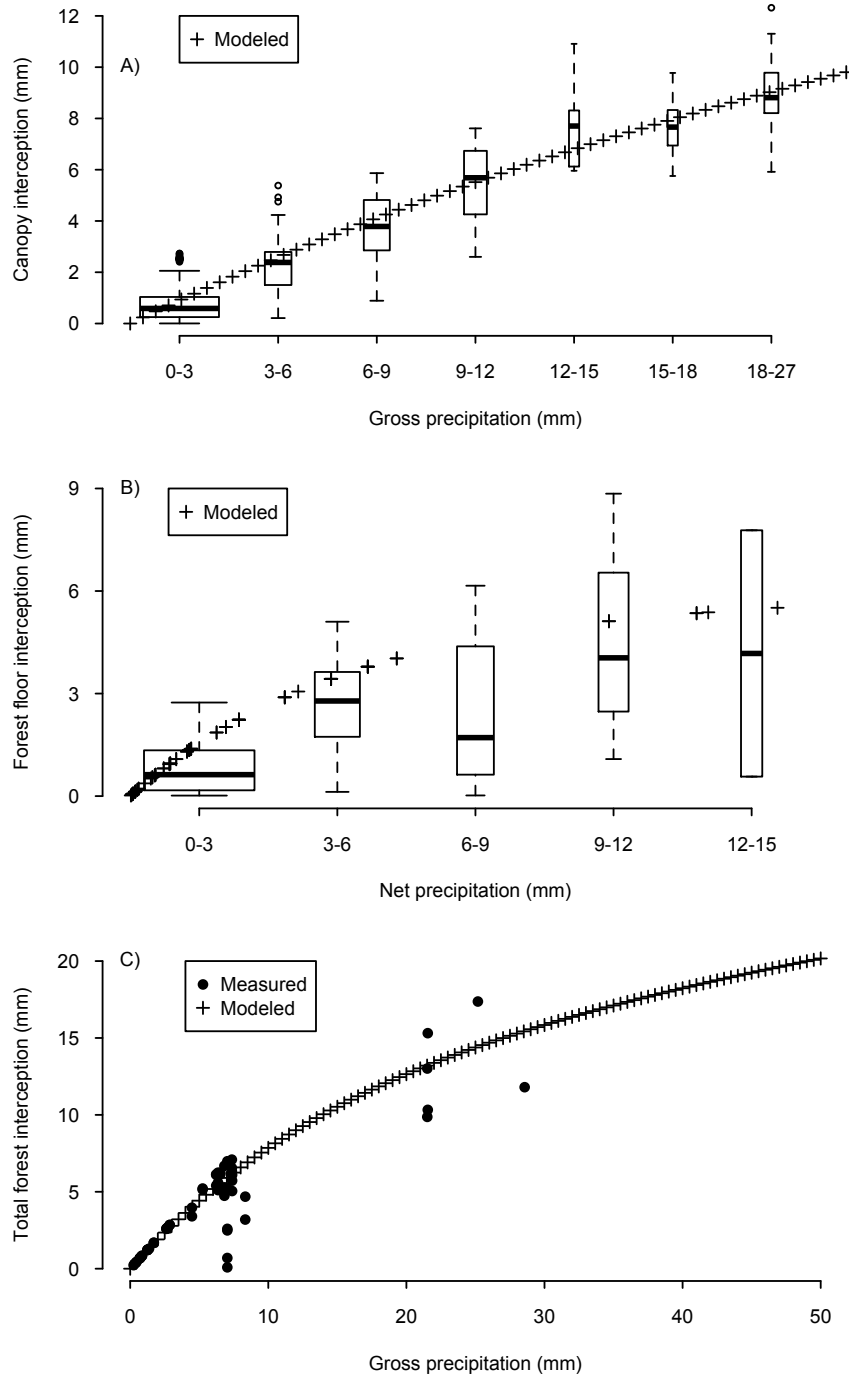


Figure 2-5. Series of forest floor water content and gross precipitation in 2009 and 2010. The dashed line represents a smoothed spline over the forest floor water content. The dashed vertical line indicated the forest floor's maximum water holding capacity.

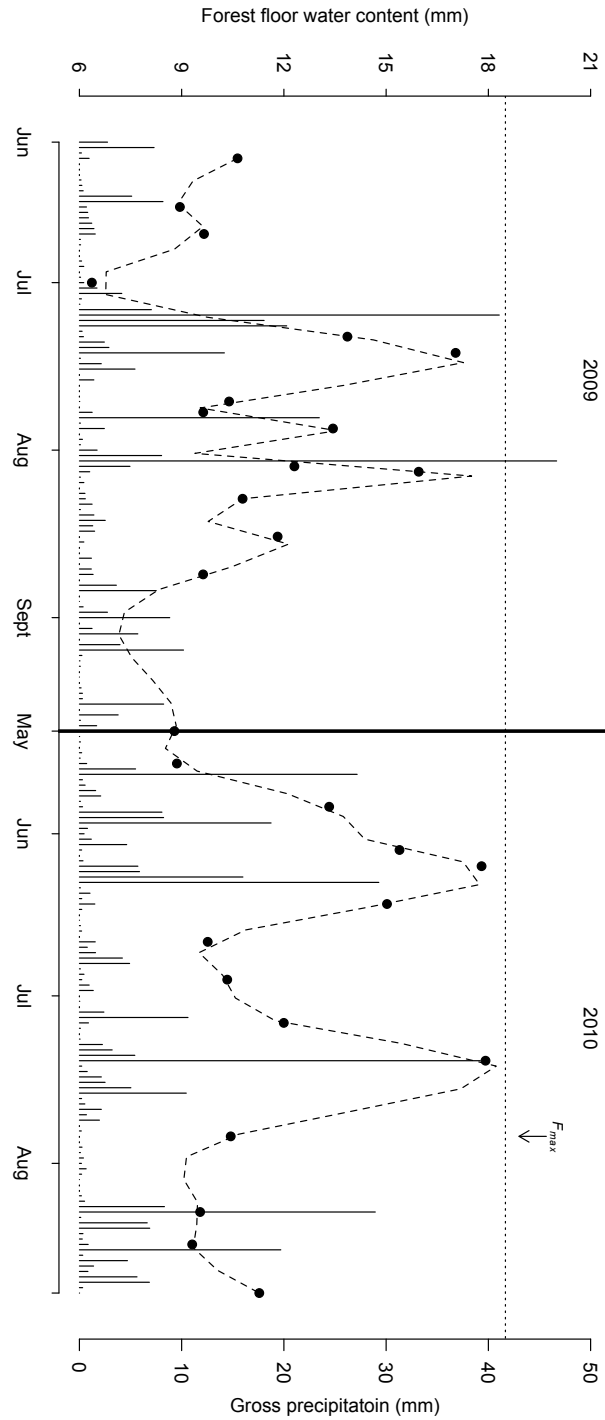


Figure 2-6. Relationships between control and treated sites for canopy interception I_c (mm) before (hollow symbols) and after (filled symbols) the treatment application. Dashed lines represent linear regressions before treatment for 50%- ($y = 0.91x + 0.01$) and 100% mortality units ($y = 0.93 + 0.03$), and after treatment for 50%- ($y = 1.02x - 0.01$) and 100% mortality units ($y = 0.96x + 0.00$). Variables were log transformed. The continuous line represents the 1:1 relationship.

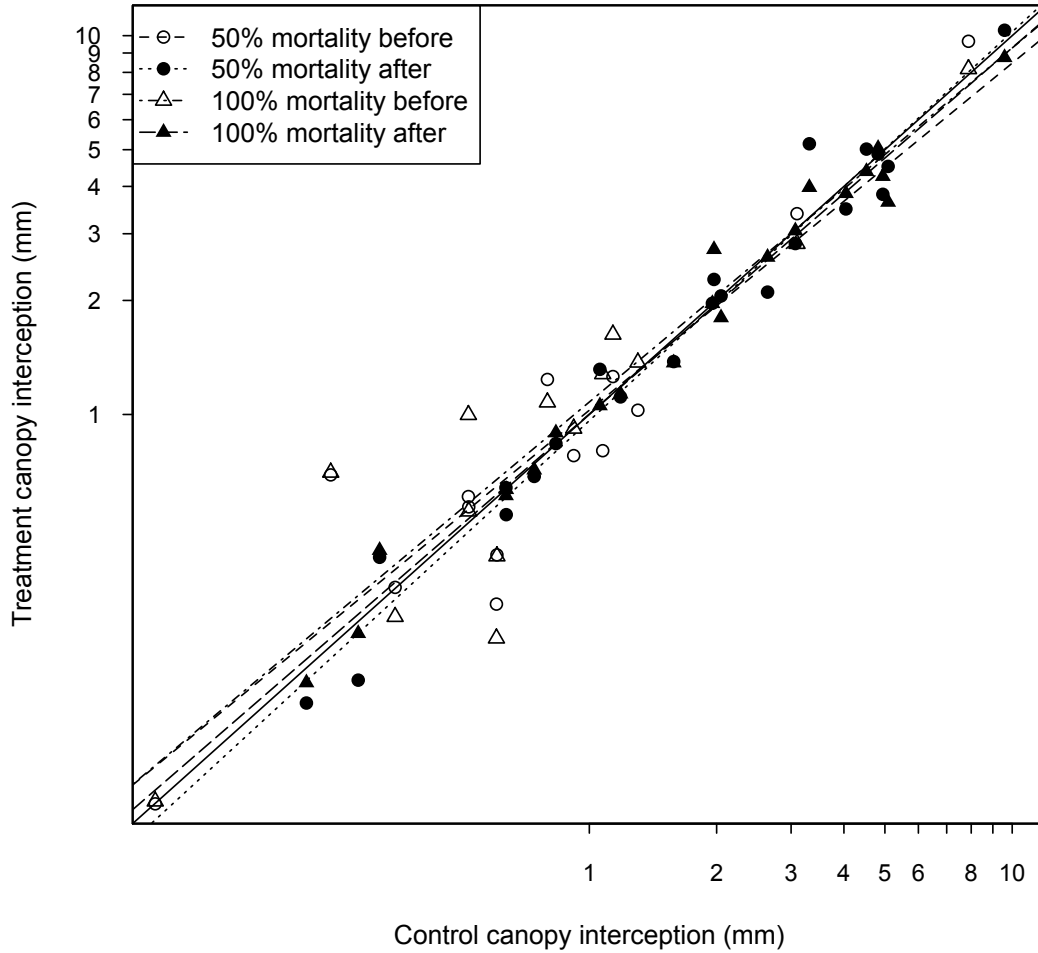


Figure 2-7. Modeled interception as a function of field measurements. Both variables were log transformed. The continuous line represents the fit of the linear regression between modeled and measured. The dashed line is the 1:1 relationship. Panel A) illustrates canopy interception, and B) forest floor interception.

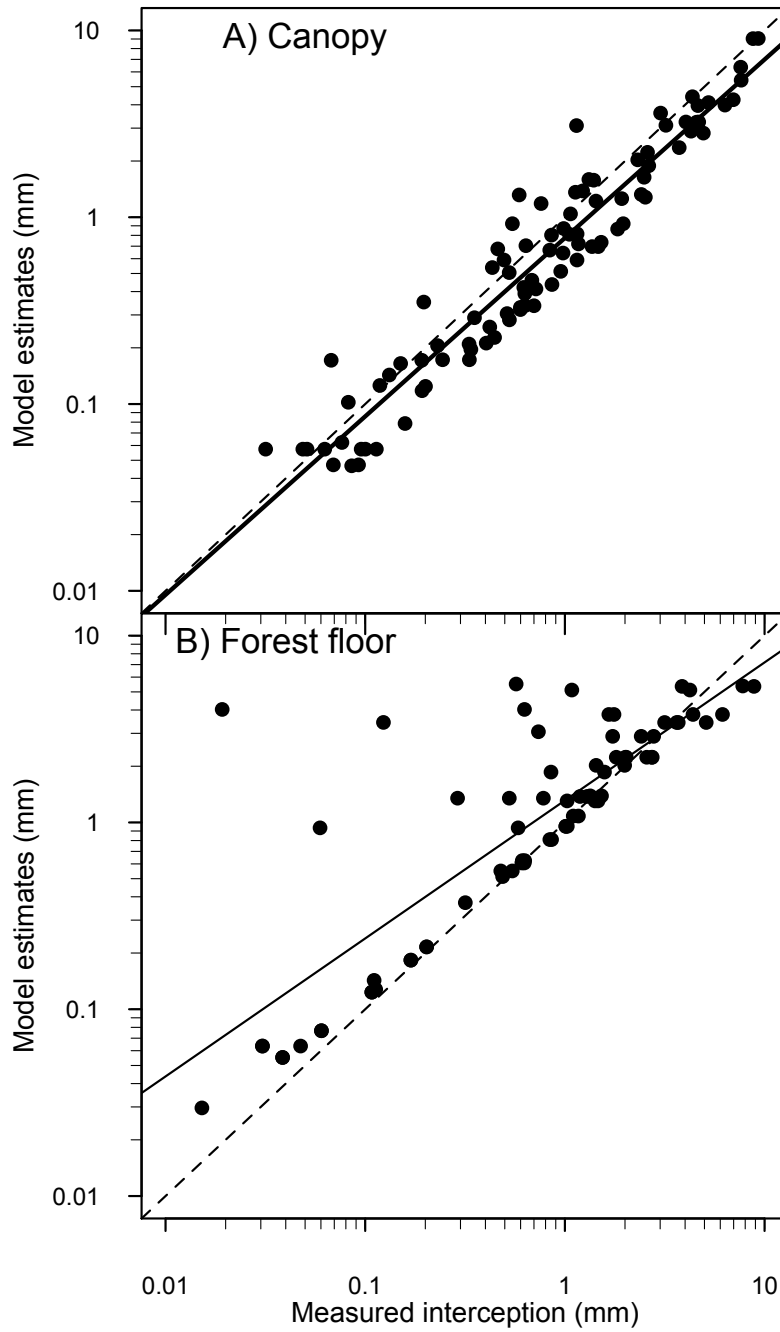
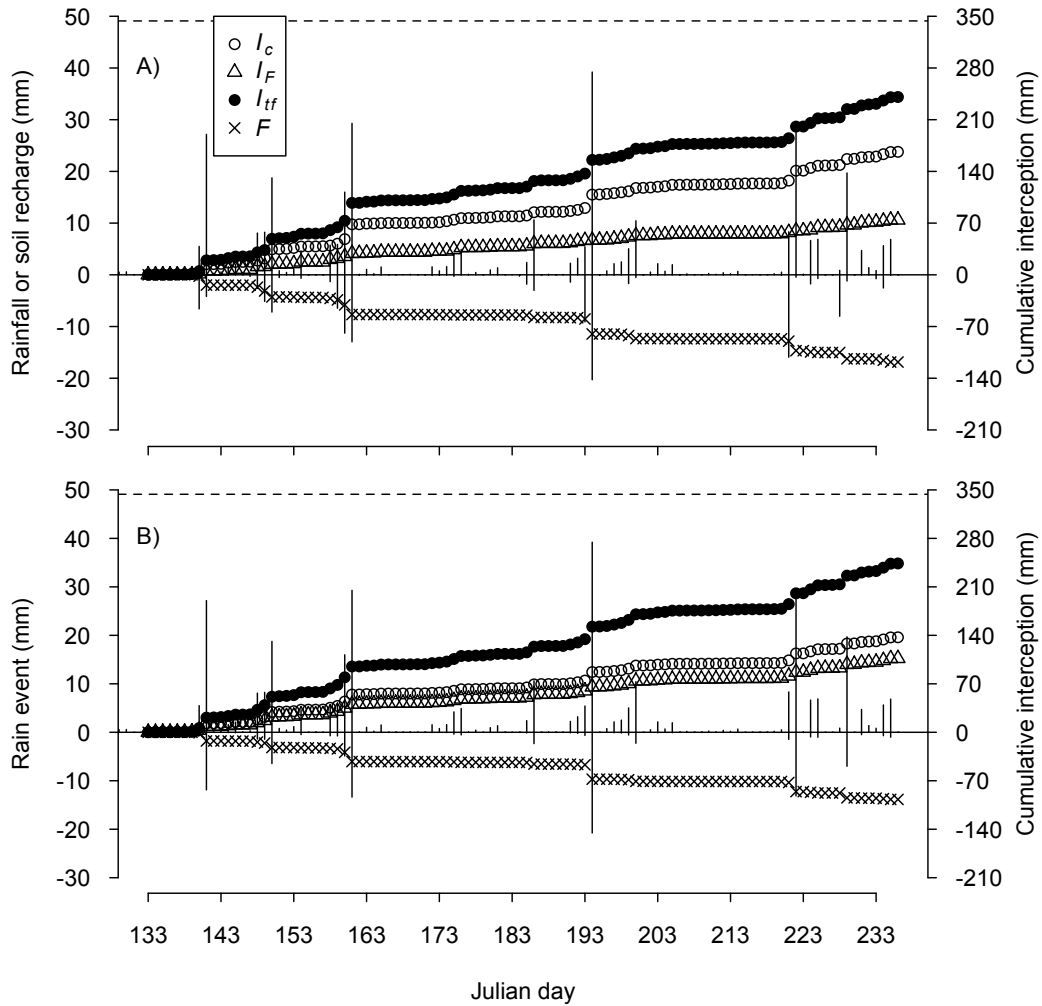


Figure 2-8. Gross precipitation and recharge (F) into the mineral soil (left axis), along with cumulative trend of canopy (I_c), forest (I_F), and total forest interception (I_{tf}) respectively for the 2010 season (right axis). Vertical lines indicate rainfall-recharge events (positive = rainfall, negative = recharge). Horizontal dashed line indicates total season gross rainfall (at end of season). A) indicates measured interception components, B) indicates measured P_G and modeled interception components.



Chapter 3. EARLY EFFECT OF VARIABLE INTENSITY MOUNTAIN PINE BEETLE ATTACK ON MICROCLIMATE AND TRANSPIRATION DYNAMICS OF LODGEPOLE PINE

3.1. Introduction

Lodgepole pine (*Pinus contorta* Dougl. ex Loud.) forest occupies 22% of forested land in western Canada and is an important component of the coniferous forest of western North America (Despain, 2001). The reproductive strategy of Lodgepole pine has evolved to enable the species to persist in environments with repeated recurrences of major landscape disturbances such as fire, insect outbreaks, mistletoe infestations, and windstorms (Raffa et al., 2008). In more recent periods, the combination of warm winter temperatures and the abundance of mature lodgepole pine stands has created optimal conditions for the development of an unprecedented outbreak of mountain pine beetle (MPB; *Dendroctonus ponderosae* Hopkins) populations (Taylor et al., 2006).

Compared to other disturbance agents such as fire and wind, MPB attack primarily affects foliage in the canopy and has no direct impacts on the understory or soil (Burton, 2008). Three phases are recognized to affect the foliage of trees successfully attacked by MPB. First, the green attack occurs during host colonization and early establishment of the beetle population. In this phase there are no apparent visual symptoms at the canopy level. Initially during this phase, attacked trees are still physiologically alive. Although trees are stressed beyond recovery, mortality does not usually occur at this stage (Chojnacky et al., 2000; Neiman and Vistintini, 2004). Inside the host tree, MPB resides in the cambial zone and inoculates fungi that occlude ray parenchyma and tracheids, resulting in reduction of water transport to tree crowns within 10 months following the initial attack (Ballard et al., 1982, 1984). Usually within approximately one year, foliage begins to die (red attack phase) and followed by transition to a grey attack phase within three years (Chojnacky et al., 2000; Neiman and Vistintini, 2004). During the red attack phase the tree canopy gradually turns red-brown, and afterwards, during the grey attack, it progressively defoliates. Some overlap is usually observed between the development of red attack and the onset of grey attack.

One major management concern with the present wide spread MPB attacks in western North America is the potential for hydrologic impacts in this region. While these include potentially large changes in water balance of lodgepole pine dominated forests after MPB attack leading to potential impacts on water production and flow regime from affected regions, few studies have directly explored the hydrologic impacts of canopy mortality from MPB attack. Boon (2009 and 2012), and Winkler et al. (2010) have shown considerable impact of the latter phases of MPB attack (grey attack) on net radiation and wind penetration into attacked stands, with subsequent impacts on snow accumulation and melt processes. However, the impact of these winter processes on overall (annual) water cycling is unclear. Few, if any, direct studies

have been conducted on hydrologic impacts of MPB on water balance of lodgepole pine forests during the growing season. Some researchers have speculated potential hydrologic impacts of MPB in some regions (Hélie et al., 2005; Uunila et al., 2006; Redding et al., 2008; Schnorbus, 2011) based on synthesis of existing literature describing individual components of water balance of healthy lodgepole pine forests (interception, transpiration, soil moisture storage), while others (Bewley et al., 2010; Alila, 2009) have attempted to predict these hydrologic impacts using models. Prediction of MPB effects on hydrology requires a clear understanding of the factors that govern the water balance in forests at the stand scale (Phillips and Oren, 2001; Simonin et al., 2007). With a gap of explicit research on MPB impacts on key hydrologic processes in lodgepole pine forests, modelling efforts have been forced to use analogous forest disturbances, or uncertain (and questionable) model parameters such as ones derived from other forest tree species.

One of the key impacts of MPB attack is the potential change of forest transpiration dynamics. In coniferous forests, the length of the transpiration season is determined by climatic conditions and stomatal response to low temperatures (Kaufmann, 1985). Stomatal sensitivity to soil water availability is particularly important for lodgepole pine (Reid et al., 2006; Bosch and Hewlett, 1982). Lodgepole pine has been identified as a conservative species (Spittlehouse, 2002) with high stomatal control in response to soil water availability (Kaufmann, 1985; Reid et al., 2006; Andrews, 2012). Transpiration can constitute a large component of the annual water balance; Kaufmann (1985) reported ~ 210 mm of an annual transpiration during a transpiration season 210-245 days long, which is in agreement with the 138 mm year⁻¹ reported by Swanson (1973). However, while MPB is known to preferentially attack mature stands, most transpiration studies in lodgepole pine have been conducted in young and/or high density stands (Knight et al., 1981; Spittlehouse, 2002; Reid et al., 2006).

While MPB infestation can be expected to severely reduce or eliminate overstory transpiration where all trees in the stand are killed, more often, all trees in the stand are not attacked or other species co-exist with lodgepole pine in mixed stands. Thus, the potential exists for surviving trees to buffer the stand from dramatic changes in transpiration after MPB attack. Reduction of transpiration within stands can increase root water availability, which has the potential to produce a positive effect on transpiration of surviving trees. Several studies have documented the effects of increased transpiration of surviving trees after partial cut harvesting or thinning (Reid et al., 2006; Bladon et al., 2006). However, because changes in microclimate after partial harvesting are strongly associated with transpiration response of surviving trees, the extent to which these positive feedbacks exist after MPB attack are highly uncertain.

The broad objectives of this study were to explore transpiration dynamics in a mature lodgepole pine forest in response to early, variable intensity MPB attack. Specific research objectives included evaluating the effect of variable intensity MPB attack on: 1) changes in the canopy micrometeorology; 2) transpiration

response of individual trees including surviving live, fading, and dying trees; 3) integrated stand-scale transpiration; and lastly, 4) model the effects on stand scale transpiration of a wider range of MPB disturbance scenarios in mature lodgepole pine forests.

3.2. Materials and methods

3.2.1. Study site description

The research was conducted in Upper Foothills sub-region of Alberta (Downing and Pettapiece, 2006). The region is characterized by pure lodgepole pine (*Pinus contorta* Dougl.), mixed conifer stands of white spruce (*Picea glauca* (Moench) Voss) and subalpine fir (*Abies lasiocarpa* (Hook.) Nutt.) (Beckingham et al., 1996). The area experiences a temperate continental climate; its mean daily maximum air temperature during the growing season ranges from 16.2 °C in May to 20.6 °C in August. The precipitation in the area is usually controlled by cyclonic activity (Nkemdirim and Weber, 1976), although localized convective storms are also frequent from late May to July (Longley, 1972). Mean monthly precipitation from May to August ranges from 57.9 mm to 82.2 mm, and the mean annual precipitation is 562.4 mm. Study sites were part of a healthy, homogeneous lodgepole pine stand of mature age classes (> 100 yrs. old). Canopy height ranged from 20.2 to 23.5 m, basal area ranged from 29.1 to 40.2 m² ha⁻¹, and stem density ranged from 906 to 1056 trees ha⁻¹. There was no presence of surface water in the area and the water table was intermittently detected with piezometers at 4 m depth.

3.2.2. Experimental design

This research was part of a study focused on describing changes in the forest water balance in response to a potential MPB attack. Measurements took place in four experimental units (2.2 ha each) during four growing seasons from May to September during 2008-2011 (Figure 3-1). The experimental design followed a “before/after; control/impact” approach (BACI) (Green, 1979; Stewart-Oaten et al., 1986, 1992). Measurements before the treatments were applied spanned approximately one whole year, from early May 2008 to mid-June 2009. Treatments were applied in mid-June 2009 and monitored for two additional post-treatment years until the end of June 2011. Samples collected in all sites were paired, in the sense that the “control” and the “impact” (treated) units were sampled simultaneously. Because the focus of the research was to describe changes in the key processes regulating transpiration dynamics as a result of the treatments, “replication” consisted of sample collection through time to measure variation of transpiration in response to the primary controls (radiation, RH, wind, soil moisture, etc.) across treatment units both the before and after treatment application. Observed differences in transpiration variables between the “treated” and the “control” units before application of the treatments was assumed to reflect an estimate of the mean difference that would have existed in the post-treatment period if there was no perturbation or had treatments not been applied (Stewart-Oaten et al., 1992). Thus, changes in the mean difference

between the pre-treatment and post-treatment periods would indicate the treated units had undergone a change relative to the control unit.

Three treatments were evaluated in this study: control (untreated), and two levels of simulated MPB attack (50% and 100% simulated MPB mortality, hereafter referred to as “50% and 100% mortality”); a fourth treatment was applied to explore the impact of a management intervention by salvage logging on soil moisture response (see Chapter 4). The simulated MPB attack treatments used glyphosate application (Glyphosate 0.15 grams per capsule, EZ-Ject lance system by Herbicide System corp.) to kill individual lodgepole pine trees. The intention was to reproduce the gross tree/stand level foliage mortality characteristic of MPB attack (sequence of green, red, and grey attack symptoms) to enable controlled study of transpiration responses to differing levels of MPB attack. As a proxy for the MPB attack, glyphosate affects basic physiological process, such as chlorophyll synthesis (Hollander and Amrhein, 1980; Lee, 1981), protein synthesis (Cole et al., 1983), auxin production (Lee, 1982) and ammonia accumulation (Cole et al., 1980). Changes in these physiological processes modify the water potential, and thereby turgor pressure of the guard cells (Shaner, 1978; Muñoz-Rueda et al., 1986). Impact of glyphosate on these metabolic processes is tightly coupled with reduction in photosynthesis, transpiration, and subsequent foliage mortality. Glyphosate therefore serves as a close analog of the effects of MPB attack. The glyphosate dosage applied to trees varied by tree size. The rate was 1 capsule per 5 cm tree diameter at breast height (dbh) per tree for trees 10–20 cm dbh (i.e., a 15 cm dbh tree would receive 3 capsules), or 1 capsule per 3cm dbh per tree for trees >20cm, with capsules equally spaced around the circumference of the tree near the base of the bole. The EZ-Ject lance drives a capsule through the bark where the glyphosate is slowly dissolved into the cambium and moves it in the tree. In the 100% mortality site, all trees ≥ 10 cm dbh (minimum size of trees attacked by MPB; Nelson et al., 2006) were injected thus all canopy trees were treated. In the 50% mortality site, while the target was to kill 50% of the trees distributed throughout the stand, only every 3rd tree ≥ 10 cm dbh was injected as some root-to-root transfer of glyphosate to neighbouring trees was anticipated because some degree of root grafting observed on similar stands (M. Mihajlovich personal communication, Fraser et al., 2005). Thus, 30% of all trees were treated instead of 50%.

3.2.3. Effectiveness of treatments

Treatment effectiveness in producing the target mortality (50% and 100% mortality) was assessed using two approaches. A stand survey using fixed area plots was conducted prior to, and after treatment applications to document crown condition in each of the treatment units. However, because of difficulty in quantifying crown condition with the surveys, survey data was combined with analysis of crown reddening evident on a digital ortho-photograph taken in the fall of 2010 to document effectiveness of the treatments. The relative proportion of live-healthy trees and dead or dying trees was estimated using both approaches (surveys and digital imagery).

The stand surveys were only used to estimate the relative proportion of live trees (r_L) on a basal area basis. While crown condition classes reflecting dying or dead trees were also included in this survey, visual assessment of varying degrees of crown reddening from these surveys were found to underestimate the likely impact of the treatments on physiological health (based on transpiration results). Surveys were conducted in the fall of 2008 (before treatment application) and again in 2010 after treatment application in the control, 50%, and 100% mortality units. Nine fixed area (8 m radius) plots were established in each unit and crown vigour class was estimated for each tree in the plot by visual assessment using binoculars. Five vigour categories were used to assess health of individual tree crowns: 1) no red needles, 2) just a few red needles, 3) intermediate amount of red needles, 4) almost all red needles, and 5) all red needles. Trees in categories 1 and 2 were considered live, and categories 3-5 were classified as dead or dying. The relative proportion of live trees r_L (crown class 1 and 2 above) in each unit was approximated from basal area and corrected to exclude natural mortality (e.g., self-thinning processes) based on existing mortality (category 3-5) observed in the control unit in 2008, where:

$$r_L = 1 - \left(\frac{\% \text{ cat.1-2 in control 2010}}{\% \text{ cat.1-2 in control 2008}} \right) - \left(\frac{\% \text{ cat.1-2 in 2010}}{\% \text{ cat.1-2 in 2008}} \right) \quad (1)$$

Because all canopy trees in the 100% mortality treatment were treated with herbicide, none of these trees were classified as healthy (i.e., $r_L = 0$)

Digital ortho-rectified imagery was used to estimate the relative proportion of plot area comprising dead foliage (r_D). The colour digital images (four band imagery collected to support both 3-band natural color (RGB) and false color infrared (CIR) orthoimage products) taken late July 2010 using fixed wing aircraft (2900 m elevation) using in a Leica ADS80 digital camera system were acquired from West Fraser Mills Ltd (Hinton Division). Image processing was performed by Northwest Group Ltd which consisted of aerotriangulation and orthorectification using Leica Xpro software package, version 4.4 and ortho mosaics were created with Inpho Orthovista 4.4. Fifteen ground control points were used during aerotriangulation. The image was analysed using a supervised classification using a maximum likelihood in the "Training Sample Manager" (ArcGIS 10) to calculate area of dead foliage as indicated by red pixels (Figure 3-1). Relative proportion of dead foliage (r_D) was calculated by subtracting the proportion of red pixel area (m^2) in the control unit from the proportion of red pixel area (m^2) in each of the treated units.

3.2.4. Micrometeorological measurements

Climate stations located at the center of each experimental unit (see details in Chapter 2) were used to measure air temperature, relative humidity, wind speed, and net radiation at approximately canopy height (21 m). All climate variables were sampled every five seconds, averaged and stored every 10 minutes using a datalogger (CR1000, Campbell Scientific, Inc., Utah, USA).

Precipitation was measured in a nearby clear-cut 300-600 m away from the sites (details found in Chapter 2).

3.2.5. Transpiration measurements

Overstory transpiration was measured using sapflow techniques (thermal dissipation method after Granier, 1985 and 1987). The thermal dissipation method for measuring sap flow has been extensively tested and a large body of literature generally reports the empirical relationships between sensor signal output to actual sap flux to be accurate (Clearwater et al. 1999; Granier 1987; Granier et al. 1990, 1994, 1996; McCulloh et al. 2007; Saugier et al. 1997; Smith and Allen 1996; Swanson 1994). Measurement of sapflow in all trees in the plots was not logistically possible. However, it was anticipated that treatments would produce distinctly different transpiration responses in several categories of trees. These included: a) live (untreated) trees in the control unit; b) live (untreated) trees surrounded by dead or dying trees in the 50% mortality unit that may experience a transpiration response reflecting improved access to growing resources (water, nutrients, etc.); c) dying trees treated with herbicide (still partially physiologically active) in both of the 50% and 100% mortality units; and, d) dead trees (no transpiration) in both of the 50% and 100% mortality units. The approach used in this study was to characterize the detailed transpiration dynamics of these groups of trees and scale these results to the treatment unit scale using the relative proportion of trees in each category to describe the overall effect of the MPB treatments.

During the pre-treatment period (2008 and May-June 2009), diurnal patterns of sap velocity were measured on seven randomly located live (healthy) trees. Trees were instrumented with one constant heat sapflow sensor (TDP-30, Dynamax, Inc, Houston, Texas) in each of the control, 50%, and 100% mortality units. Sensors were installed on the south side of trees ~1.3 m above ground level for the duration of a growing season. Tree boles were wrapped with reflective insulation (centred on the sapflow sensors) to guard against thermal noise from solar heating on sapflow measurements. Daily variation in sap velocity was measured every 20 seconds and averaged hourly over 24 hr. from July 17th to October 10th in 2008 and from May 25th to June 30th in 2009. Sensors were randomly relocated to different trees each season to avoid problems with wounding response in trees from sapflow sensors left installed during prolonged periods. Sapflow measurements during the post-treatment period (May 2nd-Sept. 27th 2010, and May 6th-June 30th 2011) were continued on seven randomly instrumented live (healthy) trees in the control unit. In the 50% mortality unit, sapflow of seven untreated live trees surrounded by herbicide treated trees (hereafter referred to as “live within dead”), and seven additional herbicide treated trees in the 100% mortality unit (hereafter referred to as “fading”) were measured for the remainder of the post-treatment period. Sapflow immediately after imposition of the treatments in late June through September 2009 was omitted to exclude the period representing the initial development of the treatment responses. Trees that died during the sapflow monitoring (i.e., trees

that developed complete red crowns and subsequently displayed noisy or incoherent diurnal sapflow signals) were excluded from the analysis. Thus transpiration of dead trees with completely red crowns was assumed to be zero.

Thermal dissipation sapflow probes consist of two thermocouple needles inserted in the sapwood, the upper one containing an electric heater. The sapflow probes measure the temperature difference between the heated upper needle and the ambient sapwood temperature at the lower needle. These differences in temperature (dT) are related to the mass flow of water, sap velocity S_v (cm S^{-1}) from the empirical calculation defined by Granier (1985; 1987):

$$S_v = 0.011119 \frac{(dT_M - dT)^{1.231}}{dT} \quad (2)$$

where dTM is the maximum dT in a given 24 hour interval. Total sap flow S_f ($\text{cm}^3 \text{s}^{-1}$) was calculated as:

$$S_f = S_v S_A \quad (3)$$

where S_A (cm^2) is the cross-sectional sapwood area at the TDP-30. Sapwood area was determined for each tree in this study from the mean sapwood thickness determined from two increment cores (sampled on the north and south sides of each tree) based on natural changes in translucence of wood color (Simonin et al., 2007) and assuming a circular bole cross-section.

Individual tree transpiration T_t (mm d^{-1}) was calculated from sap velocity as:

$$T_t = \frac{S_f}{A_L} \quad (4)$$

where A_L is the one side projected crown leaf area (m^2). A_L was estimated for each tree based on sapwood area and the linear relationship between A_L and S_A developed from the destructive sampling of eight trees as described in Chapter 2.

Transpiration per unit ground area T_g (mm day^{-1}) was calculated as:

$$T_g = T_t LAI \quad (5)$$

where LAI is the leaf area index ($\text{m}^2 \text{m}^{-2}$). Mean LAI of each treatment unit was determined from one fixed area plot per unit (8-m radius; 201 m^2 area). Height, dbh, and sapwood area was measured for each tree in the plot to determine stem density and total sapwood area for each plot. The relationship between sapwood area at breast height and A_L developed in Chapter 2 was used to estimate A_L in the fixed radius plots and subsequently, the LAI of each treatment unit.

Transpiration (T_t) was used with micrometeorological data to calculate canopy conductance g_c (m S^{-1}) given by ($g_t \times LAI$) where g_t (m s^{-1}), is the stomatal

conductance for the leaves in the canopy. g_t was calculated according to Monteith and Unsworth (1990) and the units of T_t were aggregated after Lagergren and Lindroth (2002):

$$g_t = \frac{\lambda T_t \gamma}{\rho c_p D} \quad (6)$$

where: ρ is the density of dry air (Kg m^{-3}); c_p the specific heat of air ($\text{J g}^{-1} \text{K}^{-1}$); D the vapour pressure deficit (Kpa); λ the latent heat of vaporization of water (Mj Kg^{-1}); and γ the psychrometric constant ($\text{Kpa } ^\circ\text{C}^{-1}$).

3.2.6. Scaling transpiration to the treatment unit scale

Transpiration measurements for: a) live, b) live within dead, and c) fading trees were scaled to the treatment unit scale using the proportion of trees in these categories in each treatment unit from the assessment of treatment effectiveness (r_L and r_D , section 3.2.3). Because transpiration measurements during this study indicated that visual symptoms of foliage colour (particularly for green or chlorotic foliage) did not consistently indicate physiological health of treated trees (e.g., some treated trees with green foliage had transpiration signatures indicating they were dead or close to death), the proportion of herbicide treated trees that were dying, but not yet physiologically dead (fading) could not be reliably estimated from the stand surveys. Thus the proportion of fading trees (r_F) in both the 50% and 100% mortality units were estimated from the residual of r_L (50% mortality unit only) and r_D (both 50% and 100% mortality units) as:

$$r_F = 1 - r_L - r_D \quad (7)$$

Transpiration at the stand level T_{st} (mm) was assumed to be equal to T_g of the live trees measured in the control experimental unit, whereas T_{st} in the 100% mortality site was estimated by multiplying T_g for fading trees by the relative proportion of fading (r_F) trees present in that unit (transpiration of r_D trees was assumed to be zero and no r_L trees were assumed exist in this unit). Stand level transpiration in the 50% mortality unit was similarly estimated by first multiplying T_g for live within dead, and fading trees by the proportion of trees in these categories (r_L and r_F) and summing their products (i.e., $T_{st} = (T_g \times r_L) + (T_g \times r_F)$). Because transpiration of fading trees was not directly measured in the 50% mortality unit, a linear regression (forced through the origin) between measured fading T_g in the 100% mortality unit and live within dead T_g in the 50% mortality unit enabled predicting fading T_g in the 50% mortality unit as a function of live within dead T_g in the 50% mortality unit (T_g of fading trees in 50% mortality unit = $0.53 \times T_g$ of live within dead trees in the 50% mortality unit, $P < 0.001$. $R^2 = 0.92$).

3.2.7. Scenarios for stand transpiration

Data on transpiration of live within dead trees, fading, and dead trees enabled additional scaling of transpiration results to explore the potential impact of

varying proportions of these tree classes on stand scale transpiration. Four modeled scenarios were used to explore the effects of an early MPB red attack on T_{st} from a small-scale endemic attack to full blown epidemic level attack on stand scale transpiration. These scenarios were developed to explore varying proportions of live within dead trees at four contrasting levels; 75%, 50%, 25% and 5% of total tree density in the stand. The remaining proportion of dead and fading trees in the scenarios were adjusted to preserve the proportions of these two categories measured in the field (see section 3.2.3). Stand scale transpiration (T_{st}) for these scenarios was calculated by multiplying the proportion of trees in live within dead, fading, and dead categories by T_g of trees in these classes (as above). Total stand transpiration was scaled at a daily and total seasonal basis for the 2010 season.

3.2.8. Data analysis

The effect of treatments on micrometeorological variables (air temperature, relative humidity, wind speed and net radiation) was tested by comparing linear regressions between each meteorological variable observed in control and treated units before and after the treatment application. Differences among regression slopes and intercepts were tested using Student's t after Zar (1999). Additionally, variation of meteorological variables between sites before and after treatment application was also explored using 95% confidence intervals.

Transpiration variables were not normally distributed, thus evaluating median responses was the most appropriate approach for analysis of transpiration data. Differences between median T_t of live trees before treatment with live, live within dead, and fading trees and after application of treatments was assessed using approximate 95% confidence intervals as indicated by notches in boxplots (Chambers et al., 1983), where notches in boxplots indicate $\pm 1.58 \times$ the interquartile range /square root (n). Differences in transpiration (T_g) among tree categories was also tested by comparing linear regressions between median T_g of live trees in the control unit against that of live within dead, and fading trees before and after the treatment application using Student's t tests to test equality of two population regression coefficients (slopes and intercepts) after Zar (1999). Seasonal variation of median daily T_g was assessed using bands representing upper and lower IQR around median daily T_g in 2010 to analyse patterns and strength differences among tree categories throughout the season. A complementary two-sample Kolmogorov-Smirnov (K-S) test was performed to test whether the range (distribution) of S_f among tree categories in the 50% mortality site differed from S_f in the control site before and after application of the treatments. The modeled scenarios of stand transpiration were compared using 95% confidence intervals calculated from the linear regressions between modeled scenarios as a function of control conditions. All numerical analysis were performed using R 2.15.1 (R Core Team, 2012) using $\alpha = 0.05$ as the threshold for statistical significance.

3.3. Results

3.3.1. Effectiveness of treatments

Combined results from the supervised classification of the color ortho-rectified image of the treatment units (used to estimate the proportion of dead (r_D) trees in the 50% and 100% mortality units) along with the stand mortality surveys (used to estimate the proportion of live (r_L) within dead trees in the 50% mortality unit only) indicated the relative proportion of live within dead, fading, and dead trees were 77.5%, 13.4%, and 9.1 % respectively by the fall of 2010 in the 50% mortality unit. The proportion of trees in these same categories was 0%, 83%, and 17% respectively in the 100% mortality unit. Thus, while the use of individual tree herbicide treatments as a proxy for the stand scale effects of MPB attack did not produce the target levels of 50% and 100% mortality within 1.5 years after treatment application, a strong gradient of live, fading, and dead trees characteristic of the initial phases of variable intensity MPB attack was produced between the two treatment units.

3.3.2. Micrometeorology

Mean growing season (May-September) atmospheric conditions prior to application of the treatments (2008 and May-June 2009) were slightly warmer, sunnier, and with calmer wind conditions than during post-treatment period (2010 and May-June 2011). Mean seasonal air temperature and net radiation in the untreated control unit was 14.1 °C and 129.9 W m⁻² respectively during the pre-treatment phase, whereas 11.9 °C and 110.3 W m⁻² were observed during the post-treatment phase. While no difference in mean relative humidity was observed over the course of the study (61% RH during both pre- and post-treatment periods), mean wind speed was slightly greater during the post treatment period (0.26 and 0.32 m s⁻¹ for pre- and post-treatment periods, respectively).

Mean air temperature at canopy height was 13°C across all treatments units during the study. Comparison of linear regressions between control and treated units before and after treatments indicated a significant change in the slopes of the linear regressions in both 50% and 100% mortality sites after treatment ($p < 0.05$). While this corresponded with a mean increase in air temperature of 0.5 °C in the 50% and 100% mortality units after treatment, the scatter in the relationships between treated and control sites indicated a clear overlap between pre- and post-treatment relationships (Figure 3-2). Furthermore, comparison of pre- and post-treatment 95% confidence intervals indicated this minor shift in mean air temperature for the MPB treated units (both 50% and 100% mortality units) was not significant at $\alpha = 0.05$ (Figure 3-3). Similarly, regression analysis indicated a significant ($p < 0.05$), but functionally negligible increase in relative humidity was observed at both treated sites (< 0.01 % RH) during the post-treatment period while 95% confidence intervals (Figure 3-2) suggest no meaningful change in RH after treatment was evident.

Regression analysis of mean daily wind speed and net radiation also showed a

significant ($p < 0.05$) change in the relationships between both 50% and 100% mortality treatments with the control unit after treatment (Figure 3-2). However the relative change in these variables after treatment was stronger than observed for air temperature and RH. While mean wind speed was 34% greater (and more variable) in all treatments (including the control unit) during the post-treatment period (Figure 3-3), relative to the control unit, mean wind speed declined 8% (not significant) and increased by 31% ($p < 0.05$) after treatment in the 50% and 100% mortality units (Figure 3-2). Similarly, net radiation increased relative to the control by 11% (not sig.) and 18% ($p < 0.05$) in the 50% and 100 % mortality units after treatment, respectively.

3.3.3. Transpiration

Transpiration on a unit leaf area basis T_t , of live, healthy trees was generally similar among all study units prior to treatment application, however a marginally greater median T_t was observed in the 100% mortality unit (0.15 mm d⁻¹) compared to 0.10 and 0.12 mm d⁻¹ observed the control and 50% mortality units, respectively ($p < 0.05$, Figure 3-4, Table 3-1). Median transpiration per unit ground area T_g , prior to treatment ranged from 0.48-0.71 mm d⁻¹ and differences among study units generally paralleled those evident for T_t . Variation in pre-treatment median T_t and T_g was positively associated with variation in canopy conductance g_c , among these units (Table 3-1). Transpiration variables for live trees during the post-treatment period (control unit) were lower (except S_f and g_c) than observed during the pre-treatment period, (Table 3-1).

A clear pattern of daily and seasonal variation in transpiration was observed in live trees in the control unit across the study period. T_g was lowest (near zero) in the morning (10:00) and typically peaked in late afternoon (between 17:00 and 18:00 MST) reaching ≈ 1.7 mm d⁻¹ (averaged peak over two years) during the height of the growing season (Figure 3-5). A strong seasonal pattern in transpiration was also observed, where median T_g was typically 0.1-0.2 mm d⁻¹ in early May and increased to a seasonal maximum (0.7-0.9 mm d⁻¹) during July. This pattern corresponded with the summer season maxima of environmental variables governing transpiration such as temperature, light and vapour pressure deficit. Total seasonal T_g of live trees was 57 mm in the control unit in 2010, which represented $\approx 14\%$ of summer precipitation that season.

After treatment application, transpiration increased in live within dead trees (50 % mortality unit) relative to live trees (control unit) for all transpiration variables, particularly S_f which increased by 38% (Table 3-1). Median T_t was 33% greater in live within dead compared to live trees ($p < 0.05$, Table 3-1). While sapflow (S_f) did not differ between control and the 50% mortality units prior to treatment ($D = 0.1667$ from the Kolmogorov-Smirnov test, $p = 0.08$), S_f of live within dead trees increased strongly after treatment ($D = 0.3266$, $p < 0.05$). Similarly, median T_g of live within dead trees was 41% greater than that of live trees during the post-treatment (Table 3-1). However, increases in S_f , T_t , and T_g of live within dead trees after treatment (adjusted to account for changes in transpiration of control trees before and after treatment) were 38%, 21%, and

21%, respectively (Table 3-2). The relationship between T_g of live trees with live within dead trees changed appreciably after treatment in comparison to the same relationship prior to treatment application (Figure 3-7). While some degree of overlap in the pre- and post-treatment relationships was evident, T_g of live within dead trees was greater and more responsive to changes in evaporative demand (e.g., variation in the independent variable [T_g] is driven by changes in evaporative demand) than live trees prior to treatment ($p < 0.05$ for comparison of pre- vs. post-treatment slopes and intercepts).

In contrast, a strong decline in all transpiration variables was observed after treatment in fading trees (100% mortality unit) compared to live trees (control unit, Table 3-1). Median T_t of fading trees was 0.06 mm d⁻¹ compared to 0.09 mm d⁻¹ observed for live trees ($p < 0.05$, Table 3-1). This was consistent with 56% and 20% lower median S_F and g_c (respectively) observed in fading trees compared to live trees (Table 3-1). After treatment, median T_g of fading trees was 0.28 mm d⁻¹ compared to 0.41 mm d⁻¹ observed for live trees (Table 3-1). After the relative changes in transpiration of control trees was accounted for, median g_c of fading trees appeared very strongly reduced (3% of that in live trees) in the post-treatment phase (Table 3-2). Similarly, adjusted median T_t and T_g of fading trees were both only 22% of that observed in live trees after treatment suggesting a very strong (78%) reduction in transpiration of fading trees (Table 3-2). This strong reduction in median T_g after treatment was also clearly reflected in changes in the regression relationships between live and fading trees before- and after-treatment (Figure 3-7). While the relationship between T_g of live trees in the control and 100% mortality unit prior to treatment was somewhat variable ($R^2 = 0.57$), a strong downward shift in this relationship indicating reduced T_g in fading trees was observed after treatment ($p < 0.05$ for both change in slope and intercept, Figure 3-7).

While transpiration of live within dead and fading trees followed the same general diurnal and seasonal pattern as observed in live trees, greater T_g in live within dead, and lower T_g in fading trees was generally observed at both time scales. All tree groups showed near-zero T_g in early morning, however, differences in peak T_g in late afternoon (Figure 3-5) generally paralleled the relative differences evident among groups for other transpiration variables. Compared to live trees, peak T_g in live within dead trees was $\approx 67\%$ greater, whereas peak T_g in the fading trees was 13% lower. Similarly, on a seasonal basis, median T_g and inter-quartile ranges among tree groups were greatest for live within dead and lowest for fading trees, where the strongest differences among tree groups were evident in July-Aug when transpiration was greatest (Figure 3-6).

Total stand scale transpiration T_{st} , for the herbicide treated units reflects the additive partial contribution of transpiration of live within dead, fading, and dead trees (assumed to be zero). While median T_{st} of control, 50%, and 100% mortality units prior to treatment was, 0.48, 0.57, and 0.71 mm d⁻¹, respectively, T_{st} after treatment was 0.41, 0.49, and 0.23 mm d⁻¹ for these same treatment units (Table 3-3). However, adjusted T_{st} reflecting overall treatment effects

(relative to changes in T_{st} of the control unit before and after treatment) indicated the combined median transpiration (mix of live within dead, fading, and dead trees) in the 50% mortality unit was 101% of that observed in the control unit. While the increase in daily transpiration rate (1%) might be considered negligible, over the course of the 2010 growing season, this would have resulted in 9% greater seasonal transpiration in the 50% mortality unit compared to that of the control unit. In contrast, median T_{st} in the 100% mortality unit (adjusted for changes in transpiration of the control unit) was only 8% of that observed in the control unit suggesting a 92% reduction in median total stand transpiration after treatment. Because median T_{st} does not reflect total daily T_{st} , during the 2010 season this would have resulted in 47% reduction in total seasonal transpiration in the 100 % mortality unit.

The combined effect of varying the proportions of live within dead trees, fading, and dead (transpiration assumed as zero) indicated that the intensity of MPB is a key factor governing a wide range of stand scale transpiration responses. Exploring a range of MPB attack scenarios (low to high intensity attack) using the differential transpiration rates (T_g) observed for trees in these categories indicated a strongly reduced T_{st} through moderate increases in T_{st} (Figure 3-8, Table 3-4). No difference in mean daily T_{st} was evident among the four scenarios at low T_{st} in the control (e.g., when evaporative demand is low) but scenarios showed linearly divergent responses in T_{st} with significant differences among all scenarios (separation of 95% confidence intervals) as evaporative demand increased beyond moderate levels ($T_{st} > 0.3 \text{ mm d}^{-1}$) in the control (Figure 3-8). At higher evaporative demand (0.8 mm d^{-1} in the control), mean daily T_{st} was lowest in the highest intensity MPB attack scenario D (95% fading/dead, 0.37 mm d^{-1}) and was progressively greater as the intensity of MPB attack declined through scenarios C (75% fading/dead, 0.51 mm d^{-1}) and B (50% fading/dead, 0.69 mm d^{-1}). At high evaporative demand, mean daily T_{st} for scenarios D, C, and B were 54%, 36% and 14% less than predicted for control without MPB ($T_{st} = 0.8 \text{ mm d}^{-1}$) respectively. In contrast, T_{st} of the lowest intensity MPB attack scenario A (25% fading/dead) was 8% greater than that of the control at high evaporative demand (0.8 mm d^{-1}). Total seasonal T_{st} (based on conditions present in 2010) for the four MPB scenarios was estimated at 36, 50, 67, and 85 mm for scenarios D-A respectively, compared to 77 mm observed in the control (no MPB) unit (Table 3-4). Based on the equation to calculate T_{st} in section 3.2.6, these scenarios suggest that T_{st} resulting from a partial MPB attack of 35% (fading/dead trees) with the balance of 64% live within dead trees would be equal to that of a healthy stand without MPB (e.g., control).

3.4. Discussion

Results of this research indicate that depending on the intensity of MPB attack, moderate to large early changes in transpiration dynamics of lodgepole pine stands are likely even during the initial phase of the attack (red attack). Moreover, where the intensity of such attack affects less than approximately 1/3 of the trees in the stand, total stand transpiration may remain unchanged or even increase beyond that of healthy stands. These results are novel because no

previous research (to my knowledge) has explored these early responses to MPB attack.

3.4.1. Microclimate

Microclimate and moisture availability are key environmental factors regulating transpiration of forest vegetation. Foliage density and arrangement within healthy forest canopies regulates wind penetration, radiation, air temperature, and relative humidity, that in turn, help drive canopy transpiration (Perry, 1994). While changes in some of these key microclimatic variables have been reported in the later phases (red and grey attack) of MPB attack when needles were partially or completely shed (Boon 2009 and 2012; Winkler et al., 2010), it was unclear if foliar chlorosis and reddening of crowns during the initial green and red attack phases of MPB attack would produce detectable changes in canopy microclimate in the absence of needle shedding characteristic of the later phases of MPB attack.

Results of this research indicated that either no changes in some microclimate variables, or small changes in other variables were evident. However, these small overall changes to microclimate were either unlikely to be ecologically meaningful, or were unrelated to the MPB treatments in this study. No large changes in relative humidity or air temperature were evident after treatment (5% mean increase in air temperature and only 1% change in mean RH). While the change in these variables following treatments were statistically significant, because of the powerful change detection in the BACI study design along with a very large sample size (>900 measurements), the magnitude of change was probably physiologically negligible and unlikely to be a major factor in the transpirations responses observed in this study. In contrast, comparatively large changes in wind speed and net radiation were evident during the post-treatment period relative to the control unit. Net radiation increased after treatments by 11% and 18% in the 50% and 100 % mortality units after treatments, respectively, while wind speed showed both increases and decreases after treatment (8% decline and a 31% increase in the 50% and 100% mortality units respectively). While analyses support the conclusion of a “treatment” response, the changes in net radiation were potentially not ecologically meaningful when considered in the context of the range of variability among sites during pre and post-treatment periods (Figures 3-2 and 3-3). More importantly, the effects on wind speed were not monotonic with increasing intensity of treatments across the 50- and 100% mortality units, suggesting these effects were likely unrelated to the MPB treatments. Indeed, some extensive harvesting took place immediately outside of the study area during the post-treatment period and this likely affected wind dynamics within the study plots (including the control) as evidenced by some isolated, but not insignificant blowdown of trees within the study plots. This feature alone was probably implicated in both the increased variability in wind speed (because of greater wind penetration into the canopy) and the more minor changes in net radiation during the post-treatment period. However, this was unlikely to have driven the changes observed in transpiration observed in the study. A decrease in wind speed would counteract the effects on

evaporative demand produced by an increase in net radiation observed in the 50% mortality unit; whereas a decrease in transpiration was observed in the 100% mortality unit despite the increase in both net radiation and wind observed after treatment in that unit. Thus the variable intensity MPB attack simulated using herbicide in this study produced no clear evidence of changes to microclimate after treatments.

While no studies to my knowledge have described coupled changes in growing season microclimate and forest evaporative losses after MPB attack, numerous studies have documented such changes after other types of forest disturbance such as fire, clear-cut harvesting, partial cutting, or thinning (Stednick, 1996; Andreassian, 2004; Brown et al., 2005; Shakesby and Doerr, 2006; Montes-Helu et al., 2009). Large changes in daytime radiation reaching the ground surface leading to increased air temperatures (Hungerford 1980), decreased afternoon relative humidity (Miller et al. 1983), and potentially large diurnal air temperature variation (Keenan and Kimmins 1993) have all been reported after severe canopy disturbance from clear-cut harvesting. However, moderate to large changes in microclimate have also been reported after less severe canopy disturbance associated with partial-cut harvesting systems. Man and Lieffers (1999) and Zheng et al. (2000) reported lower relative humidity and higher temperature and vapor pressure deficit at near ground levels (~0.2 m) following thinning. In particular, wind speed and its associated influence on microclimate appears strongly responsive to canopy disturbance (Bladon et al., 2006; Marenholtz et al., 2010). Rudnicki et al. (2003) observed a three-fold increase in wind speed at the canopy level following a moderate thinning treatment that removed only understory spruce and suppressed/intermediate crown classes in a lodgepole pine stand. Similarly, Bladon et al. (2006) reported that both increased canopy wind penetration and increased mid-day net radiation after low intensity variable retention-harvesting were strongly coupled with increased transpiration of aspen, balsam poplar, white spruce, and lodgepole pine. Consistent with my results, Bladon et al. (2006) did not observe large changes in relative humidity, air temperature and vapor pressure deficit at canopy height, and concluded that the impact of partial harvesting on those microclimate variables were physiologically negligible.

Given the microclimate responses measured in this study were not strongly, nor clearly evident, changes observed in transpiration dynamics of live within dead trees in the 50% mortality unit were likely driven entirely by increased below ground soil moisture due to the reduced transpiration of neighbouring trees (fading/dead). This suggests that early MPB attacks are notably different than those observed in harvested systems (clear-cut or partial cut) because microclimate was not a factor in the transpiration responses observed.

3.4.2. Transpiration dynamics of individual trees

Results of this study also indicated clear differences in transpiration of both live within dead, and fading trees, which are important components of stand transpiration response after MPB attack. Increases in S_F , T_t , and T_g of live within

dead trees after treatment (adjusted to account for changes in transpiration of control trees before- and after treatment) were 38%, 21%, and 21%, respectively (Table 3-2). In contrast, a strong decline in all transpiration variables was observed after treatment in fading trees (100% mortality unit) compared to live trees (Table 3-1). Adjusted median T_t and T_g of fading trees were both only 22% of that observed in live trees after treatment suggesting a very strong (78%) reduction in transpiration of fading trees (Table 3-2). Again, while there is currently no published research (to my knowledge) documenting transpiration responses in lodgepole pine during the initial phases of MPB attack, results of this study strongly suggest the variable responses among different categories of trees are key to understanding how MPB attack is likely to affect water balance of MPB forests. While the mechanisms involved in disruption of transpiration from herbicide treatments differ from that of MPB attack, the stand scale effects of the MPB treatments were analogous in terms of effects on tree mortality and canopy structural composition. In particular, the MPB directly disrupts the hydraulic conductivity of tree vascular systems through occlusion of tracheids by fungal mycelia whereas the overall effect of glyphosate interferes with physiological processes that indirectly generate steep reduction in stomatal conductance. While the trees to which herbicide was applied in the 100% mortality site experienced a steep reduction in g_c (Table 3-1 and 3-2), transpiration still paralleled the seasonal and diurnal patterns of atmospheric drivers of moisture demand (Figure 3-5 and 3-6). This generally is consistent with the impacts of xylem cavitation and loss of sapwood hydraulic conductivity in lodgepole pine, which results in strongly reduced transpiration (Reid et al., 2006; Andrews et al., 2012). Thus the overall effect of both MPB attack and herbicide treatments used in this study on tree physiologic controls over water loss are highly similar and support the interpretation of herbicide application as an adequate surrogate for MPB attacked on tree transpiration dynamics. However, while results of this study show fading trees have a potentially important role on stand water use during the initial green to red attack phases, once these fading trees die, their contribution to stand level transpiration will likely drop to zero.

In contrast to fading trees, the role of live within dead trees will likely continue to constitute an important component of MPB attacked stands where <100% of the trees are attacked, as is more commonly the case. The transpiration responses of live within dead trees observed in this study were generally similar to response of trees after thinning or partial-cut harvesting. Observations of improved soil water access following thinning in lodgepole pine stands, together with the close link between stomatal behaviour and soil water availability experiencing periodic drought stress, suggest that the whole tree canopy stomatal conductance in lodgepole pine is closely linked to soil water availability (Bosch and Hewlett, 1982; Reid et al., 2006; Andrews et al., 2012). Thus, the potential exists for surviving trees to buffer the stand from dramatic changes in stand water use after MPB attack. Reduction of transpiration within stands can increase root water availability, which has the potential to produce a positive effect on transpiration of surviving trees. For example, changes in stand conditions such as a thinning can trigger a compensatory response of surviving

trees on overall water loss from stand, where reduction of demand for water can result in increased water availability in the rooting zone. Reid et al. (2006) reported increased water use in thinned lodgepole pine stands was associated with greater soil moisture after the first growing season following thinning. However, because changes in micro-climate after partial harvesting are strongly associated with transpiration response of surviving trees (Reid et al. 2006; Bladon et al. 2006), results of this previous research are not directly comparable to the present study, where no meaningful change in microclimate was observed. Thus transpiration responses of live within dead trees observed in this study are unique and most likely a response to improved access to rooting zone moisture resulting from death of neighbouring trees

3.4.3. Transpiration response of lodgepole pine to variable intensity MPB attack

Stand scale transpiration after MPB attack reflects the additive contribution of transpiration from surviving (live within dead), and fading trees which makes predicting overall transpiration response to MPB attack difficult. However, because the transpiration response of trees in these categories was measured, this study enabled documenting the overall effect of variable intensity, early phase MPB attack. Results from scaling individual tree transpiration to the stand scale clearly indicated that the additive contribution of differing tree categories to total stand transpiration in the 50% mortality site was not different from that of the reference control stand. The increased transpiration from live within dead trees, strongly support the idea of a compensatory response on transpiration at the stand level in lodgepole pine forests. While greater transpiration of younger forests with species that have high water use has been previously reported (see Hornbeck et al., 1993, and 1997), results showing surviving trees of the same species can actually compensate for dying trees has not been shown anywhere (to my knowledge).

Furthermore, results from varying the proportions of live within dead trees in four hypothetical modeled scenarios (Figure 3-8), suggests that surviving or live within dead trees play a critical role in governing the stand scale response across a gradient of intensity of MPB attack. In particular, results indicate that stand scale transpiration in stands with less than 1/3 of the trees killed by MPB are unlikely to be less than transpiration of healthy pine stands. Where the intensity of MPB attack affects less than 1/3 of the stand, stand level transpiration of partially attacked stands may actually exceed that of healthy stands while increasing intensity of MPB attack affecting greater 1/3 of the stand is likely to produce proportional decreases in stand level water use.

Schmid et al. (1991) argued that different tree strata should be considered in evaluating stand hydrological responses to the MPB attack because differential transpiration among strata can result in more conservative transpiration responses to disturbance at the stand-level (Kelliher et al., 1993; Roberts, 1983; Phillips and Oren, 2001). Indeed, my results provide strong evidence in support of this argument. This compensatory response represents a buffered response in

transpiration at the stand level and reflects the integrated stand-scale effect of the differential transpiration responses of remaining strata in the stands. While previous efforts at modelling impacts of MPB on forest water balance have summarized forest transpiration only in terms of live and dead trees (see review in Uunila et al., 2006), results of the present study highlight the importance of understanding the effects of MPB on lodgepole pine transpiration at both the tree and stand levels.

3.5. Conclusions

This study represents the first research (to my knowledge) documenting the early impacts of MPB attack on micro-climate and transpiration dynamics in lodgepole pine. While no meaningful changes in microclimate were evident during the early green-red attack phases of simulated MPB attack, strong variation in transpiration of several distinct categories of trees were observed. The additive contribution of both increased transpiration by surviving trees and decreased transpiration by fading and dead trees resulted in no meaningful change in overall stand transpiration in a stand with 50% MPB attack, whereas a 92% reduction in transpiration was observed in another stand with 100% MPB attack. This study also highlights the importance of understanding the effects of MPB on transpiration at both the tree- and stand-levels where the compensatory response at the stand-scale would depend on the relative distribution of dying and live trees. These results demonstrated that transpiration response to variable intensity MPB attack is unique in the research literature, yet a critical component to understanding how MPB is likely to impact forest water balance and hydrology of vulnerable landscapes.

3.6. References

- Alila, Y., D. Bewley, et al. (2009). Effects of pine beetle infestations and treatments on hydrology and geomorphology: integrating stand-level data and knowledge in mesoscale watershed functions. Mountain Pine Beetle Working Paper. Victoria, BC, Natural Resources Canada, Canadian Forest Service, Pacific Forestry Centre: 69.
- Andreassian, V. (2004). "Waters and forests: from historical controversy to scientific debate." Journal of Hydrology **291**(1-2): 1-27.
- Andrews, S. F., L. B. Flanagan, et al. (2012). "Variation in water potential, hydraulic characteristics and water source use in montane Douglas-fir and lodgepole pine trees in southwestern Alberta and consequences for seasonal changes in photosynthetic capacity." Tree Physiology **32**(2): 146-160.
- Ballard, R. G., M. A. Walsh, et al. (1982). "Blue-stain fungi in xylem of lodgepole pine - a light-microscope study on extent of hyphal distribution." Canadian Journal of Botany-Revue Canadienne De Botanique **60**(11): 2334-2341.
- Ballard, R. G., M. A. Walsh, et al. (1984). "The penetration and growth of blue-stain fungi in the sapwood of lodgepole pine attacked by mountain pine-beetle." Canadian Journal of Botany-Revue Canadienne De Botanique **62**(8): 1724-1729.
- Beckingham, J. D., J. H. Archibald, et al. (1996). Field guide to ecosites of west-central Alberta. Edmonton, Northern Forestry Centre.
- Bewley, D., Y. Alila, et al. (2010). "Variability of snow water equivalent and snow energetics across a large catchment subject to Mountain Pine Beetle infestation and rapid salvage logging." Journal Of Hydrology **388**(3-4): 464-479.
- Bladon, K. D., U. Silins, et al. (2006). "Differential transpiration by three boreal tree species in response to increased evaporative demand after variable retention harvesting." Agricultural And Forest Meteorology **138**(1-4): 104-119.
- Boon, S. (2009). "Snow ablation energy balance in a dead forest stand." Hydrological Processes **23**(18): 2600-2610.
- Boon, S. (2012). "Snow accumulation following forest disturbance." Ecohydrology **5**(3): 279-285.
- Bosch, J. M. and J. D. Hewlett (1982). "A review of catchment experiments to determine the effect of vegetation changes on water yield and evapotranspiration." Journal of Hydrology **55**(1-4): 3-23.
- Brown, A. E., L. Zhang, et al. (2005). "A review of paired catchment studies for determining changes in water yield resulting from alterations in vegetation." Journal of Hydrology **310**(1-4): 28-61.
- Burton, P. J. (2008). "The mountain pine beetle as an agent of forest disturbance: From Lessons Learned to Community-based Solutions Conference Proceedings." BC Journal of Ecosystems and Management **9**(3): 9-13.
- Chambers, J. M., W. S. Cleveland, et al. (1983). Graphical methods for data analysis. Boston, Wadsworth & Brooks/Cole.
- Chojnacky, D. C., B. J. Bentz, et al. (2000). Mountain pine beetle attack in ponderosa pine: Comparing methods for rating susceptibility Research Paper. Fort Collins, U.S. Department of Agriculture, Forest Service, Rocky Mountain Research Station: 10 p.

- Clearwater, M. J., F. C. Meinzer, et al. (1999). "Potential errors in measurement of nonuniform sap flow using heat dissipation probes." Tree Physiology **19**(10): 681-687.
- Cole, D. J., J. C. Caseley, et al. (1983). "Influence of glyphosate on selected plant processes." Weed Research **23**(3): 173-183.
- Cole, D. J., A. D. Dodge, et al. (1980). "Some biochemical effects of glyphosate on plant meristems." Journal of Experimental Botany **31**(125): 1665-1674.
- Despain, D. G. (2001). "Dispersal ecology of lodgepole pine (*Pinus contorta* Dougl.) in its native environment as related to Swedish forestry." Forest Ecology and Management **141**: 59-68.
- Downing, D. J. and W. W. Pettapiece (2006). Natural regions and subregions of Alberta. Edmonton, Government of Alberta.
- Fraser, E. C., V. J. Loeffers, et al. (2005). "Age, stand density, and tree size as factors in root and basal grafting of lodgepole pine." Canadian Journal of Botany **83**(8): 983-988.
- Granier, A. (1985). "A new method of sap flow measurement in tree stems." Annales Des Sciences Forestieres **42**(2): 193-200.
- Granier, A. (1987). "Evaluation of transpiration in a douglas-fir stand by means of sap flow measurements." Tree Physiology **3**(4): 309-319.
- Granier, A., T. Anfodillo, et al. (1994). "Axial and radial water-flow in the trunks of oak trees - a quantitative and qualitative-analysis." Tree Physiology **14**(12): 1383-1396.
- Granier, A., P. Biron, et al. (1996). "Comparisons of xylem sap flow and water vapour flux at the stand level and derivation of canopy conductance for Scots pine." Theoretical And Applied Climatology **53**(1-3): 115-122.
- Granier, A., V. Bobay, et al. (1990). "Vapor flux-density and transpiration rate comparisons in a stand of maritime pine (*pinus-pinaster ait*) in les-landes forest." Agricultural and Forest Meteorology **51**(3-4): 309-319.
- Green, R. H. (1979). Sampling design and statistical methods for environmental biologists. New York, Wiley.
- Hélie, J. F., D. L. Peters, et al. (2005). Review and synthesis of potential hydrologic impacts of mountain pine beetle and related harvesting activities in British Columbia. Victoria, Natural Resources Canada, Canadian Forest Service, Pacific Forestry Centre. **Mountain Pine Beetle Initiative Working Paper 2005-23**: 34.
- Hollander, H. and N. Amrhein (1980). "The site of the inhibition of the shikimate pathway by glyphosate .1. inhibition by glyphosate of phenylpropanoid synthesis in buckwheat (*Fagopyrum-esculentum* moench)." Plant Physiology **66**(5): 823-829.
- Hornbeck, J. W., M. B. Adams, et al. (1993). "Long-term impacts of forest treatments on water yield - a summary for northeastern USA." Journal Of Hydrology **150**(2-4): 323-344.
- Hornbeck, J. W., C. W. Martin, et al. (1997). "Summary of water yield experiments at Hubbard Brook Experimental Forest, New Hampshire." Canadian Journal of Forest Research-Revue Canadienne De Recherche Forestiere **27**(12): 2043-2052.
- Hungerford, R. D. (1980). Microenvironmental response to harvesting and residue management. Environmental consequences of timber harvesting in Rocky Mountain coniferous forest, Ogden, Utah, USDA, Forest Service, Intermountain Forest and Range Experiment Station.

- Kaufmann, M. R. (1985). "Annual transpiration in subalpine forests: large differences among four tree species." Forest Ecology and Management **13**: 235-246.
- Keenan, R. J. and J. P. Kimmins (1993). "The ecological effects of clear-cutting." Environmental Reviews **1**(2): 121-144.
- Kelliher, F. M., R. Leuning, et al. (1993). "Evaporation and canopy characteristics of coniferous forests and grasslands." Oecologia **95**(2): 153-163.
- Knight, D. H., T. Fahey, et al. (1981). "Transpiration from 100-yr-old Lodge Pole pine forests estimated with whole-tree potometers." Ecology **62**(3): 717-726.
- Lagergren, F. and A. Lindroth (2002). "Transpiration response to soil moisture in pine and spruce trees in Sweden." Agricultural and Forest Meteorology **112**(2): 67-85.
- Lee, T. T. (1981). "Effects of glyphosate on synthesis and degradation of chlorophyll in soybean and tobacco cells." Weed Research **21**(3-4): 161-164.
- Lee, T. T. (1982). "Mode of action of glyphosate in relation to metabolism of indole-3-acetic-acid." Physiologia Plantarum **54**(3): 289-294.
- Longley, L. W. (1972). Precipitation in the canadian praires. Atmospheric Environment Service, Toronto, Canadian Department of the Environment.
- Man, R. Z. and V. J. Liefers (1999). "Effects of shelterwood and site preparation on microclimate and establishment of white spruce seedlings in a boreal mixedwood forest." Forestry Chronicle **75**(5): 837-844.
- Marenholtz, E. H., V. J. Liefers, et al. (2010). "Evaporative demand across a range of microsites in partial-cut boreal forests." Scandinavian Journal of Forest Research **25**(2): 118-126.
- McCulloh, K. A., K. Winter, et al. (2007). "A comparison of daily water use estimates derived from constant-heat sap-flow probe values and gravimetric measurements in pot-grown saplings." Tree Physiology **27**(9): 1355-1360.
- Miller, A., J. C. Thompson, et al. (1983). Elements of meteorology. Columbus, Charles E. Merrill Publishing Company.
- Monteith, J. L. and M. H. Unsworth (1990). Principles of environmental physics. New York, Edward Arnold.
- Montes-Helu, M. C., T. Kolb, et al. (2009). "Persistent effects of fire-induced vegetation change on energy partitioning and evapotranspiration in ponderosa pine forests." Agricultural and Forest Meteorology **149**(3-4): 491-500.
- Muñoz-Rueda, A., C. Gonzalez-Murua, et al. (1986). "Effects of glyphosate [n-(phosphonomethyl)glycine] on photosynthetic pigments, stomatal response and photosynthetic electron-transport in medicago-sativa and trifolium-pratense." Physiologia Plantarum **66**(1): 63-68.
- Natural Regions Committee (2006). Natural regions and subregions of Alberta. D. D.J. and W. W. Pettapiece, Government of Alberta.
- Neimann, K. O. and F. Visintini (2004). Assessment of potential for remote sensing detection of bark beetle-infested areas during a green attack: a literature review. Mountain Pine Beetle Initiative. Victoria, Natural Resources Canada, Canadian Forest Service.
- Nelson, T., B. Boots, et al. (2006). "Rating the susceptibility of forests to mountain pine beetle infestations: the impact of data." Canadian Journal of Forest Research-Revue Canadienne De Recherche Forestiere **36**(11): 2815-2825.

- Nkemdirim, L. C. and L. Weber (1976). "Wet and dry sequences in precipitation regimes." *Geografiska Annaler Series a-Physical Geography* **58**(4): 303-315.
- Perry, D. A. (1994). *Forest Ecosystems*. Baltimore, USA, Johns Hopkins University Press.
- Phillips, N. and R. Oren (2001). "Intra- and inter-annual variation in transpiration of a pine forest." *Ecological Applications* **11**(2): 385-396.
- R Core Team (2012). *R: A language and environment for statistical computing*. Vienna, R Foundation for Statistical Computing.
- Raffa, K. F., B. H. Aukema, et al. (2008). "Cross-scale drivers of natural disturbances prone to anthropogenic amplification: The dynamics of bark beetle eruptions." *Bioscience* **58**(6): 501-517.
- Redding, T. E., R. D. Winkler, et al. (2008). *Mountain pine beetle and watershed hydrology: A synthesis focused on the Okanagan*. One Watershed – One Water, Kelowna, BC, Canadian Water Resources Association.
- Reid, D. E. B., U. Silins, et al. (2006). "Sapwood hydraulic recovery following thinning in lodgepole pine." *Annals of Forest Science* **63**: 329-338.
- Roberts, J. (1983). "Forest transpiration - a conservative hydrological process." *Journal Of Hydrology* **66**(1-4): 133-141.
- Rudnicki, M., V. J. Lieffers, et al. (2003). "Stand structure governs the crown collisions of lodgepole pine." *Canadian Journal of Forest Research-Revue Canadienne De Recherche Forestiere* **33**(7): 1238-1244.
- Saugier, B., A. Granier, et al. (1997). "Transpiration of a boreal pine forest measured by branch bag, sap flow and micrometeorological methods." *Tree Physiology* **17**(8-9): 511-519.
- Schmid, J. M., S. A. Mata, et al. (1991). "Net Precipitation Within Small Group Infestations of the Mountain Pine Beetle." *USDA Forest Service, Rocky Mountain Forest and Range Experiment Station Research Note RM-508*: 4.
- Schnorbus, M. (2011). A synthesis of the hydrological consequences of large-scale mountain pine beetle disturbance. *Mountain Pine Beetle Working Paper 2010-01*. Victoria, Natural Resources Canada, Canadian Forest Service, Pacific Forestry Centre: 30.
- Shakesby, R. A. and S. H. Doerr (2006). "Wildfire as a hydrological and geomorphological agent." *Earth-Science Reviews* **74**(3-4): 269-307.
- Shaner, D. L. and J. L. Lyon (1979). "Somatal cycling in *Phaseolus-vulgaris* l in response to glyphosate." *Plant Science Letters* **15**(1): 83-87.
- Simonin, K., T. E. Kolb, et al. (2007). "The influence of thinning on components of stand water balance in a ponderosa pine forest stand during and after extreme drought " *Agricultural and Forest Meteorology* **143**: 266-276.
- Smith, D. M. and S. J. Allen (1996). "Measurement of sap flow in plant stems." *Journal of Experimental Botany* **47**(305): 1833-1844.
- Spittlehouse, D. L. (2002). *Sap flow and transpiration of old lodgepole pine trees*. 26th Conference on Agricultural and Forest Meteorology, Norfolk, Virginia, American Meteorological Society.
- Stednick, J. D. (1996). "Monitoring the effects of timber harvest on annual water yield." *Journal Of Hydrology* **176**(1-4): 79-95.
- Stewart-Oaten, A., J. R. Bence, et al. (1992). "Assessing effects of unreplicated perturbations: no simple solutions." *Ecology* **73**(4): 1396-1404.
- Stewart-Oaten, A., W. W. Murdoch, et al. (1986). "Environmental-impact assessment - pseudoreplication in time." *Ecology* **67**(4): 929-940.

- Swanson, R. H. (1994). "Significant historical developments in thermal methods for measuring sap flow in trees." Agricultural and Forest Meteorology **72**(1-2): 113-132.
- Taylor, S. W., A. L. Carrol, et al. (2006). Forest, climate and mountain pine beetle dynamics. The mountain pine beetle: A synthesis of its biology, management and impacts on lodgepole pine. L. Safranyik and W. B., Natural Resources Canada, Canadian Forest: 67-94.
- Uunila, L., B. Guy, et al. (2006). "Hydrologic effects of mountain pine beetle in the interior pine forests of British Columbia: key questions and current knowledge." Streamline **9**(2): 1-6.
- Winkler, R., S. Boon, et al. (2010). "Assessing the effects of post-pine beetle forest litter on snow albedo." Hydrological Processes **24**(6): 803-812.
- Zar, J. (1999). Biostatistical analysis. Upper Saddle River, Prentice Hall.
- Zheng, D. L., J. Q. Chen, et al. (2000). "Effects of silvicultural treatments on summer forest microclimate in southeastern Missouri Ozarks." Climate Research **15**(1): 45-59.

3.7. Tables

Table 3-1. Median sap velocity (S_v), sap flow (S_f), transpiration per unit leaf area (T_t), transpiration per unit ground area (T_g), and canopy conductance (g_c) before and after treatment application of live, live within dead (50% mortality unit), and fading trees (100% mortality unit). Live 1, 2 and 3 correspond to transpiration measured in the control (Cnt), 50% and 100% mortality sites prior to treatment application, respectively.

Variable	Before			After		
	Live 1 (Cnt)	Live 2 (50%)	Live 3 (100%)	Live 1 (Cnt)	Live w/dead (50%)	Fading (100%)
S_v (cm d ⁻¹)	33.4	26.4	34.9	29.5	24.1	20.1
S_f (g d ⁻¹)	4082	4071	4506	5678	7840	2489
T_t (mm d ⁻¹)	0.10	0.12	0.15	0.09	0.12	0.06
T_g (mm d ⁻¹)	0.48	0.57	0.71	0.41	0.58	0.28
g_c (mm s ⁻¹)	1.19	1.53	2.11	1.38	1.87	1.10

Table 3-2. Relative change in median sap velocity (S_v), sap flow (S_f), transpiration per unit leaf area (T_t), transpiration per unit ground area (T_g), and canopy conductance (g_c) after application of treatments for live, live within dead, and fading trees adjusted relative to live trees in the control. Relative change for each variable after treatment was calculated as $1 + [((\text{post-treatment treated unit})/(\text{post-treatment live1 unit})) - ((\text{pre-treatment treated unit})/(\text{pre-treatment Live1 unit}))]$ where 1 indicates no relative adjusted change after treatment.

Variable	Live (Control)	Live w/dead (50% mortality)	Fading (100% mortality)
S_v (cm d ⁻¹)	1.00	1.03	0.64
S_f (g d ⁻¹)	1.00	1.38	0.33
T_t (mm d ⁻¹)	1.00	1.21	0.22
T_g (mm d ⁻¹)	1.00	1.21	0.22
g_c (mm s ⁻¹)	1.00	1.07	0.03

Table 3-3. Median T_{st} (mm d⁻¹) before and after treatment application in the control, 50% and 100% mortality (mort.) sites.

Variable	Before			After		
	Control	50% mort.	100% mort.	Control	50% mort.	100% mort.
T_{st}	0.48	0.57	0.71	0.41	0.49	0.23

Table 3-4. Percentage of trees in three categories used in scenarios and corresponding total seasonal (May-Sept, 2010) stand-scale transpiration (T_{st}) for each of four scenarios of partial MPB attack. The reference T_{st} (control conditions) was 77 mm.

Live within dead (%)	Fading trees (%)	Dead trees (%)	T_{st} (mm)
75	15	10	85
50	30	20	67
25	45	30	50
5	56	39	36

The baseline proportion of fading and dead trees in scenarios was based on their relative proportions measured in the 50% Mortality unit in 2010: live within dead 77.5%, fading 13.4%, and dead 9.1%.

3.8. Figures

Figure 3-1. Study location and layout of treatment units (2.2 ha. each), climate stations, sapflow measurements. Dotted pattern indicates presence of dead trees (red foliage) from supervised classification of a color orthophoto taken in 2010. Asterisks indicate the approximate location of sapflow measurements (re-located within units every year).

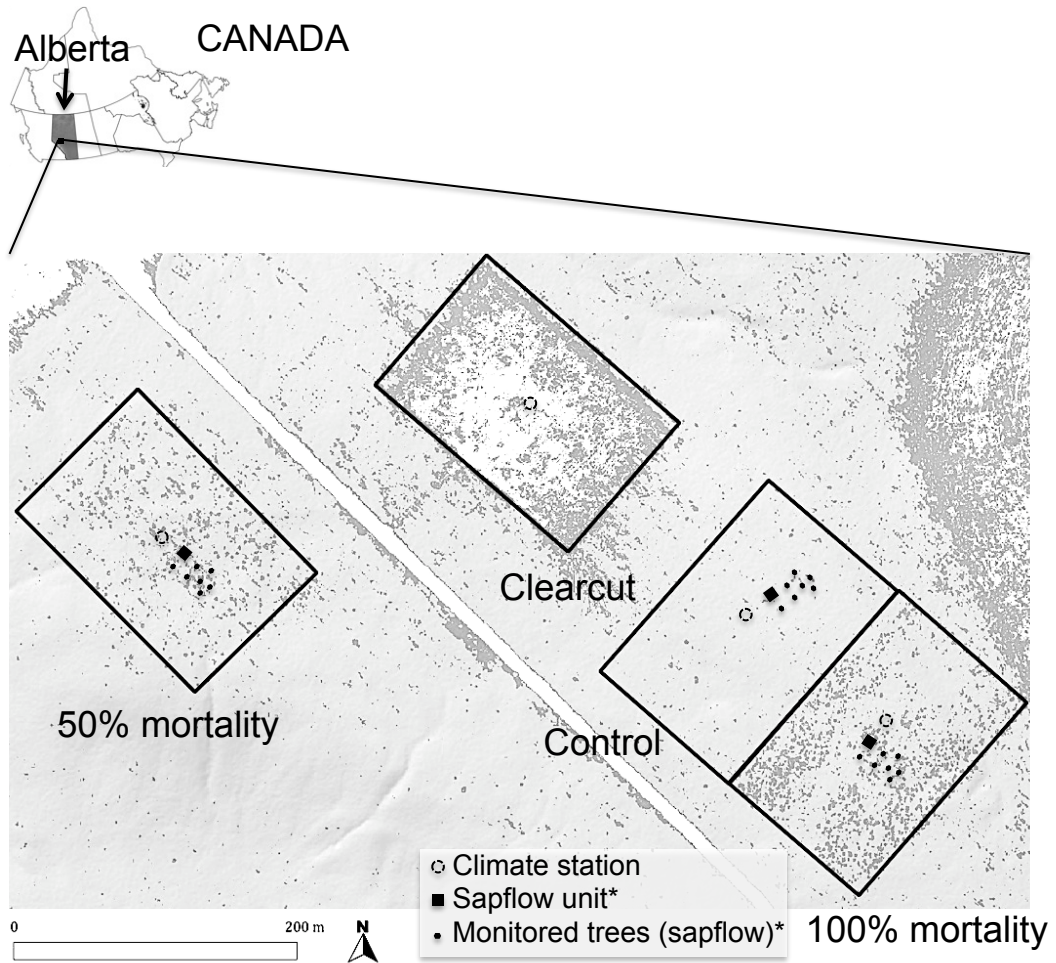


Figure 3-2. Relationship of mean daily air temperature ($T^{\circ}\text{C}$), relative humidity (RH), wind speed (m s^{-1}), and net radiation (W m^{-2}) in the 50% (left) and 100% (right) mortality units with that of the control unit before (filled symbols) and after (hollow symbols) treatment application.

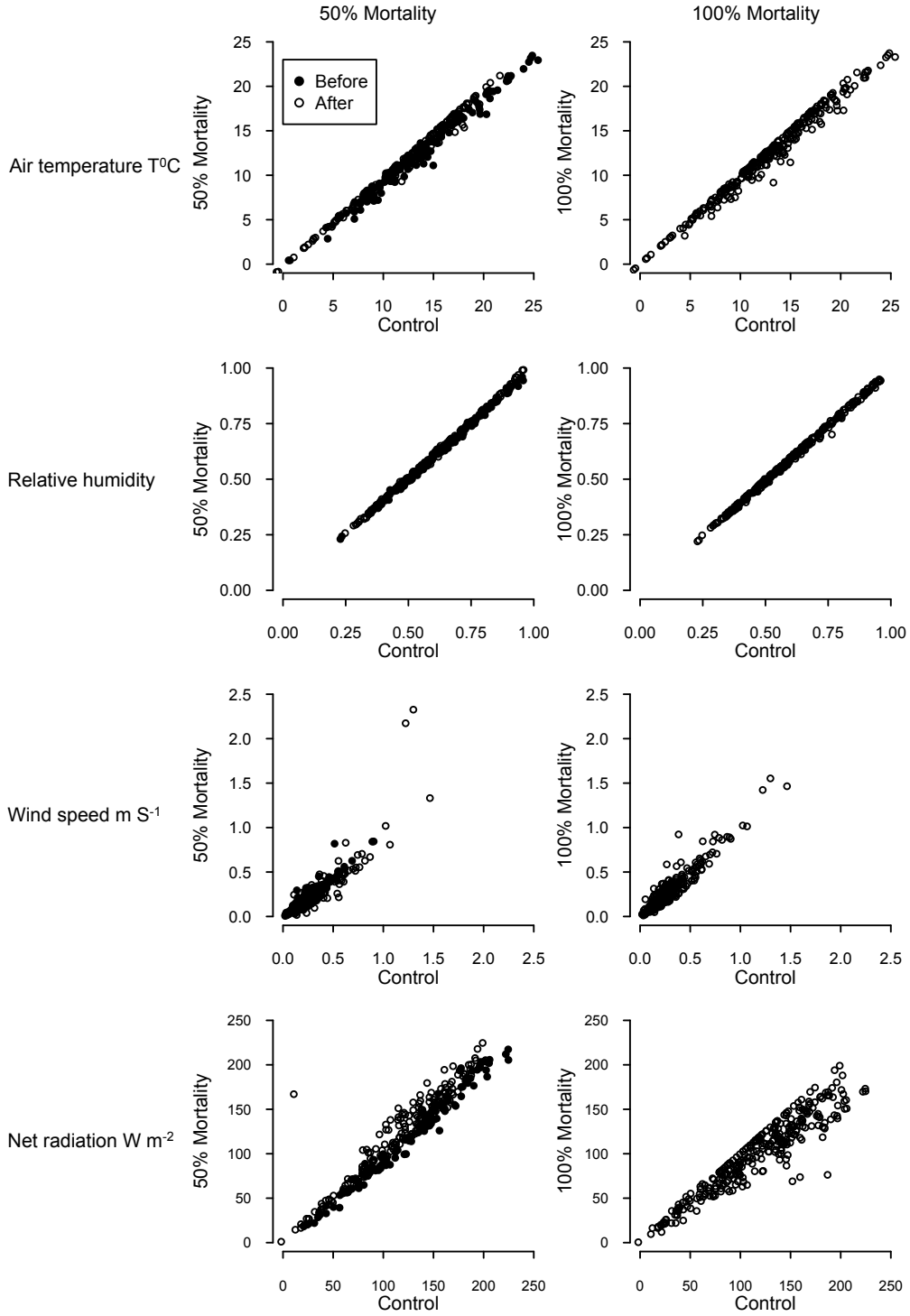


Figure 3-3. Mean air temperature (T °C), relative humidity (RH), wind speed ($m s^{-1}$), and net radiation ($W m^{-2}$) of control, 50% and 100% mortality units before and after treatment application. Error bars indicate 95% confidence intervals.

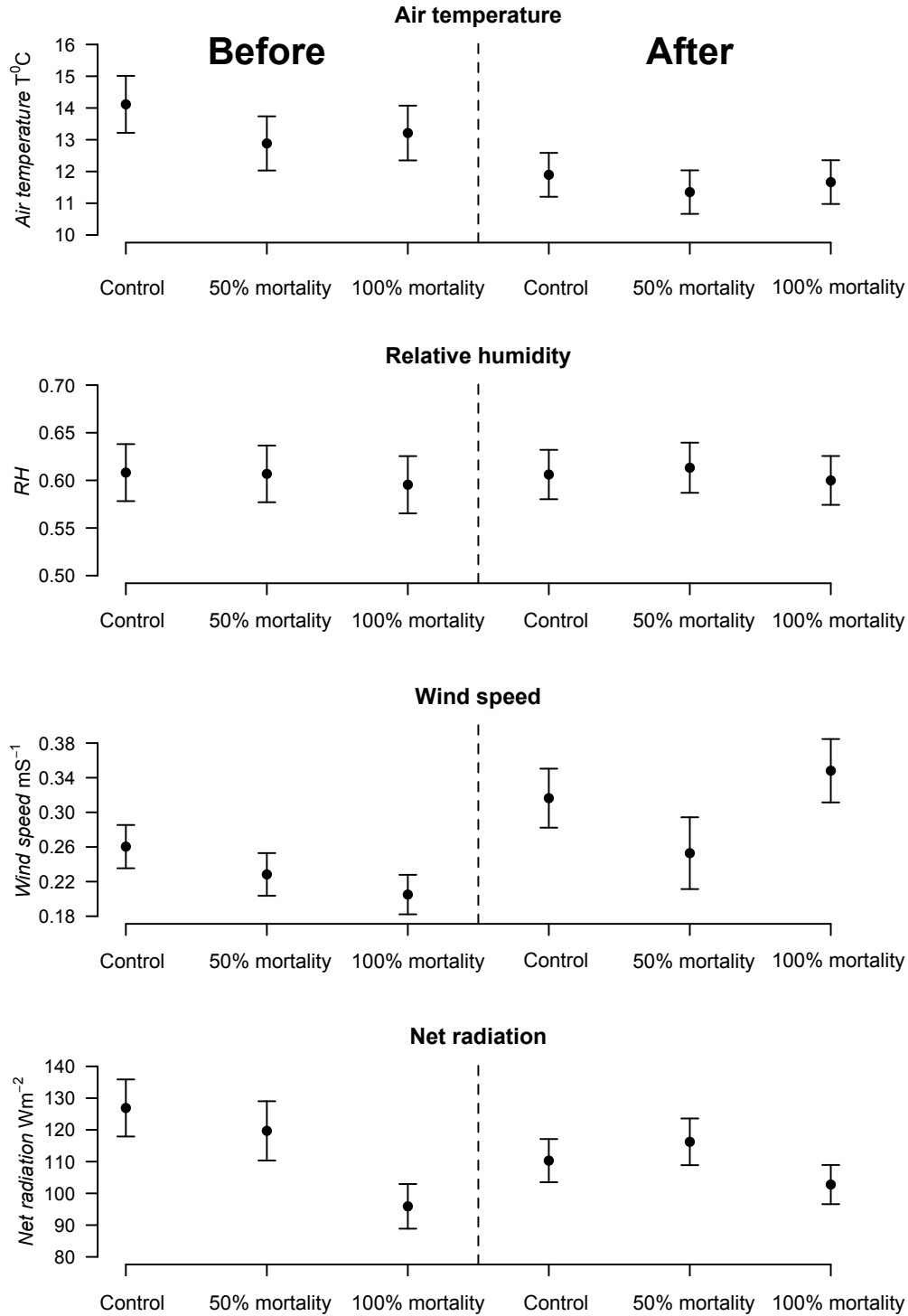


Figure 3-4. Distribution of transpiration (T_t , $m^3 m^2 day^{-1}$) of live, live within dead, and fading trees before and after treatment application. Dark horizontal lines on boxplots indicate median, boxes indicate interquartile range (IQR), whiskers (extremes) indicate extreme range ($1.5 \times IQR$), box widths are proportional to square root (n), and notches indicate approximate 95% confidence intervals [$\pm 1.58 IQR/\text{square root } (n)$].

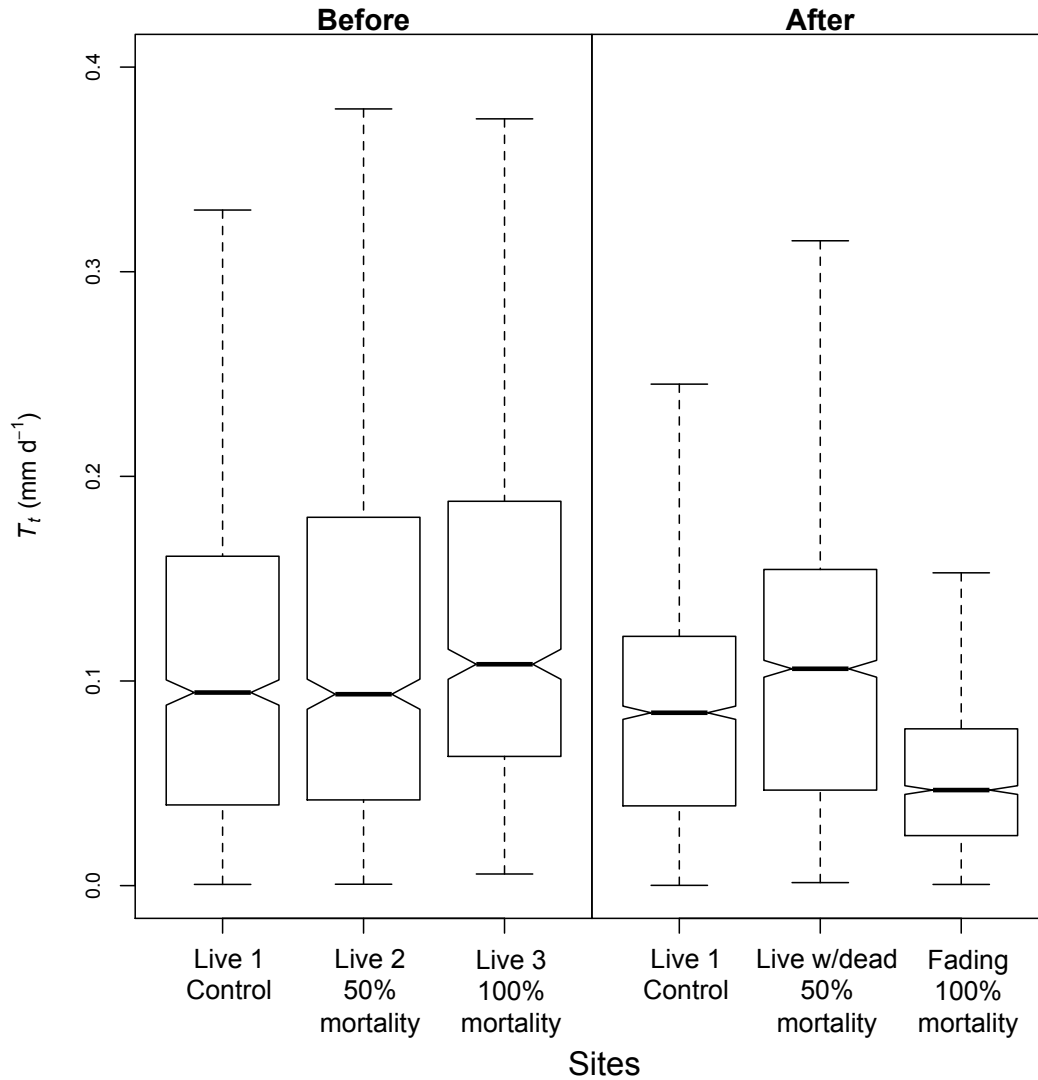


Figure 3-5. Typical diurnal patterns of median hourly transpiration (T_g , mm d⁻¹, unit ground area basis) of live, live within dead, and fading trees in the control, 50%, and 100% mortality sites, respectively, during sunny, clear-sky conditions (Julian days 133-135, 2011).

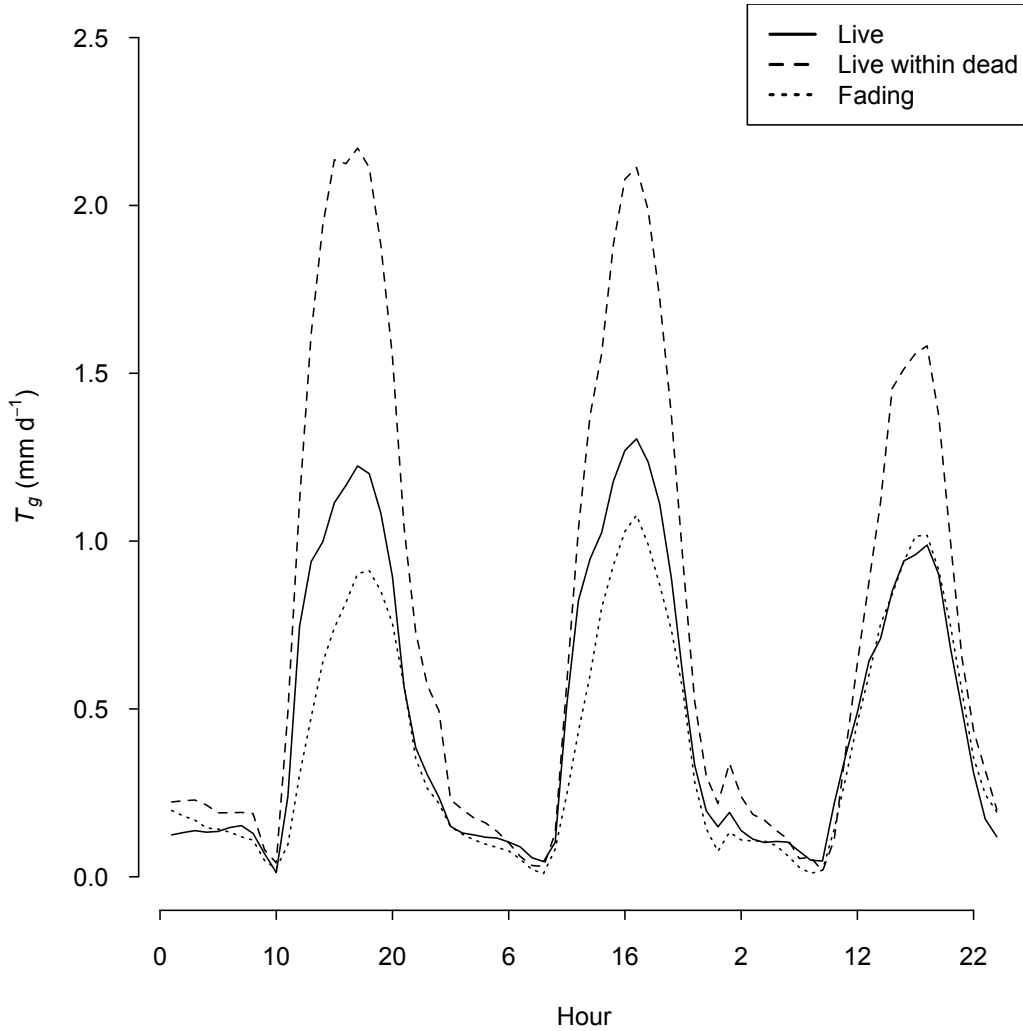


Figure 3-6. Median daily transpiration per unit ground area (T_g , mm) of live, live within dead and fading trees in 2010. Symbols indicate daily medians (n=7) embedded in shaded bands/edge lines representing the upper and lower inter-quartile range of each tree category.

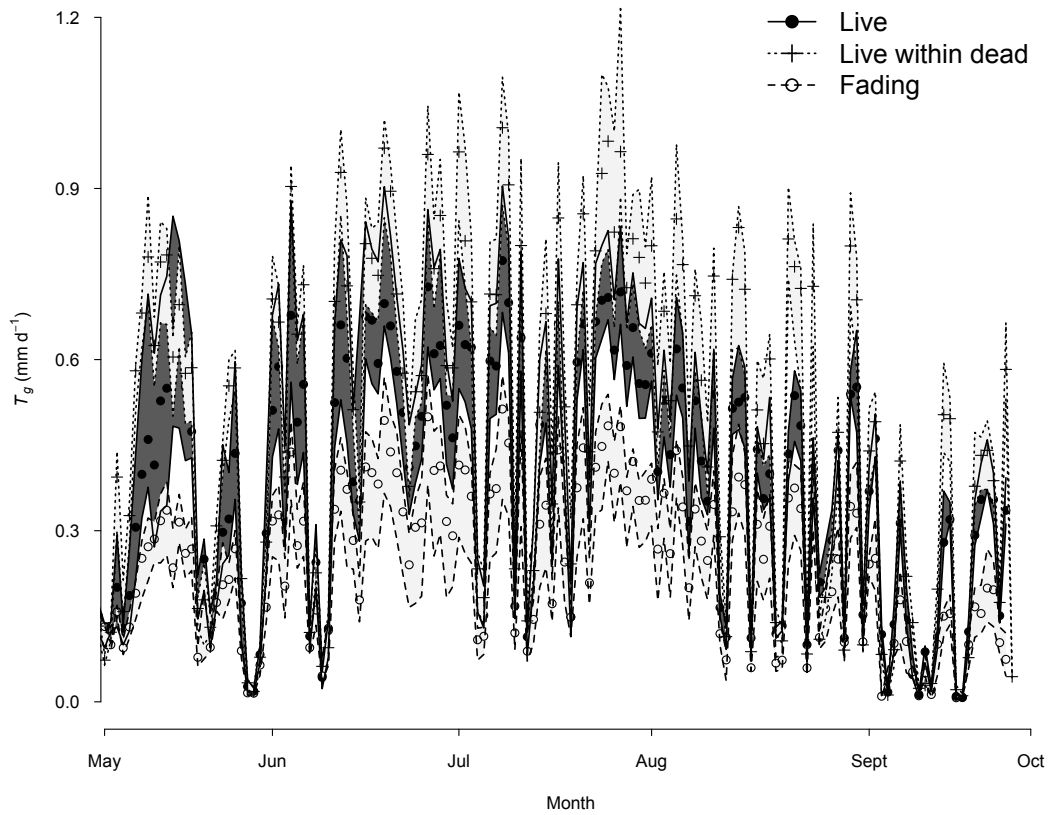


Figure 3-7. Relationships between median daily transpiration per unit ground area (T_g , mm) of live within dead (50 % mortality unit), and fading trees (100% mortality unit) trees with live trees (control unit) before (filled symbols) and after (hollow symbols) treatment application. Short-dashed lines indicate linear regressions before treatment for 50% ($y = 0.85x + 0.13$, $R^2 = 0.63$) and 100% mortality ($y = 0.99 + 0.20$, $R^2 = 0.57$) units, whereas long-dashed lines indicate relationships after treatment for 50% ($y = 1.29x + 0.01$, $R^2 = 0.84$), and 100% mortality ($y = 0.70x + 0.00$, $R^2 = 0.75$) units.

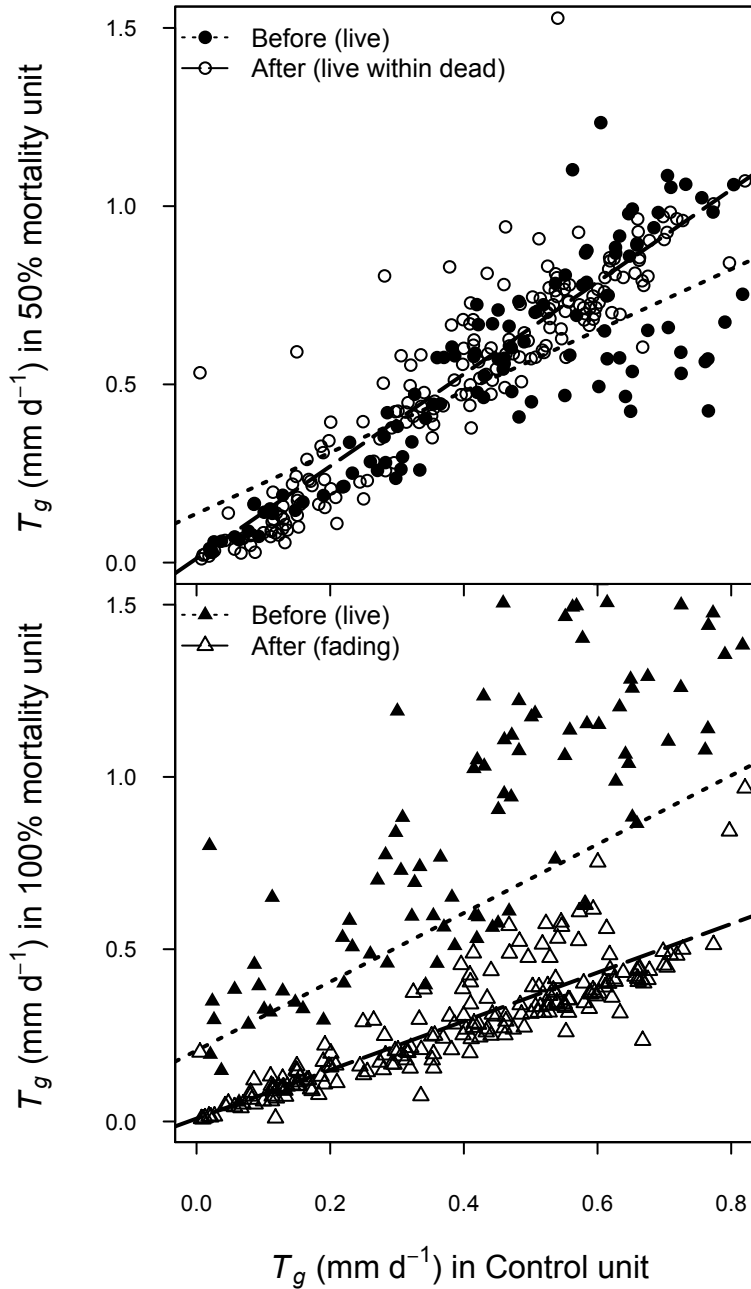
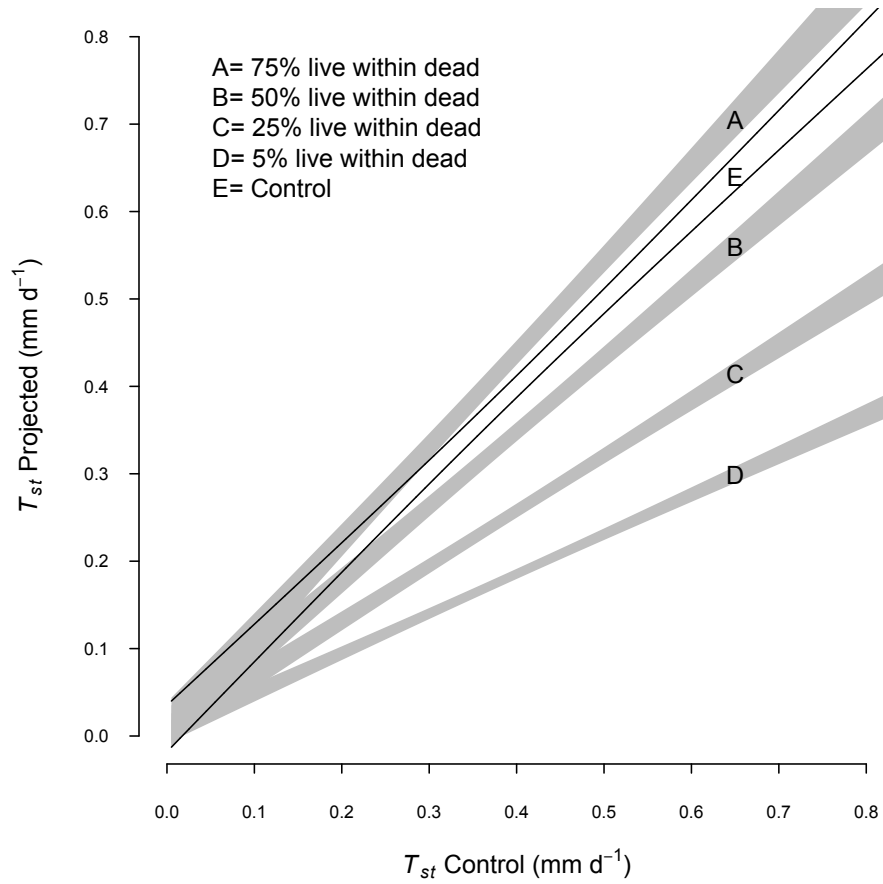


Figure 3-8. Relationship between mean daily estimated stand scale transpiration (T_{st} , mm day⁻¹) for four scenarios of partial MPB attack comprised of 75- (A), 50- (B), and 25% (C), and (D) 5% live trees (surrounded by fading and dead trees) and control (E - 100% live trees) with that of control conditions. Grey bands indicate 95% confidence intervals.



Chapter 4. EARLY EFFECTS OF FOREST HARVESTING AND VARIABLE INTENSITY MOUNTAIN PINE BEETLE ATTACK ON SOIL MOISTURE IN MATURE LODGEPOLE PINE FORESTS OF WESTERN ALBERTA

4.1. Introduction

The linkages between climate, soil and vegetation are critical for understanding and managing forest ecosystems. Soil moisture both influences, and is controlled by vegetation (Rutter, 1966; Tanner, 1968; Rodríguez-Iturbe et al., 1999; Porporato et al., 2004; Guswa, 2005).

The impact of mountain pine beetle (MPB, *Dendroctonus ponderosae* Hopkins) on soil moisture conditions in forests susceptible to attack by this insect has received surprisingly little research attention and remains highly uncertain (Schnorbus 2011) despite recent projections of the importance of MPB (Raffa et al., 2008) and its potential to impact ecohydrological processes (Adams, 2012). Nonetheless, numerous studies have documented changes in soil moisture after other types of forest disturbance such as fire, clear-cut harvesting, and partial cutting or thinning (e.g., DeBano, 2000; Lewis et al., 2006; Shakesby and Doerr, 2006; Lane et al., 2010, Madrid et al., 2006; Sajedi et al., 2012; Ebel et al. 2012). Mountain Pine Beetle attack, forest harvesting, and fire all result in reductions in overstory canopy cover that regulate net precipitation inputs and evaporative losses of moisture from the forest, yet important distinctions exist among these differing disturbances and their effects on the soil moisture. Large increases in soil moisture typically occur after forest harvesting (particularly clear cut harvesting) because the strong effect of canopy removal on increasing net precipitation (reduced interception of precipitation) and reduction of transpiration from the forest (Sajedi et al., 2012). Harvesting usually increases soil moisture during the growing season, though the magnitude of change is governed by the precipitation regime of the region along with site factors such as the amount and distribution of slash remaining on the site, the type and degree of soil disturbance, and the characteristics of residual and developing vegetation (Weber et al., 1985; Chrosiewicz, 1989). Although both MPB and fire leave dead standing snags while harvest does not, some types of forest harvesting practices have potentially similarities with the likely effects of MPB that fire does not. MPB effects on forest structure often resemble a 'thinning-from-above' harvesting treatment, where larger trees are selectively removed from the stand since larger trees are often more likely to be killed during MPB attack (Mueller et al., 2005; Floyd et al., 2009; Klenner and Aresenault, 2009). Reduced tree density after partial cutting silvicultural treatments has been shown to increase soil moisture in approximate proportion to the intensity of canopy removal (Bosch and Hewlett, 1982; Stednick, 1996; Bladon et al., 2006). Nevertheless, forest harvesting or other types of forest disturbance produce impact on soil moisture regimes that are fundamentally different from those likely produced by MPB attack. Forest harvesting, wildfire, and late grey attack phase MPB attack produce increases in soil moisture driven by both increases net precipitation (reduced rainfall interception) and reduction in evaporative losses by transpiration whereas early green-red phase MPB attack only affects transpiration losses. Thus, while studies have documented increases in soil

moisture after partial-cut harvesting or thinning due to reduction of canopy cover (decrease in transpiration and canopy interception), the extent of these effects after MPB attack are highly uncertain.

While fire is the predominant natural disturbance affecting lodgepole pine forests in western Canadian, the MPB has been expanding its range as a dominant disturbance agent (Nealis and Peter 2008). Furthermore, MPB distribution is not considered to be constrained by the availability of suitable host tree species (Carroll et al. 2006) but by climate, and more specifically by low winter temperatures (Safranyik 1978, Carroll et al. 2004). Over the last decade, favorable climate (mild winters) has been associated with significant expansion of MPB (Logan and Powell 2001; Carroll et al. 2004) across western North America including rapid expansion in lodgepole pine dominated forests in Alberta (Safranyik et al. 2010). Although the future course of the MPB affected forests in Alberta is not yet known, MPB is likely to remain as a significant agent of forest disturbance in Alberta (Schneider et al. 2010) due to both climate and vegetation shifts (Mbogga et al., 2009; Gray and Hamman, 2011). As a result, MPB will likely modify the historic disturbance regimes for Alberta's pine forests which have previously been dominated by wildfire. Forests attacked by MPB experience a sequence of symptoms as stands transition from a green to red and grey attack stage (Chojnacky et al. 2000). External (foliar) symptoms of trees attacked by MPB include crown foliar chlorosis (green attack) followed by death and retention of dead needles in the crown (red attack) for a period of 1-3 years (Chojnacky et al., 2000; Neiman and Vistintini, 2004). These dead needles are eventually shed during the final phase of the attack (grey attack).

Because of the critical role of the forest canopy in regulating water cycling in pine forests, a growing body of research has explored (mainly by modelling) the potential impact of MPB attack in western North American forests (Adams et al., 2011; Schnorbus, 2011). However, surprisingly little direct research has been conducted on how this growing agent of forest disturbance affects key processes that regulate water cycling in these forests. While changes in the structure of the canopy in the later grey attack phase of MPB attack have been linked to changes in microclimate conditions regulating snowpack accumulation and melt dynamics (Boon 2009, 2012; Winkler et al., 2010), little insight is currently available on broader changes in water cycling. In particular, no studies (to my knowledge) have documented the impact of MPB on soil moisture. This represents a crucial information gap because changes in soil moisture are likely to be strongly coupled with larger scale hydrologic changes in MPB affected landscapes such as groundwater recharge and runoff generation (Brooks and Vivoni, 2008) that are likely to govern streamflow regimes in these landscapes (Redding et al., 2008).

Accordingly, the objectives of this study were to determine the impact of variable intensity MPB green and red attack along with and salvage logging on 1) differential soil moisture response in both shallow and increasingly depth soil profile layers, 2) to explore how these changes in soil moisture vary temporally throughout the growing season, and 3) to explore the spatial variability in soil

moisture response within stands affected by differing intensities of MPB attack.

4.2. Materials and Methods

4.2.1. Study site description

The research was conducted in the upper montane forested region of west-central Alberta, Canada. The region is characterized by pure lodgepole pine (*Pinus contorta* Dougl.), mixed conifer stands of white spruce (*Picea glauca* (Moench) Voss), and subalpine fir (*Abies lasiocarpa* (Hook.) Nutt. (Beckingham et al., 1996). The area experiences a temperate continental climate where mean daily maximum air temperatures during the growing season range from 16.2 °C in May to 20.6 °C in August. The precipitation in the area is usually controlled by cyclonic activity (Nkemdirim and Weber, 1976), although localized convective storms are also frequent from late May to July (Longley, 1972). Mean monthly precipitation from May to August ranges from 57.9 mm to 82.2 mm, and the mean annual precipitation is 562.4 mm.

4.2.2. Site description and experimental design

Study sites were part of a healthy, homogeneous lodgepole pine stand of old age classes (> 100 yrs. old). Tree height ranged from 20.2 to 23.5 m, basal area ranged from 32.8 to 54.9 m² ha⁻¹, and stem density ranged from 1044 to 1343 trees ha⁻¹. Soils in this stand are brunisolic gray luvisols, with a silt-loam texture, bulk density of 1.2 g cm⁻³ and volumetric water content at field capacity of 0.38 cm³ cm⁻³. There was no presence of surface water in the area and the water table was intermittently detected with piezometers at 4 m depth.

This research was part of a study focused on describing changes in the forest water balance in response to a potential MPB attack in the foothills region of west-central Alberta, Canada. Soil moisture was measured in four treatment units (2.2 ha each) during three growing seasons from May to September during 2008-2010 (Figure 4-1). The units contained internal research plots surrounded by a 20 m treated buffer to minimize edge effects within interior portions of the sites. To avoid interference in other research instrumentation in site, each research plot was randomly split into a 100 x 100 m site, where the majority of measurements were conducted (Figure 4-1). The experimental MPB treatments were applied using a “before/after; control/impact” study design (BACI) (Green, 1979; Stewart-Oaten et al., 1986, 1992). Soil moisture measurements before treatment application spanned approximately one year, from beginning-May 2008 to mid-June 2009. Three treatments were applied to four experimental units or sites: control (untreated), two levels of simulated MPB attack (50% and 100% mortality), and a fourth experimental unit that was harvested to represent a salvage logged management treatment comparison (Figure 4-1). Individual tree application of glyphosate was used (“EZ-Ject” lance system, Herbicide System corp., MA, USA) to kill individual lodgepole pine trees as this type of treatment closely approximates the external morphological symptoms of post-MPB green-, red-, and grey-attack phases (i.e., foliar chlorosis followed by

reddening of crowns and eventual needle cast as trees die). The pre-treatment period ran from May 2008 to mid-June 2009. At the completion of the pre-treatment measurement period, treatments were applied to all three experimental units in the last two weeks of June 2009. Treatments were applied in mid-June 2009 and monitored for one and a half additional post-treatment years until the end of 2010. Measurements in all treatment units were paired, in the sense that the “control” and the “impact” (treated) sites were sampled simultaneously. Replication consisted of sample collection through time to capture variation in soil moisture in response to treatments across experimental units both the before and after treatment applications on a paired basis (e.g., control versus each treated unit). Observed differences in soil moisture between the “treated” and the “control” units before application of the treatments was assumed to reflect an estimate of the mean difference that would have existed in the post-treatment period if there was no perturbation or had treatments not been applied (Stewart-Oaten et al., 1992). Thus, changes in the mean difference between the pre-treatment and post-treatment periods would indicate changes at treated units relative to the control unit.

4.2.3. Micrometeorological measurements

Climate stations were established approximately in the center of each of the four sites (see details in Chapter 2). Air temperature, relative humidity, wind speed, and net radiation were measured at canopy height (21 m) at each climate station. The climate stations continuously sampled meteorological variables every five seconds to produce 10 minutes averages using a CR1000 system (Campbell Scientific, Inc., Utah, USA). Precipitation was measured in a nearby clear-cut 300-600 m away from the sites (details found in Chapter 2).

4.2.4. Soil moisture measurements

Soil moisture during the pre- and post-treatment periods was measured using a combination of time domain reflectometry (TDR) and TDR capacitance type soil moisture sensors.

4.2.4.1. Continuous soil moisture series

Volumetric soil water content (VWC; $\text{cm}^3 \text{cm}^{-3}$) and soil temperature ($^{\circ}\text{C}$) were continuously measured using capacitance type TDR probes (CS616; Campbell Scientific, Inc., Utah, USA) and thermocouples (type T) installed at 20, 40 and 60 cm belowground at each climate station. All sensors were calibrated in the laboratory by developing linear relationships between sensor output and actual moisture content ($R^2=0.98$). Because these measurements were not replicated within each of the treatment units, continuously measured soil moisture data was used only to explore gross temporal trends in soil moisture recharge by snowmelt or rainfall and soil moisture depletion during the growing season for each of the treatment units. Soil VWC was converted to total soil moisture storage (mm) for the top 60 cm of the soil profile using the mean VWC across each of the three soil depths. Additionally, because VWC differed among the

treatment units (likely reflecting variation in soil moisture retention properties and/or micro-topographic effects among climate station locations) soil moisture storage was scaled or standardized to the lowest water storage (mm) observed in each treatment unit over ~2.5 years. Thus the scaled continuous soil moisture storage (0-60 cm depth) reflected relative changes in total soil profile water storage scaled to 0 mm (lowest storage observed in each treatment unit).

4.2.4.2. Spatially distributed soil moisture

Spatially distributed VWC was measured using TDR techniques employing stainless steel rods as wave guides where the signal delay was measured with using Tektronix Inc. cable tester (model 1502c, Tektronix Inc., Beaverton, OR, USA) after Topp et al. (1980). Measurements were conducted on a weekly basis during the growing season from 2008 to 2010. In 2008 measurements started in the late summer, spanning from early August to end of September; while in 2009 and 2010 weekly measurements were conducted from May to September. Soil moisture was measured in eight randomly located plots in each unit. Plots were randomly selected from the corners of a 10 x 10 m grid established on each experimental unit (Figure 4-1). Three stainless steel wave guides (20, 40, and 60 cm long) were installed vertically in each plot to enable measurement of VWC in three increasingly deep soil layers (0-20, 0-40, and 0-60 cm). Volumetric soil water content was calculated from the time delay measured with the cable tester using the empirical relationship for mineral soils developed by Topp et al. (1980). VWC measured using the three wave guides (differing length) was calibrated against actual soil moisture content after Topp et al. (1980) with R^2 of 0.94, 0.91 and 0.96 corresponding each to 0-20, 0-40 and 0-60 cm soil layers respectively.

An additional extensive set of spatially distributed soil moisture measurements was added for the 2010 growing season (May to September) to explore spatial patterns of surface soil moisture in the treated units. VWC for the first 0-5 cm of the soil profile was measured using a ML2x - ThetaProbe (Delta-T Devices Ltd, Cambridge UK). Soil moisture storage (mm) for the top 0-5 cm of the soil profile was calculated from VWC. Soil moisture measurements using the probe were also calibrated against field moisture content ($R^2 = 0.96$). Each site was randomly split into a 100 x 100 m sub-site in order to avoid interference in other research instrumentation (Figure 4-1). The grid over each sub-site consisted a total of 82 sampling points that were measured on a weekly basis (May-September, 2010).

4.2.5. Data analysis

Statistical analyses were performed using R 2.15.1 (R Core Team, 2012), using mgcv (Wood, 2006), geoR (Ribeiro Jr. and Diggle, 2001) and gstat (Pebesma, 2004) analysis libraries.

4.2.5.1. Soil moisture response by depth

Treatment effects on soil moisture for both the continuous time series (using mean daily VWC) and manually sampled TDR datasets were explored using tests for coincident regressions (F tests) to determine if changes in the relationship between soil moisture in the control and treated units occurred between pre- and post-treatment periods after Zar (1999). Because of the highly variable soil moisture within and among treatment units, the manually sampled TDR dataset was further explored using a generalized additive mixed model (GAMM; Wood, 2004 and 2006) to filter the data to remove any random effects including spatial variability within and among treatment units along with experimental error (Mastrorilli et al., 1998, Guo et al., 2002; Ford et al., 2005). The GAMM is an extension of generalized additive models (GAM) in which the random effects and correlation structures are employed primarily to model residual correlation in the data (Wood, 2004). This approach filters the data leaving only variation in soil moisture due to the fixed effects including the four main treatments, soil profile depth (0-20, 0-40, and 0-60 cm layers), and temporal variation among sampling periods. The smooth functions used were based on a thin plate regression spline that was constructed by starting with the basis and penalty for a full thin plate spline and then truncating this basis in an optimal manner, to obtain a low rank smoother. The GAMM routine calculates a posterior covariance matrix for the coefficients of all the terms in the fixed effects formula, including the smooth functions. Once the optimal model structure was found by using AIC (Akaike, 1971), the original values in the GAM model covariates were used to obtain a linear predictor. The linear predictor was then used to explore the soil moisture relationships between treatment units both before and after imposition of treatments. Because mean soil VWC of all treatment units was generally greater during the post-treatment period (after June 2009), the relative change in GAM modeled soil moisture storage in treated units (50%, 100% mortality and the clearcut units) after application of treatments was scaled (adjusted) using the mean difference in moisture storage observed in the control unit before and after treatment application. This was done to more clearly illustrate the change in soil moisture storage after application of treatments. Mean adjusted soil moisture storage was calculated as; mean modelled soil moisture storage after treatment = $1 + \left[\frac{\text{mean post-treatment moisture storage in treated unit}}{\text{mean post-treatment moisture storage in control unit}} - \frac{\text{mean pre-treatment moisture storage in treated unit}}{\text{mean pre-treatment moisture storage in control unit}} \right]$ where 1 indicates no relative (adjusted) change after treatment.

4.2.5.2. Spatial patterns in surface soil moisture

Four dates were selected to analyze and compare the distribution of soil moisture at 5 cm depth between sites. The dates were selected to capture the early, mid and late summer periods that represented contrasting stages of soil moisture throughout the growing season. These dates were also selected to exclude periods immediately following precipitation events to ensure soil moisture conditions were more representative of gross seasonal trends rather than that produced by discrete rainfall events. Mean soil moisture storage (mm)

of each site (n=82) was compared using 95% confidence intervals.

The analysis of spatial patterns in soil moisture was conducted in three steps. First, variograms were developed to explore spatial variation of soil moisture storage (mm) at each site using several Gaussian models with constant mean and exponential correlations. The model parameters were estimated based on maximum likelihood; models providing the lowest AIC were retained (Akaike, 1973). Second, ordinary krigings (based on parameters identified in the variograms) were used to produce interpolated spatial soil moisture surfaces for each treatment unit. Kriging was performed using a 2 x 2 m grid resolution for each site. For each kriging prediction, Monte Carlo simulation was used to generate a sample of 1000 independent conditional soil moisture surfaces (Diggle and Ribeiro, 2007). Each simulation represented the predicted spatial distribution of surface soil moisture storage over the research units. Kernel density estimates (Venables and Ripley, 2002) were used to visually compare the distribution of the mean and standard variation of the 1000 spatial simulations. Third, the samples obtained in the Monte Carlo simulations were used to explore the proportion of area in the treated sites that exceeded average soil moisture storage of undisturbed (control) conditions. To do this, the arithmetic mean soil moisture storage in the control site was used as a threshold y for each of the sites. The y threshold was used to extract the area (i.e., number of cells in the 2 x 2 m grid) that exceeded y on each simulation. This process was conducted separately on each date. Thus, for each date, a sample of 1000 individual soil moisture surfaces was used to represent the proportion of total area where soil moisture depth (mm) exceeded y . As with the kriging simulations, Kernel density estimates were used to compare the means and standard variations between sites and throughout the season. All the statistical analysis were performed with $\alpha = 0.05$ as the threshold for statistical significance.

4.3. Results

4.3.1. Soil moisture response

4.3.1.1. Seasonal patterns of soil moisture

Soil water storage in the top 60cm of the soil profile declined during the fall/early winter season (~September to December) prior to formation of deep ground frost in 2008-2010 (Figure 4-2). However, rapid increases in soil water storage took place during April when spring snowmelt recharged soil water. Melt associated recharge was approximately 16 mm in April 2009 and 39 mm in April 2010. The initial moisture recharge of the soil profile by snowmelt corresponded with the timing of ground frost recession in the early spring. Soil moisture storage in the spring increased steadily to peak storage in June-July 2009 and 2010. Although the main period of soil moisture recharge was during the spring melt, soil moisture storage in the top 60cm showed a clear positive response after rain events larger than approximately 8 mm (Figure 4-2). The maximum moisture storage in the profile was 58 mm (corresponding to 0.32 mean θ) which was generally observed after rain events > 30 mm or after

periods of consecutive rain events > than 20 mm (Figure 4-2).

4.3.1.2. Soil moisture response to canopy disturbance

While the scaled continuously sampled soil moisture for the top 60cm of the soil profile at climate stations showed no clear pattern of change after imposition of the treatments (June-July 2009), soil moisture storage was somewhat greater in the latter portion of the growing season in the 50%- and 100% mortality sites. However a clear gradient in soil moisture storage reflecting relative intensity of MPB treatments (undisturbed, 50%-, 100% mortality, and harvested) was not evident (Figure 4-2). Nonetheless, comparison of pre- and post-treatment regressions of mean daily VWC by depth in the control unit and all treated sites indicated a strong change (increase) in soil water content at 20, 40, and 60 cm depth in the harvested unit after treatment (Table 4-1). The treatment effects were less consistent in the MPB treatment units where strong changes ($P < 0.001$) in VWC were evident at 20 and 60 cm depth (but not at 40 cm depth) in the 100% mortality unit and only at 20 cm depth in the 50% mortality unit.

While treatment effects were evident in continuously sampled soil moisture at climate stations, the spatially replicated (manually sampled TDR dataset) provided a more robust description of soil moisture response to treatments. While VWC was variable among sites, mean weekly VWC in the first 20 of the soil profile was greater after treatment ($P < 0.04$) in each of the 50%-, 100% mortality, and clearcut units (Table 4-1, Figure 4-3). Differences in mean VWC of treated and control units in the top 20 cm of the soil profile were greatest under wetter conditions (high VWC) than when conditions were drier as reflected in greater slopes in the relationship between mean VWC of control and treated units after treatment. However, weaker treatment effects were generally evident for increasingly deep soil profile depths (e.g. 0-40 and 0-60cm depths) than observed in the surface 0-20cm. While mean VWC in all treatment units was generally greater during the post-treatment period (including in the control unit), differences in relationships between mean VWC between the control and clearcut units before and after treatment were evident in the top 0-40 cm of the soil profile ($P = 0.03$) and between the control and 50% MPB unit from 0-60 cm (Table 4-1, Figure 4-3). Relative differences in mean VWC among treatments adjusted to account for changes in mean VWC of the untreated control unit before and after treatment indicated that the 50% and 100% mortality and clearcut sites were 25%, 31% and 30% wetter, respectively, for the first 20 cm of the soil profile during the post-treatment period (Table 4-2). In contrast, the same comparisons for the deeper 0-40 cm depth soil indicated only a 2%, 4% and 7% increase in soil moisture in the 50% and 100% mortality and clearcut sites. Little if any change in total water storage was evident for the deepest soil profile (0-60 cm) in the 100% mortality and clearcut units, however, the relative adjusted VMC in 50% mortality unit was 7% lower after treatment. (Table 4-2).

The modeled VWC (using the GAM model) helped clarify treatment effects on soil moisture by filtering the data to retain only variation in VWC due to treatment and depth effects (along with temporal variability from weekly

sampling). The GAM model selected indicated a large inter-annual variability of one sample variance per year in the repeated measures. Variation in modelled VWC among treatment units and increasingly deep soil profile layers was consistent with inferences suggested by comparison of linear regressions of measured VWC before and after application of treatments. Comparatively strong treatment effects were evident in the 50%-, 100% mortality and clearcut units after treatment (Figure 4-4). While the 100% mortality and clearcut units (more severe treatments) showed greater moisture storage for the deeper 0-40 cm profile, little clear effect was evident for the deepest (0-60 cm) soil layer. However, when adjusted to account for the change in modeled VWC of the control unit before and after treatment, relative (adjusted) VWC after application of treatments suggested smaller effects of treatment than indicated by mean measured VWC. Modeled VWC adjusted for changes in the control unit after treatment indicated a 2-9% increase in VWC of the 0-20cm layer, while at the 0-40cm layer no treatment effect was evident in the 50% unit and only 2% and 6% increases were observed in the 100% mortality and clearcut units, respectively (Table 4-2). Constant with relative (adjusted) changes measured VWC in the deepest soil profile (0-60cm), changes in adjusted modeled VWC after treatment suggest soil moisture decreased by 2-7% after treatment of the 50%-, 100% mortality units and the clearcut unit (Table 4-2).

4.3.2. Spatial patterns of soil moisture

Soil moisture at 5 cm depth showed a clear treatment effect throughout the 2010 season. Mean soil moisture storage at 5 cm depth was 33%, 13%, and 10% greater than the control in the clearcut, 100% and 50% mortality units from May-August, respectively (Table 4-3). Spatial variability of soil moisture storage was greatest during the early part of the growing season (May) when the soil moisture was closer to field capacity (Figure 4-5, Table 4-3). The widest confidence intervals (Table 4-3) along with high values for signal variance (nugget + Partial sill, Table 4-4) were observed at this time. Soil moisture declined after May with lowest soil water storage occurring in August (Julian day 238). Variability in soil moisture storage among treatment units was also least during August (Table 4-3, Figures 4-5 and 4-6) when soil moisture storage was most similar among treatments. Differences in surface soil water storage among treatments was greatest near the peak of the growing season in July when soil moisture storage was 52%, 26%, and 11% greater than the control in the clearcut, 100% and 50% mortality units, respectively (Table 4-3, Figure 4-5). Across the 2010 growing season, the clearcut site was consistently the wettest and the control unit was driest, whereas the 50% and 100% mortality sites did not show differences in surface soil moisture storage except in the month of July (Table 4-3, Figures 4-5 and 4-6). Soil moisture storage at 5 cm depth was most spatially variable in the clearcut and 50% mortality treatments as reflected in a wider range of soil moisture in the probability density functions (PDF) and coefficients of variation compared to the other sites (Table 4-5, Figure 4-6).

The proportion of area in each of the treatments exceeding the mean soil moisture storage in the control unit clearly illustrate the gradient in soil

moisture storage across control, clearcut, 100%, and 50% mortality treatments (Table 4-6). The mean proportion of area exceeding average soil moisture conditions in the untreated control unit across the 2010 growing season was 90%, 76%, and 70% in the clearcut, 100%, and 50% mortality treatments, respectively, compared to only 52% observed in the control unit (Table 4-6, Figure 4-7). Again, the differences among treatment units were greatest in July when 99%, 94%, and 71% of the area within the clearcut, 100%, and 50% mortality units exceeded the mean soil moisture storage of the control unit (Table 4-6, Figure 4-7).

4.4. Discussion

Results of this research showed a clear gradient of increasing soil moisture during the growing season related to the intensity of canopy disturbance across stands that had been harvested or represented differing intensities of early MPB attack. Soil moisture storage increased during this early phase of MPB attack and these effects were greatest in surface soil layers and during the period of time when evaporative demand by the forest was at its peak in mid-summer. These findings are novel because while the effects of harvesting on soil moisture status of forests are well known, impacts of MPB attack and particularly that of the early green and red phases of MPB attack on soil moisture have not been previously reported.

4.4.1. Soil moisture response to canopy disturbance

The change in soil moisture after disturbance was strongly associated with the gradient in canopy disturbance where the increase in soil moisture was greatest in the clearcut, followed by the 100% and 50% mortality sites, and lowest in the control site. In contrast to MPB effects on soil moisture, effects of harvesting on soil moisture are well known (Sajedi et al., 2012). Harvesting usually increases soil moisture and soil temperature during the growing season, which can potentially result in expansion of the growing season length (Ahlgren, 1981; Viereck et al., 1993; Chen et al., 1995). The magnitude of soil moisture responses largely depend on the precipitation regime of the region, and on amount and distribution of slash, the type and degree of soil disturbance, and the characteristics of residual and re-developing vegetation (Weber et al., 1985; Chrosiewicz, 1989). Partial cutting in silvicultural treatments have also shown that reduction of tree density is associated with increased soil moisture (Bosch and Hewlett, 1982; Stednick, 1996; Bladon et al., 2006). However while most studies conclude increases in soil moisture storage following harvesting can be expected, no clear patterns in the degree of soil moisture responses observed among silvicultural treatments are evident other than the degree of canopy removal among clearcut and partial cutting strategies (Madrid et al., 2006).

Forest harvesting or other types of forest disturbance produce impact on soil moisture regimes that are fundamentally different from those likely produced by MPB attack. Forest harvesting, wildfire, and late grey attack phase MPB attack produce increases in soil moisture driven by both increases net precipitation

(reduced rainfall interception) and reduction in evaporative losses by transpiration, whereas early green-red phase MPB attack only affects transpiration losses. In the present study, soil water content was increased by 25% and 31% in the top 20 of the soil profile for the 50% and 100% mortality treatments representing early green attack and transition to red attack phases of MPB attack, respectively, and this was likely driven entirely by the reduction in transpiration reported on in Chapter 3 of this thesis. Thus, the finding of increased soil water in both 50% and 100 % mortality units is unique in the literature as these changes would have been produced solely by reduction in stand scale transpiration without any other changes in stand structure affecting soil water inputs.

A clear gradient in the strength of treatment effects on soil water content and soil water storage was observed among differing soil profile depths where effects were greatest in the surface 0-5 cm and 0-20 cm depth layers (Table 4-2 and Table 4-3). While harvesting increased mean soil moisture content by 30% in the surface 0-20 cm layer after harvesting (Table 4-2), this was approximately the same magnitude of soil moisture increase observed in the 100% mortality unit (31%). Furthermore, the 25% increase in soil water content observed in the 50% mortality unit was also in the same approximate magnitude of effect size as that produced by the 100% mortality treatment. While the effects of treatments were considerably lower for the top 40 cm of the soil profile, 2%, 4%, and 7% increases in bulk soil water content of this deeper layer were still evident in the 50%, 100% mortality and clearcut treatments, respectively. While these early effects of green-red attack on soil moisture storage were not as severe as those observed after grey attack such as the severe water logging that was observed after late phase MPB attack in the Vanderhoof Forest District of British Columbia (Rex and Dube, 2006), these early increases in soil water storage may be important in driving subsequent ecological and hydrologic changes in these sites. Increases in soil water content are likely to increase water available for plant growth or microbial communities. Indeed, the increased transpiration I observed by surviving trees in the 50% mortality site (Chapter 3) was likely a direct result of the increased soil moisture status observed in the present chapter and constitutes some of the first evidence of this ecohydrological feedback after MPB attack. Similarly, increased soil moisture would play an important role in understory plant growth that would be a critical component governing vegetation recovery of lodgepole pine stands after MPB attack. However, because of the breadth of ecological processes regulated by soil moisture, interactions among ecosystem components are not easily predicted. For example, in an early simulated MPB attack experiment in Wyoming, USA, there was an increase in soil moisture and water percolation below the rooting zone that increased nitrogen mineralization and nutrient leaching from the stand (Knight et al., 1991).

4.4.2. Spatial and temporal variability in soil moisture responses

Spatial variation in soil water storage in the surface 0-5 cm depth differed strongly across the 2010 growing season. Spatial variation in soil water storage

across treatment units was most similar in May and Aug (beginning and end of the summer growing season) when soil moisture storage was greatest and least, respectively (Figure 4-6). These periods during the growing season also correspond to the times when evaporation was likely lowest. While soil moisture was greatest in May, evaporative demand would also have been low. Similarly, while evaporative demand was high in August, soil water and moisture availability would have limited evaporation. In contrast, the spatial variability of soil moisture within and among treatment units was greatest in July when evaporative demand and transpiration (Chapter 3) was highest. Thus is likely that changes in spatial variability of soil moisture storage during the growing season were strongly influenced by the magnitude of stand evaporative losses during the season. This is consistent with the suggestion that soil and vegetation interactions tend to result in spatial patterns of soil moisture that are highly variable over time (Guo et al. 2002).

The highest spatial variability in soil moisture storage within treatments was generally observed in the clearcut and 50% mortality units. High spatial variability in soil moisture in the clearcut was not unexpected given the large variation in microsites composed of different substrates such as logging slash composed of crowns, branches and woody debris, along with moss and bare ground in that treatment. These variable microsites would have likely produced spatial variation in evaporative losses driving spatial variability in soil moisture status. Similarly, the 50% mortality treatment had relatively uniform distribution of live, dying (fading), and dead trees. This mix of living, fading, and dead trees produced a strongly differential in transpiration response (Chapter 3), presumably resulting in strong differences in the rate of soil water extraction. Furthermore, measurements of soil moisture near to the trunks of dead and dying trees (data not shown) indicated a clear gradient in soil moisture, where soil moisture immediately nearby dying and dead trees was 20% and 54% higher, respectively, than soil moisture near to the boles of live trees. This is consistent with previous reports of increased spatial variability in soil moisture in a 40-year-old *Pinus elliottii* plantation, followed by a rapid return to undisturbed conditions two years after the application of commercial harvesting and chemical girdling (Guo et al. 2002). These findings support the idea that plants could alter the spatial patterns of soil properties including soil moisture conditions (Hendrickson and Robinson 1984; Breshears et al. 1997; Finzi et al. 1998).

Schume *et al.* (2003) argued that two key elements drive variation in the water content of forested soils: a) soil moisture rewetting responses governed by antecedent soil moisture conditions (e.g. drying history); and b) the influence of evapotranspiration. In this study, the beginning of the growing season (May) was characterized by snowmelt and soil thawing processes that can be characterized as a rewetting response to overwinter antecedent soil moisture conditions and thus, could be thought of as an input driven period (Figure 4-3). During this period, the differences in soil moisture between the clearcut and control units were greatest presumably due to significantly higher snow pack and snow water equivalent in the clearcut site (data not shown). In contrast, the

middle of the growing season (July) could be characterized as an output driven period governed by evaporative processes. The greatest differences in both soil moisture among treatments and spatial variability of soil moisture within treatments was observed at this time. Thus, the soil moisture conditions during this output driven period were best explained by interaction of stand vegetation with evaporative demand. This is further illustrated by the fact that the greatest difference in soil moisture status and variability of soil moisture between the 50% and 100 % mortality treatments was observed in July (Table 4-5, Figure 4-6).

4.5. Conclusion

Results of this research showed a clear gradient of increasing soil moisture during the growing season related to the intensity of canopy disturbance across stands that had been harvested or represented differing intensities of early (green and red phase) MPB attack. Effects of MPB attack on soil moisture storage were associated with the intensity of the MPB attack and while the strongest impact on soil moisture status was evident in the top 0-5 cm soil layer, soil moisture storage was increased in the surface 0-20 cm after both levels of MPB attack and was still evident in the surface 0-40 cm soil layer under the most severe level of attack.

While, harvesting and early phase MPB attack produce fundamentally differing effects on processes governing soil moisture dynamics in forests; increases in soil moisture after harvesting are driven by both increases net precipitation (reduced rainfall interception) and reduction in evaporative losses by transpiration while early MPB attack only affects transpiration losses. While effects of variable intensity green or red attack showed the most dramatic increases in soil moisture in the top 0-5 and 0-20 cm soil layers, increased soil moisture after early variable intensity green-red attack in the absence of disturbance effects on water inputs to stands (e.g. interception and net precipitation) are novel and have not been previously reported.

4.6. References

- Adams, H. D., C. H. Luce, et al. (2011). "Ecohydrological consequences of drought- and infestation- triggered tree die-off: insights and hypothesis." Ecohydrology **5**(2): 145-159.
- Ahlgren, C. E. (1981). "17-year changes in climatic elements following prescribed burning." Forest Science **27**(1): 33-39.
- Akaike, H. (1971). Information theory and an extension of the maximum likelihood principle. Second International Symposium on Information Theory, Budapest, Hungary, Akademiai Kiado.
- Bladon, K. D., U. Silins, et al. (2006). "Differential transpiration by three boreal tree species in response to increased evaporative demand after variable retention harvesting." Agricultural And Forest Meteorology **138**(1-4): 104-119.
- Boon, S. (2009). "Snow ablation energy balance in a dead forest stand." Hydrological Processes **23**(18): 2600-2610.
- Boon, S. (2012). "Snow accumulation following forest disturbance." Ecohydrology **5**(3): 279-285.
- Bosch, J. M. and J. D. Hewlett (1982). "A review of catchment experiments to determine the effect of vegetation changes on water yield and evapotranspiration." Journal of Hydrology **55**(1-4): 3-23.
- Breshears, D. D., P. M. Rich, et al. (1997). "Overstory-imposed heterogeneity in solar radiation and soil moisture in a semiarid woodland." Ecological Applications **7**(4): 1201-1215.
- Brooks, P. D. and E. R. Vivoni (2008). "Mountain ecohydrology: quantifying the role of vegetation in the water balance of montane catchments." Ecohydrology **1**(3): 187-192.
- Carroll, A. L., J. Régnière, et al. (2006). Impacts of climate change on range expansion by the mountain pine beetle. Victoria, Natural Resources Canada, Canadian Forest Service, Pacific Forestry Centre: 20.
- Carroll, A. L., S. W. Taylor, et al. (2004). Effects of climate change on range expansion by the mountain pine beetle in British Columbia. Mountain Pine Beetle Symposium: challenges and solutions, Kelowna, B.C., Natural Resources Canada, Canadian Forest Service, Pacific Forestry Centre.
- Chen, J. Q., J. F. Franklin, et al. (1995). "Growing-season microclimatic gradients from clear-cut edges into old-growth douglas-fir forests." Ecological Applications **5**(1): 74-86.
- Chojnacky, D. C., B. J. Bentz, et al. (2000). Mountain pine beetle attack in ponderosa pine: Comparing methods for rating susceptibility Research Paper. Fort Collins, U.S. Department of Agriculture, Forest Service, Rocky Mountain Research Station: 10 p.
- Chrosiewicz, Z. (1989). "Prediction of forest-floor moisture-content on jack pine cutovers." Canadian Journal of Forest Research-Revue Canadienne De Recherche Forestiere **19**(2): 239-243.
- DeBano, L. F. (2000). "The role of fire and soil heating on water repellency in wildland environments: a review." Journal of Hydrology **231**: 195-206.
- Diggle, P. J. and P. J. Ribeiro Jr. (2007). Model-based Geostatistics. New York, Springer.

- Ebel, B. A., E. S. Hinckley, et al. (2012). "Soil-water dynamics and unsaturated storage during snowmelt following wildfire." Hydrology and Earth System Sciences **16**(5): 1401-1417.
- Finzi, A. C., N. Van Breemen, et al. (1998). "Canopy tree soil interactions within temperate forests: species effects on soil carbon and nitrogen." Ecological Applications **8**(2): 440-446.
- Floyd, M. L., M. Clifford, et al. (2009). "Relationship of stand characteristics to drought-induced mortality in three Southwestern pinon-juniper woodlands." Ecological Applications **19**(5): 1223-1230.
- Ford, C. R., C. E. Goranson, et al. (2005). "Modeling canopy transpiration using time series analysis: A case study illustrating the effect of soil moisture deficit on *Pinus taeda*." Agricultural and Forest Meteorology **130**(3-4): 163-175.
- Gray, L. K. and A. Hamann (2011). "Strategies for reforestation under uncertain future climates: guidelines for Alberta, Canada." PLoS ONE **6**(8): e22977.
- Green, R. H. (1979). Sampling design and statistical methods for environmental biologists. New York, Wiley.
- Guo, D., P. Mou, et al. (2002). "Temporal changes in spatial patterns of soil moisture following disturbance: an experimental approach." Journal of Ecology **90**(2): 338-347.
- Guswa, A. J. (2005). "Soil-moisture limits on plant uptake: an upscaled relationship for water-limited ecosystems " Advances in Water Resources(28): 543-552.
- Hendrickson, O. Q. and J. B. Robinson (1984). "Effects of roots and litter on mineralization processes in forest soil." Plant and Soil **80**(3): 391-405.
- Klenner, W. and A. Arsenault (2009). "Ponderosa pine mortality during a severe bark beetle (Coleoptera: Curculionidae, Scolytinae) outbreak in southern British Columbia and implications for wildlife habitat management." Forest Ecology and Management **258**: S5-S14.
- Knight, D. H., J. B. Yavitt, et al. (1991). "Water and nitrogen outflow from lodgepole pine forest after 2 levels of tree mortality." Forest Ecology and Management **46**(3-4): 215-225.
- Lane, P. N. J., P. M. Feikema, et al. (2010). "Modelling the long term water yield impact of wildfire and other forest disturbance in Eucalypt forests." Environmental Modelling & Software **25**(4): 467-478.
- Lewis, S. A., J. Q. Wu, et al. (2006). "Assessing burn severity and comparing soil water repellency, Hayman Fire, Colorado." Hydrological Processes **20**(1): 1-16.
- Longley, L. W. (1972). Precipitation in the canadian praires. Atmospheric Environment Service. Toronto, Canadian Department of the Environment.
- Madrid, A., A. G. Fernald, et al. (2006). "Evaluation of silvicultural treatment effects on infiltration, runoff, sediment yield, and soil moisture in a mixed conifer New Mexico forest." Journal of Soil and Water Conservation **61**(3): 159-168.
- Mastrorilli, M., N. Katerji, et al. (1998). "Daily actual evapotranspiration measured with TDR technique in Mediterranean conditions." Agricultural and Forest Meteorology **90**(1-2): 81-89.

- Mbogga, M. S., A. Hamann, et al. (2009). "Historical and projected climate data for natural resource management in western Canada." Agricultural and Forest Meteorology **149**(5): 881-890.
- Mueller, R. C., C. M. Scudder, et al. (2005). "Differential tree mortality in response to severe drought: evidence for long-term vegetation shifts." Journal of Ecology **93**(6): 1085-1093.
- Nealis, V. G. and B. Peter (2008). Risk assessment of the threat of mountain pine beetle to Canada's boreal and eastern pine forests. Information Report Victoria, Natural Resources Canada, Canadian Forest Service, Pacific Forestry Centre. **BC-X-417**: 38.
- Neimann, K. O. and F. Visintini (2004). Assessment of potential for remote sensing detection of bark beetle-infested areas during a green attack: a literature review. Mountain Pine Beetle Initiative. Victoria, Natural Resources Canada, Canadian Forest Service.
- Nkemdirim, L. C. and L. Weber (1976). "Wet and dry sequences in precipitation regimes." Geografiska Annaler Series a-Physical Geography **58**(4): 303-315.
- Pebesma, E. (2004). "Multivariate geostatistics in S: the gstat package." Computers and Geosciences **30**: 683-691.
- Porporato, A., E. Daly, et al. (2004). "Soil water balance and ecosystem response to climate change." The American Naturalist **164**(5).
- R Core Team (2012). R: A language and environment for statistical computing. Vienna, R Foundation for Statistical Computing.
- Raffa, K. F., B. H. Aukema, et al. (2008). "Cross-scale drivers of natural disturbances prone to anthropogenic amplification: The dynamics of bark beetle eruptions." Bioscience **58**(6): 501-517.
- Redding, T. E., R. D. Winkler, et al. (2008). Mountain pine beetle and watershed hydrology: A synthesis focused on the Okanagan. One Watershed – One Water, Kelowna, BC, Canadian Water Resources Association.
- Rex, J. and S. Dubé (2006). "Predicting the risk of wet ground areas in the Vanderhoof Forest District: project description and progress report." BC Journal of Ecosystems and Management **7**(2): 57-71.
- Ribeiro Jr., P. J. and P. J. Diggle (2001). "geoR: A package for geostatistical analysis." R-NEWS **1**(2): 15-18.
- Rodríguez-Iturbe, I., A. Porporato, et al. (1999). "Probabilistic modelling of water balance at a point: the role of climate, soil and vegetation." Proceedings of the Royal Society of London. Series A **455**: 3789-3805.
- Rutter, A. J. (1966). "Studies on water relations of *Pinus sylvestris* in plantation conditions. 4. direct observations on rates of transpiration evaporation of intercepted water and evaporation from soil surface." Journal of Applied Ecology **3**(2): 393-&.
- Safranyik, L. (1978). Effects of climate and weather on mountain pine beetle populations. Symposium on theory and practice of mountain pine beetle management in lodgepole pine forests, University of Idaho, Moscow, Idaho, Washington State University, Pullman, Washington.
- Safranyik, L., A. L. Carroll, et al. (2010). "Potential for range expansion of mountain pine beetle into the boreal forest of North America." Canadian Entomologist **142**(5): 415-442.

- Sajedi, T., C. E. Prescott, et al. (2012). "Relationships among soil moisture, aeration and plant communities in natural and harvested coniferous forests in coastal British Columbia, Canada." Journal of Ecology **100**(3): 605-618.
- Schneider, R. R., M. C. Latham, et al. (2010). "Effects of a severe mountain pine beetle epidemic in western Alberta, Canada under two forest management scenarios." International Journal of Forestry Research(417595): 7.
- Schnorbus, M. (2011). A synthesis of the hydrological consequences of large-scale mountain pine beetle disturbance. Mountain Pine Beetle Working Paper 2010-01. Victoria, Natural Resources Canada, Canadian Forest Service, Pacific Forestry Centre: 30.
- Schume, H., G. Jost, et al. (2003). "Spatio-temporal analysis of the soil water content in a mixed Norway spruce (*Picea abies* (L.) Karst.) - European beech (*Fagus sylvatica* L.) stand." Geoderma **112**(3-4): 273-287.
- Shakesby, R. A. and S. H. Doerr (2006). "Wildfire as a hydrological and geomorphological agent." Earth-Science Reviews **74**(3-4): 269-307.
- Stednick, J. D. (1996). "Monitoring the effects of timber harvest on annual water yield." Journal Of Hydrology **176**(1-4): 79-95.
- Stewart-Oaten, A., J. R. Bence, et al. (1992). "Assessing effects of unreplicated perturbations: no simple solutions." Ecology **73**(4): 1396-1404.
- Stewart-Oaten, A., W. W. Murdoch, et al. (1986). "Environmental-impact assessment - pseudoreplication in time." Ecology **67**(4): 929-940.
- Tanner, C. B. (1968). Evaporation of water from plants and soil. Water deficits and plant growth. T. Kozlowski. New York, Academic Press. **I**: 73-106.
- Topp, G. C., J. L. Davis, et al. (1980). "Electromagnetic determination of soil-water content - measurements in coaxial transmission-lines." Water Resources Research **16**(3): 574-582.
- Venables, W. N. and B. D. Ripley (2002). Modern Applied Statistics with S. New York, Springer.
- Viereck, L. A., K. Vancleve, et al. (1993). "Climate of the tanana river floodplain near fairbanks, alaska." Canadian Journal of Forest Research-Revue Canadienne De Recherche Forestiere **23**(5): 899-913.
- Weber, M. G., I. R. Methven, et al. (1985). "The effect of forest floor manipulation on nitrogen status and tree growth in an eastern ontario jack pine ecosystem." Canadian Journal of Forest Research-Revue Canadienne De Recherche Forestiere **15**(2): 313-318.
- Winkler, R., S. Boon, et al. (2010). "Assessing the effects of post-pine beetle forest litter on snow albedo." Hydrological Processes **24**(6): 803-812.
- Wood, S. (2006). Generalized Additive Models: An introduction with R. England, Chapman and Hall/CRC Press.
- Wood, S. N. (2004). "Stable and efficient multiple smoothing parameter estimation for generalized additive models." Journal of the American Statistical Association **99**(467): 673-686.
- Zar, J. (1999). Biostatistical analysis. Upper Saddle River, Prentice Hall.

4.7. Tables

Table 4-1. Tests for coincidental regressions ($P > |F|$) among regression relationships between mean daily soil moisture in treated units and the control unit by depth before and after treatment application. Relationships are based on mean daily VWC for the continuously measured dataset and on mean of weekly measurements for three increasingly deep soil profiles in the manually sampled dataset. R^2 indicates goodness of fit of the linear regressions before and after treatments and * indicates $P < 0.05$.

Dataset	Depth (cm)	Treatment	R^2 (before-after)	Coincidental Regression test $P > F $
Continuous measurement	20	50% mortality	0.51-0.44	0.919
		100% mortality	0.59-0.14	<0.001*
		Clearcut	0.37-0.52	<0.001*
	40	50% mortality	0.47-0.42	0.779
		100% mortality	0.79-0.43	0.863
		Clearcut	0.37-0.06	<0.001*
	60	50% mortality	0.02-0.26	0.407
		100% mortality	0.02-0.29	<0.001*
		Clearcut	0.51-0.40	<0.001*
Manually sampled	0-20	50% mortality	0.13-0.89	<0.001*
		100% mortality	0.19-0.71	0.002*
		Clearcut	0.07-0.85	0.004*
	0-40	50% mortality	0.65-0.93	0.178
		100% mortality	0.76-0.68	0.205
		Clearcut	0.41-0.61	0.030*
	0-60	50% mortality	0.89-0.66	0.014*
		100% mortality	0.90-0.66	0.622
		Clearcut	0.89-0.63	0.106

Table 4-2. Mean manually measured (TDR dataset) and modeled (GAMM) VWC for three increasingly deep soil profiles before (Bfr) and after (Aft) treatment application. BACI columns refer to the scaled relative (adjusted) treatment effect relative to control conditions where 1 indicates no relative adjusted change after treatment. The Error column indicates the difference between measured and modeled BACI.

Depth (cm)	Site	Measured			Modeled			Error
		Bfr	Aft	BACI	Bfr	Aft	BACI	
0-20	Control	0.22	0.21	1.00	0.21	0.26	1.00	0.00
	50%	0.25	0.30	1.25	0.26	0.32	1.02	0.22
	100%	0.22	0.28	1.31	0.23	0.30	1.09	0.22
	Clearcut	0.26	0.32	1.30	0.27	0.33	1.04	0.26
0-40	Control	0.30	0.33	1.00	0.28	0.32	1.00	0.00
	50%	0.29	0.33	1.02	0.29	0.32	1.00	0.02
	100%	0.29	0.33	1.04	0.28	0.32	1.02	0.02
	Clearcut	0.28	0.33	1.07	0.27	0.33	1.06	0.02
0-60	Control	0.27	0.34	1.00	0.25	0.30	1.00	0.00
	50%	0.29	0.35	0.93	0.29	0.33	0.93	0.00
	100%	0.27	0.35	1.02	0.27	0.32	0.97	0.05
	Clearcut	0.28	0.35	0.99	0.27	0.32	0.98	0.01

Table 4-3. Mean monthly soil moisture storage (mm) for each experimental unit at 5 cm depth. Confidence intervals (95%) shown in brackets.

Month	Control (mm)	Clearcut (mm)	100% mortality (mm)	50% mortality (mm)
May	17.86 (17.22-18.51)	22.92 (22.07-23.78)	19.09 (18.51-19.70)	19.85 (19.05-20.70)
June	11.73 (11.27-12.20)	14.65 (14.05-15.27)	12.51 (12.06-12.96)	13.14 (12.68-13.62)
July	10.60 (10.04-11.18)	16.08 (15.51-16.70)	13.39 (12.92-13.87)	11.72 (11.07-12.39)
Aug	10.25 (9.81-10.70)	12.47 (11.98-13.00)	11.45 (11.11-11.80)	10.94 (10.47-11.41)

Table 4-4. Coefficients for exponential models fit to soil moisture storage (mm) at 5 cm depth.

Plot	Month	β	Nugget	Partial Sill	Range
Control	May	17.86	6.15	2.21	0.45
	June	11.70	3.86	0.56	7.49
	July	10.54	5.52	1.24	9.59
	Aug	10.25	3.41	0.57	0.49
Clearcut	May	22.97	0	14.90	3.56
	June	14.81	0	7.70	5.44
	July	16.08	5.20	1.61	0.46
	Aug	12.49	2.30	2.57	5.12
100% mortality	May	18.99	5.94	1.18	26.07
	June	12.51	0.78	3.37	0.13
	July	13.39	1.07	3.65	0.59
	Aug	11.45	0.73	1.655	0.28
50% mortality	May	19.81	0	13.07	5.65
	June	13.14	0	4.50	4.15
	July	11.66	0	9.07	7.23
	Aug	10.93	0	4.48	5.24

Table 4-5. Summary of the 1000 Monte Carlo simulations of soil moisture storage (mm) drawn from the probability density functions for soil moisture storage at 5 cm depth.

Site	Month	Mean (mm)	Variance	Standard deviation	Coefficient of variation (%)
Control	May	17.86	0.02	0.15	0.66
	June	11.72	0.04	0.20	1.62
	July	10.58	0.16	0.40	3.67
	Aug	10.25	0.02	0.13	1.16
Clearcut	May	22.94	1.81	1.35	5.84
	June	14.74	1.84	1.36	9.19
	July	16.08	0.02	0.14	0.68
	Aug	12.47	0.30	0.54	4.31
100% mortality	May	19.18	0.27	0.52	2.66
	June	12.51	0.00	0.07	0.22
	July	13.39	0.02	0.14	0.86
	Aug	11.46	0.00	0.05	0.19
50% mortality	May	19.83	3.23	1.80	9.07
	June	13.15	0.71	0.84	6.40
	July	11.62	2.79	1.67	14.35
	Aug	10.93	1.00	1.00	9.14

Table 4-6. Mean percentage of samples (n= 1000) from Monte Carlo simulations exceeding the mean soil moisture storage of the reference site (control). Values shown in brackets indicate the mean % difference between treatments and the control site.

Month	Control (%)	Clearcut (%)	100% (%)	50% (%)
May	48	90 (42)	67 (19)	69 (21)
June	45	84 (39)	60 (15)	70 (25)
July	59	99 (40)	94 (35)	71 (12)
Aug	55	87 (32)	83 (28)	68 (13)
Mean	52	90	76	70

4.8. Figures

Figure 4-1. Layout of the four treatment units (2.2 ha size with 20 m treated inner-buffers). Filled circles indicate the sampling locations for the manual TDR measurements of 3 increasingly deep soil layers (2008-2010), and hollow circles denote the sampling grid for the surface (5 cm depth) soil measurements (2010 only).

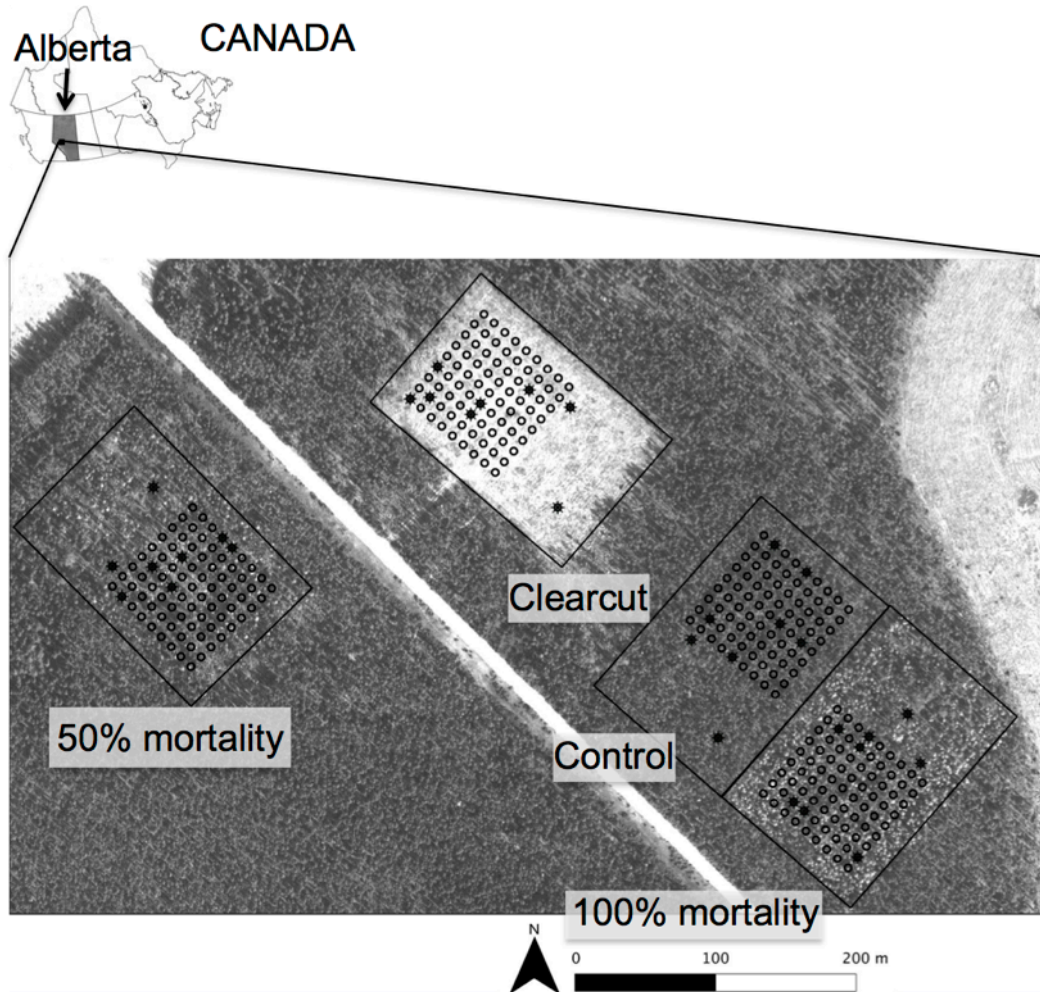


Figure 4-2. Scaled relative soil moisture storage (mm) in the top 60cm of the soil profile during the frost-free period from Sept. 2008 to Dec. 2010. Relative soil moisture storage represents the actual storage minus the minimum value of storage recorded in the series for each site. The blank frames represent the periods of frozen soil. Vertical bars indicate daily gross precipitation (mm).

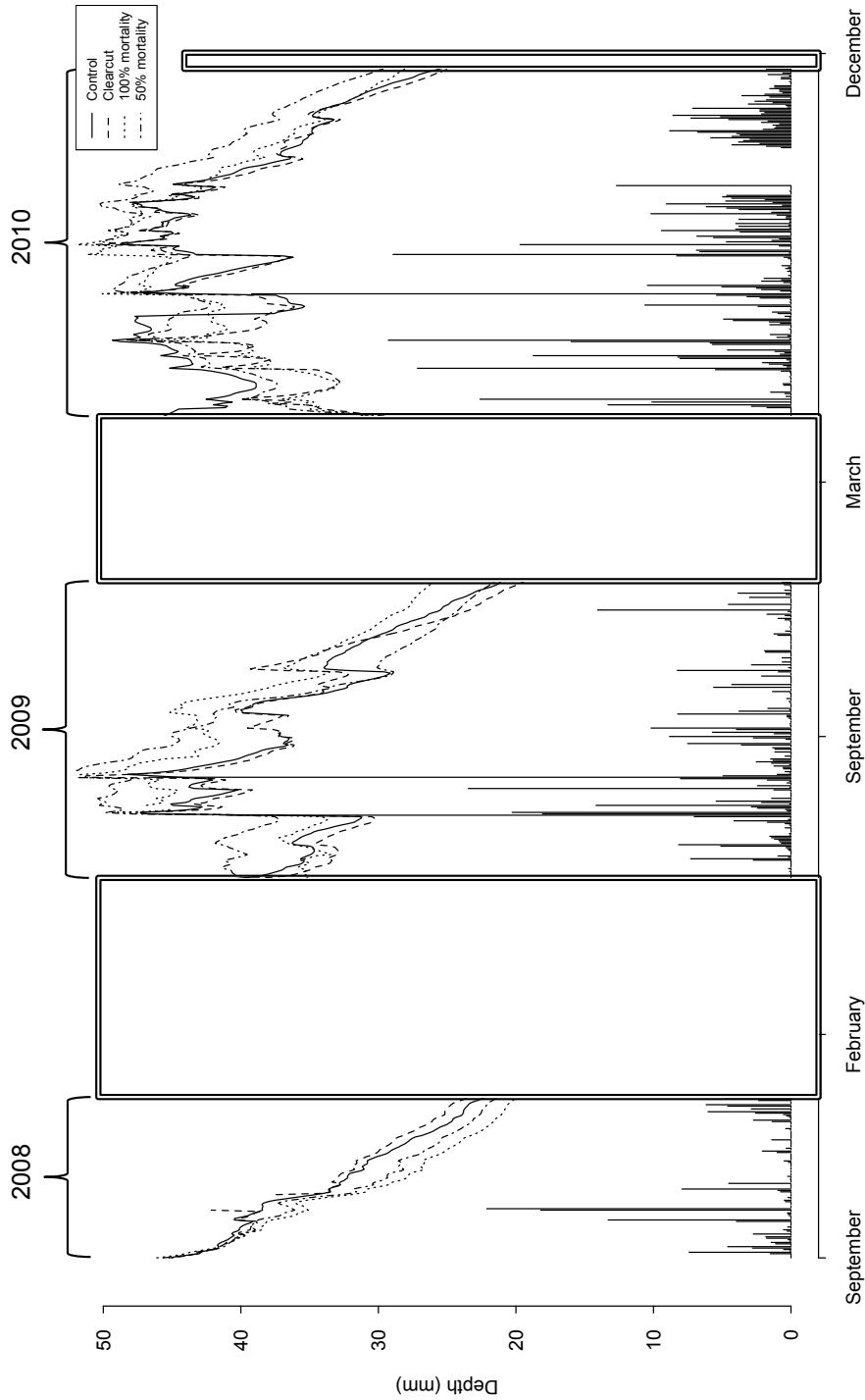


Figure 4-3. Relationship between mean weekly manually sampled VWC (n=8) in the control and treated units before and after treatment application for three increasingly deep soil profile depths. Lines indicate linear regressions before (long-dashed) and after (short-dashed) treatment application for 50%, 100% and clearcut units.

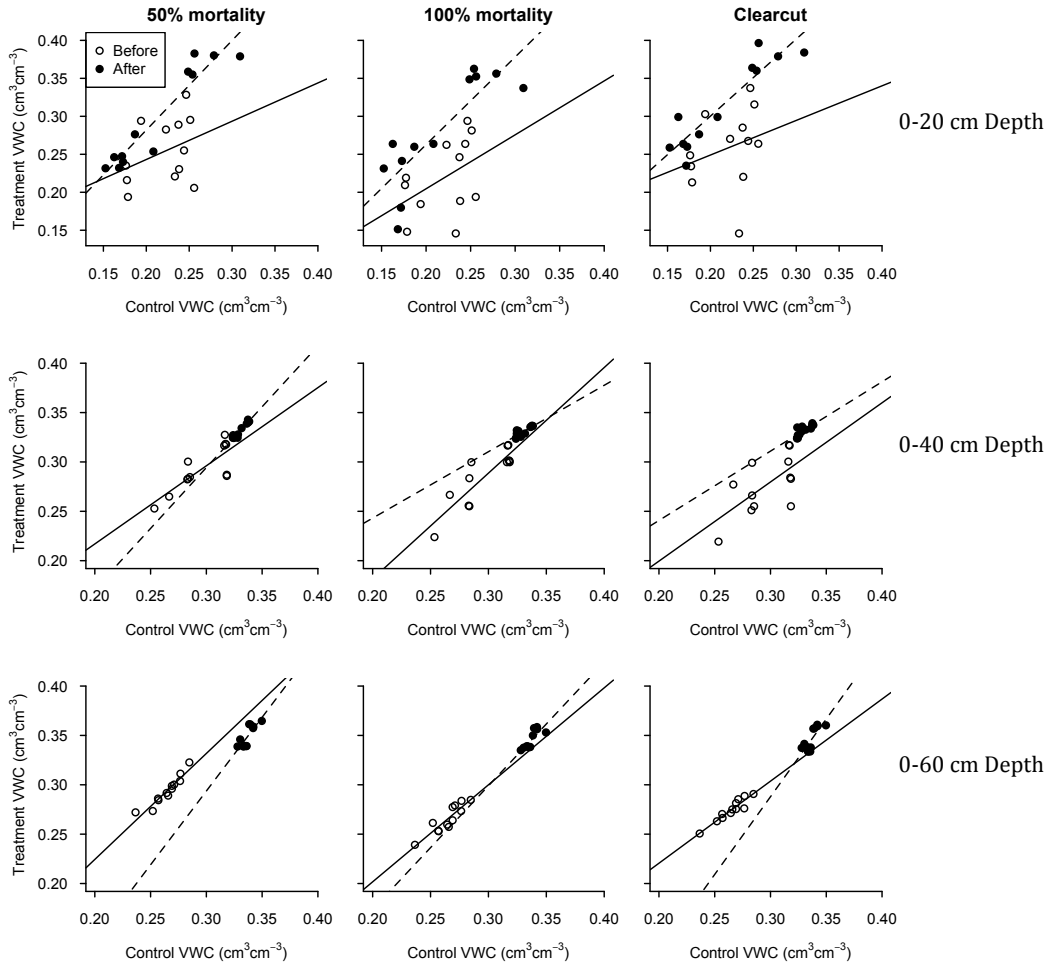


Figure 4-4. Relationship between mean modeled VWC (n=8) in the control and treated units before and after treatment application for three increasingly deep soil profile depths. GAM modeled VWC reflects variation in moisture content due to only the fixed effects of treatment, the three profile depths, and time.

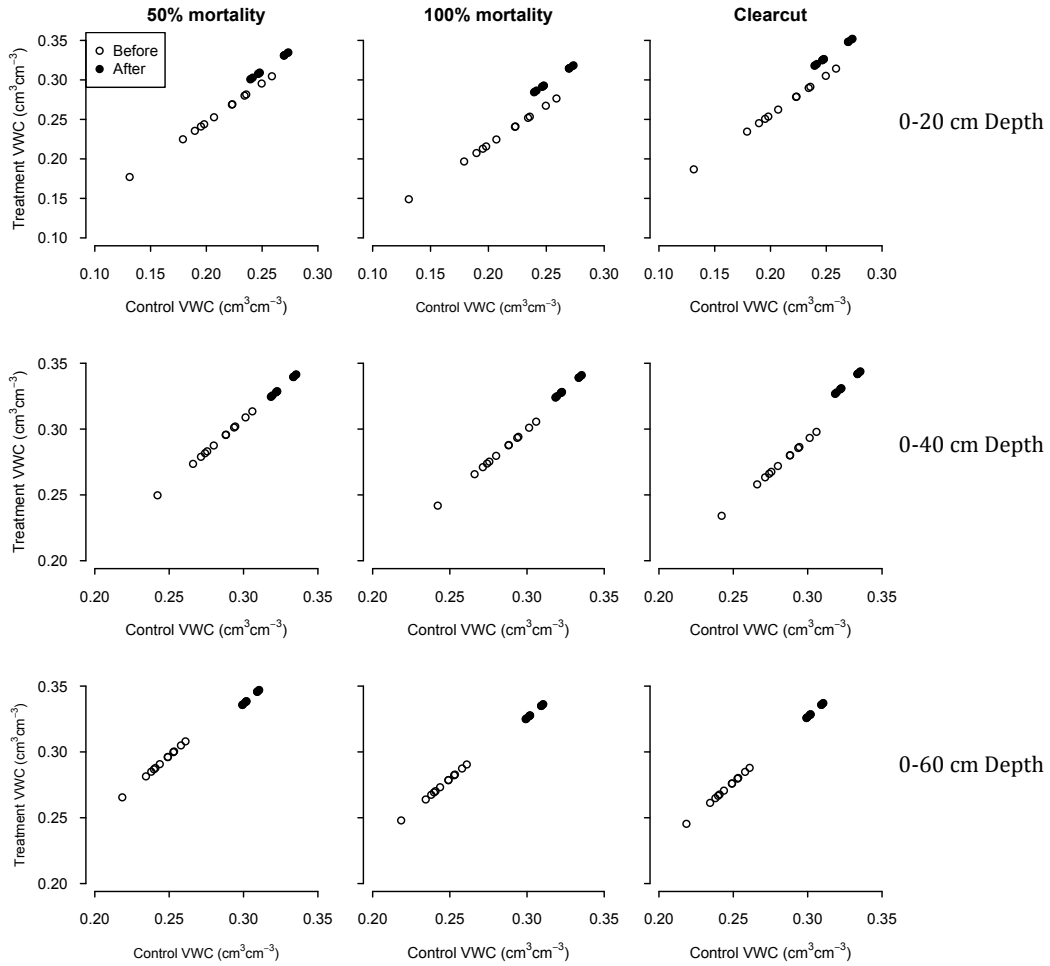


Figure 4-5. Precipitation (mm) and median (n=81) soil VWC (cm³ cm⁻³) at 5 cm depth in 2010. Arrows indicate the four dates used for the spatial analysis.

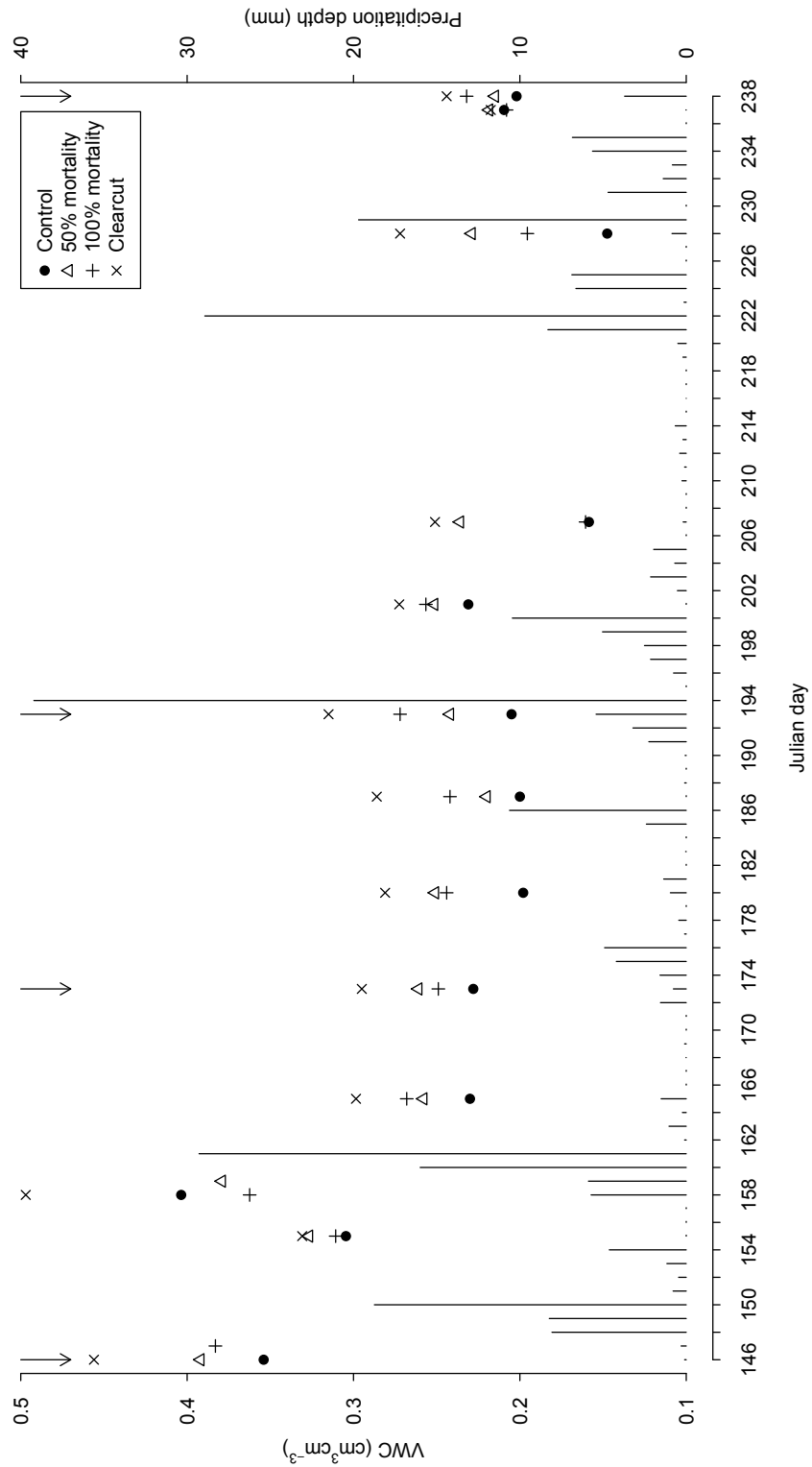


Figure 4-6. Probability Density Functions (PDF) of the simulations (n= 1000) of moisture storage at 5 cm depth for four treatment units. The panels represent the four dates used in the spatial analysis.

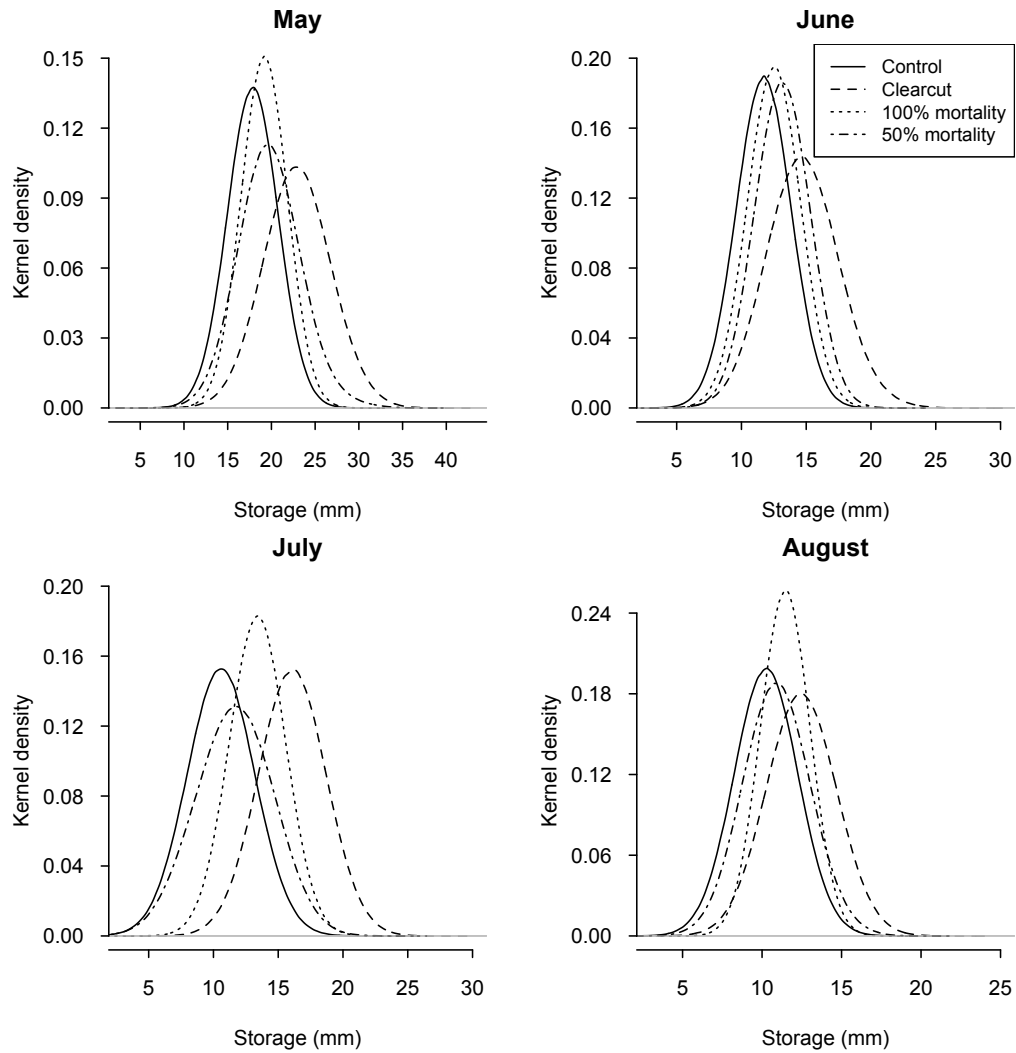
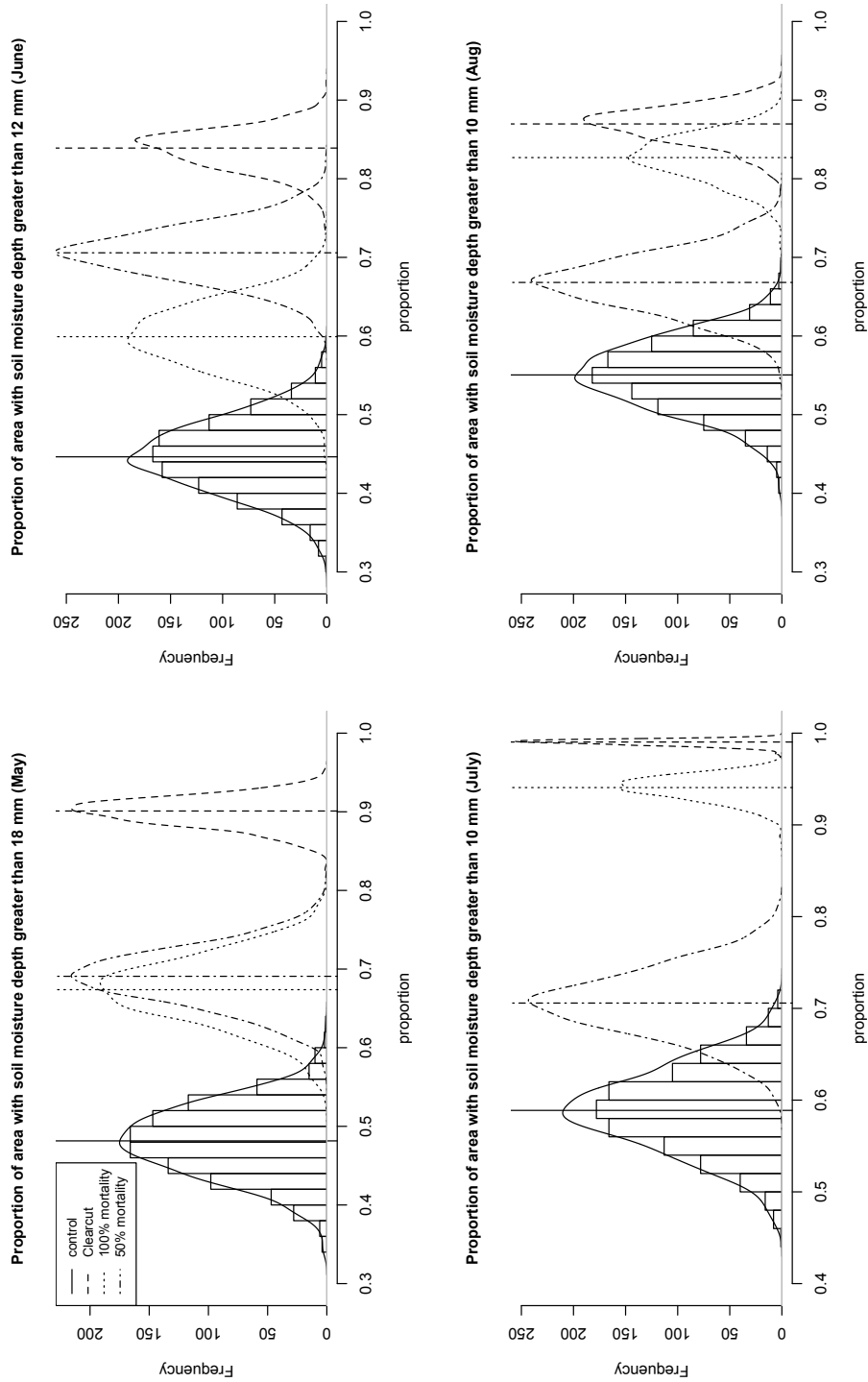


Figure 4-7. Proportion of area in each treated unit exceeding the mean soil moisture storage (mm) at 5 cm depth of the control unit (indicated in titles for each date) for four dates during 2010. Vertical lines indicate the mean proportion of area for each site.



Chapter 5. IMPACT OF VARIABLE INTENSITY MOUNTAIN PINE BEETLE ATTACK ON VERTICAL WATER BALANCE OF MATURE LODGEPOLE PINE FORESTS IN WESTERN ALBERTA

5.1. Introduction

Predicting future water availability is challenged by the likelihood of future changes in both climate and vegetation (Jackson et al., 2009; Wilcox 2010) including those predicted in west central Canada (Mbogga et al., 2009; Gray and Hamman, 2011). Vegetation dynamics, unlike other physical attributes of the landscape occur within relatively short time frames that reflect seasonality, development changes, as well as disturbance conditions. Thus, climate and vegetation shifts have strong potential to impact human use of water because of large scale hydrological changes driven by the interaction of these elements (Troch et al., 2009). Of particular concern is the strength of continental-scale trajectories of drought and warmer temperatures, which have triggered widespread infestations of pathogens and pests (Allen et al., 2010). This is particularly true for lodgepole pine forests (*Pinus contorta* Dougl. ex Loud.) in western North America where the combination of warm winter temperatures and an abundance of mature stands has created optimal conditions for the development of an unprecedented outbreak of mountain pine beetle (MPB; *Dendroctonus ponderosae* Hopkins) (Taylor et al., 2006; Robertson et al., 2007).

The potential impacts of MPB on the forest's hydrology have prompted a wide range of research traditionally focused on evaluating alterations to water yield, peak flows and low flows, channel changes associated with increased runoff, as well as impacts on aquatic habitat and drinking water (Uunila et al., 2006; Redding et al., 2008; Schnorbus, 2011). This research however, is usually limited to potential impacts on the landscape or watershed scale hydrology. Catchment water balance studies have provided the fundamental information regarding the effects of forest development and land-use on evapotranspiration (Bosch and Hewlett 1982, many others). These estimations represent the combined effect or integrated effects of disturbance on individual components regulating water cycling in forests including interception, transpiration, and soil evaporation, which are processes that are not easily separated. However, understanding how disturbance influences these individual factors is required to predict of how MPB is likely to affect water cycling of bark-beetle affected regions across a range of scales (Phillips and Oren, 2001; Simonin et al., 2007; Adams et al., 2011). Changes in stand scale water balance aggregate to manifest at the scale of regional surface and groundwater resources (Brooks and Vivoni, 2008), where an increase in soil moisture results in an increase in groundwater recharge and runoff generation in MPB affected landscapes.

Unfortunately, comparatively little direct research has been conducted on MPB impacts to water balance of lodgepole pine stands. Boon (2009 and 2012), and Winkler et al. (2010) observed large changes in net radiation and wind penetration during the latter phases of MPB attack that produced subsequent

increases in snow accumulation and melt processes though the impact of these winter processes on overall (annual) water cycling remains unclear. Unpublished research by Spittlehouse (2002; 2006) in the Upper Penticton Creek Watershed Experiment in BC, showed considerable impact of different levels of MPB attack on transpiration and rainfall interception processes. These, in turn, were used in water balance modeling efforts that showed both increases and decreases in drainage below the rooting zone of partially and severely attacked stands were produced by changes in interception and evaporation between stand types. Many more authors have attempted to describe potential hydrologic impacts of MPB based conceptual changes in water cycling based on synthesis of existing literature describing individual components of water balance of healthy lodgepole pine forests such as interception, transpiration, soil moisture storage (Hélie et al., 2005; Uunila et al., 2006; Redding et al., 2008; Schnorbus, 2011) while others (Bewley et al., 2010; Alila, 2009) have attempted to predict these impacts using models based on other crudely analogous types of forest disturbances, or uncertain (and questionable) model parameters such as ones derived from other forest tree species.

The present research encompasses several significant direct studies documenting the impact of differing intensities of MPB attack on key components regulating water cycling in beetle affected stands including rainfall interception by the canopy and forest floor layers, transpiration, and soil moisture dynamics (chapters 2, 3, and 4). However, the combined (integrated) effects of these components are uncertain as MPB impacts to individual water balance components may produce interactions among water balance components that could moderate overall system response in ways that are not easily predicted.

The present study represents an integration of the relationships developed in the vertical water balance components of Chapters 2 and 3 to provide insights into the likely stand or forest scale impacts of MPB attack in Alberta. The primary objectives of this study were: 1) to examine rainfall interception, transpiration, and drainage dynamics across a range of MPB attack intensities using historical precipitation regimes characteristic of the region supporting lodgepole pine forests in Alberta; and 2) to examine the interaction these components in regulating overall vertical water balance of the lodgepole pine forest in Alberta.

5.2. Materials and methods

The study area encompassed the entire geographic region of lodgepole pine occurrence in the western portion of Alberta (Figure 5-1) reported in "Atlas of United States Trees" (U.S. Geological Survey, 1999). Historic climate records for daily rainfall (P_G , mm d⁻¹) and mean daily air temperature (TC , °C) were obtained from climate stations distributed across this region (Environment Canada, 2011a and 2011b). Daily precipitation and air temperature data for the summer growing season (May-Sept) from 1979 to 2010 were as abstracted for 54 stations across this region (Figure 5-1). Climate stations with > 10 contiguous

days of missing records between May-Sept. were omitted from the analysis..

Records for daily precipitation and air temperature across the region were used input data for the rainfall interception model described in Chapter 2 (see Section 2.2.7) and a transpiration model (below) to predict daily canopy and forest floor interception and transpiration in healthy lodgepole pine stands (baseline scenario). The parameters developed in Chapter 2 (Table 2-3) were used in to model the expected daily rainfall interception by the canopy and forest floor that would occur across the daily precipitation records for each climate station. A similar approach was used for predict transpiration (below) using relationships between potential evapotranspiration (evaporative demand of the atmosphere) and total daily transpiration of the different categories of trees that existed in the stands described in Chapter 3. Thus the model outputs for both interception and transpiration (for healthy trees) would be representative of what would be expected for a healthy, mature lodgepole pine stand. The healthy forest condition (hereafter referred to as “control”) was a lodgepole pine stand >100 years old, 20–24 m tall, with 48% of canopy cover, and a well developed forest floor mainly composed of bryophytes species.

5.2.1. Interception

Daily canopy and forest floor interception for the period of record for each climate station was calculated using the canopy and forest floor sub-models developed in Chapter 2 and linked in series to predict total daily rainfall interception loss by the forest. Canopy interception I_c (mm) was calculated as:

$$I_c = C_m \left[1 - \exp \left(- \frac{(1-p)}{C_m} P_G \right) \right] \left[1 - \frac{E_c}{(1-p)R} \right] + \frac{E_c}{R} P_G \quad (1)$$

where C_m (mm) is the stand storage capacity; p is the canopy gap fraction (or canopy openness), which represents the proportion of throughfall that reaches the forest floor by passing directly through the canopy; and E_c (E^*c , mm) and R (mm) represent the mean evaporative and rainfall rate respectively.

Similar to canopy interception, forest floor interception I_F (mm) was calculated as:

$$I_F = S_{Fl} \left[1 - \exp \left(- \frac{1}{S_{Fl}} P_n \right) \right] \left[1 - \frac{E_F}{R_{net}} \right] + \frac{E_F}{R_{net}} P_n \quad (2)$$

where E_F (mm) is the evaporative demand in the forest floor, P_n (mm) represents net precipitation ($P_n = T_h$); R_{net} (mm) is the mean rate of net precipitation; and S_{Fl} (mm) is the forest floor storage capacity. The sum of I_c and I_F represents total forest interception I_{tf} (mm). The recharge into the mineral soil F (mm) was calculated by subtracting I_{tf} from P_G .

One control and three different scenarios of increasing MPB attack intensity were modeled. For the interception component, the MPB attack scenarios representing a gradient of attack intensity were modeled using increasing

canopy gap fraction or openness (parameter p above) relative to the control scenario. MPB1 represented a 25%, MPB2 a 50% and MPB3 a 75% increase in p , respectively.

5.2.2. Transpiration

Since this modeling exercise employed historical data on precipitation for forest interception, a simple formulation of evapotranspiration allowed the parallel calculations using means, minimums and maximums of available daily temperature data. Transpiration was modeled using relationships between potential evapotranspiration and observed transpiration of trees reported in Chapter 3. Potential transpiration ET_0 (mm d^{-1}) was calculated using the empirical Hargreaves evapotranspiration equation (Hargreaves and Allen, 2003):

$$ET_0 = 0.0023 * R_a * (TC + 17.8) * TR^{0.5} \quad (3)$$

where R_a is the extraterrestrial radiation ($\text{MJ m}^2 \text{d}^{-1}$), TC is air temperature ($^{\circ}\text{C}$) and TR is the difference between daily maximum and minimum temperatures. Extra-terrestrial radiation was estimated from latitude for each station and Julian Day in the record for each station after (Duffie and Beckman, 1980):

$$R_a = \left(\frac{24*60}{\pi}\right) G_{sc} d_r [\omega_s \sin\delta \sin\phi \cos\delta \sin\omega_{\square}] \quad (4)$$

where G_{sc} ($0.082 \text{ MJ m}^2 \text{min}^{-1}$) is a solar constant; d_r is the correction for eccentricity of Earth's orbit around the sun on a day i of the year:

$$d_r = 1 + 0.033 \cos\left(\frac{2\pi}{365} i\right) \quad (5)$$

ω_s is the sunrise hour angle (radians):

$$\omega_s = \cos^{-1}(-\tan\phi \tan\delta) \quad (6)$$

δ is the declination of the sun above the celestial equator in radians on a day i of the year:

$$\delta = 0.409 \sin\left(\frac{2\pi}{365} i - 1.39\right) \quad (7)$$

ϕ is the latitude in radians converted from latitude (L) in degrees:

$$\phi = \frac{\pi * L}{180} \quad (8)$$

Transpiration of live, live within dead, and fading (dying) trees as a function of ET_0 was calculated using relationships between daily ET_0 (mm d^{-1}) and mean daily transpiration per unit ground area (T_g , mm d^{-1}) of trees in these categories in measured during the 2010 growing season as reported on in chapter 3

(Figure 5-2). Cloudy days with rain or days with minimum temperatures below zero were excluded from the relationships between measured T_g and ET_0 to avoid introducing bias into the relationships caused by poor coupling of transpiration with evaporative demand. This resulted in approximately 24, relatively clear-sky, rain free days spanning May-Aug used to develop these relationships (Figure 5-2).

Four scenarios including a control and three different intensities of MPB attack were simulated using transpiration from the control unit and three categories of trees comprising MPB attack conditions: a) live (untreated) trees surrounded by dead or dying trees (hereafter referred to as “live within dead”) show positive transpiration response due to improved access to growing resources (water, nutrients, etc.); b) dying trees with strongly reduced transpiration (hereafter referred to as “fading” trees), and c) trees with completely red crowns that are no longer transpiring (hereafter referred to as “dead”). Stand level transpiration (T_{st} , mm d⁻¹) in the control scenario was based on the T_g from live trees in the control experimental unit (T_g control = $0.14 \times ET_0 - 0.10$, $R^2 = 0.76$, Figure 5-2). T_{st} in the MPB1 scenario light-moderate attack where stand level transpiration response of dead and fading trees was buffered by approximately 75% live within dead (un-attacked) trees. The following proportion of trees was used to define the MPB1 scenario (from chapter 3); 77.5% live within dead trees ($T_g = 0.14 \times ET_0 - 0.09$, $R^2 = 0.59$, Figure 5-2), 13.4% fading (treated) trees ($T_g = 0.08 \times ET_0 - 0.02$, $R^2 = 0.71$, Figure 5-2), and 9.1% dead trees ($T_g = 0$). T_{st} in the MPB2 scenario was based on the assumption that all trees in the stand were attacked and fading and was calculated using only T_g from fading trees (above). All trees in the MPB3 scenario were considered dead (i.e., T_g and $T_{st} = 0$).

5.2.3. Evapotranspiration and Water balance

Evapotranspiration E_t (mm d⁻¹) was assumed to be the sum of I_{tf} and T_{st} . The water balance calculated from the residual of P_g and E_t as:

$$Q = P_G - E_t \quad (9)$$

thus Q (mm) represents both storage and drainage below the rooting zone.

Because T_{st} in the MPB3 scenario was set to 0, E_t was entirely represented by total forest rainfall interception (I_{tf}) for that scenario. Thus the canopy gap fraction of 25% used to model rainfall interception in MPB3 was meant to represent the rainfall interception by tree trunks, branch, and the forest floor that would still be present in a completely dead stand.

5.2.4. Statistical analysis

The data analysis was performed using R version 2.15.1 (R Core Team, 2012). A Student's t test testing equality of two population regression coefficients (Zar, 1999) was performed to test for significant changes in the slope lines and intercepts between I_{tf} in the MPB scenarios as a function of I_{tf} in the control

scenario. This same approach was used to compare Q among scenarios. The strength of the relationship between Q and P_G was tested with linear regressions for each scenario on a daily and annual basis. Differences in the relationships with P_G between scenarios evaluated using 95% confidence intervals that resulted from the linear regressions between I_{tf} and Q as a function of P_G on an annual basis.

5.3. Results

5.3.1. Regional water balance

A total of 48 climate stations (out of 54) had continuous historical records (32 years) of both daily rainfall and air temperature in the study region to enable water balance modeling (Table 5-1). Annual summer growing season median P_G for the region was 273 mm (mean of 272, Table 5-2), with lower and upper interquartile ranges of 202 mm and 342 mm respectively (Figure 5-2). Mean growing season P_G was unrelated to elevation in this region ($R^2=0.07$, $P=0.08$) suggesting that most of the summer P_G was dominantly associated with convective storms opposed to cyclonic systems where elevation gradients and precipitation lapse rates would drive spatial patterns of greater precipitation at higher elevations. On average, the south and north portions of the studied region were dry compared to the central region, where Markerville station had the lowest growing season P_G with 163 mm (ID MARK33, Table 5-2), and Winfield station had the highest P_G with 390 mm (ID WINF48, Table 5-2). The temporal distribution in of growing season P_G indicated a dryer period beginning in approximately 1998 until present, when total summer P_G of nine out of thirteen years was below the regional 32 year median P_G (Figure 5-2). Mean annual water balance components for healthy forest conditions across the stations indicated that E_t was the dominant component of the water balance comprising 92% of P_G (251 mm, Table 5-2) across the region. I_{tf} was the main source of E_t , representing 72% of P_G and 78% of E_t (Table 5-2). While Q calculated at daily or annual time steps represents both drainage and changes in storage, long-term mean Q represents only drainage since positive and negative changes in storage tend to approach zero when averaged over long periods. The coefficients of variation of water balance components indicated a large spatial variability of these components across the region. Mean growing season Q across the region was only 20 mm (7.4% of P_G) and was the most variable component in the water balance; coefficients of variation for P_G , E_t , and Q were 0.2, 0.15, and 0.55, respectively (Table 5-2).

5.3.2. Effect of the MPB in the water balance

5.3.2.1. Rainfall interception and total evapotranspiration

Mean long-term I_c and I_F across the region were generally similar in magnitude in the healthy forest condition, comprising 40% (110 mm/yr) and 32 % (87 mm/yr) of mean growing season precipitation (196 mm/yr) respectively (Table 5-2, Table 5-3). However, the predicted effect of MPB produced very different responses in these two components of total rainfall interception. Canopy

interception dominated total annual forest interception under control conditions, whereas forest floor interception dominated total forest interception in the MPB scenarios. Rainfall interception by the canopy was strongly reduced across the gradient of MPB attack scenarios where mean annual I_c of 110mm/yr in the control scenario was progressively reduced to 31 mm/yr in the MPB3 scenario (Table 5-3). In contrast, mean rainfall interception by the forest floor was progressively increased across the scenarios (87 mm/yr. in the control scenario through 115 mm/yr in MPB3). However, because canopy interception represented > 56% of total rainfall interception losses (Table 5-2) the combined effect of decreased and increased I_c and I_f resulted in decreasing total forest interception across the gradient of increasing MPB attack intensity. Mean long-term I_{tf} was 196, 185, 168, and 148 in the control, MPB1, MPB2, and MPB3 scenarios respectively. Furthermore, because rainfall interception comprised 78% of total forest evaporative losses (E_t), the gradient of scenarios representing increasing intensity of MPB attack strongly reduced mean growing season E_t from 251 mm/yr in the control scenario to 148 mm/yr in the MPB3 scenario (Table 5-3).

Very little variability in I_{tf} among the MPB scenarios was evident when total daily rainfall was below 10mm/day, however, larger differences were predicted for increasingly greater daily rainfall magnitudes up to 40 mm/day (Figure 5-4 A). These differences in I_{tf} among MPB scenarios as a percentage of daily rainfall were particularly concentrated within the range of 17 and 18.5 mm (vertical lines in Figure 5-4 A), when I_{tf} was 66% of rainfall under control conditions, and I_{tf} was 59%, 51% and 42% of rainfall in the MPB1, MPB2 and MPB3 scenarios respectively. Similar to daily I_{tf} , lower variability in I_{tf} among the MPB scenarios was evident when total annual rainfall was below 210mm/year, however, larger differences were predicted for increasing annual rainfall magnitudes up to 350 mm/year (Figure 5-4 B). Total annual I_{tf} had a strong linear relationship with total seasonal rainfall (Figure 5-4 B) where R^2 of linear regressions were 0.94 for control conditions, and 0.93, 0.92 and 0.89 in the MPB1, MPB2 and MPB3 scenarios respectively. There were no statistically significant differences between the slopes of the linear regressions of the control conditions and MPB1 scenario, but there were significant differences between the slopes of the linear regressions of the control conditions and the MPB2 and MPB3 scenarios. None of the intercepts of the regressions were significantly different from control conditions.

Nonlinear relationships between daily F and I_{tf} with P_G were evident (Figure 5-5). The point at which daily recharge into the mineral soil equaled daily I_{tf} indicates a threshold in rainfall magnitude beyond which recharge into the mineral soil increases rapidly. This threshold rainfall magnitude was greatest in the control scenario (33.4 mm) and progressively decreased to 25.9, 18.4, and 12.6 mm for the MPB1, MPB2, and MPB3 scenarios respectively. While daily rainfall was large enough for F to exceed I_{tf} in only 1% of days across the record in the control scenario, this threshold was reached in 3%, 6% and 12% of the days with rain in the MPB1, MPB2, and MPB3 scenarios.

Mean growing season E_t decreased as the magnitude of the MPB attack increased (Table 5-4). E_t was the dominant component in the water balance, however since E_t decreased following an increase of MPB attack, the contribution of Q to the water balance increased to a point where Q dominated the water balance in the MPB3 scenario (Table 5-4).

5.3.2.2. Storage and drainage

The effects of changes in mean evaporative losses among MPB scenarios also produced strong increases in water drainage beneath the forest floor. While F increased from 73 to 127 mm/yr across the four scenarios, the largest change in any of the components of the water balance was observed for Q . Mean growing season Q increased from 20, 30, 71, and 127 mm/yr in the control through to the MPB3 scenario, respectively (Table 5-3). The mean Q predicted in the most severe MPB scenario (127 mm/yr in MPB3) represented a 6.4 fold increase over that predicted in the control scenario.

Mean daily Q across years and stations in the control and MPB1 scenarios did not indicate a clear pattern of seasonality throughout the growing season (Figure 5-6). Instead, storage and drainage in these two scenarios ranged between zero and one indicating close 1:1 ratio between precipitation inputs and evaporative losses. While mean daily Q throughout the growing season in the MPB1 scenario was only slightly higher than that of control conditions, mean daily Q in the MPB2 and MPB3 each progressively greater than the control scenario which was particularly evident near the peak of the growing season in July (Figure 5-6). Linear regressions between daily Q and P_G (relationships not shown) indicated progressively stronger relationships were evident along the disturbance gradient from control to MPB3 scenarios; R^2 were 0.56, 0.79, 0.89 and 0.97 for control, MPB1, MPB2 and MPB3 scenarios respectively. Thus, the gradient in growing season Q from control through MPB3 scenarios was likely driven by increasing sensitivity of Q to seasonal variation daily rainfall with increasing intensity of MPB attack (Figure 5-6). Similarly, increasingly stronger linear relationships were observed between mean annual Q with mean annual P_G across the gradient of disturbance scenarios (Figure 5-7 A). The R^2 of these relationship for control conditions was 0.83, and increased to 0.88, 0.91 and 0.94 in the MPB1, MPB2 and MPB3 scenarios respectively indicating closer coupling between precipitation and Q along this disturbance gradient. Very little variability in growing season Q among the control and MPB1 scenarios was evident when total annual rainfall was below 270mm/yr, however, larger differences were predicted for increasing growing season rainfall magnitudes up to 350 mm/yr (Figure 5-7 A). In contrast, total annual Q in the MPB2 and MPB3 scenarios was clearly greater than Q under control conditions across the same range in precipitation. Comparison of regression relationships (control versus MPB scenarios) indicated significant differences in the intercepts for both MPB2 and MPB3 scenarios, where both slopes and intercepts differed among control and MPB3 scenarios.

The regression models for control and MPB1 conditions indicated that $Q < 0$

would be expected where growing season P_G was between ~230 to 200 mm (Figure 5-6 A) and these two scenarios were the only scenarios where $Q < 0$ across the 32 year historic climate record (Figure 5-7 B). These years were mainly concentrated between 1998 and 2010 (Figure 5-7 B) and corresponded to dry years where annual P_G was below the long-term rainfall median (< 273 mm, Figure 5-3).

5.4. Discussion

Results of this research showed a clear gradient of increasing storage and drainage in mature lodgepole pine stands during the growing season across the disturbance gradient of increasing intensity of MPB attack. Furthermore, these effects increased in magnitude where growing season precipitation was greater. Evapotranspiration was the dominant component in the water balance, where total rainfall interception was the main source of this evaporative loss. However, as evapotranspiration decreased along the gradient of increasing intensity of MPB attack, the contribution of storage and drainage in the water balance increased strongly. These findings are novel because while the effects of MPB attack on water balance of lodgepole pine stands have been previously explored via modeling using unconfirmed parameters or parameters based on other tree species or disturbance types, impacts of MPB attack on stand water balances in this study reflect the combined outcome of carefully measured, representative water components in mature lodgepole pine that have not been previously reported. Thus the effects of MPB attack modeled herein reflect considerably greater certainly than previous efforts.

5.4.1. Effects of MPB on rainfall interception

Combined rainfall interception by the canopy and forest floor (I_{tf}) accounted for over 78% of total evaporative losses across the range of climatic conditions supporting lodgepole pine forests in Alberta, suggesting that the interaction of changes in I_{tf} after MPB attack and rainfall magnitude are very important drivers of hydrologic response to MPB at both short (daily) and longer (growing season) time scales. Because the variability of water balance components in the MPB scenarios was strongly positively related to rainfall magnitude, only larger rainfall events (> 10 mm) were sufficient produce a clear gradient in I_{tf} between MPB scenarios. Based on literature review of likely MPB effects on rainfall interception, Schnorbus (2011) argued that the MPB attack is unlikely to produce strong changes in rainfall interception except in the case of considerable canopy cover loss such as during the latter grey attack phase of attack. While this is generally consistent with findings from this study, the proportional reduction in canopy over of 25, 50, and 75% across MPB1-MPB3 scenarios in this study did not produce a linearly proportional response in water balance. While a strong linear reduction in I_{tf} was predicted across the disturbance gradient ($R^2=0.999$), linear increases in I_F ($R^2=0.996$) and highly non-linear (increased followed by decreased) changes in transpiration produced a muted response to increasing severity of MPB attack where these latter components compensated or buffered the direct changes of canopy interception

on overall water balance. Because these interacting processes have not been previously measured nor represented in recent efforts to predict hydrologic changes after MPB attack, these results are novel as they reflect the documented interaction among major components governing stand water balance in lodgepole pine forests.

The relationships illustrating variation in rainfall event sizes where daily recharge into the mineral soil equalled to total forest interception (Figure 5-5) indicated a threshold representing a switch in response to rainfall dominated either by upward evaporative loss (total forest interception, I_{tf}) or to downward gain of soil water (recharge into the mineral soil, F). Because F increased and I_{tf} decreased along the gradient of MPB attack scenarios, these thresholds were associated with progressively smaller rainfall events (Figure 5-5). Thus increasing severity of MPB attack is likely to drive progressive increases in the likelihood of growing season rainfall producing a downward gain of soil moisture (i.e., F) or groundwater recharge. This idea is generally consistent with unpublished research by Spittlehouse (2007) in the Upper Pentiction Creek Watershed Experiment in B.C. which showed variation in drainage among healthy, partially attacked, and severely attacked stands was largely due to differences in interception and evaporation between stand types. However, intensively attacked stands in that study showed greater drainage than healthy forest, while a partially attacked stand showed slightly higher drainage than the healthy forest (Spittlehouse, 2007). In contrast, my results suggest progressive (though non-linear) increases in drainage can be expected with increasing intensity of MPB attack.

The mean growing season components of rainfall interception (I_c , I_f and F) across the forest disturbance scenarios also illustrated the particular importance of the forest floor in regulating total forest evaporative loss (Table 5-3). In particular in the MPB1 scenario, an increase in the forest floor interception (as a result of a decrease in I_c) resulted in a mean annual I_{tf} very close to the mean annual I_{tf} under control conditions (9 mm less). This suggests that under moderate MPB attack conditions forest floor interception has the capacity to attenuate a direct decrease in canopy interception, whereas under more severe MPB attack conditions the forest floor interception could represent the main source of forest rainfall interception and thus, the main source of evaporative loss. While previous authors also speculated that the forest floor layer could compensate for the loss of overstory in beetle-killed stands (Carlyle-Moses, 2007; Silins, 2007; Stednick and Jensen 2007), this study is the first (to my knowledge) to explicitly explore the contribution of this component to overall interception dynamics of MPB affected forests and represents an additional novel contribution of this work.

5.4.2. Effects of MPB on water balance

Total forest interception was the main source of evaporative loss and was followed by stand transpiration. Combined total forest interception and transpiration represented 96% and 92% of the total rainfall on a daily and

annual basis respectively. These results are in contrast to previous (unpublished) modelling efforts of MPB impacts on water balance of lodgepole pine forests (Spittlehouse 2002, 2006, and Silins et al. 2007). Spittlehouse (2002; 2006) reported that overstory transpiration was the main source of evaporative loss in lodgepole pine forests. While Spittlehouse (2002; 2006) reported nearly identical estimates for daily and annual E_t of 90% to 92% of rainfall as the present study, the contribution of the forest floor layer to rainfall interception was not measured, but was represented as understory evaporative loss instead. However, the explicit measurement and modeling of I_F in both Chapter 2 and the present study, along with the findings by Carlyle-Moses (2007) and Silins et al. (2007) all support the notion that the storage capacity of the forest floor represents an important component forest rainfall interception. Indeed, a modest increase in the contribution of total forest interception ($\sim 10\%$) to E_t , based on the magnitude of the other water balance components reported by Spittlehouse (2002; 2006), total forest rainfall interception would be the main source of evaporative loss in lodgepole pine forests in those studies. Similarly, Silins et al. (2007) also concluded that transpiration is the largest component of E_t in lodgepole pine forests. In that case, Silins et al. (2007) used estimates of canopy interception from 25-year-old juvenile pine stands after Brabender (2005) where rainfall interception losses were lower than those measured for mature stands in this study, and transpiration rates from other juvenile stands based on a study by Reid et al. (2005). Thus, while transpiration may have dominated the evaporative losses in juvenile stands modeled by Silins et al. (2007), interception was clearly the dominant component of stand water balance in the mature stands measured in Chapters 2 and 3 and modeled in the present study. This idea is further supported by Brabender (2005) who reported canopy interception of mature stands that varied only $\sim 10\%$ and 2% from the measured and modeled canopy interception values reported in Chapter 2.

Results of seasonal variation in the mean daily storage and drainage (Q) among MPB scenarios also closely paralleled the seasonal pattern of precipitation. Although the daily time series in Q did not show a clear pattern of seasonal variation in the control and MPB1 scenarios, the MPB2 and particularly the MPB3 scenarios reflected the bell-shape pattern reflecting the long-term distribution of rainfall across the growing season. This progressive increase in coupling between Q and daily precipitation with increasing intensity of MPB attack suggests that the magnitude of MPB impacts on water cycling are strongly modified by rainfall regimes that govern variation in daily and seasonal precipitation among regions. This was also supported by very strong linear relationships between mean seasonal Q with total seasonal precipitation across the 48 climate stations representing the range of precipitation regimes for lodgepole pine forests in Alberta. The greatest impact of the MPB scenarios was evident at the wetter range of seasonal precipitation. These results suggest that larger impacts of MPB attack can be expected in regions with greater mean summer precipitation, greater convective storm activities, or across regions in wetter years as compared to drier years.

Indeed, in addition to the influence of climate on vulnerability of forests to bark-

beetle attack, variability of climate in the future may play an important role in the hydrologic impacts of forests already attacked by these insects. The variation in annual water balance of the previous 32 years (Figure 5-7 B) indicated a dry trend for the past 13 years where P_G was generally below the region's long-term median P_G (Figure 5-3). During this same period there was higher frequency of years with annual $Q < 0$ in both the control and MPB1 scenarios where the impact of the MPB1 scenario on Q was very small or negligible and the MPB2 and MPB3 scenarios were much smaller than those of average or wet years. This suggests that dry years ($P_G \leq 230$ mm) could buffer impacts of MPB on Q under moderate levels of MPB attack where impacts of MPB of runoff from these stands would likely be indistinguishable from that of healthy forests. However, no meaningful conclusions on long-term trends and likely future precipitation can be drawn from this precipitation record.

5.5. Conclusions

Results of this research showed a clear gradient of changes to the components governing water cycling in response to increasing intensity of MBP attack in mature lodgepole forests including up to 6.4 fold increases in drainage for the most severe MPB attack scenario. Evapotranspiration was the dominant component in the water balance, and in contrast to previous research, total rainfall interception was the main source of this evaporative loss. However, both the role of increased rainfall interception by the forest floor, and highly variable changes in transpiration responses produced interactions among components of stand water balance that buffered or moderated the impacts of MPB on water balance across the gradient of increasing intensity of MPB attack modeled in this study. The impact of MPB on all water cycling components increased in magnitude during wetter years or where growing season precipitation was greater suggesting that the impact of bark-beetle attack are likely to be greatest in the regions of Alberta where growing season precipitation is greatest.

While effects of MPB attack on water balance of lodgepole pine stands have been modeled by others using uncertain model parameters, impacts of MPB attack on stand water balances explored in this study reflect the combined outcome of carefully measured, representative water components in mature lodgepole pine that have not been previously reported. Thus the effects of MPB attack predicted in this study reflect considerably greater certainly than previous efforts.

5.6. References

- Adams, H. D., C. H. Luce, et al. (2011). "Ecohydrological consequences of drought- and infestation- triggered tree die-off: insights and hypothesis." Ecohydrology 5(2): 145-159.
- Alila, Y., D. Bewley, et al. (2009). Effects of pine beetle infestations and treatments on hydrology and geomorphology: integrating stand-level data and knowledge in mesoscale watershed functions. Mountain Pine Beetle Working Paper. Victoria, BC, Natural Resources Canada, Canadian Forest Service, Pacific Forestry Centre: 69.
- Allen, C. D., A. K. Macalady, et al. (2010). "A global overview of drought and heat-induced tree mortality reveals emerging climate change risks for forests." Forest Ecology and Management 259(4): 660-684.
- Beckman, W. A. and J. A. Duffie (1980). Solar heat in industrial processing. Proceedings of the Meat Industry Research Conference, Chicago, USA.
- Bewley, D., Y. Alila, et al. (2010). "Variability of snow water equivalent and snow energetics across a large catchment subject to Mountain Pine Beetle infestation and rapid salvage logging." Journal Of Hydrology 388(3-4): 464-479.
- Boon, S. (2009). "Snow ablation energy balance in a dead forest stand." Hydrological Processes 23(18): 2600-2610.
- Boon, S. (2012). "Snow accumulation following forest disturbance." Ecohydrology 5(3): 279-285.
- Bosch, J. M. and J. D. Hewlett (1982). "A review of catchment experiments to determine the effect of vegetation changes on water yield and evapotranspiration." Journal of Hydrology 55(1-4): 3-23.
- Brabender, B. (2005). Scaling Leaf Area Index and rainfall interception in lodgepole pine. Renewable Resources. Edmonton, University of Alberta. Master of Science: 91.
- Brooks, P. D. and E. R. Vivoni (2008). "Mountain ecohydrology: quantifying the role of vegetation in the water balance of montane catchments." Ecohydrology 1(3): 187-192.
- Carlyle-Moses, D. E. (2007). Measurement and modelling of mountain pine beetle impacts on annual forest water balance. Final Report, Ministry of Forests and Range: 26.
- Environment Canada. (2011, 2011-05-18). "National Climate data and Information Archive." Climate Data Online Retrieved 2011-07-07, 2011, from http://www.climate.weatheroffice.gc.ca/climateData/canada_e.html.
- Environment Canada. (2011, 2011-05-18). "National Climate data and Information Archive." Canadian Climate Normals or Averages 1971-2000 Retrieved 2011-07-07, 2011, from http://climate.weatheroffice.gc.ca/climate_normals/index_e.html.
- Gray, L. K. and A. Hamann (2011). "Strategies for reforestation under uncertain future climates: guidelines for Alberta, Canada." PLoS ONE 6(8): e22977.

- Hargreaves, G. H. and R. G. Allen (2003). "History and evaluation of Hargreaves evapotranspiration equation." Journal of Irrigation and Drainage Engineering-ASCE 129(1): 53-63.
- Jackson, R. B., H. J. Schenk, et al. (2000). "Belowground consequences of vegetation change and their treatment in models." Ecological Applications 10(2): 470-483.
- Knight, D. H., J. B. Yavitt, et al. (1991). "Water and nitrogen outflow from lodgepole pine forest after 2 levels of tree mortality." Forest Ecology and Management 46(3-4): 215-225.
- Mbogga, M. S., A. Hamann, et al. (2009). "Historical and projected climate data for natural resource management in western Canada." Agricultural and Forest Meteorology 149(5): 881-890.
- Phillips, N. and R. Oren (2001). "Intra- and inter-annual variation in transpiration of a pine forest." Ecological Applications 11(2): 385-396.
- R Core Team (2012). R: A language and environment for statistical computing. Vienna, R Foundation for Statistical Computing.
- Redding, T. E., R. D. Winkler, et al. (2008). Mountain pine beetle and watershed hydrology: A synthesis focused on the Okanagan. One Watershed – One Water, Kelowna, BC, Canadian Water Resources Association.
- Robertson, C., T. A. Nelson, et al. (2007). "Mountain pine beetle dispersal: the spatial-temporal interaction of infestations." Forest Science 53(3): 395-404.
- Schnorbus, M. (2011). A synthesis of the hydrological consequences of large-scale mountain pine beetle disturbance. Mountain Pine Beetle Working Paper 2010-01. Victoria, Natural Resources Canada, Canadian Forest Service, Pacific Forestry Centre: 30.
- Silins, U., V. J. Lieffers, et al. (2007). Stand water balance in absence of mountain pine beetle: Synthesis of several Alberta studies to characterize "reference" water use of lodgepole pine. Proceedings of the Mountain Pine Beetle and Watershed Hydrology Workshop: Preliminary Results of Research from BC, Alberta, and Colorado. Kelowna, BC, FORREX, BC Ministry of Environment, Forest Service BC, Canadian Water Resources Association: 21-22.
- Simonin, K., T. E. Kolb, et al. (2007). "The influence of thinning on components of stand water balance in a ponderosa pine forest stand during and after extreme drought " Agricultural and Forest Meteorology 143: 266-276.
- Spittlehouse, D. L. (2002). Sap flow and transpiration of old lodgepole pine trees. 26th Conference on Agricultural and Forest Meteorology, Norfolk, Virginia, American Meteorological Society.
- Spittlehouse, D. L. (2006). Annual water balance of high elevation forest and clearcuts. 27th Conference on Agricultural and Forest Meteorology, San Diego, American Meteorological Society.
- Spittlehouse, D. L. (2007). Influence of the mountain pine beetle on the site water balance. Mountain Pine Beetle and Watershed Hydrology Workshop: Preliminary results of research from BC, Alberta, and Colorado, Kelowna, BC, FORREX, BC Ministry of Environment, Forest Service BC, Canadian Water Resources Association.

- Stednick, J. D. and R. Jensen (2007). Effects of pine beetle infestations on water yield and water quality at the watershed scale in northern Colorado. Unpublished technical report, Report to Colorado Water Resources Research Institute.
- Taylor, S. W., A. L. Carrol, et al. (2006). Forest, climate and mountain pine beetle dynamics. The mountain pine beetle: A synthesis of its biology, management and impacts on lodgepole pine. L. Safranyik and W. B., Natural Resources Canada, Canadian Forest: 67-94.
- Troch, P. A., G. F. Martinez, et al. (2009). "Climate and vegetation water use efficiency at catchment scales." Hydrological Processes 23(16): 2409-2414.
- U.S. Geological Survey. (1999, 2010). "Digital representation of "Atlas of United States Trees" by Elbert L. Little, Jr." Digital Version 1.0. from <http://esp.cr.usgs.gov/info/veg-clim/>.
- Uunila, L., B. Guy, et al. (2006). "Hydrologic effects of mountain pine beetle in the interior pine forests of British Columbia: key questions and current knowledge." Streamline 9(2): 1-6.
- Wilcox, B. P. (2010). "Transformative ecosystem change and ecohydrology: ushering in a new era for watershed management." Ecohydrology 3(1): 126-130.
- Winkler, R., S. Boon, et al. (2010). "Assessing the effects of post-pine beetle forest litter on snow albedo." Hydrological Processes 24(6): 803-812.
- Zar, J. (1999). Biostatistical analysis. Upper Saddle River, Prentice Hall.

5.7. Tables

Table 5-1. Climate stations in the study region with 32 years of continuous records (May-September) of daily rainfall and air temperature. Station locations (easting and northing) are UTM coordinates for zone 11 using ellipsoid GRS80 and datum NAD83. Elevation units are in meters.

Station	ID	Easting	Northing	Elevation (m)
BANFF	BANF1	600177	5671189	1384
BEAVER MINES	BEAV2	705281	5483194	1257
BEAVERLODGE CDA	BEAV3	347256	6119675	745
BIGHORN DAM	BIGH4	545443	5796469	1341
CALMAR	CALM5	709981	5908419	720
CAMERON FALLS	CAME6	725282	5437594	1311
CAMPSIE	CAMP7	652508	5999019	671
CLEARDALE	CLEA8	346474	6245949	643
CLEARWATER	CLEA9	620179	5760631	1280
COLEMAN	COLE10	674501	5500669	1341
CONNELLY CREEK	CONN11	702315	5497924	1249
CROSS LAKE	CROS12	700156	6056552	655
ECKVILLE SOUTH	ECKV13	678484	5795777	960
EDMONTON STONY PLAIN	EDMO14	692189	5935515	766
EDMONTON WOODBEND	EDMO15	715970	5923544	671
EDSON A	EDSO16	535308	5937297	927
ELBOW RS	ELBO17	661728	5641224	1400
ELMWORTH CDA EPF	ELMW18	324548	6109374	754
ENTRANCE	ENTR19	453422	5913289	991
EUREKA RIVER	EURE20	393255	6261222	665
FAIRVIEW	FAIR21	413876	6214362	670
FORT ASSINIBOINE	FORT22	635349	6026319	671
GHOST RS	GHOS23	644073	5685215	1417
GLENEVIS	GLEN24	663545	5964131	732
GRANDE CACHE RS	GRAN25	362026	5974439	1250
GRANDE PRAIRIE A	GRAN26	380033	6114957	669
GROVEDALE RS	GROV27	384911	6098127	701
JASPER EAST GATE	JASP28	428224	5859825	1003
KANANASKIS	KANA29	637945	5653519	1391
KANANASKIS POCATERRA	KANA30	632998	5618156	1610
KAYBOB 3	KAYB31	525067	5994716	1003
LAKE LOUISE	LAKE32	554452	5698306	1524
MARKERVILLE	MARK33	696266	5777891	914
NORDEGG RS	NORD34	564488	5817076	1320

PEACE RIVER A	PEAC35	473126	6230279	571
PEKISKO	PEKI36	683717	5582590	1439
ROBB RS	ROBB37	502225	5898228	1130
ROCKY MTN HOUSE	ROCK38	641629	5811278	988
SHINING BANK	SHIN39	567977	5967328	829
SIMONETTE	SIMO40	452412	6030130	884
SION	SION41	689505	5974395	701
SLAVE LAKE A	SLAV42	640725	6130414	581
SUNWAPTA	SUNW43	469418	5811186	1555
VALLEYVIEW RS	VALL44	482970	6102243	762
WANHAM CDA	WANH45	413246	6182832	561
WATERTON RIVER CABIN	WATE46	731060	5445255	1281
WHITECOURT A	WHIT47	579495	5999041	782
WINFIELD	WINF48	662358	5869442	910

Table 5-2. Long-term mean (32 years) growing season rainfall (P_G), canopy interception (I_c), throughfall (T_h), forest floor interception (I_F), total forest interception (I_{tf}), recharge into the mineral soil (F), transpiration (T), evapotranspiration (E_t), and drainage and storage (Q) from 48 climate stations across the study region. Summaries below stations refer to mean, standard deviation (Std) and coefficient of variation (CV) across stations. The CV of Q was adjusted to account for the presence of negative numbers.

ID	P_G	I_c	T_h	I_F	I_{tf}	F	T	E_t	Q
BANF1	231	96	132	80	176	49	55	231	-8
BEAV2	255	100	155	73	172	81	55	225	27
BEAV3	231	98	129	78	181	49	60	240	-2
BIGH4	257	108	149	87	197	68	51	246	15
CALM5	340	126	199	100	225	91	64	292	29
CAME6	341	130	208	94	222	104	56	279	51
CAMP7	305	122	177	93	213	79	60	274	19
CLEA8	232	93	141	79	173	66	59	236	8
CLEA9	277	115	164	94	209	79	47	256	29
COLE10	215	93	121	78	172	46	51	225	-9
CONN11	209	87	119	65	154	62	52	207	8
CROS12	334	132	194	102	235	86	60	295	26
ECKV13	331	137	191	106	245	87	55	296	39
EDMO14	310	124	180	96	221	86	58	279	26
EDMO15	287	116	169	94	211	74	63	264	12
EDSO16	282	119	161	98	220	68	58	278	9
ELBO17	245	101	146	74	176	83	43	215	41
ELMW18	267	110	153	89	198	65	61	258	-1
ENTR19	293	119	170	92	210	72	53	264	28
EURE20	214	89	123	75	163	51	57	224	-9
FAIR21	239	101	144	78	184	68	61	244	11
FORT22	297	123	174	100	223	80	58	288	23
GHOS23	283	112	168	90	202	81	45	244	36
GLEN24	310	114	193	94	205	100	62	271	39
GRAN25	266	112	152	87	200	68	49	248	29
GRAN26	253	105	143	82	187	56	62	250	-4
GROV27	238	99	138	77	174	61	62	227	3
JASP28	304	123	176	102	225	73	57	285	16
KANA29	284	112	171	90	205	86	51	261	29
KANA30	172	75	96	66	140	34	39	184	4
KAYB31	304	122	177	98	219	76	53	278	27
LAKE32	180	78	100	69	144	30	40	190	-14
MARK33	163	62	100	44	105	57	24	129	34
NORD34	263	110	148	85	196	76	43	239	36
PEAC35	196	83	113	73	157	51	62	219	-13
PEKI36	237	100	143	81	185	70	49	231	27
ROBB37	372	147	220	103	250	110	57	307	53

ROCK38	353	132	213	93	224	108	52	269	59
SHIN39	290	119	167	100	218	73	58	276	16
SIMO40	335	135	195	102	239	85	54	288	33
SION41	294	113	179	89	202	84	59	261	24
SLAV42	245	100	144	81	180	64	56	240	13
SUNW43	175	75	98	66	140	32	41	185	-10
VALL44	292	112	171	90	202	80	60	262	20
WANH45	238	93	138	74	163	60	61	223	0
WATE46	271	93	162	76	163	84	51	220	28
WHIT47	355	142	209	111	252	99	59	311	44
WINF48	390	150	232	120	266	114	57	324	55
Mean	272	110	159	87	196	73	54	251	20
Std	54	19	33	14	33	19	8	37	19
CV	0.20	0.18	0.21	0.16	0.17	0.26	0.15	0.15	0.55

Table 5-3. Mean growing season canopy interception (I_c), forest floor interception (I_f), total forest interception (I_{tf}), recharge into the mineral soil (F), evapotranspiration (E_t), and drainage and storage (Q) across the 48 climate stations. Mean growing season rainfall (P_G) was 272 mm. Values in brackets indicate the percentage of P_G .

Scenario	Component of water balance					
	I_c	I_f	I_{tf}	F	E_t	Q
Control	110 (40%)	87 (32%)	196 (72%)	73 (27%)	251 (92%)	20 (7%)
MPB1	85 (31%)	98 (36%)	185 (68%)	86 (32%)	244 (90%)	30 (11%)
MPB2	60 (22%)	106 (39%)	168 (62%)	105 (39%)	205 (75%)	71 (26%)
MPB3	31 (11%)	115 (42%)	148 (54%)	127 (47%)	148 (54%)	127 (47%)

5.8. Figures

Figure 5-1. Distribution of lodgepole pine in Alberta and location of climate stations used in this study.

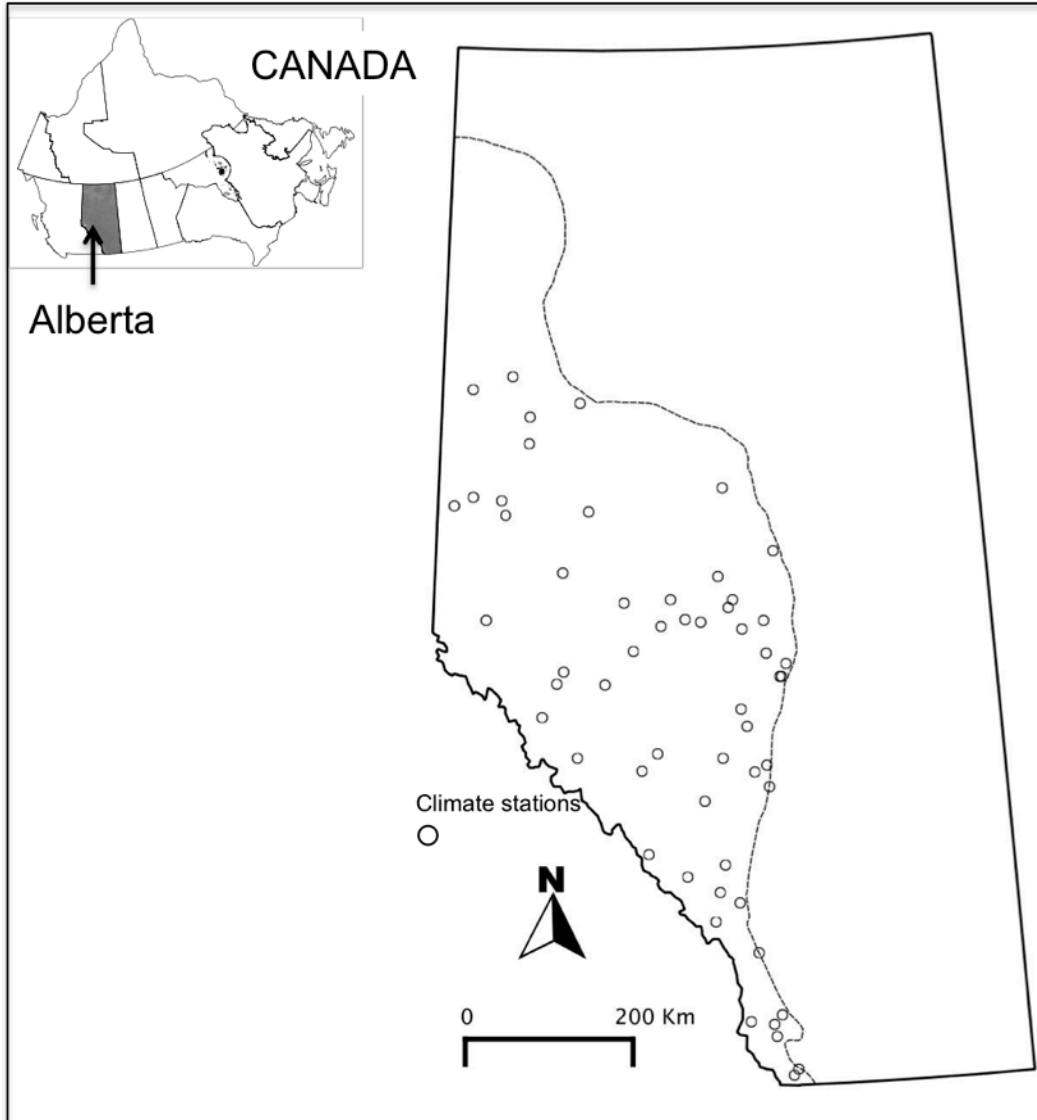


Figure 5-2. Linear relationships between mean daily tree transpiration (T_g) in 2010 for three categories of trees after MPB attack and potential evapotranspiration. Live trees ($y = 0.14 \times ET_0 - 0.10$, $R^2 = 0.76$); live within dead trees ($y = 0.14 \times ET_0 - 0.09$, $R^2 = 0.59$); and dying (fading) trees ($y = 0.08 \times ET_0 - 0.02$, $R^2 = 0.71$).

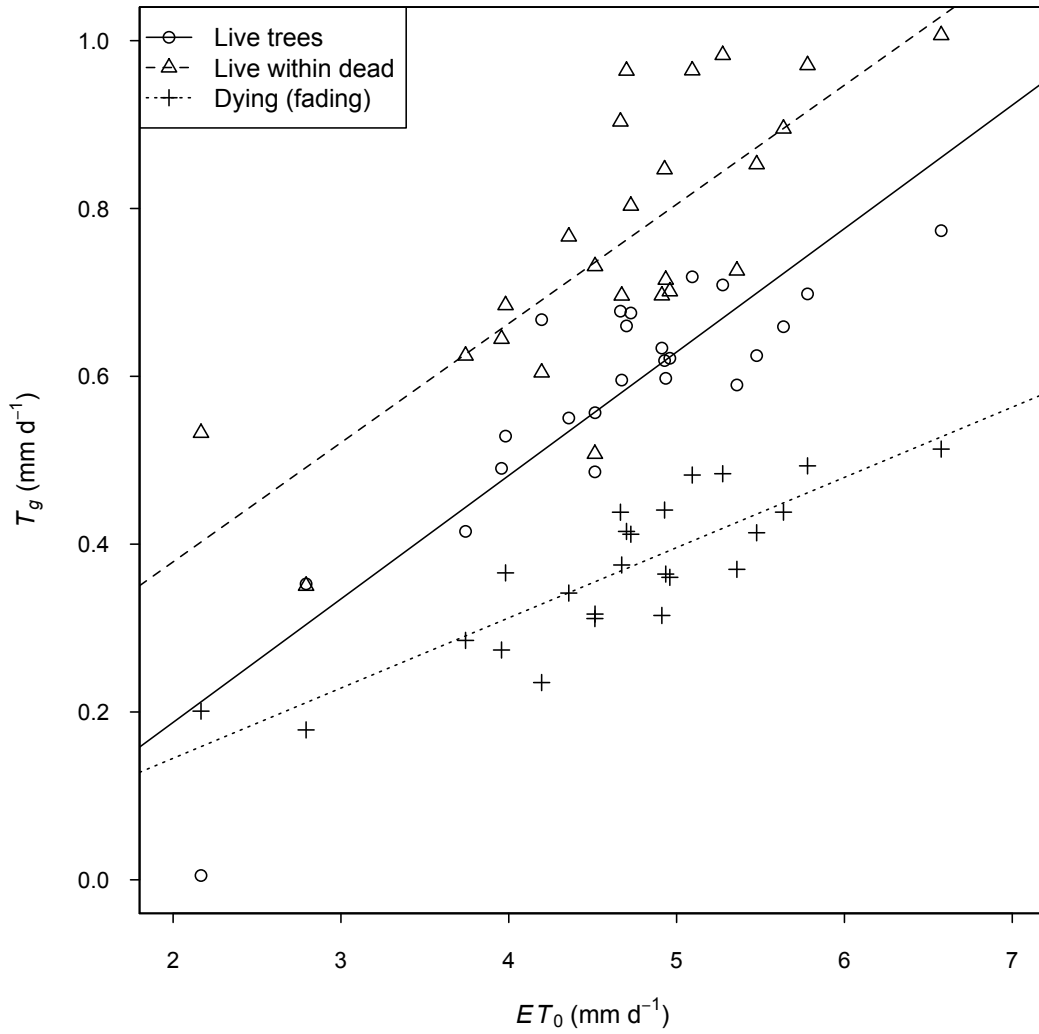


Figure 5-3. Boxplots of total growing season rainfall across 54 climate stations in the study region (1979-2010). The boxplots width is proportional to sample size (i.e., number of stations with data available for the respective year). Horizontal dashed lines indicate median (273 mm) and both upper (342 mm) and lower (202 mm) interquartile range (IQR), whiskers indicate extremes (1.5 x IQR), and circles indicate outliers.

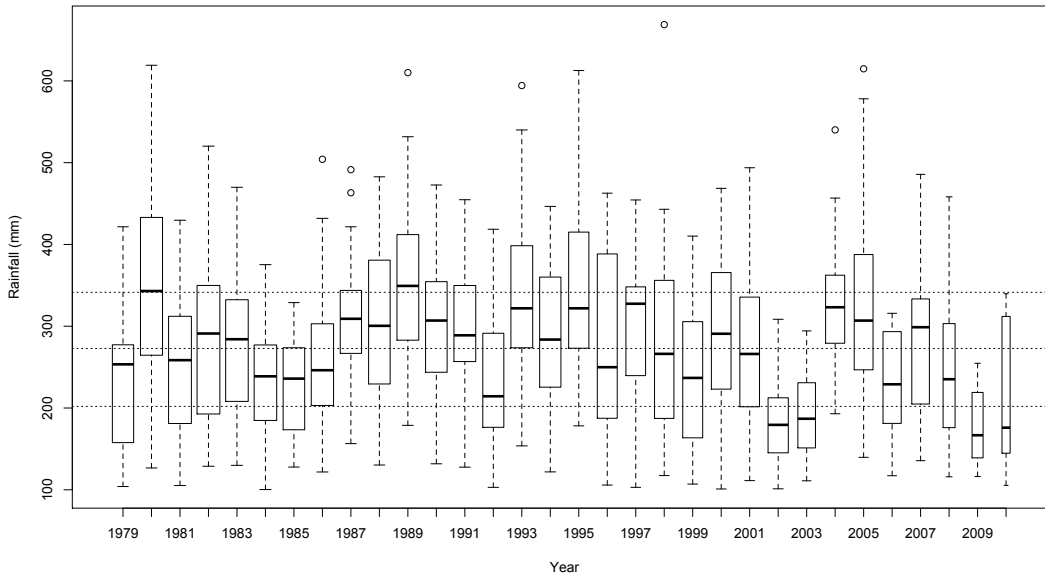


Figure 5-4. Mean daily (A, mm and %) and annual (B, mm/yr) rainfall interception I_{rf} across the 48 climate stations for control, MPB1, MPB2 and MPB3 scenarios. Vertical lines in panel A represent the range of daily rainfall where the maximum percentage difference between the control and the MPB scenarios was evident. Lines shown in panel B indicate the linear fit, upper and lower 95% confidence intervals.

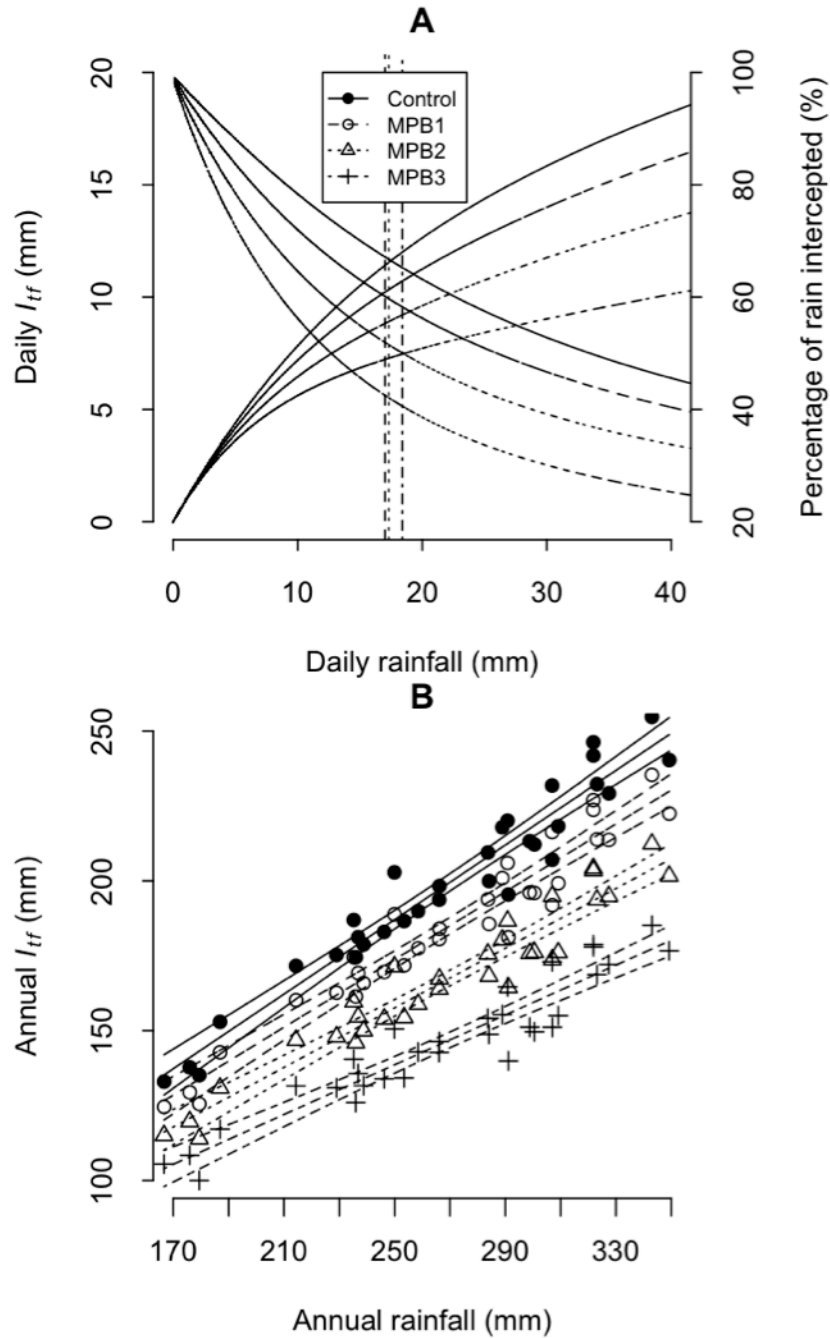


Figure 5-5. Relationships between daily recharge into the mineral soil F , and total rainfall interception I_{tf} , as a function of daily rainfall. Exponential trends in both panels represent F . Quasi-asymptotic trends represent I_{tf} . Vertical and horizontal lines denote the points where I_{tf} is equal to F in the control and three mountain pine beetle attack scenarios.

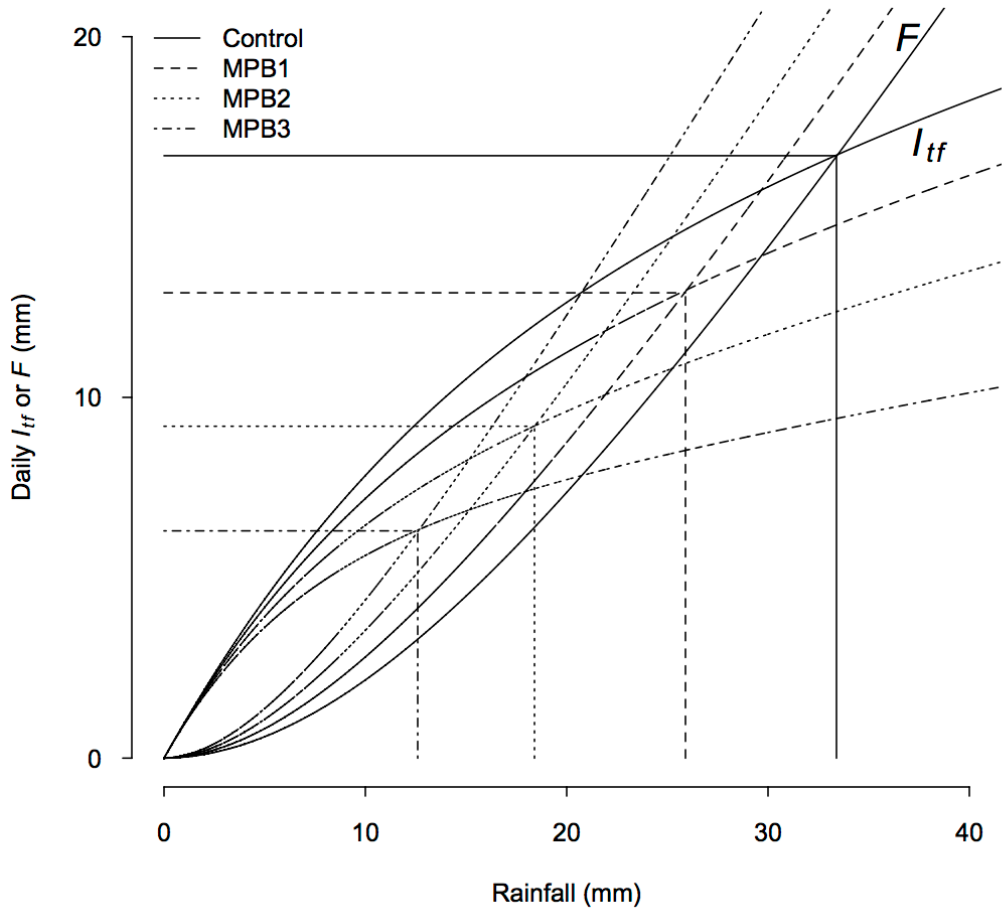


Figure 5-6. Mean daily storage and drainage (Q) across the 48 climate stations for control, MPB1, MPB2 and MPB3 scenarios.

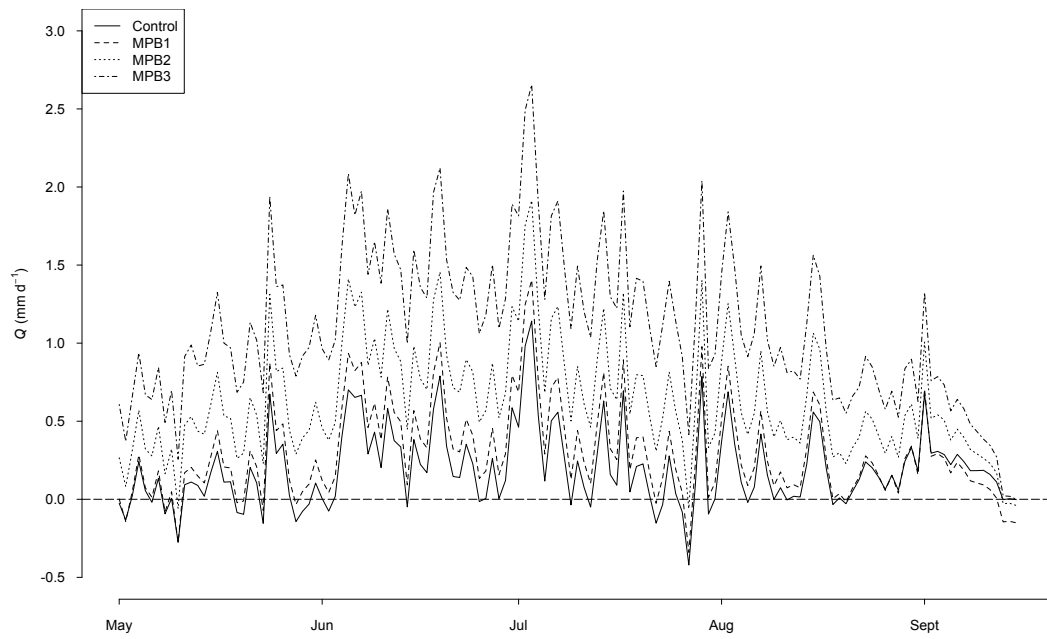
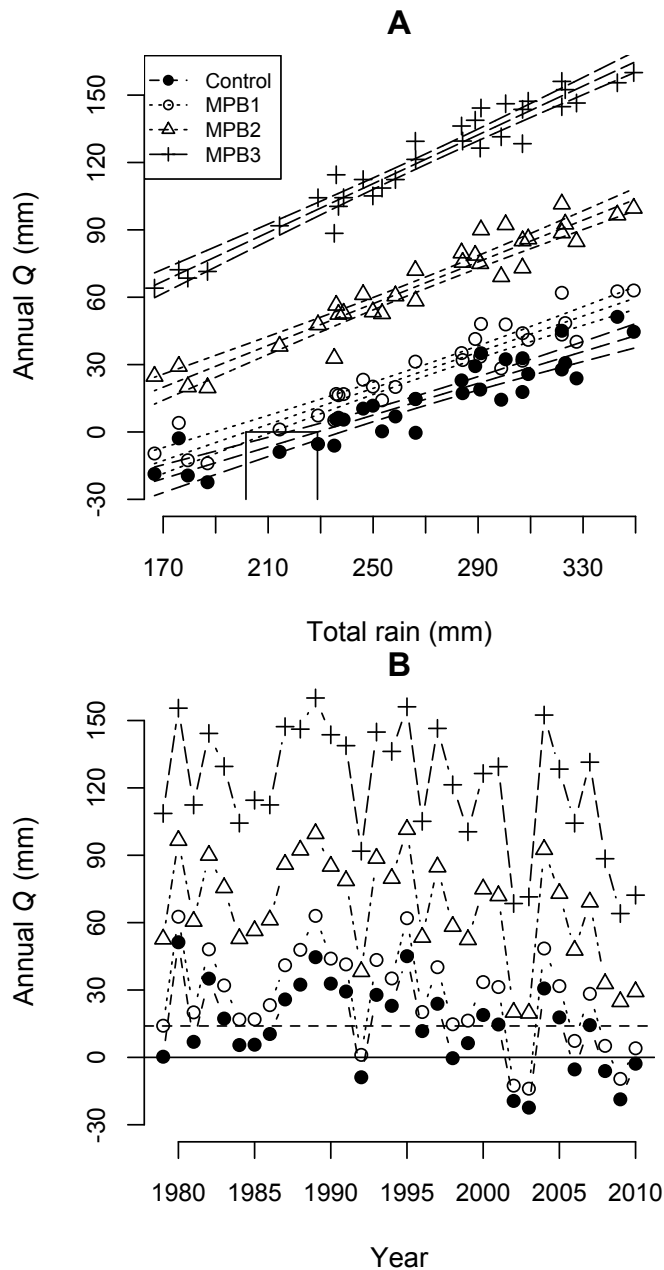


Figure 5-7. The relationship between mean annual storage and drainage (Q) and mean growing season precipitation across the 48 climate stations for control, MPB1, MPB2 and MPB3 scenarios (panel A) and mean annual Q across 32 years for these scenarios. The dashed lines in panel A indicate the linear relationship, upper and lower 95% confidence intervals for each scenario. The solid lines refer to the range of value in rain where Q equalled zero in the control and MPB1 scenario. The horizontal dashed line in panel B indicates the long-term mean Q for control conditions across all years, and the solid line indicates zero Q .



Chapter 6. SYNTHESIS OF CONCLUSIONS

Climate change represents a new dimension in the issue of future forest sustainability (Mbogga et al., 2009; Gray and Hamman, 2011). Mountain pine beetle (MPB) is increasingly considered an established disturbance regime in the landscape of west central Canada (Schneider et al. 2010), thus the impact of this disturbance will likely be an important component affecting water resources in this region (Hélie et al., 2005; Uunila et al., 2006). The hydrologic changes resulting from MPB mortality are primarily related to the loss of canopy cover. Despite the widespread recognition of the potential changes in landscape dynamics due to MPB, there has been limited direct research explicitly focused on how this disturbance affects key hydrological processes in lodgepole pine forests throughout west central Alberta or other parts of North America (see review in Schnorbus, 2011). The limited management options for preventing MPB spread across extensive areas highlight the importance of future research to improve our ability to predict the hydrological consequences of MPB. Although increased water yield caused by MPB could be desirable in some regions, usually the threats of excessive flooding and reduction in water quality require land managers to consider intervention or mitigation strategies. Options for mitigating MPB effects will likely involve strategies aimed at promoting eco-hydrological recovery from this disturbance (Millar et al., 2007). Nonetheless, as a consequence highly limited existing research, land managers dealing with eco-hydrological changes after MPB attack have to be particularly cautious in considering climate and forest type in relation to site-specific objectives.

The need for research addressing important knowledge gaps in ecohydrology of lodgepole pine and how MPB is likely to affect water cycling in these forests is not new. In particular, there has been a need for carefully controlled short- to long-term stand-level field studies (Hélie et al., 2005; Uunila et al., 2006). Key research priorities include transpiration, rainfall interception and soil moisture dynamics (Hélie et al., 2005; Adams et al., 2011). The present analysis of the impacts of simulated MPB attack on the water balance in lodgepole pine forests represents a significant advance in understanding of key components regulating stand water balance and their response to disturbance. As expected, the present research met much of this need, but also raised many other questions.

6.1. Research contributions

The following generalizations correspond to water balance relationships developed throughout Chapters 2 to 5, which should be applicable to mature lodgepole pine dominated stands at risk from MPB attack in western Alberta (>100 years old, 20–24 m tall, with well developed forest floor layers):

Lodgepole pine forests in this region are strongly snowmelt-dominated systems. Most of the rain reaching the forest is lost through rainfall interception and overstory transpiration. Storage and/or drainage dynamics have a weak relationship with rainfall inputs and thus, do not show clear seasonality during the growing season. These findings are

novel because while the water balance of lodgepole pine stands have been previously explored via modeling using unconfirmed parameters or parameters based on other tree species, this study reflect the combined outcome of carefully measured, representative water components in mature lodgepole pine that have not been previously reported.

- Forest rainfall interception is the dominant source of evaporative loss in these lodgepole pine forests, however, both canopy and forest floor layers contribute to this process. As no previous studies have documented all of the components regulating rainfall interception losses in lodgepole pine, the results of this study constitute an important contribution to understanding the vertical dynamics of rainfall interception processes in lodgepole pine. Previous research on rainfall interception dynamics in other forest types has usually neglected the role of the forest floor layer and focused primarily on the canopy layer. Thus, the present research highlights the importance of analyzing the process of rainfall interception as a dual layer.
- During periods of high evaporative demand, transpiration in lodgepole pine is highly conditioned by soil water availability. Thus, individual trees have the potential of differential responses in transpiration under contrasting conditions of soil water availability. Microclimate and moisture availability are key environmental factors regulating transpiration of forest vegetation. While numerous studies have documented such relationships in the context of changes after forest disturbance such as fire, clear-cut harvesting, partial cutting, or thinning, no studies to my knowledge have described coupled changes in growing season microclimate and forest evaporative losses after MPB attack. Given the microclimate responses measured in this study were not strongly, nor clearly evident, changes observed in transpiration dynamics of surviving trees in partially attacked stands were likely driven entirely by increased below ground soil moisture due to the reduced transpiration of neighbouring trees (fading/dead). This suggests that early MPB attacks are notably different than those observed in harvested systems (clear-cut or partial cut) because microclimate was not a factor in the transpiration responses observed.
- The influence of aboveground conditions on soil moisture dynamics is mainly associated with the first 20 cm layer of the soil profile and most clearly evident at 5 cm depth. Studies relating soil moisture to ecological processes, and more specifically disturbance, are rare and usually focused only on the shallow portion of the soil profile (up to depths of 30-40 cm), limited to one or two years, and accounting only for soil moisture. In particular, no studies (to my knowledge) have documented the impact of MPB on soil moisture. This represents a crucial information gap because changes in soil moisture are likely to be strongly coupled with larger scale hydrologic changes in MPB affected landscapes such as

groundwater recharge and runoff generation that are likely to govern streamflow regimes in these landscapes.

6.1.2. Effects of MPB on water balance of lodgepole pine forests in Alberta

Adams et al. (2011) employed a hypothesis tree of potential effects of tree die-off on key water budget components in forest stands, using changes in canopy cover as an indicator of disturbance intensity. In this particular case, a reduction in canopy cover of ~25% could be defined as a threshold for statistical separation of partial and intense MPB attacks in mature lodgepole pine forests (Figure 6-1). The hypothesis tree in Figure 6-1 could serve as a framework to evaluate interactions among components regulating stand water balance in MPB attacked stands:

- Changes in the canopy cover produced by MPB can significantly increase the importance of the forest floor in overall forest rainfall interception. As a consequence, the forest floor can become the main component in the forest evaporative loss after MPB and thus, provide stronger insight into the relationships between water inputs and drainage after MPB attack. Given both the broad importance of lodgepole pine and the impacts of MPB attack affecting these forests in western North America, information on rainfall interception dynamics is a keystone component of understanding water balance and hydrology of these western forests. As no previous studies have documented all of the components regulating rainfall interception losses in lodgepole pine, the results of this study constitute an important contribution to understanding the vertical dynamics of rainfall interception processes in lodgepole pine.

A partial MPB attack can result in a slight reduction in total forest interception (~5% less, MPB1 scenario in Figure 6-2) due to an increase in net precipitation and a subsequent increase in forest floor interception (Figure 6-3). With the reduction of forest canopy cover in MPB attacked forests the role of forest floor interception in the forest water balance becomes critical (Figure 6-3). A MPB attack can also trigger an increase in the recharge into the mineral soil, regardless of the intensity of the attack (Figure 6-3). Increases in soil moisture drives subsequent increases in transpiration of surviving trees, which results in compensatory effect buffering changes in overall stand transpiration (Figure 6-1):

- MPB attack can produce a clear gradient of increasing soil moisture during the growing season related to the intensity of canopy disturbance. This can be extended to include changes produced by harvesting or by differing intensities of MPB attack. Increases in soil moisture after harvesting are driven by both increases in net precipitation (reduced rainfall interception) and reduction in evaporative losses by transpiration, while early MPB attack only affects transpiration losses. While effects of variable intensity green or red attack showed the most dramatic increases in soil moisture in the top 0-5 and 0-20 cm soil layers,

increased soil moisture after early variable intensity green-red attack in the absence of disturbance effects on water inputs to stands (e.g. interception and net precipitation) are novel and have not been previously reported.

- While no meaningful changes in microclimate likely occur during the early green-red attack phases of MPB attack, strong variation in transpiration of several distinct categories of trees are likely. The differential transpiration of individual trees may compensate or buffer stand scale changes in transpiration. This study highlights the importance of understanding the effects of MPB on transpiration at both the tree- and stand-levels, where the compensatory response at the stand-scale would depend on the relative distribution of dying and live trees. These results demonstrate that transpiration response to variable intensity MPB attack is unique in the research literature, yet a critical component to understanding how MPB is likely to impact forest water balance and hydrology of vulnerable landscapes.

A compensatory response in partially MPB attacked stands can result in little changes in the stand transpiration from healthy forest conditions. These changes in transpiration result in little changes in evapotranspiration (Figures 6-2 and 3):

- The water balance as storage and/or drainage in partially MPB attacked forests may not differ meaningfully from healthy forest conditions due to increases in the forest floor interception, along with the compensatory response in transpiration. The role of increased rainfall interception by the forest floor, and highly variable changes in transpiration responses produce interactions among components of stand water balance that can buffer or moderate the impacts of MPB on water balance across a gradient of increasing intensity of MPB attack.

Intensively MPB attacked stands show overall decreases in evapotranspiration, regardless of the compensatory transpiration response (Figure 6-1). Intensively MPB attacked stands that lack of transpiration will have a dramatic increase in the amount of water available for storage or drainage. Storage or drainage will end being equal to recharge into the mineral soil (Figure 6-3). Stands where the storage or drainage fluxes are close to evapotranspiration (I_{tf} in Figure 6-2) will likely show strong growing season variation in soil moisture (Figure 6-1):

- Intensively MPB attacked forests can exhibit strong seasonal variation in storage and/or drainage that parallels the distribution of rain during the growing season. Thus, soil moisture during the growing season in these stands may not be as reliant on strong snowmelt recharge as healthy forests. In healthy forests, evapotranspiration is the dominant component in the water balance, where total rainfall interception represents the main source of this evaporative loss. However, as

evapotranspiration decreases along a gradient of increasing intensity of MPB attack, the contribution of storage and drainage in the water balance increases strongly. These findings are novel because while the effects of MPB attack on water balance of lodgepole pine stands have been previously explored via modeling using unconfirmed parameters or parameters based on other tree species or disturbance types, impacts of MPB attack on stand water balances in this study reflect the combined outcome of carefully measured, representative water components in mature lodgepole pine that have not been previously reported. Thus the effects of MPB attack modeled herein reflect considerably greater certainly than previous efforts.

Drier climatic conditions (past 13 years) result in smaller changes in the hydrology of MPB attacked forests than under previous moister climates. Furthermore, since the impact of MPB on all water cycling components increased in magnitude following an increase in precipitation (both daily and annual), the impact of MPB on all components water cycling will increase in magnitude during wetter years or where growing season precipitation is greater. The latter suggests that the impact of bark-beetle attack is likely to be greatest in the regions of Alberta where growing season precipitation is greatest.

6.2. Unanswered questions

The rainfall interception study (Chapter 2) did not detect a change in rainfall interception during the early green-red attack phase of MPB attack. However, the sensitivity analysis in the model implemented for canopy rainfall interception suggested that changes in canopy openness should result in major shifts in canopy interception:

- What are the effects of late stage (grey attack) MPB attack on forest rainfall interception?

Since the latter grey attack phase of MPB attack results in a direct increase in canopy openness in the stands, canopy rainfall interception should decrease in proportion to the reduction in canopy cover. Furthermore, a decrease in canopy interception represents an increase in net precipitation. Trends in forest floor water content along with the results in forest floor water storage capacity study suggest that an increase in net precipitation would result in a significant increase in forest floor interception. Since MPB attacked stands should experience increases in net precipitation, forest floor interception should increase because of the large water storage capacity in the forest floor layer. There might be potential for a negative effect in the forest floor storage capacity by increase in understory moss mortality via photoinhibition (due to an increase in the canopy gap fraction). Nonetheless, since the main composition of the forest floor layer is coarse material, a significant reduction in the forest floor storage capacity may not counteract an increase in forest floor interception.

The soil moisture study (Chapter 4) indicated that trees in a partially MPB

attacked stand had a dynamic influence in the spatial pattern of soil moisture throughout the growing season. This influence in the spatial pattern of soil moisture was associated with the spatial location of live, dying and dead trees. However, the monitoring of soil moisture was not specifically associated with a tree response but with a stand response:

- What is the intra and inter-annual response in soil moisture associated with the distribution of trees representative of MPB attacked stands (i.e., live, dying and dead)?

Since the stand reflecting partial MPB attack produced a dynamic increase in soil moisture spatial heterogeneity, then the hypothesis will be that the soil moisture in the proximity of trees will be directly associated with their life status, and this dynamic influence will be explained by root-soil interactions.

6.3 Final statement

While effects of MPB attack on water balance of lodgepole pine stands have been modeled by others using uncertain model parameters, impacts of MPB attack on stand water balances explored in this study reflect the combined outcome of carefully measured, representative water components in mature lodgepole pine that have not been previously reported. Overall, the results of this dissertation have provided novel insights into the ecohydrology of lodgepole pine forests, in particular in mature stands in the face of early MPB attack. These results can be applied to forest management and silvicultural practices in pine forests by providing an increased understanding of the linkages between individual water balance components and the likely response of these forests to MPB attack. Results indicated clear differences between MPB and other disturbances (e.g., fire or harvesting) commonly used as surrogates to understand the effects of MPB in the landscape.

As a summary, the main take-home messages are:

1. Given both the broad importance of lodgepole pine and the impacts of MPB attack affecting these forests in western North America, information on rainfall interception dynamics is critical to understand the hydrology of these western forests.
2. MPB attack can produce a clear gradient of increasing soil moisture during the growing season related to the intensity of canopy disturbance. This can be extended to include changes produced by harvesting or by differing intensities of MPB attack. Nonetheless, while increases in soil moisture after harvesting are driven by both increases in net precipitation (reduced rainfall interception) and reduction in evaporative losses by transpiration, early MPB attack only affects transpiration losses.

3. While no meaningful changes in microclimate likely occur during the early green-red attack phases of MPB attack, strong variation in transpiration of several distinct categories of trees are likely.
4. The differential transpiration of individual trees may compensate or buffer stand scale changes in transpiration. This study highlights the importance of understanding the effects of MPB on transpiration at both the tree- and stand-levels, where the compensatory response at the stand-scale would depend on the relative distribution of dying and live trees.
5. In healthy forests, evapotranspiration is the dominant component in the water balance. However, as evapotranspiration decreases along a gradient of increasing intensity of MPB attack, the contribution of storage and drainage in the water balance increases strongly.

6.3. References

- Adams, H. D., C. H. Luce, et al. (2011). "Ecohydrological consequences of drought- and infestation- triggered tree die-off: insights and hypothesis." Ecohydrology **5**(2): 145-159.
- Carver, M., M. Weiler, et al. (2009). Development and application of a peak-flow hazard model for the Frazer basin (British Columbia). Mountain Pine Beetle Working Paper 2009-14. Victoria, B.C., Natural Resources Canada, Canadian Forest Service, Pacific Forestry Centre.
- Gray, L. K. and A. Hamann (2011). "Strategies for reforestation under uncertain future climates: guidelines for Alberta, Canada." PLoS ONE **6**(8): e22977.
- Hélie, J. F., D. L. Peters, et al. (2005). Review and synthesis of potential hydrologic impacts of mountain pine beetle and related harvesting activities in British Columbia. Mountain Pine Beetle Initiative Working Paper. Victoria, Natural Resources Canada, Canadian Forest Service, Pacific Forestry Centre. **2005-23**: 34.
- Mbogga, M. S., A. Hamann, et al. (2009). "Historical and projected climate data for natural resource management in western Canada." Agricultural and Forest Meteorology **149**(5): 881-890.
- Millar, C. I., N. L. Stephenson, et al. (2007). "Climate change and forests of the future: managing in the face of uncertainty." Ecological Applications **17**(8): 2145-2151.
- Redding, T. E., R. D. Winkler, et al. (2008). Mountain pine beetle and watershed hydrology: A synthesis focused on the Okanagan. One Watershed – One Water, Kelowna, BC, Canadian Water Resources Association.
- Schneider, R. R., M. C. Latham, et al. (2010). "Effects of a severe mountain pine beetle epidemic in western Alberta, Canada under two forest management scenarios." International Journal of Forestry Research(417595): 7.
- Schnorbus, M. (2011). A synthesis of the hydrological consequences of large-scale mountain pine beetle disturbance. Mountain Pine Beetle Working Paper 2010-01. Victoria, Natural Resources Canada, Canadian Forest Service, Pacific Forestry Centre: 30.
- Uunila, L., B. Guy, et al. (2006). "Hydrologic effects of mountain pine beetle in the interior pine forests of British Columbia: key questions and current knowledge." Streamline

6.4. Figures

Figure 6-1. A hypothesis tree of potential effects of MPB on key water budget components in a mature lodgepole pine forest after Adams et al. (2011). Possible effects include decreases and increases in total forest interception (I_{tf}), soil moisture, stand transpiration (T_{st}), evapotranspiration (E_t) and soil moisture storage or drainage. Important factors for determining these outcomes include the total amount of annual rainfall during the growing season, the dominance of snowmelt on water flows, percent tree cover lost from mortality, the degree of development of forest floor and rainfall interception response, and the effect of tree mortality and the compensatory response in stand transpiration. These hypotheses represent an assessments of the empirical analysis conducted in Chapters 2 to 5.

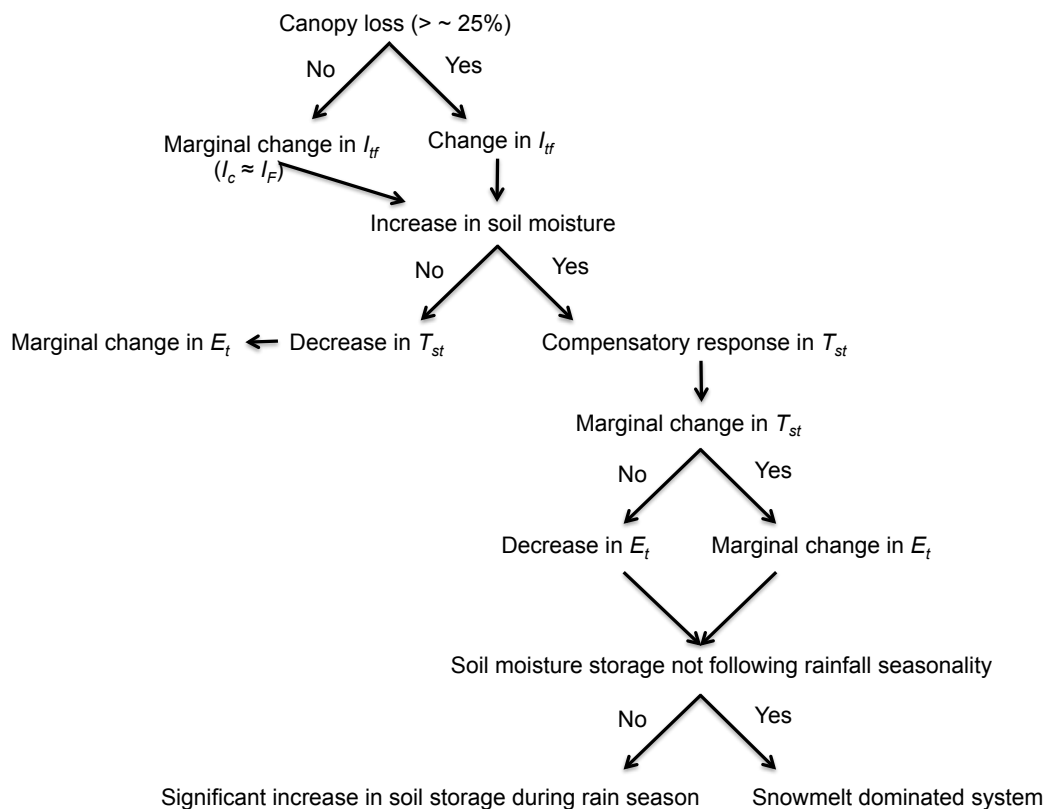


Figure 6-2. Changes in components of forest water balance with increasing intensity of MPB attack. Components include total forest interception I_{tf} , stand overstory transpiration T_{st} , and water balance (storage and/or drainage) Q as a percentage of annual rainfall in healthy forests and MPB scenarios reflecting a gradient of intensity from MPB1-MPB3 (after Chapter 5). Scenarios were defined by decreasing both canopy cover and overstory transpiration.

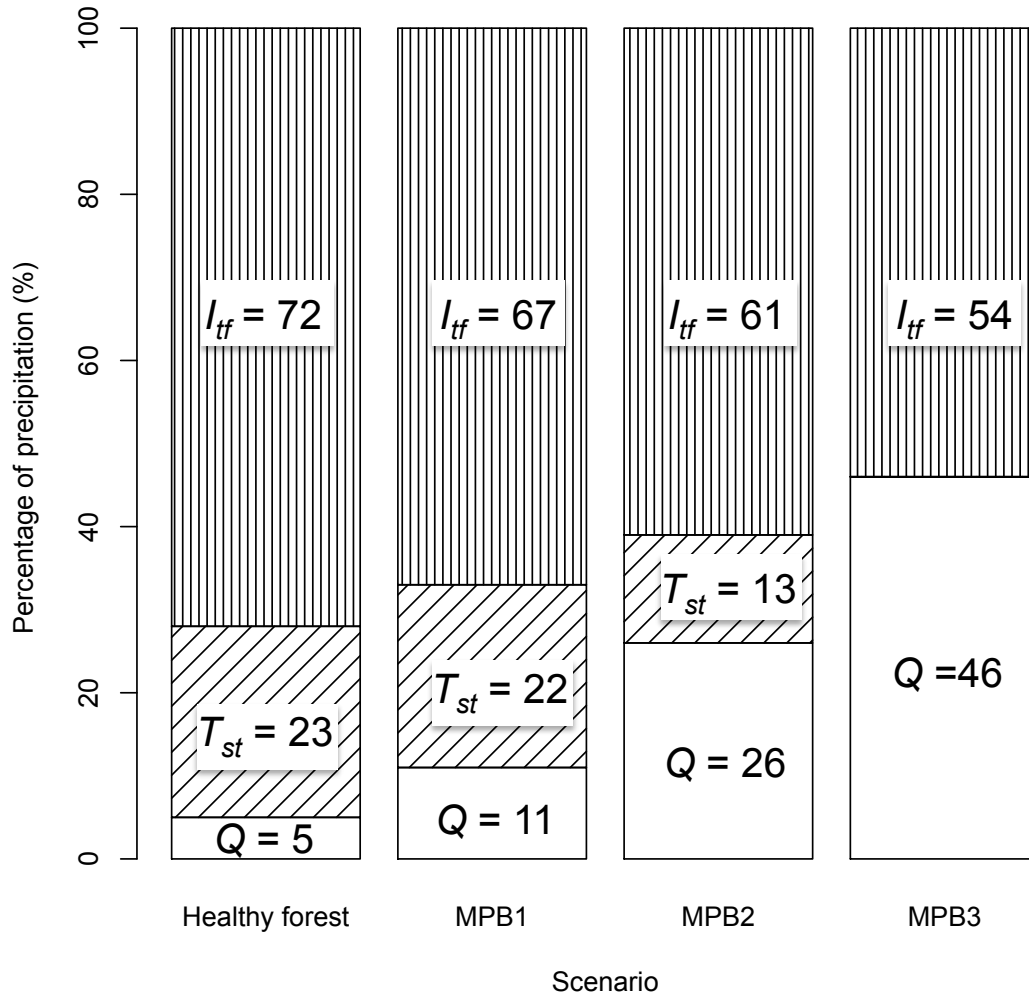


Figure 6-3. Components of water balance in healthy forests and MPB scenarios reflecting a gradient of intensity in MPB attack from MPB1- MPB3 (after Chapter 5). Scenarios were defined by decreasing both values of canopy cover and of overstory transpiration. The width of the each box corresponds to the percentage of rainfall during the growing season.

